Shedding light on the role of bHLH transcription factors in *Arabidopsis thaliana* male reproductive development

Jordan Kirsty Robson, BSc (Hons)

Thesis submitted to the University of Nottingham
for the degree of Doctor of Philosophy

March 2021

ACKNOWLEDGMENTS

First of all, my deepest thanks to my supervisor Zoe Wilson for all her guidance, insight and support, not only within my own project and thesis-writing, but also in getting us all back into the lab to safely continue experiments after the first Covid-19 lockdown. I'm incredibly grateful that I've had the opportunity to learn from the best and hope that we can continue working together for many years to come.

Thank you also to Steve Thomas and Peter Hedden for the discussions that have shaped the GA story and to Ari Sadanandom for bringing the SUMO-bHLH connection to light.

Within the Wilson group itself, I'd especially like to thank Alison for taking me under her wing as a new PhD student and teaching me everything I know. I'm very thankful to all lab members, past and present, for providing such a wonderful working environment and helping me throughout my PhD; particularly Joan, Helen and Marie for always being counted upon to turn up the tunes and keep me positive.

Naturally, I must say a massive thank you to all my friends and family for their love and encouragement, I really couldn't have got through my PhD without you. Thank you to Mum for teaching me how to be strong, always looking after me and showing an interest in my science even when it's complicated. For my Dad and sister Beth, who are always keen to discuss the possibility of creating invisible plants, I wrote Chapter 8 especially for you.

Last but by no means least, thank you to Jason who has weathered the PhD storm alongside me since day 1 and kept me afloat. There's no person I'd rather have had by my side writing our theses in a global pandemic, but I can't wait to get back to adventuring now that it's over.

ABSTRACT

Development of viable pollen in the anther locule is crucial for plant reproduction, and relies upon secretion of proteins, lipids, polysaccharides and other essential molecules from the surrounding tapetum tissue. Tapetum development in *Arabidopsis thaliana* is regulated by a number of genes including the basic Helix Loop Helix (bHLH) transcription factors DYSFUNCTIONAL TAPETUM (DYT1) and ABORTED MICROSPORES (AMS), which interact competitively with bHLH010, bHLH089 and bHLH091 to regulate downstream targets involved in synthesis and secretion of pollen wall components. Disruption of genes within the tapetum development pathway leads to male sterility and previous research has shown that *ams, dyt1* and *bhlh089 bhlh010 amiR-bHLH091* knockout mutants are completely male sterile, whereas the single and double *bhlh010*, *-089* and *-091* mutants are mostly fertile due to a high level of functional redundancy.

In this thesis *bhlh089 bhlh091* and *bhlh089 bhlh010* double mutants are revealed to show light-sensitive sterility, alongside recent observations of thermosensitive male sterility. In low light conditions, both *bhlh* double mutants exhibit severe pollen wall defects; however, whereas the *bhlh89,10* double mutant shows later recovery of fertility, *bhlh89,91* remains sterile throughout development suggesting that bHLH89, -91 and -10 have distinct functions in maintaining fertility in response to environmental stress.

RNASeq analysis of wild type and *bhlh89,91* mutant light response highlighted differential regulation of genes related to sexual reproduction and hormonal responses. As transient assays demonstrated that bHLH89, 91 and -10 interact with DELLA proteins and MYB33/65, and bHLH-AMS heterodimers were found to more strongly induce target gene expression, it's proposed that DELLA-dependent sequestration of bHLHs in different light environments regulates formation of AMS-bHLH dimers that activate genes involved in pollen development. bHLH89, -91 and -10 are further shown to undergo post-translational modifications leading to a new hypothesis on their role in regulating reproductive development in adverse conditions.

TABLE OF CONTENTS

1 INTRODUCTION

1.1 MALE FERTILITY & HYBRID VIGOUR

With the global population rising there is increasing pressure on the agricultural industry to meet demands for food. Hybrid varieties of crops such as maize and rice have been instrumental in increasing crop productivity since the 1960s. Plants with 'hybrid vigour', a phenomenon also known as heterosis, have a higher disease resistance, reduced susceptibility to abiotic stress and increased yield (Brewbaker, 1964). However, preventing self-pollination and producing hybrid seed on a large scale is highly labour intensive. Many methods promoting outcrossing are employed, including manual removal of male flowers or stamens, but this is impractical for large-scale production of many crops. Male sterile lines are a popular alternative, reducing labour demands and expenses of hybrid crop production.

Crop breeders use two main types of male sterility system in hybrid breeding. Cytoplasmic Male Sterility (CMS) is fixed and irreversible, requiring a third genetic line to provide restorer genes and therefore sometimes called three-line breeding. Environmentally-Sensitive Genetic Male Sterility (EGMS) on the other hand is more flexible, with plants remaining male sterile under certain conditions and regaining fertility in a different environment. Commonly these lines are temperature and photoperiod-sensitive (Kim and Zhang, 2018) but there have also been reports of humidity-sensitive lines (Xue *et al.*, 2018). Studies in Maize showed that moderate transient heat stress applied to plants undergoing the tetrad stage of development reduced starch content, decreased enzymatic activity and reduced pollen germination, ultimately resulting in sterility (Begcy et al., 2019).

1.2 ARABIDOPSIS REPRODUCTION

To develop male sterile lines an understanding of the genetics underlying male reproductive development is crucial. *Arabidopsis thaliana*, commonly known as Thale Cress or Mouse-Ear Cress, has a small stature, relatively short lifecycle and orthologous genes in many major crop species; making it the perfect model organism for studying the impact of the environment on reproduction.

The Arabidopsis flower is made up of four concentric whorls: 4 sepals, 4 petals, 6 stamen and 1 carpel (Figure 1.1). As in all flowering plants, or Angiosperms, the male reproductive organ is the stamen comprised of a filament topped by an anther. Floral development occurs in 12 stages outlined by Smyth et al. (1990). Development of the anther, beginning at floral developmental stage 5, can further divided into 14 distinct developmental stages (Sanders et al., 1999). L1, L2 and L3

layers of the stamen primordia undergo a series of divisions to produce a bilaterally symmetrical, four-lobed anther, with each lobe containing developing microspores in a locule surrounded by four somatic tissues: the epidermis, endothecium, middle layer (ML) and tapetum (Figure 1.2). Over the course of development, the middle layer degenerates and microspores undergo meiosis. Subsequently, the tapetum also degenerates and microspores under two rounds of mitosis, forming distinct microspore stages that can be identified through DAPI staining of DNA (Figure 1.3).

Much focus in the male sterility field has been on genes acting within the tapetum, since this is the tissue layer that secretes proteins, lipids, polysaccharides and other molecules necessary for the development of viable pollen (Piffanelli et al., 1998). Mutations in genes within the tapetum development pathway lead to defects in tapetum secretion and production of non-viable pollen (Section 1.2.2).

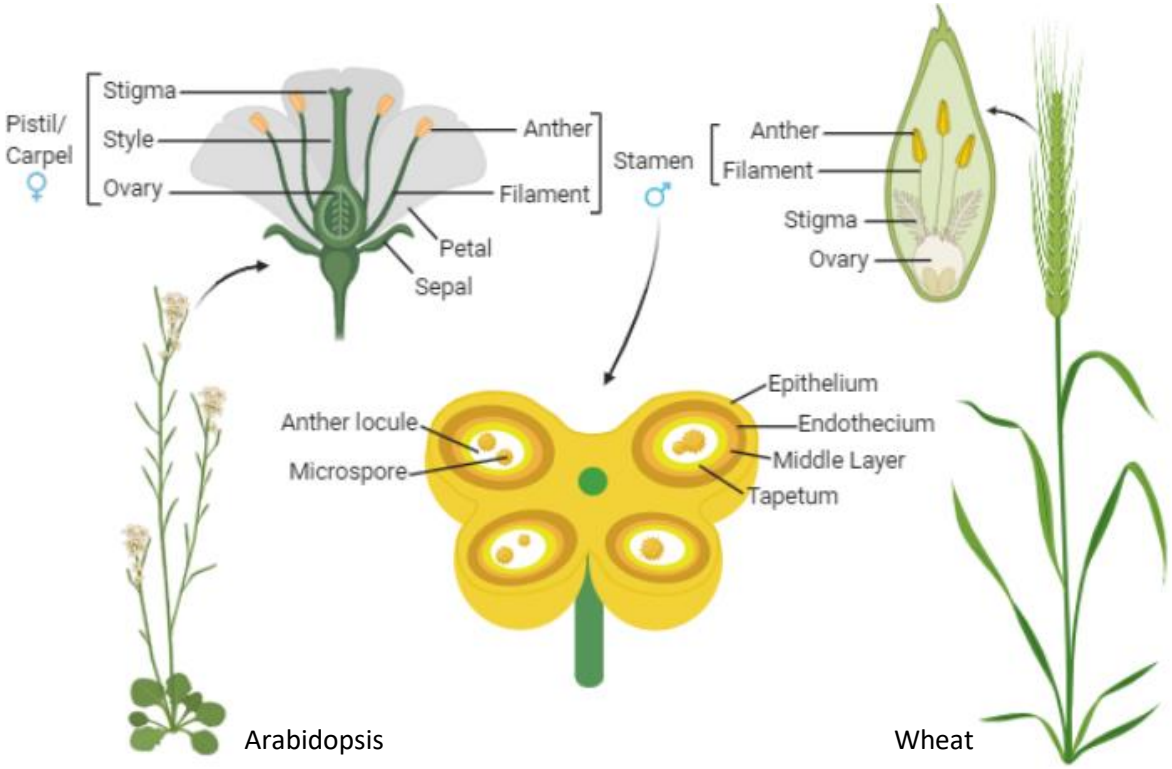

Figure 1.1. Diagrammatic view of Arabidopsis vs wheat flower morphology and tissue layers in cross-section of the Anther. Created using BioRendr.

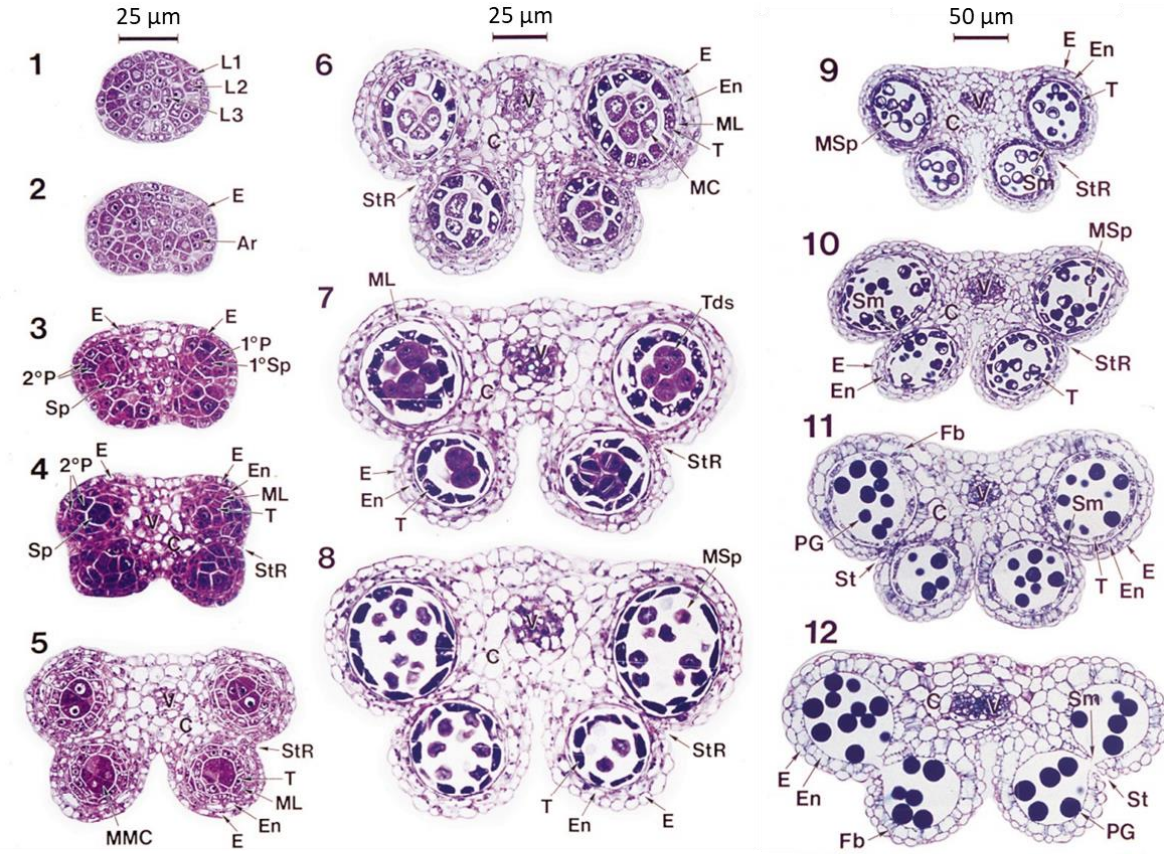

Pollen Stage	Anther Stage	Anther Morphology	Flower Stage
	1	Emergence of stamen primordia	5
	2	Archesporial cells arise from L2	
	3	Parietal and sporogenous layers derive from archesporial cells	7
	4	Anther develops into 4 distinct lobes	8
PMC	5	Locules established, all anther cell types present	9
	6	Microspore meiosis, middle layer degenerates, tapetum vacuolates and anther increases in size	
Tet	7	Meiosis completed, tetrads free within locules	
SM	8	Degradation of the callose wall surrounding tetrads, single microspores released	10
	9	Exine wall develops, microspores become vacuolated	
	10 - 11	Tapetum degenerates	11-12
BM, TM	11	Pollen mitosis, endothecium expands and thickens, septum begins to degenerate	
MP	12	Pollen grains are tricellular, septum breaks to form bilocular anther	
	13	Anther dehiscence, pollen released	13-14
	14	Stamen senesces, anther cells shrink	15-16

Figure 1.2. Pollen stages referred to in this thesis (PMC- Pollen Mother Cells, Tet- Tetrad, SM/BM/TM- Single/ Bicellular/ Tricellular Microspores, MP- Mature Pollen), corresponding stages of anther and flower development (Sanders et al., 1999; Smyth et al., 1990) *and morphological changes associated with these stages. Ar, archesporial; C, connective; E, epidermis; En, endothecium; L1, L2, and L3, 3 layers of the stamen primordia; MC, meiocyte; ML, middle layer; MMC, microspore mother cell; MSp, microspore; 2°P, secondary parietal layer; PG, pollen grains; Sm, septum; Sp, sporogenous cells; St, stomium; T, tapetum; Tds, tetrads; V, vascular.*

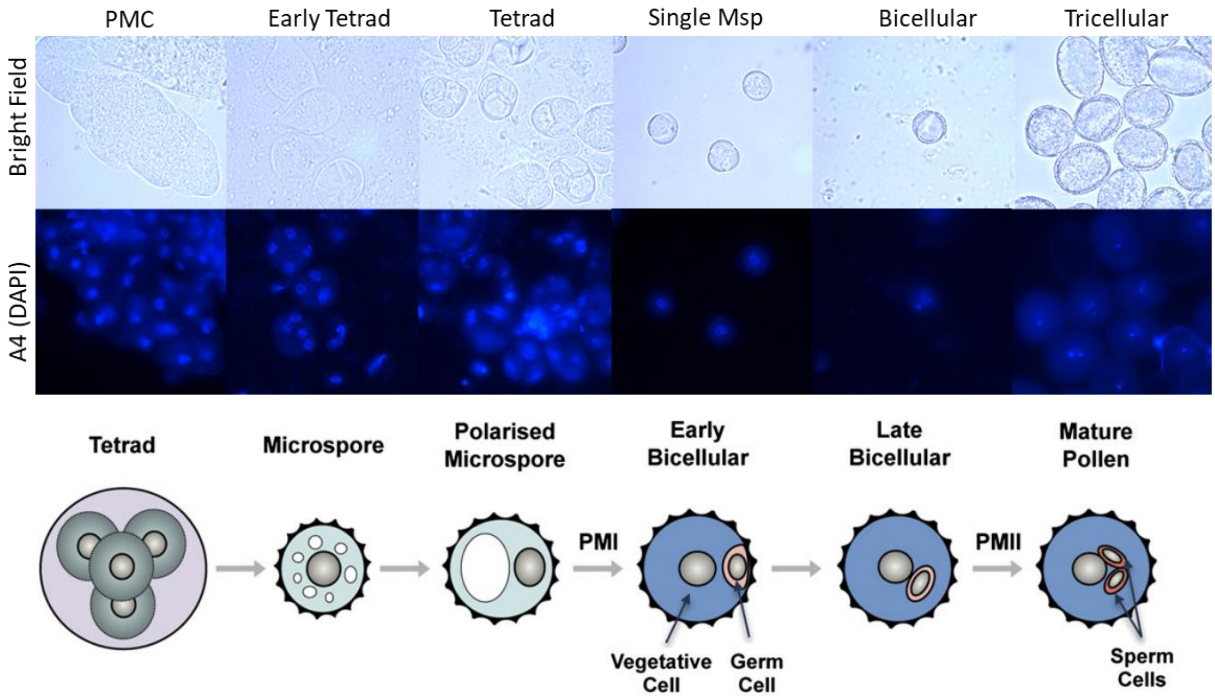

Figure 1.3 Stages of microspore development, as identified through 4',6-diamidino-2-phenylindole (DAPI) fluorescent staining of DNA under A4 fluorescent filter. Diagram from Borg et al. (2009)

1.2.1 Establishing Male Identity

According to ABCDE model for flower development, floral organ identity is defined by overlapping expression of five classes of homeotic genes: A, B, C, D and E (Rijpkema et al., 2010). Male stamen identity is specified by a protein complex of B-, C- & E- classes of MADS box transcription factors; specifically B-class APETALA3 (AP3) and PISTILLATA (PI), C-class AGAMOUS (AG) and partially redundant E-class SEPALLATA proteins: SEP1, -2, -3 and -4.

AG and AP3/PI initiate anther cell differentiation through induction of *SPOROCYTELESS/ NOZZLE* (*SPL/ NZZ*) (Wuest et al., 2012; Ito et al., 2004). Periclinal division of archesporial cells doesn't occur in *spl /nzz* mutants stage 3 anthers, and thus the endothecium, middle layer, tapetum and microsporocytes do not develop (Yang et al., 1999; Schiefthaler et al., 1999). SPL/ NZZ positively regulates the leucine-rich repeat receptor like kinases (LRR-RLKs) *BARELY ANY MERISTEM 1* and *-2* (*BAM1* and *-2*) which in turn restrict expression of SPL/NZZ, forming a regulatory loop (Figure 1.5; Hord et al., 2006).

Downstream of SPL/NZZ, another LRR-RLK EXCESS MICROSPOROCYTES1/EXTRA SPOROGENOUS CELL (EMS1/EXS) binds TAPETUM DETERMINANT1 (TPD1), a putative signal peptide, to activate pathways promoting tapetum specification (Jia et al., 2008). Two other redundant LRR-RLKs, SOMATIC EMBRYOGENESIS RECEPTOR-LIKE KINASE1 and 2 (SERK1 and -2), seemingly function within this same space with overlapping mutant phenotypes: *ems1/exs*, *serk1 serk2* and *tpd1* mutant anthers all develop a normal endothecium and middle layer however lack a tapetum and generate excess

microsporocytes which degenerate by anther stage 7 (Figure 1.4; Canales et al., 2002; Zhao et al., 2002; Albrecht et al., 2005; Colcombet et al., 2005; Yang et al., 2003). Thus it seems that EMS1/EXS forms a complex with SERK1/2 (Li et al., 2017b) binding TPD1 to specify tapetum identity (Figure 1.5).

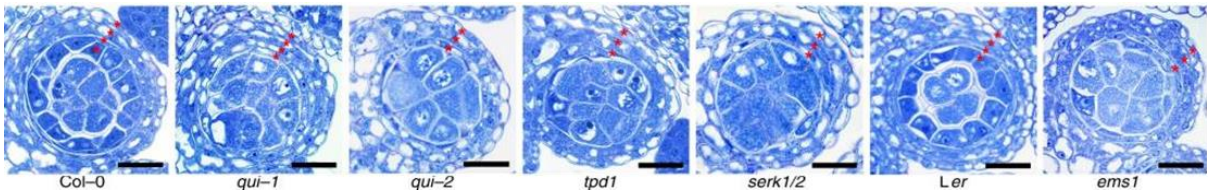

Figure 1.4 Semi-thin sections of stage 6 anthers stained with toluidine blue from Chen et al. (2019). WT Col-0 and Ler with four somatic tissue layers (indicated by red asterisks) is compared to qui-1 (bes1-1 bzr1-1 beh1-1 beh3-1 beh4-1), which also has 4 but tapetum is impaired, qui-2 (bes1-c1 bzr1-1 beh1-1 beh3-1 beh4-c1), tpd1, serk1/2 and ems1 mutants which all lack the tapetum. All mutant anthers have excessive microspores. Scale bar 20µm.

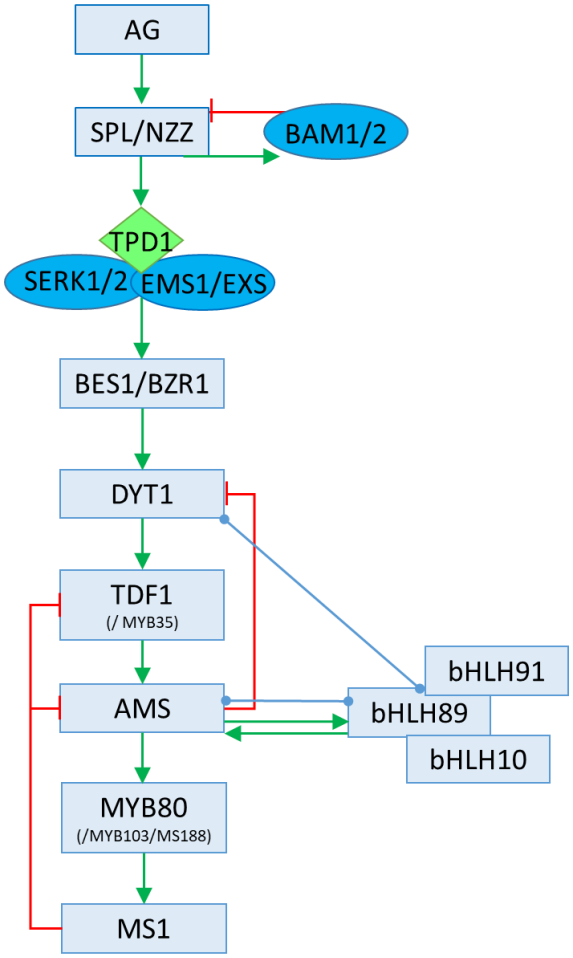

Figure 1.5. Summary of genetic control of tapetum development from initiation of anther cell differentiation by AG induction of SPL/NZZ, through to tapetum specification by the TPD1-SERK-EMS complex and then transcription factor cascades crucial to later anther development. Boxes represent transcription factors, ovals LRR-RLKs and diamond ligands.

1.2.2 Tapetum development pathways

The EMS1-TPD1-SERK1/2 signalling pathway activates *BRI1 EMS SUPPRESSOR 1* (*BES1*) expression, which alongside family members including *BRASSINAZOLE RESISTANT 1* (*BZR1*) play an essential role in regulating early tapetum development (Figure 1.4; Chen et al., 2019).

Downstream of BES1, cascading interactions of key transcription factors form a series of feedback and feedforward loops to regulate tapetum development (Figure 1.5; Ferguson et al., 2017; Zhu et al., 2011). The earliest transcription factor to act within this pathway is DYSFUNCTIONAL TAPETUM1 (DYT1; Zhang et al., 2006), a basic Helix Loop Helix (bHLH) transcription factor. This regulates a second bHLH *ABORTED MICROSPORES* (*AMS*; Sorensen et al., 2003) via a putative R2R3 MYB transcription factor *DEFECTIVE IN TAPETAL DEVELOPMENT AND FUNCTION 1* (*TDF1*; Gu et al., 2014; Zhu et al., 2008). AMS in turn regulates *MALE STERILE 1* (*MS1*; Wilson et al., 2001) through *MYB80*, another R2R3 MYB which is also sometimes referred to as *MYB103* or *MS188* (Zhang et al., 2007; Lu et al., 2020). In addition to DYT1 and AMS, three other bHLH proteins have been shown to function in tapetum development, seemingly downstream of AMS (Table 1.1): *bHLH010*, *bHLH089* and *bHLH091* (Xu et al., 2010; Feng et al., 2012).

Table 1.1. Expression (log2FC) of key tapetal transcription factors in male sterile mutant backgrounds according to published microarray data (Feng et al., 2012; Zhu et al., 2015; Lou et al., 2017; Ma et al., 2012; Phan et al., 2011; Yang et al., 2007). Blue shows downregulation, with upregulation in red and non-significant (q>0.05) changes in white.

	Male Sterile mutant					
Gene	***dyt1***	***tdf1***	***ams***	***tri-bhlh***	***myb80***	***ms1***
DYT1	1.40	0.94	0.79	1.21	-0.17	
TDF1	-3.59	-0.67	0.13		0.37	1.74
AMS	-3.92	-3.23	0.25		0.74	0.85
bHLH010	-1.56	-1.43	-1.81		0.28	
bHLH089	-1.98	-1.11	-1.64		0.25	-0.49
bHLH091	-1.80	-1.93	-1.79		0.44	0.89
MYB80	-3.87	-4.05	-4.25		0.77	0.58
MS1	-4.36	-4.33	-4.66	-4.19	-4.41	

Knock-out mutants of these key genes are male sterile, with defective tapetum and pollen development resulting in the production of inviable pollen (Figure 1.6). The tapetum cells of *dyt1, tdf1* and *ams* mutants are enlarged with increased vacuolation and reduced cytoplasm from anther stage 5/6 onwards, with unreleased tetrad meiocytes within the anther locule crushed by the swollen tapetal layer later in development (Sorensen et al., 2003; Zhu et al., 2008; Zhang et al., 2006). Whilst *dyt1, tdf1* and *ams* all function early in tapetum development, vacuolisation appears to be most severe in *dyt1* mutants, with less severe defects in *tdf1* mutants and lesser still in the *ams* mutants, consistent with their later expression patterns (Zhu et al., 2011). *myb80*/ *myb103* knockout

mutants exhibit complete male sterility with early tapetum degeneration, reduced callose breakdown, abnormal exine deposition, loss of cytoplasm in microspores and eventual collapse of most microspores by stage 12 (Higginson et al., 2003; Li et al., 2007; Zhang et al., 2007). The tapetum and microspores of the *ms1* mutant are unusually granular and heavily vacuolated immediately after dissolution of the callose wall which leads to eventual collapse of both the microspores and the tapetum; abnormal exine structures and intine formation were also observed on the microspores (Wilson et al., 2001; Vizcay-Barrena and Wilson, 2006).

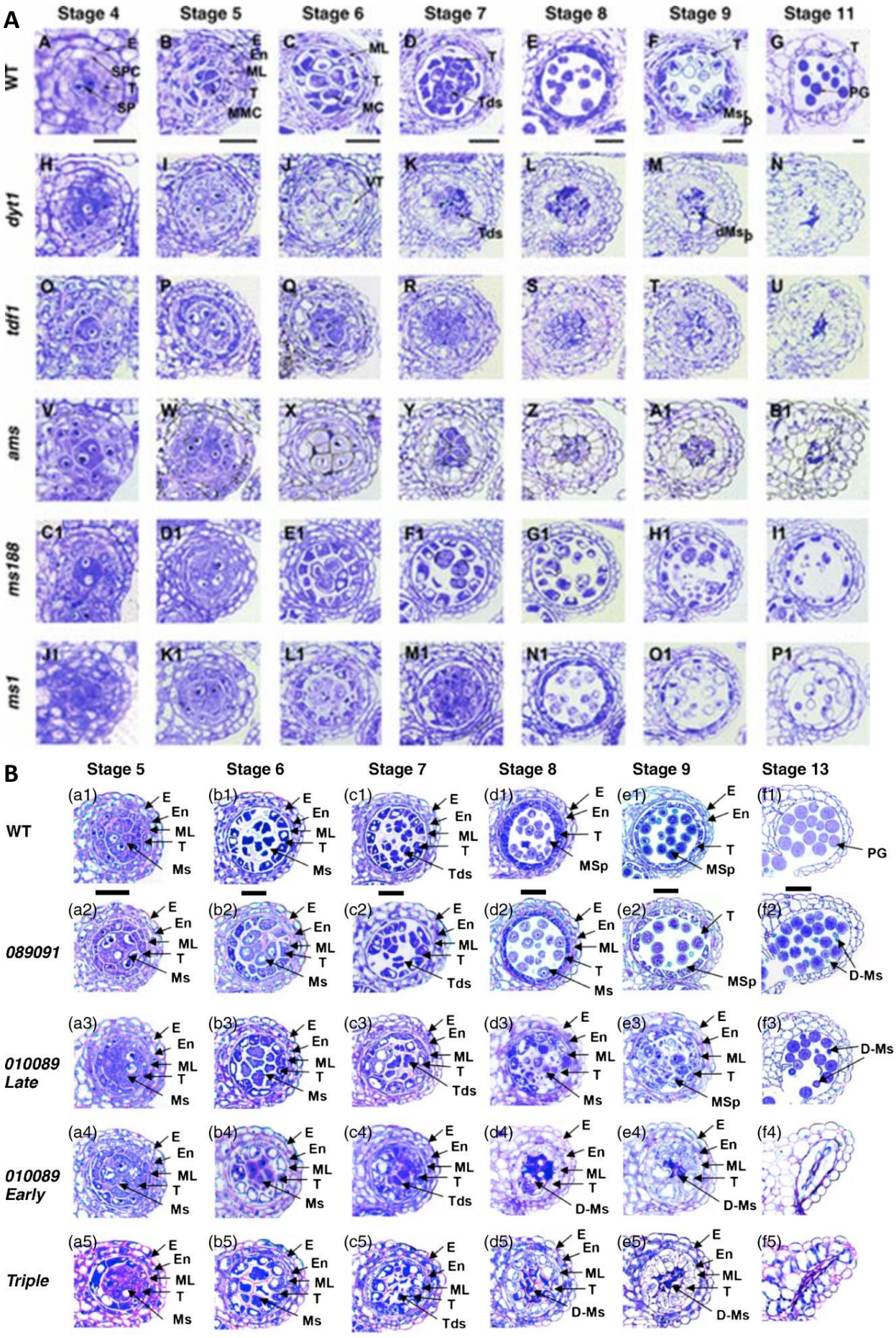
A
Stage 4
Stage 5
Stage 6
Stage 7
Stage 8
Stage 9
Stage 11
WT
dyt1
tdf1
ams
ms188
ms1
B
Stage 5
Stage 6
Stage 7
Stage 8
Stage 9
Stage 13
WT
089091
010089 Late
010089 Early
Triple
E
En
ML
T
Ms
Tds
MSp
D-Ms
PG

Figure 1.6 (previous page) Comparison of stages of anther development in A) WT Ler vs dyt1, tdf1, ams, ms188/myb80 and ms1 mutant anthers (Zhu et al., 2011). *B) WT Col-0 vs bhlh089 bhlh091, early- and late- bhlh089 bhlh010 and triple bhlh089 bhlh010 amiR-bHLH091 mutants (Zhu et al., 2015). Swollen tapetum layers in dyt1, tdf1, ams and early 8910 and triple bhlh mutant anthers leads to microspore collapse whilst impaired pollen development is seen in ms188/myb80 and mas1 mutants. Msp, degenerated microspores; E, epidermis; En, endothecium; MC, meiocytes; ML, middle layer; MMC, microspore mother cells; Msp, microspores; PG, pollen gain; SP, sporocytes; SPC, secondary parietal cell layer; T, tapetum; Tds, tetrads; VT, vacuolated tapetum. Scale bar represents 20µm.*

1.2.3 Tapetum transcription factors regulate pollen development

The core tapetum transcription factors regulate the expression of a multitude of downstream targets involved in pollen wall formation (Xu et al., 2014; Lu et al., 2020).

The mature pollen wall is made up of two main layers: the outer sporopollenin-based exine, with its characteristic sculpture-like baculae and tecta structures, and the intine which is made up of pectin, cellulose and proteins (Scott, 2004). The exine layer can be further divided into two sub-layers the inner nexine and outer sexine (Figure 1.7). As the anther develops the callose wall accumulates first on the microspore surface and then the tapetum secretes lipid precursors which are deposited between the plasma membrane and callose wall to form the primexine matrix. Precursors of Sporopollenin, a biopolymer of fatty acids and phenols, are then secreted and deposited onto this primary scaffold to form the ornate exine wall with its sculptural tecta and electron dense baculae, patterning of which depends on undulations of the plasma membrane below (Xiong et al., 2020). The nexine layer develops under the sexine as the callose wall dissolves, forming an intact pollen wall which protects the microspore from the external environment. The resulting pollen coat thus consists of veritable cocktail of waxes, lipids, sterols, sugars, proteins and polyamines such as spermidine (Shi et al., 2015).

AMS has been shown to be a master regulator of pollen wall formation, controlling the synthesis of critical lipids, phenols and flavonols (Xu et al., 2014). qCHIP-PCR demonstrated that AMS directly binds to the promoters of 29 genes involved in pollen wall development (Xu et al., 2010, 2014) including two GLYCINE-RICH PROTEINS (GRP18 and GRP19), four cytochrome P450 enzymes (CYP703A2, CYP704B1, CYP98A8, and CYP98A9), three EXTRACELLULAR LIPASES (EXL4, -5 & -6), LIPID TRANSFER PROTEIN12 (LTP12) and the ATP-binding cassette (ABC) transporter ABCG26/ WBC27 (Figure 1.7).

In a later study, AMS was also found to directly regulate the AT-hook nuclear localized (AHL) family protein TRANSPOSABLE ELEMENT SILENCING VIA AT-HOOK (TEK), which is critical to the formation of the nexine and intine layers (Lou et al., 2014). This in turn represses CALLOSE SYNTHASE5 (CalS5) to halt callose wall synthesis in order to achieve callose dissolution and proper patterning of the pollen wall (Xiong et al., 2020; Figure 1.7).

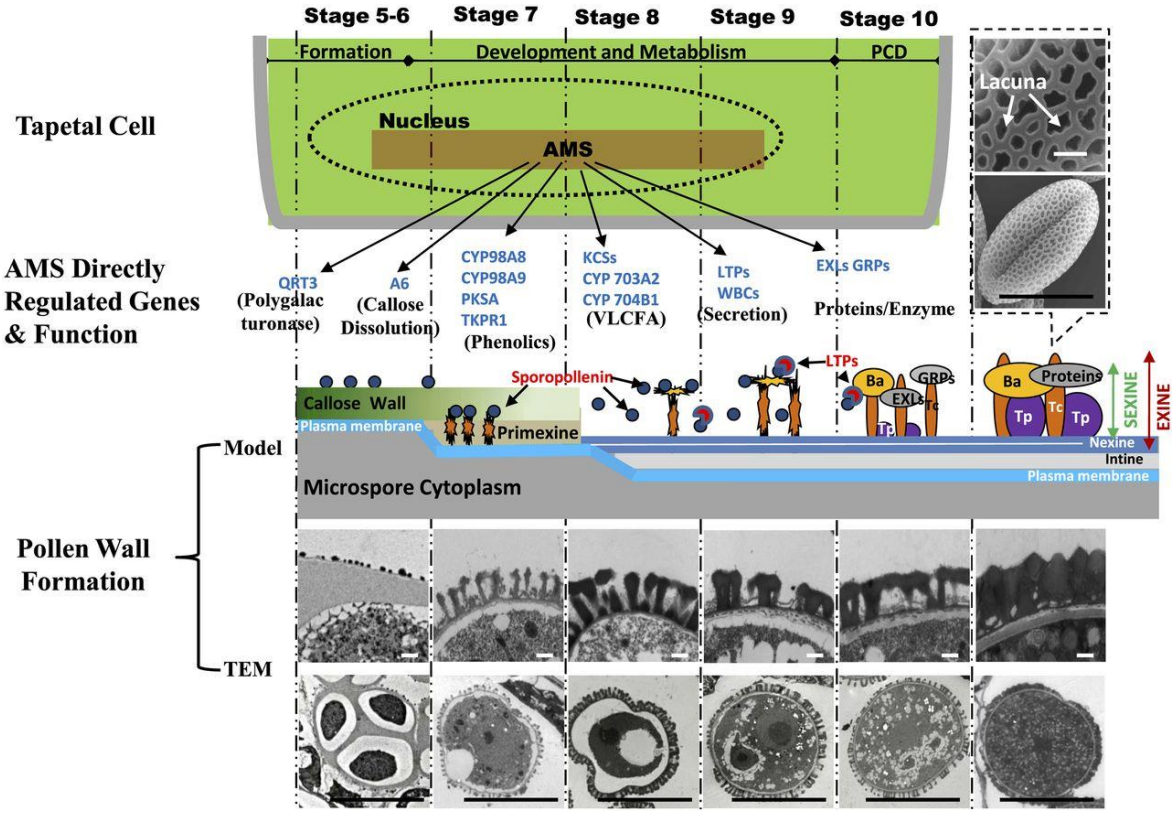

Figure 1.7. AMS is master regulator of pollen wall development, directly regulating genes involved in callose degeneration, fatty acid/ phenol synthesis, metabolism and secretion, and pollen exine development (Xu et al., 2014)

Xu *et al.* (2014) demonstrated that *cyp98a8 cyp98a9-RNAi, exl5* and *exl6* mutants all have microspores with abnormal exine layers and irregular bacula and tecta (Xu et al., 2014). Although exine structure of other mutants were not reported, previous work has shown that *wbc27* mutants have defective exine (Dou et al., 2011). The *exl4* mutant exhibits a delay in pollen hydration after contact with the stigma (Updegraff et al., 2009), and this phenotype is echoed in the *grp17* mutant – one of six closely related oleosin-proteins (Mayfield and Preuss, 2000; Mayfield et al., 2001), suggesting that these genes might also play an important (and perhaps redundant) role in AMS-mediated pollen coat formation.

CYP98A8 and CYP98A9 are partially redundant and function in spermidine biosynthesis (Matsuno et al., 2009). A BAHD acyltransferase involved in the same biosynthetic pathway- SPERMIDINE HYDROXYCINNAMOYL TRANSFERASE (SHT) was also reported to be downregulated in the *ams* mutant but a direct interaction was not shown. The *sht* knockout mutant has also been shown to have reduced spermidine derivatives and pollen coat irregularities (Grienenberger et al., 2009).

In some cases more than one key-regulator is required for activation of these downstream genes. The aforementioned CYP703A2 is activated by an AMS-MYB80 complex (Xiong et al., 2016). Transient dual-luciferase assays also imply that the AMS-MYB80 complex increases activation of CYP704B1 and TETRAKETIDE α-PYRONE REDUCTASE1 (TKPR1). The fatty acid reductase MS2 was also

found to be direct target of MYB80, however as expression was not fully restored in the pAMS:MS188 *ams* transgenic line (in which MYB80 is expressed normally but AMS is absent), it seems that full MS2 expression also requires both AMS and MYB80 (Wang et al., 2018). All of these genes are considered essential to synthesising the fatty acid components of sporopollenin for pollen wall formation: with *ms2, cyp704b1* and *tkpr1* mutant microspores all displaying a defective exine layer (Aarts et al., 1997; Dobritsa et al., 2009; Grienenberger et al., 2010).

1.2.4 Orthology in tapetum development

Despite vast differences in floral morphology between monocot and dicot species, rice and wheat anthers have a similar structure to *Arabidopsis* (Figure 1.1). Tapetum development in many crop species is also regulated by orthologous genes (Figure 1.8). In Rice, these transcription factors form an almost identical network. UNDEVELOPED TAPETUM 1 (UDT1), the homolog of *Arabidopsis* DYT1, is upstream of OsTDF1 (Jung et al., 2005; Cai et al., 2015). The bHLH transcription factors, TAPETUM INTERACTING PROTEIN 2 (TIP2) and ETERNAL TAPETUM 1 (EAT1) fulfil the role of AtbHLH089, -091 and -010. UDT1 regulates TIP2, which in turn activates expression of the AMS homolog TAPETUM DEGENERATION RETARDATION 1 (TDR1) and EAT1 (Fu et al., 2014; Ko et al., 2014). TDR1 directly regulates OsMS188 (Han et al., 2021) which is upstream of PERSISTENT TAPETAL CELL1 (PTC1), the MS1 homolog (Li et al., 2011; Pan et al., 2020).

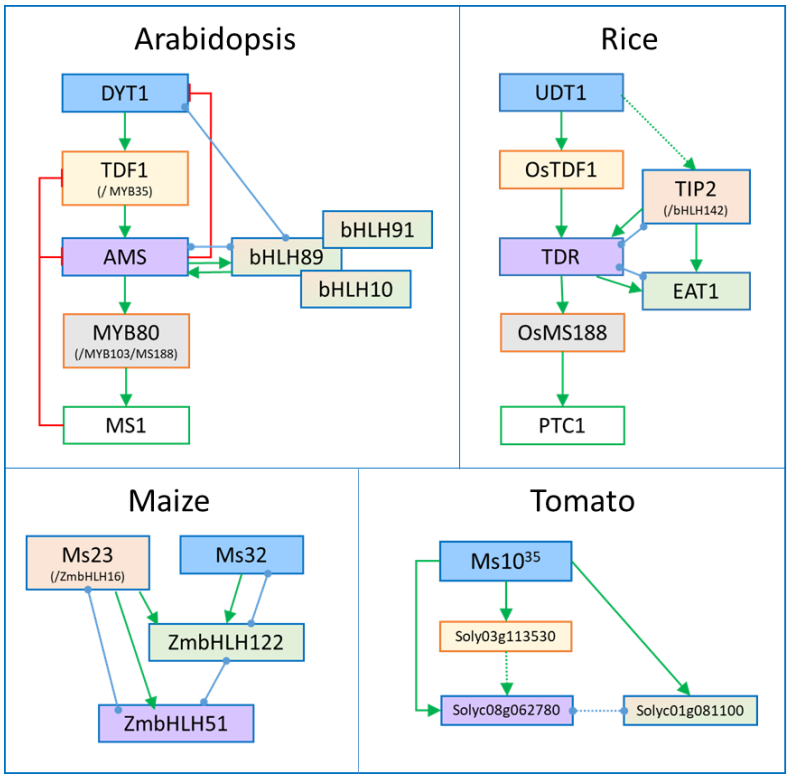

Figure 1.8. Tapetum development pathway in Arabidopsis thaliana (A) and orthologous pathways in Oryza sativa (B), Zea mays (C) and Solanum lycopersicum (D). Coloured fill represents homologous gene in each pathway and box outline colour relates to transcription factor type with blue for bHLHs, orange for MYBs and green for PHD proteins. Gene activation is shown by green arrows, protein interactions by blue lines and inhibition by red blunt ended arrows. Pathways modified from Ferguson et al., 2017; Cai et al., 2015; Nan et al., 2017; Jeong et al., 2014

Homologous bHLH transcription factors and pathways are further seen in other food crops such as Maize (Nan et al., 2017), Tomato (Jeong et al., 2014; Liu et al., 2019) and Pepper (Guo et al., 2018; Cheng et al., 2018). By understanding regulation of the pathways in *Arabidopsis*, findings can thus be extrapolated to a broad range of crops.

1.2.5 basic Helix Loop Helix transcription factors

The basic Helix Loop Helix (bHLH) transcription factors constitute one of the largest families in *Arabidopsis*, second only to the MYBs (Riechmann et al., 2000). The bHLH domain was first identified by Murre *et al.* (1989) and the first plant bHLH motif was recognised soon after: the maize Lc protein encoded by the R gene (Ludwig et al., 1989). Since then 167 *Arabidopsis* bHLHs have been identified and sorted into 32 sub-families based on their conserved protein motifs (Figure 1.10; Carretero-Paulet et al., 2010).

Five key basic Helix Loop Helix (bHLH) proteins function in the core *Arabidopsis* tapetum development pathway: DYT1, AMS and bHLH89, 91 and 10. bHLHs constitute the second largest family of transcription factors in Arabidopsis (Riechmann et al., 2000) and are characterised by a basic region at the amino (N)-terminus and a Helix Loop Helix region at the carboxyl (C)-terminus.

The HLH region functions as a dimerization domain (Murre et al., 1989; Ferré-D'Amaré et al., 1994) whilst the basic region consists of around 15 amino acids and is involved in DNA binding (Toledo-Ortiz et al., 2003; Atchley et al., 1999). bHLH proteins recognise and bind to a consensus DNA sequence motif called the E-box (Figure 1.9). This hexanucleotide, 5'-CANNTG-3', has many variants with altered binding-specificity determined by the two central bases. However the palindromic G-box, 5'-CACGTG-3', is the most common E-box variant (Toledo-Ortiz et al., 2003).

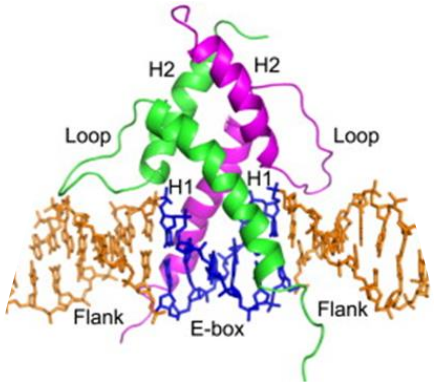

Figure 1.9. bHLH dimer binding to E-box motif (Gordân et al., 2013)

bHLH proteins can be divided into two major categories: DNA binding and non-DNA binding. Out of the 147 bHLHs identified by Toledo-Ortiz *et al.* (2003), 120 were predicted to bind DNA and only 109 were characterised as E-box binders. These each contain the Glu-13 & Arg-16 residues which are

vital to the E-box recognition motif and can be further divided into 89 G-box binders and 20 proteins which bind to E-boxes other than the G box. The 11 Non-E-box binding bHLHs contain unusual basic regions which lack the E-box binding residues, thus they are likely to lack specificity. In DNA binding bHLHs there are an average of 5.8 basic residues in the basic region. Non-DNA binding bHLHs are much less basic and are therefore often known simply as HLHs. These are believed to be negative regulators of bHLHs, as HLH-bHLH heterodimeric complexes can disrupt the formation of active bHLH-bHLH complexes, acting antagonistically by interfering with DNA binding.

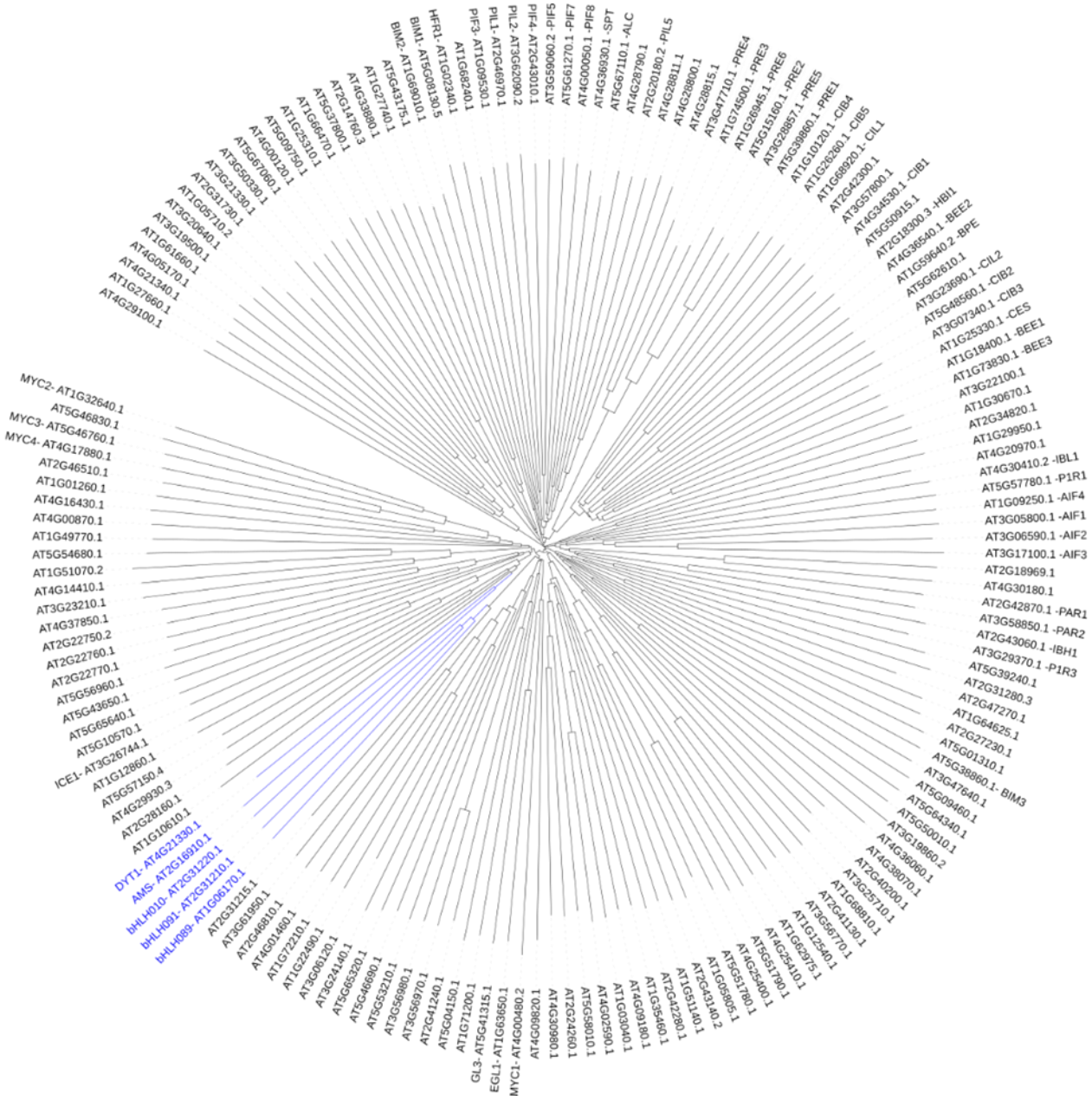

Figure 1.10. bHLH phylogeny as determined by CLUSTAL multiple sequence alignment of the 167 Arabidopsis bHLHs identified in Carretero-Paulet et al., 2010. Key identified bHLHs have been labelled and core bHLHs within the tapetum development pathway have been highlighted in blue.

1.2.5.1 bHLH010, -089 and -91 show high functional redundancy

bHLH010, -089 and -091 diversified from a common gene ancestor over two duplication events (Haberer, 2004; Zhu et al., 2015); each has three exons and a highly conserved protein structure (Appendix II), with 44-60% amino acid identity and 58-70% amino acid similarity. In particular, all three have a highly conserved C-terminus and the HLH domain of bHLH89 and -10 is remarkably similar. With such conservation, bHLH89, 91 and 10 sit in a distinct clade of the bHLH phylogenetic tree (Figure 1.10; Carretero-Paulet et al., 2010).

bHLH89, -91 and -10 are expressed in the anther from stage 6 onwards, with the same expression patterns (albeit at different levels of expression; Figure 1.11 A-E) and have been shown to play a redundant role in male reproductive development (Zhu et al., 2015). Whilst, *bhlh* single mutants are indistinguishable from wild type (WT), double and triple *bhlh* mutants exhibit increasingly defective anther development and decreased pollen viability, such that the *bhlh089 bhlh010* double mutant shows initial sterility that later recovers and the *bhlh089 bhlh010 amiR-bHLH091* is totally male sterile. Triple *bhlh* mutant anthers and the early anthers of the *bhlh089 bhlh010* double mutant showed abnormally large and disorganised tapetal cells with increased vacuolation at stage 6 and notably thinner callose walls which remain visible at stage 8, by which point they should have already degraded (Figure 1.6B). Tapetal cell size is uneven and the tapetum layer less organised than WT in *bhlh089 bhlh091* and late *bhlh089 bhlh010* anthers. Developing microspores in stage 11 WT anthers auto-fluoresces, due to phenols in the pollen exine (Roshchina, 2003), however there was no autofluorescence in stage 11 triple and early *bhlh010 bhlh089* mutant anthers (Zhu et al., 2015), which suggests that bHLH010, -089 and -010 contribute to exine deposition and thus pollen wall formation. But whilst *bHLH010*, *-089* & *-091* are expressed in the meiocytes, according to RNA *in situs*, chromosome spread experiments indicate that meiotic division is normal in all the mutants and thus these genes may not be essential to meiosis (Zhu et al., 2015).

Significant similarity in the promoter sequences of *bHLH010* and *bHLH091* has been reported (Haberer, 2004) but there are key differences in their cis-elements. *bHLH091* contains the fewest cis-elements in the 1000bp upstream of its coding DNA sequence (CDS) with just 88 compared to 109 in *bHLH010* and 112 in *bHLH089*. The upstream region of *bHLH091* has three W-boxes and two MYB2 elements (Zhu et al., 2015; Figure 1.12) Since *AtMYB2* is synthesised following the accumulation of the phytohormone abscisic acid (ABA) in response to abiotic stress and the WRKY-binding W-boxes are also implicated in ABA signalling (Shang et al., 2010; Shinozaki and Yamaguchi-Shinozaki, 2007), this could indicate a role for bHLH091 in stress response. Indeed much of this thesis will focus on the role of bHLHs in maintaining reproductive development in a low light environment and a recent study has also implicated bHLHs in heat-sensitive fertility (Fu et al., 2020).

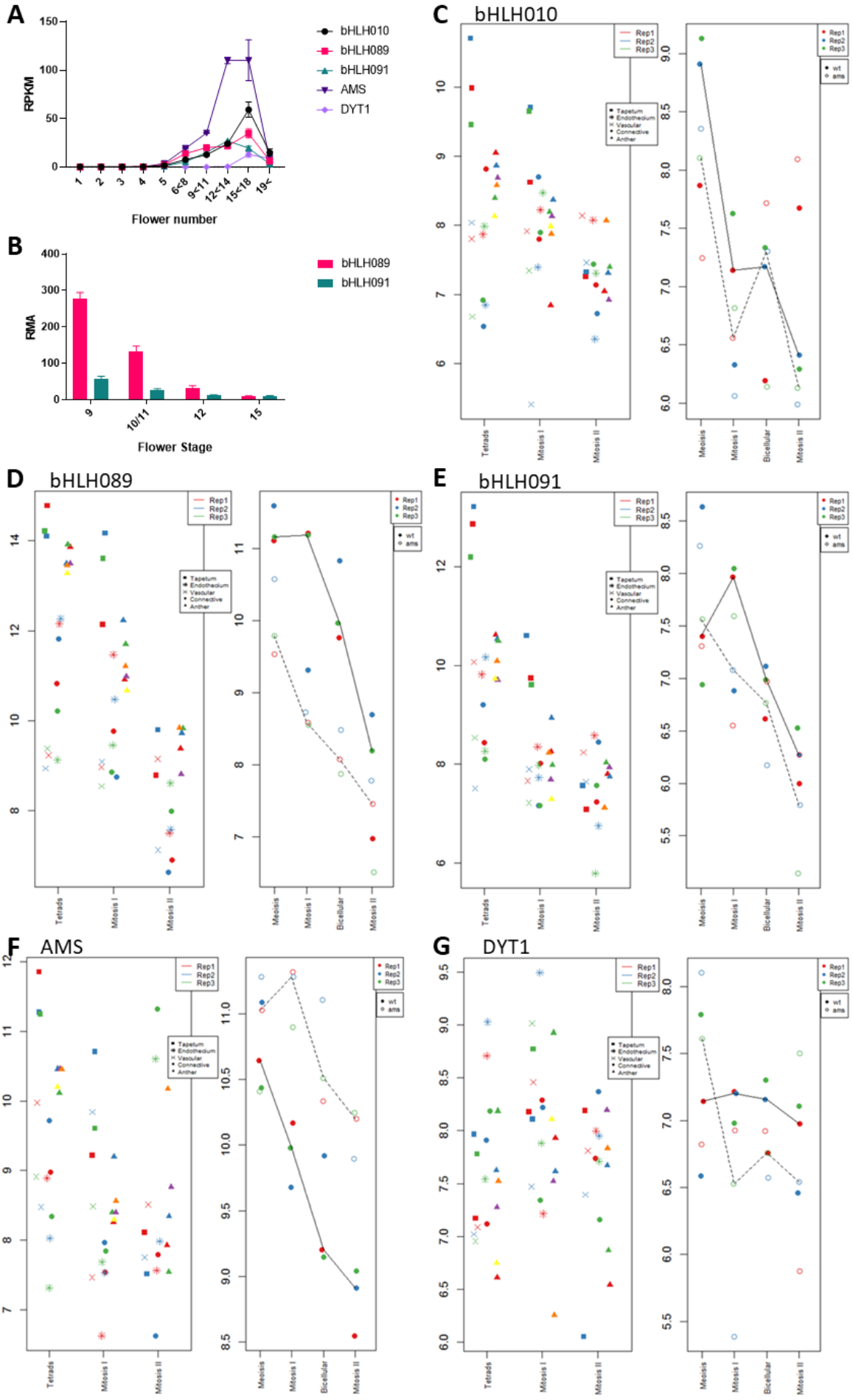
A
RPKM
Flower number
bHLH010
bHLH089
bHLH091
AMS
DYT1
B
RMA
Flower Stage
C bHLH010
D bHLH089
E bHLH091
F AMS
G DYT1
Rep1
Rep2
Rep3
Tapetum
Endothecium
Vasular
Connective
Anther
wt
ams
Tetrads
Mitosis I
Mitosis II
Meiosis
Bicellular

Figure 1.11 (previous page) Expression of core bHLHs in reproductive development. A) RPKM expression of bHLHs in inflorescences according to RNAseq atlas data (Klepikova et al., 2016). B) Developmental RMA expression data of bHLH089 and bHLH091 (Schmid et al., 2005). C-G) Tissue and stage-specific expression patterns of bHLHs with y-axis showing RMA expression (log2). Panel 1: Unpublished Laser Capture Microscopy (LCM) sectioning data showing expression of bHLHs in wild-type anther tissues: Tapetum (■), Vascular (x), Endothecium (*), Connective Tissues (●) and the whole Anther (▲) at different stages of development (Wilson group). Panel 2: Comparison of wild-type (●) and ams (○) mutant anther data from two-colour arrays across different stages of development, published in Xu et al (2010). For both panels each colour represents a single replicate.

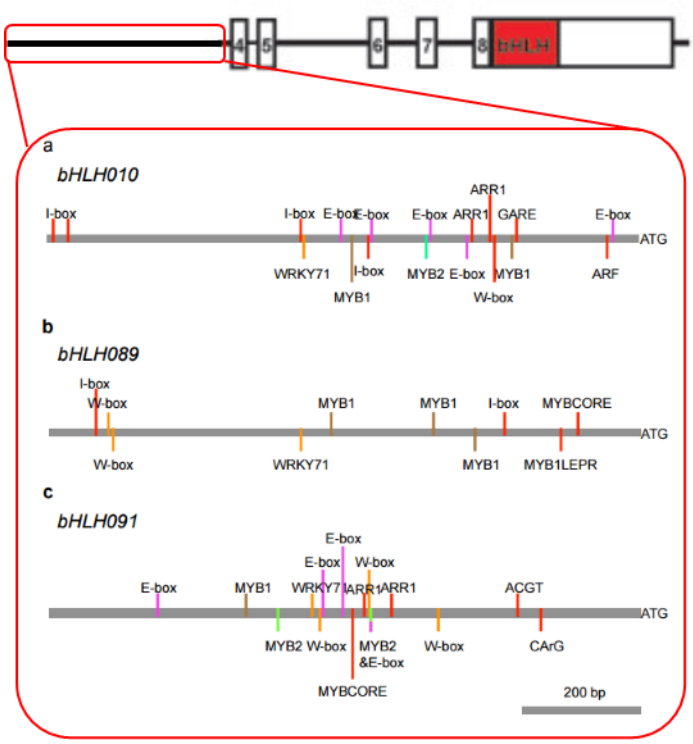

Figure 1.12 Conserved domains of bHLH010, -089 & -091 are represented by numbered white boxes. Highlighted promoter region shows cis-elements of a) bHLH010, b) bHLH089 and c) bHLH091. Adapted from Heim et al. (2003) and Zhu et al. (2015).

1.2.5.2 DYT1 interacts with bHLH89/91/10

DYSFUNCTIONAL TAPETUM1 (*DYT1*) is a bHLH transcription factor expressed in the tapetum at stages 5-6 and at a lower level in developing microspores. It is a central regulator of tapetum and pollen development, upstream of numerous transcription factors (Feng et al., 2012). The *dyt1* mutant has enlarged, heavily vacuolated tapetal cells and meiocytes are surrounded by an abnormally thin callose cell wall (Figure 1.6A, Zhang et al., 2006).

Studies have shown that DYT1 binds to the G-box of promoters (Feng et al., 2012) however previous work determined that *DYT1* regulates the expression of downstream genes primarily via *TDF1* which lacks a G-box in the promoter region, instead containing three E-box motifs (Gu et al., 2014). Therefore, in order to bind to the *TDF1* promoter it is likely then that DYT1 must form a complex with other bHLHs. The interaction of bHLH089, -091 and -010 proteins with DYT1 has been relatively well characterised, with binding determined by a Yeast 2 Hybrid (Y2H) assay and later confirmed *in*

planta via bimolecular fluorescence complementation (BiFC) assays in Tobacco (Zhu et al., 2015; Feng et al., 2012).

Transcriptomic and molecular analyses suggest that bHLH010, bHLH089 and bHLH091 proteins act downstream of DYT1 (Zhu et al., 2015); but despite this *DYT1* expression is increased in the *bhlh* triple mutant (Table 1.1) which suggests repression by an unknown negative feedback mechanism.

bHLH89, 91 and 10 increase DYT1 function through enhancement of the Nuclear Localisation Signal (NLS; Cui et al., 2016). A transient expression system was set up in tobacco with EYFP-tagged DYT1 expressed alone or in combination with each of the bHLH proteins. bHLH010, -089, & -091 were found to have a strong, specific NLS suggesting that DYT1, possessing a weak NLS, depends on a dimeric partner for strong nuclear localisation. A basal level of DYT1 in the nucleus may activate low-level expression of bHLH010, -089 and -091 which interact with DYT1 and facilitate nuclear localisation so that the bHLHs are increasingly expressed in a positive feedback loop. As such, DYT1 is localised to the nucleus in an anther stage-dependent manner: during stage 5 the DYT1 signal is localised to both the cytoplasm and the nucleus but from stage 6 onwards, when bHLHs 89, 91 and 10 are expressed, DYT1 is more strongly localised to the nucleus (Cui et al., 2016).

The findings of Cui *et al.* (2016) suggest that, although bHLH89, 91 and 10 are functionally redundant, different DYT1-bHLH combinations show differential transcriptional activation. The DYT1-bHLH089 heterodimer, for example, binds to the MYB35 promoter and highly activates expression, whereas DYT1 or bHLH089 alone does not. Thus different combinations of bHLH010/089/091 in complex with DYT1 may have distinct functions in regulating downstream genes.

RNAseq data of stage 4-7 anthers showed that 1114 genes were differentially expressed in the bHLH triple mutant compared to WT, of these 975 were down-regulated and 139 up-regulated (Zhu et al., 2015). Genes related to regulation of transcript, transport, development, stress and minor carbohydrate metabolism were significantly enriched in the down-regulated group, indicating bHLH89, 91 and 10 mediated positive regulation of these processes. Zhu *et al.* (2015) compared the *bhlh* triple mutant transcriptome to previous RNAseq from the *dyt1* mutant (Feng et al., 2012) and found that *bHLH010*, *bHLH089*, *bHLH091* and *DYT1* regulate both overlapping and discrete sets of genes, thus the bHLH proteins can also function independently to DYT1.

1.2.5.3 AMS and bHLH interactions

ABORTED MICROSPORES (*AMS*) is in the MYC sub-family of bHLH transcription factors that resides on chromosome II. Disruption of the gene causes premature tapetal degeneration and abortion of microspores. The *ams* mutant has an abnormally large, vacuolated tapetum (Figure 1.6A) which contributes to a failure in post-meiotic pollen development, and subsequent formation of viable pollen, resulting in undeveloped siliques devoid of seed. Filaments of *ams* mutant flowers are also shorter, containing on average two cells less than WT. Aside from this, the gross morphology of the *ams* mutant is indistinguishable from WT (Sorensen et al., 2003).

AMS plays a dual role in early and late pollen development with two peaks in AMS protein levels: during pollen meiosis at anther stages 6-7 and again during mitosis I at stage 10. However qRT-PCR indicates that *AMS* expression levels reach just one prolonged peak (Ferguson et al., 2017). Since AMS protein levels inversely correlate to expression of the downstream MS1 protein, Ferguson *et al.* hypothesised that MS1 promotes AMS protein degradation in a negative feedback loop.

AMS is known to interact with bHLH089 and bHLH091 from Y2H and Glutathione S-transferase (GST) pulldown assays (Xu et al., 2010). However the interaction of the bHLHs with AMS has not been characterised as fully as with DYT1 and there has been nothing published in relation to an interaction with bHLH010.

Models by Ferguson *et al.* (2017) suggest that due to competitive binding, bHLH089 & bHLH091 may associate earlier with DYT1 than AMS causing a delay in the production of AMS-regulated genes such as MYB80 and MS1 until DYT1 levels are lower and the bHLHs are free to associate with AMS. Although this competitive behaviour fits with the mathematical modelling it has not been tested *in situ*.

According to microarray data, *bHLH089* is downregulated in *ams* meiosis-stage buds (Xu et al., 2010), however it seems that *bHLH91* and *bHLH10* expression is unaffected (Figure 1.11 C-E). That said, bHLH89, -91 and -10 are all upregulated 8 hours after AMS is induced by dexamethasone (DEX) treatment in an *ams* background (Ferguson et al., 2017). This suggests that, as well as interacting on a protein level, AMS may enhance the transcription of *bHLH089, -091* and *-010*.

1.3 THESIS AIMS

This thesis aims to further characterise the role of bHLH89, 91 and 10 transcription factors in *Arabidopsis thaliana* male reproductive development in an effort to elucidate their role in an environmental context.

One of the key aims of this thesis was to understand how the fertility of *bhlh* double mutants is affected in response to decreased light availability, focussing on changes to tapetum and pollen development through scanning electron, confocal and brightfield microscopy (Chapter 3).

This thesis further aims to investigate the transcriptomic changes underlying this conditionally sterile phenotype (Chapter 4) and highlight light-responsive genes and pathways that are influenced by bHLH89 and -91 by RNAseq analysis of the *bhlh89,91* double mutant in response to low light.

Another objective is to explore a potential role for bHLH89/91/10 in regulating Gibberellin (GA) responses through interactions with DELLA proteins, by *in vivo* interaction assays and GA profiling (Chapter 5).

Finally, this thesis aims to assess possible post-translational regulation of bHLH proteins by Small Ubiquitin-like Modifications (SUMO, Chapter 6) to develop a proposed new model for the integration of environmental signals into tapetum development.

2 MATERIALS & METHOD

2.1 PLANT MATERIALS & GROWTH CONDITIONS

T-DNA insertion lines were obtained from SALK and GABI-KAT collections at the Nottingham Arabidopsis Stock Centre. Lines used in this study were GK-055H02 for *bhlh010,* SALK-123106 for *bhlh089* and GK-345C08 for *bhlh091.* These lines were crossed to produce the double mutants *bhlh089 bhlh010* and *bhlh089 bhlh091.* The triple mutant line *bhlh089 bhlh010 amiR-bHLH091* was obtained from Zhu *et al.* (2015).

Arabidopsis thaliana Columbia (Col-0) ecotype and mutants were sown into pots containing a 3:1 mix of Levington M3 compost: Vermiculite with T34 biological control. All plants were grown at 22°C in 16h days under fluorescent lighting, with a 3:3:1 ratio of red:green:blue light (Figure 2.1), and watered at 2-3 day intervals with weekly applications of Hypoline™ (Bioline AgroSciences) to prevent scarid larval infestation. At the onset of flowering, just before bolting, low light and/or hormone treatments were commenced as appropriate. In normal light conditions, plants were illuminated with a Photosynthetic Photon Flux Density (PPFD) of 205(± 8.6 SD) µmol/m^2/s, while the low light plants received 53 (± 5) µmol/m^2/s PPFD through use of net shading. Light availability and spectra was recorded by a Li-180 Spectrometer (Licor) at plant base (rosette level; Figure 2.1, Figure 2.2). Trays were rotated every week to minimise localised environmental effects.

2.1.1 Hormone Treatments

Plants were grown until bolting as in Section 2 at which point they were sprayed every 2-3 days with either a control solution of 0.5% (v/v) EtOH and 0.1% (v/v) Tween-20 or test solutions of 1, 5, 10, 25 or 50µM Paclobutrazol (PAC) or GA_3 (in 0.5% EtOH and 0.1% Tween-20).

2.1.2 Arabidopsis seedling growth on Agar plates

Arabidopsis seedlings were sterilised with 50% (v/v) bleach and then washed in 0.05% Triton 5 times before plating onto ½ MS media (2.2 g/L Murashige and Skoog media, Sigma) with 6g/L Sucrose and 1% Bacto-Agar (10 g/L) at a pH of 5.8. Seeds were stratified 4°C for 2 days before transferring to growth cabinets (Conviron) at 23°C for 16h photoperiod at 100 µmol/m^2/s.

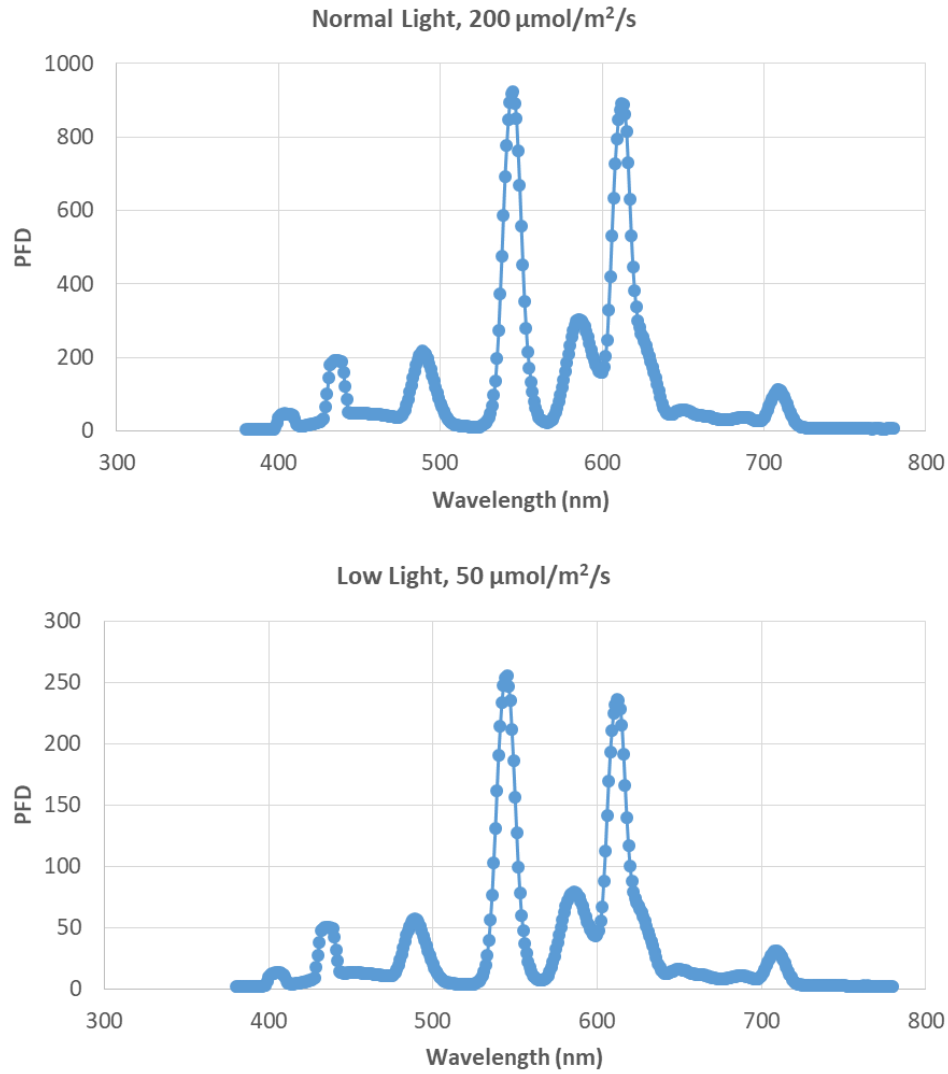

Figure 2.1. Spectra of normal and low light treatments with Photon Flux Density (PFD) plotted against wavelength, shows that spectra is not changed between light treatments aside from intensity.

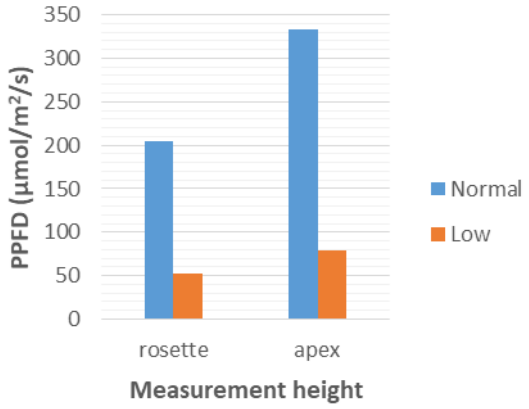

Figure 2.2. Light availability measured at different growth stages of plant / height in Normal and Low light conditions.

2.1.3 Accession numbers

AMS (AT2G16910), bHLH010 (AT2G31220), bHLH089 (AT1G06170), bHLH091 (AT2G31210), DYT1 (AT4G21330), GAI (AT1G14920), MS1 (AT5G22260), MS2 (AT3G11980), MYB80 (AT5G56110), MYB33 (AT5G06100), MYB65 (AT3G11440), RGA (AT2G01570), RGL1 (AT1G66350), RGL2 (AT3G03450), RGL3 (AT5G17490), TDF1 (AT3G28470)

2.1.4 Genotyping *Arabidopsis* T-DNA lines

DNA was extracted from crushed young leaf tissue using a extraction buffer (50mM Tris-Cl pH 7.5, 300mM NaCl, 300mM Sucrose). Extracted genomic (g)DNA was heated to 99°C for 10 min, returned to 4°C and then 1µl was added to a REDTaq® Polymerase Chain Reaction (PCR) mix (Table 2.1) using SALK/GK specific primers (Table 2.2) and amplified using a Veriti™ 96-Well Thermal Cycler (Applied Biosystems).

Table 2.1 RedTaq PCR reaction components and thermocycler settings, Annealing temperature (*) and extension time dependant on primers used.

Component	Volume (µl)
REDTaq® ReadyMix™ PCR Reaction Mix (Sigma-Aldrich)	5
Forward primer	0.25
Reverse primer	0.25
Template (1µl gDNA/ 0.1µl plasmid)	1/ 0.1
H_2O	to 10µl
Temperature (°C)	**Time (min)**
94	3
94	0.5
*	0.5
72	1/kb
72	4

Table 2.2. Primers for bhlh mutant genotyping

Primer	Sequence	Gene
GK_055H02F	TTTGATTCACCAAATGGCTTC	bHLH010
GK_055H02R	ACCTGCAACATGGTGAAGATC	bHLH010
Salk _123106R	CCATCTTTCTTAGCCCTTTGG	bHLH089
Salk_123106F	CAAGAAACTGTGGTGCTCTCC	bHLH089
GK-345C06-LP	TTGGGAAGAGAAGCCATGTAG	bHLH091
GK-345C06-RP	TGGGGTGTTTCTGAAGACAAC	bHLH091
Lbb1.3	ATTTTGCCGATTTCGGAAC	SALK
o8474	ATAATAACGCTGCGGACATCTACATTTT	GK

2.2 Expression Analysis

2.2.1 Staging and RNA extraction

Staged samples were separated into early (pre-mitosis I, up to and including single microspore stage) and later (post-mitosis I) stages by bud size. DAPI staining was used to confirm that bud sizing was consistent at different stages in the different lines and light treatments. Single microspore stage buds, which marked the early-late stage threshold, were consistent in size at ~1mm in all conditions and lines. RNA was extracted using an RNeasy Kit (Qiagen) from both whole and staged inflorescences

2.2.2 RNASeq

RNA was isolated from early-stage buds as in Section 2.2.1 from 4 factor groups (*bhlh089 bhlh091* Low, *bhlh089 bhlh091* Norm, Col-0 Low, Col-0 Norm), each with 4 biological replicates (16 samples in total) and was sequenced using the BGISEQ-500 platform (BGI).

Total RNA Sample QC was checked using an Agilent 2100 Bio analyser and then the library was constructed (Figure 2.3). First, Poly-A containing mRNA molecules were purified using poly-T oligo-attached magnetic beads. The purified mRNA was then fragmented into small pieces using divalent cations under elevated temperature. Cleaved RNA fragments were copied into first strand cDNA using reverse transcriptase and random primers, followed by second strand cDNA synthesis using DNA polymerase I and RNase H. A single 'A' base was then added to the cDNA fragments and subsequently ligated to an adapter, purified and enriched with PCR amplification. PCR yield was quantified by Qubit and samples were pooled together to make a single strand DNA circle (ssDNA circle), which make up the final library. DNA nanoballs (DNBs) were generated with the ssDNA circle by rolling circle replication (RCR) to enlarge the fluorescent signals at the sequencing process. The DNBs were loaded into the patterned nanoarrays and pair-end reads of 100 bp were read through on the BGISEQ-500 platform, which combines DNA nanoball-based nanoarrays and stepwise sequencing using Combinational Probe-Anchor Synthesis Sequencing Method.

BGI's internal software SOAPnuke v1.5.2 (available at https://github.com/BGI-flexlab/SOAPnuke) was used to filter reads by removal of reads with adaptors, unknown bases more than 1% and low quality reads (percentage of base which quality is lesser than 15 is greater than 40% in a read).

Clean reads were mapped to Arabidopsis Thaliana Reference Transcript Dataset 2 (AtRTD2; Zhang *et al.*, 2017) using the Salmon tool on UseGalaxy.eu (Patro et al., 2017). The 3D-RNASeq app was then used for differential expression (DE), differential alternative splicing (DAS) gene and differential transcript usage (DTU) analysis (Guo et al., 2019; Calixto et al., 2018).

Read counts and transcript per million reads (TPMs) were generated using tximport R package version 1.10.0 and length Scaled TPM method (Soneson et al., 2016). Low expressed transcripts and genes were filtered based on analysis of the data mean-variance trend, with an optimal filter of low expression set at ≥ 1 of the 16 samples with a count per million reads (CPM) ≥ 1 (Figure 2.4). The TMM method was then used to normalise gene and transcript read counts to $\log_2$-CPM (Bullard et al., 2010). Batch effects were checked for using a principal component analysis (PCA) plot and showed the RNASeq dataset did not have distinct batch effects.

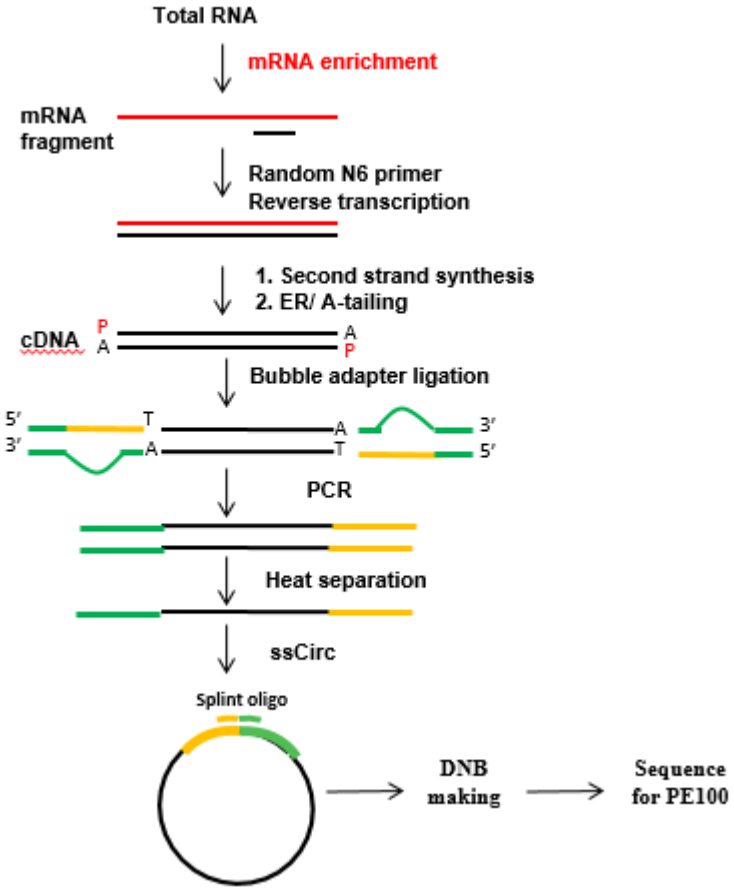

Figure 2.3. Library construction for BGISEQ-500 platform.

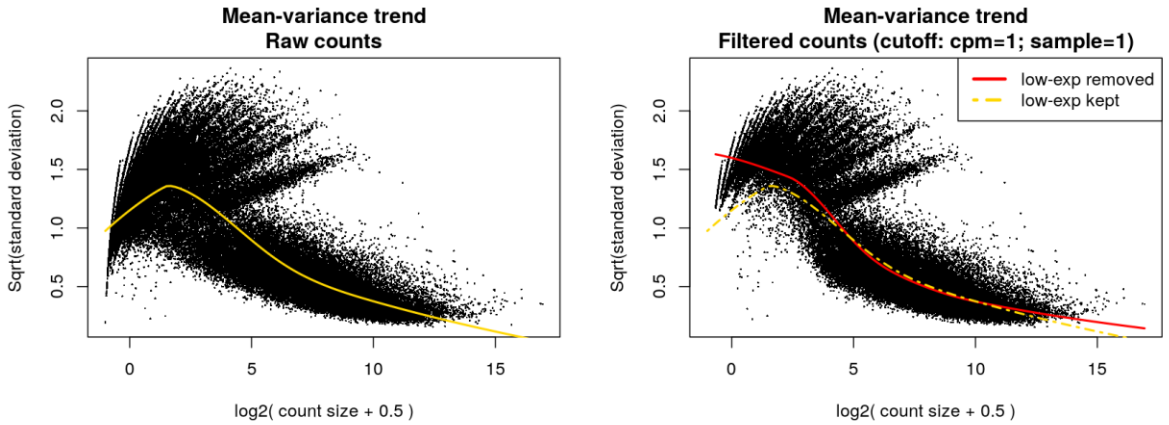

Figure 2.4 Filtered read counts based on mean-variance trend, filtering low expression with a cut-off of more than 1 of the 16 samples with a count per million (CPM) reads of more than 1.

The Limma R package was used for 3D expression comparison of contrast groups (Ritchie et al., 2015; Law et al., 2014). For DE genes/transcripts, the $\log_2$ fold change ($\log_2$FC) of gene/transcript abundance were calculated based on contrast groups and significance of expression changes were determined using t-test. P-values of multiple testing were adjusted by the Benjamini-Hochberg method to correct false discovery rate (FDR) (Benjamini and Yekutieli, 2001). A gene/transcript was significantly DE in a contrast group if it had an FDR adjusted p-value (q) < 0.01 and $\log_2$FC ≥ 1.

At the alternative splicing level, DTU transcripts were determined by comparing the $\log_2$FC of a transcript to the weighted average of $\log_2$FCs, with weights based on standard deviation, of all remaining transcripts in the same gene. A transcript was determined as significant DTU if q < 0.01 and Δ Percent Spliced (ΔPS) ratio ≥ 0.1. For DAS genes, each individual transcript $\log_2$FC were compared to gene level $\log_2$FC, which was calculated as the weighted average of $\log_2$FC of all transcripts of the gene. Then p-values of individual transcript comparison were summarised to a single gene level p-value with F-test. A gene was significantly DAS in a contrast group if it had a q < 0.01 and any of its transcript had ΔPS ratio ≥ 0.1.

Hierarchical clustering was used to partition the DE genes into 10 clusters based on euclidean distance and ward.D clustering algorithm and heatmaps were generated using ComplexHeatmap R package version 1.20.0 (Gu et al., 2016).

KEGG pathway enrichment analysis was performed using the online Database for Annotation, Visualization and Integrated Discovery (DAVID) v6.8 (https://david.ncifcrf.gov/home.jsp, accessed 2020) (Huang et al., 2009a, 2009b). Mapping of expression changes to KEGG pathways was carried out with Pathview in R (Luo and Brouwer, 2013).

2.2.3 qRT-PCR

1µg cDNA was synthesised from 1µg RNA using SuperScript III Reverse Transcriptase (ThermoFisher) and tested for gDNA contamination alongside minus-RT samples by RT-PCR using PP2A3 primers (Table 2.3).

qRT-PCR was performed in a LightCycler 480 (Roche Life Science) with primers listed in Table 2.3. To calculate Relative Gene Expression (E), Ct values were adjusted according to previously calculated primer efficiencies (x) and then normalised to the housekeeping gene PP2A3 (H) using the equation $E = 100x^{H-Ct}$.

Due to low sample sizes (2-4 biological replicates) data normality could not be assessed thus a non-parametric Kruskall-Wallis rank sum test was performed to assess variance between groups and post-hoc Dunn tests were then carried out.

Table 2.3. qPCR primers

Primer	Sequence	Gene
PP2A3_1355F	CGTGACCCCTCCAAGCTGCA	PP2A3
PP2A3_1677R	CACCAAGCATGGCCGTATCA	
bHLH10_957F	TGGTGAAGGAGGAGGAGGAGAA	bHLH010
bHLH10_1246R	CACCAATCTGTCCACCTGCAAC	
1g06170_1118R	TGGTGCTCTCCGATTTGTGC	bHLH089
1g06170_929F	CCTTGAGATGCTCATGGCTCA	
2g31210_1144R	CTCCGGCAACATGGTGAAGA	bHLH091
2g31210_927F	GAAGAAGCCGGAGAGCGATG	
DBAMS3R	GTTCTCTTCAAGCTCGTCTTGAAGCTCC	AMS
DBAMS4F	CACCAAAGGATCTCAAGCCAAGAACCTG	
4g21330_DYT_1F	ATGGGTGGAGGAAGCAGATTTC	DYT1
4g21330_DYT_406R	CCCCAATCTTACACAATTGCACA	
TDF1_F	CGGACCCGGTTCCTCAAGTA	TDF1
TDF1_R	ACGAAGGAACTCGCGGAATG	
MS1_a_F	CGAACAGACCATCAGCAACA	MS1
MS1_a_R	CCGAACGTCTTCAGCCTAA	
MS2_qPCR_F	ATCGAGCGGCTAAAGAACG	MS2
MS2_qPCR_R	TGAAAGACATGTAAGATGCTCCA	
MYB33_qPCR_F	TGGGTAATAGATGGGCACGTA	MYB33
MYB33_qPCR_R	CTCGTTGTCGCCTCTTGATAC	
MYB65_qPCR_F	TGGGAAATAAATGGGCACAG	MYB65
MYB65_R	AGATGGGAAATAAATGGGCAC	
MYB80_455F	CCCTCGGCTGTTTCAAGGACGA	MYB80
MYB80_742R	CGTGACCCCTCCAAGCTGCA	
RGA-qPCR_R	TAGATCCGCCGCGCTAAAG	RGA
RGAseqF	CAAATCGGATGCTTAGCTGTGTC	
GAI_qPCR_F	TGAAATGCTCAAACGGCGTC	GAI

GAI_qPCR_R	GTTCTCCTGCGAGTCAACCA	
RGL1_qPCR_F	CGTTTAGTCCACGCGCTATT	RGL1
RGL1_qPCR_R	AGTAACCCCACGTGCTTCAC	
RGL2_qPCR_F	AATTCCGGGTCTTTCTGCGT	RGL2
RGL2_qPCR_R	GAGAGTCAACGAGCACCAC	
ATA1_g761_F	GGAGTTTGCTGACCGGAAGA	ATA1
ATA1_g848_R	TGAACCCCGACGATTCTTGG	
ABCG26_g88_F	TCATGCCACAAGCTTACCTCA	ABCG26
ABCG26_g194_R	AGAAAGATGGGAAGAGGGGC	
RGP3_g1283_F	TGGAATGGTCACCTGGATCG	RGP3
RGP3_g1363_R	TTTTGCCTTTTGGTGCCTCAG	
GLP8_g656_F	TTTCGATAGCCAGCTTCCCG	GLP8
GLP8_g778_R	TCTTCTGAATCTCTGGTGCTGC	
RBOHE_g2311_F	AGACCTCGTCATGTGGTTCAA	RBOHE
RBOHE_g2389_R	AACCCAGCTTCTTTGCCAGT	
NPF41_g862_F	CAGCAGGGAGTCCTTTGACC	NPF4.1
NPF41_g955_R	GTGTCACCACCTCTGCATCC	
GID1A_g1298_F	GCGATTGGTACTGGAAAGCG	GID1A
GID1A_g1337_R	CCTCTCGGGCTAAACGGATT	
GID1B_g294_F	TTACAAAGTCCTCCGTCGCC	GID1B
GID1B_g388_R	GTCGAGGGGGAAAGAGTTGG	
GID1C_g545_F	GCTTACAATCTCCTGCGTCG	GID1C
GID1C_g626_R	ATTTGCAGGGACTTTCCGGT	
CYP703A2_a_F	TCCCTCTTCGCTGTTCTCAT	CYP703A2
CYP703A2_a_R	TAGGCAATCTTGGTGGACCT	
AT1G02813_qPCR_F	CTTCTGTATCCGTCTCCGGC	AT1G02813
AT1G02813_qPCR_R	ACGTGGTGTTGAAACGGACT	
AT1G47980_qPCR_F	CAGTTTGCTTGGCAAGAGGT	AT1G47980
AT1G47980_qPCR_R	AAATCAAGTTGTGGCCTTGC	
AT1G76470_qPCR_F	TGTTACGCTCTGTCCGTCTG	AT1G76470
AT1G76470_qPCR_R	ACACCAACAAAAGCGCATCC	
AT4G26830_qPCR_F	CCTTCCTCTCAGCCATTGAC	AT4G26830
AT4G26830_qPCR_R	GGCGACGGGAGATTGTTAG	
AT5G16920_qPCR_F	TGCCCTAGCAGTCACAACAA	AT5G16920
AT5G16920_qPCR_R	TTGGCTGGCTAATCGGACTG	

2.2.4 Analysis of published Microarray datasets

bhlh089 bhlh010 amiR-bHLH091 RNASeq datasets SRS838170 and SRS838173 (Zhu *et al*., 2015) were obtained from NCBI Sequence Read Archive. Gene expression levels were calculated in TPM (Soneson et al., 2016), and the Limma R package was used to calculate $\log_2$FC and FDR (q) values (Ritchie et al., 2015). Genes were classed as differentially expressed if they had a $\log_2$FC≥1, q≤0.05. This RNASeq data was compared against previous *ams* microarray data (Lou et al., 2017) using VENNY (https://bioinfogp.cnb.csic.es/tools/venny/, accessed 2018, Oliveros, 2007). Gene Ontology

(GO) enrichment analysis was performed using PANTHER Overrepresentation Test (http://pantherdb.org/, accessed 2018, Mi *et al.*, 2017).

2.3 CLONING

2.3.1 Translational Fusions

bHLH genes lacking a stop codon and driven by various sized native promoters were amplified from genomic DNA by Phusion™ high fidelity DNA polymerase (Thermo Fisher Scientific). The CDS and a 1kb and 1.9kb upstream region of bHLH089 was amplified by PCR using the bHLH89CDS-nostop_R primer paired with bHLH89pro-1080_F and bHLH89pro-1933_F respectively, and the bHLH091 CDS including a 1.7kb upstream region was amplified using bHLH91pro-1706_F with bHLH91CDS-nostop_R (Table 2.4). PCR products were then purified using GenElute™ PCR Clean-Up Kit (Sigma-Aldrich).

Purified PCR products were inserted into pcr8 entry vectors by TOPO™ TA Cloning™ (Invitrogen) and subsequently transformed into One Shot™ TOP10 chemically competent *E. coli* cells. These entry constructs were then cloned into LR compatible destination vectors with fluorescent tags, as in Table 2.5, using Gateway™ LR Clonase™ II (Invitrogen) and transformed in dh5α *E. coli* cells.

Positive colonies were screened by colony PCR (see Section 2.3.1) with construct specific ROligo_New_CompR and gene specific bHLH89gDNA1211_F / bHLH91gDNA774_F primers (Table 2.4). They were confirmed by sequencing (Source Bioscience) before transformation into GV3101 Agrobacteria through electroporation. Col-0 *Arabidopsis thaliana* was transformed via the Floral Dip method (Clough and Bent, 1998). T1 seed were either sown onto plates as in Section 2.1.2, with 25mg/L Hygromycin-B, or sown onto soil and seedlings sprayed with 120 mg/L BASTA 2-3 times from emergence every 8-10 days.

2.3.2 Transcriptional Fusions

Native bHLH091 and bHLH010 promoters were amplified from genomic DNA by Phusion™ high fidelity PCR (Thermo Fisher Scientific) using bHLH10pro-1997_F & bHLH10pro-0_R and bHLH91pro-1706_F & bHLH91pro-0_R primers (Table 2.4). As in Section 2.3.1, PCR products were purified then cloned into entry vectors by TOPO™ TA cloning and subsequently into pGWB3 constructs through Gateway™ Cloning (Table 2.5). Constructs were checked by colony PCR, sequenced and transformed into Agrobacteria for floral dipping as in the previous section.

Table 2.4. Primers used to generate and screen constructs

Primer	Sequence	Loci
bHLH10pro-1997_F	TGGGGACAGTCGCAGT	AT2G31220
bHLH10pro-0_R	GGAAATGGTTCAACGAGTACTC	AT2G31220
bHLH89pro-1080_F	ATTTTTCCAAAAGACAATGCGAAAA	AT1G06170
bHLH89pro-1933_F	TGATGAATCCTCTCGTCAATAAGA	AT1G06170
bHLH89CDS-nostop_R	ATCACTAGAGTAACAGTGATAACCA	AT1G06170
bHLH89pro-446_R	TTGTGGTCTAACGGGGAACA	AT1G06170
bHLH89g48_F	TGCTCCGGCAGAAATGAC	AT1G06170
bHLH89-gDNA1211_F	TGTTCAACGCCAAGGTTTGT	AT1G06170
bHLH91pro-1706_F	GAGCAAGCAAGATTGCTATGTCTATTC	AT2G31210
bHLH91pro-0_R	TTTCAACTGATTTTTTTCTGCAACCAA	AT2G31210
bHLH91CDS-nostop_R	ATAGTTACTGTTGGGAAGAGAAGCCA	AT2G31210
bHLH91pro-1004_R	CTTTTGGCCACAACGGCAAT	AT2G31210
bHLH91-gDNA774_F	ATCTCCAATGGCACTTTGCT	AT2G31210
bHLH91pro-69_F	GGCTTTTGTCTTAAAGATTAATTATGGTTGTG	AT2G31210
ROligo_New_CompF	GTTTTCCCAGTCACGACGTT	construct
ROligo_New_CompR	GAGCTGCCAGGAAACAGCTA	construct
GFP_PGWB5_R	AAGTCGTGCTGCTTCATGTG	GFP
EGFPR	CTTGTACAGCTCGTCCATGCC	GFP
pK7colF1	TTTTGCGGACTCTAGCATGG	construct
UBQ10_F1	CGAAGACGATTTTCTGGGTTT	UBQ10
LUC5Rv	CCATCTTCCAGCGGATAGAATG	LUC
VENUS-R2	CACATGAAGCAGCACGACTT	YFP
EGFPR	CTTGTACAGCTCGTCCATGCC	GFP
RFP R2	GAGCCGTACTGGAACTGAGG	RFP
GUSpGWB3_138R	AGCAATTGCCCGGCTTTCTT	GUS
GUSpGWB3_20F	CCCCAACCCGTGAAATCAAA	GUS
Luc_R	GCTGCGAAATGCCCATACTG	LUC
Luc_F	AGAGATACGCCCTGGTTCCT	LUC
MS2pro-2218_F	AGGGAAACCTGCGATTCACAAG	AT3G11980
MS2pro-0_R	CACAAGCTATAAGAAATAAGAAATAGAGGAAGGG	AT3G11980
GAI_CDS_no_stop_R3	ATTGGTGGAGAGTTTCCAAG	AT1G14920
GAI_1525_F	GTGACGGCTGTCTCATGTTG	AT1G14920
RGL2_cds_F	ATGAAGAGAGGATACGGAGAAACATG	AT3G03450
RGL2_nstp_R	GGCGAGTTTCCACGCC	AT3G03450
RGL3_cds_F	ATGAAACGAAGCCATCAAGAAACGT	AT5G17490
RGL3_nstp_R	CCGCCGCAACTCCGC	AT5G17490
MYB33_CDS_F	ATGAGTTACACGAGCACTGACA	AT5G06100
MYB33_nstp_R	GGGTAGTTCTGTCATTTGACAGAC	AT5G06100
RGL2_1600_F	AGACGCGACCACTCATCAC	AT3G03450
RGL3_1510_F	GGCAAACGAAACCTCTAATCG	AT5G17490
nYFP_R	AAGTCGTGCTGCTTCATGTG	nYFP
cYFP_R	GAACTCCAGCAGGACCATGT	cYFP

2.3.3 Transient expression constructs

bHLH10/89/91, AMS, DYT1, MYB33/65, GAI, RGL2/3 transcription factor CDSs were amplified by Phusion™ high fidelity DNA polymerase, using gene specific primers (Table 2.4). As in Section 2.3.1, PCR products were purified and transferred into entry vectors by TOPO-TA cloning and then into pUBC-YFP/ pUBC-cYFP/ pUBC-nYFP destination vectors via a Gateway LR reaction. Likewise, the MS2 promoter was cloned into pGREENII-0800-LUCGW (Table 2.5).

Table 2.5. Reporter & Transient Expression constructs, detailing promoter type or size of native promoter (kb), presence of CDS, marker protein and construct purpose.

Gene	Promoter (/kb native)	CDS	Marker	Construct	Purpose
bHLH091	1.7	✓	mCerulean	pGHGWC-bHLH091	Reporter
	1.7	✓	mVenus	pGBGWY-bHLH091	Reporter
	1.7	x	GUS	pGWB3-bHLH091	Reporter
	UBQ10	✓	YFP	pUBC-bHLH091-YFP	DLRA, IP
	UBQ10	✓	cYFP	pUBC-bHLH091-cYFP	BiFC
	UBQ10	✓	nYFP	pUBC-bHLH091-nYFP	BiFC
bHLH089	1.1	✓	GFP	pGHGWG-bHLH089-1	Reporter
	1.1	✓	mCherry	pGWB453-bHLH089-1	Reporter
	1.9	✓	GFP	pGHGWG-bHLH089-2	Reporter
	1.9	✓	mCherry	pGWB453-bHLH089-2	Reporter
	UBQ10	✓	YFP	pUBC-bHLH089-YFP	DLRA, IP
	UBQ10	✓	cYFP	pUBC-bHLH089-cYFP	BiFC
	UBQ10	✓	nYFP	pUBC-bHLH089-nYFP	BiFC
bHLH010	2	x	GUS	pGWB3-bHLH010	Reporter
	UBQ10	✓	YFP	pUBC-bHLH010-YFP	DLRA, IP
	UBQ10	✓	cYFP	pUBC-bHLH010-cYFP	BiFC
	UBQ10	✓	nYFP	pUBC-bHLH010-nYFP	BiFC
AMS	UBQ10	✓	YFP	pUBC-AMS-YFP	DLRA
DYT1	UBQ10	✓	YFP	pUBC-DYT1-YFP	DLRA
MS2	2.2	x	LUC	pGREEN-MS2-LUC	DLRA
MYB33	UBQ10	✓	cYFP	pUBC-MYB33-cYFP	BiFC
MYB65	UBQ10	✓	cYFP	pUBC-MYB65-cYFP	BiFC
GAI	UBQ10	✓	cYFP	pUBC-GAI-cYFP	BiFC
RGL2	UBQ10	✓	cYFP	pUBC-RGL2-cYFP	BiFC
RGL3	UBQ10	✓	cYFP	pUBC-RGL3-cYFP	BiFC

2.3.4 Colony PCR

Single bacterial colonies were isolated, transferred into 20µl H_2O and denatured for 5 minutes at 98°C. 1µl of this is added to 5µl REDTaq® ReadyMix™ (Sigma-Aldrich), 0.25µl of forward and reverse primer stocks (10µM) and 3.5µl H_2O. Typically, thermocycler conditions were 98°C for 3mins;

followed by 30 cycles of 30secs at 98°C, 30secs at 58°C and 1min per kb amplicon at 72°C; and then a final extension at 72°C for 10mins. PCR products were then run by Agarose Gel Electrophoresis.

2.3.5 Agarose Gel Electrophoresis

DNA was separated on agarose gels (1-2%) using Agarose gel electrophoresis: 10µl of PCR product was loaded onto the gel alongside 5µl HyperLadder™ 1kb/ 50bp (Bioline) and run at 100V in 0.5x TBE buffer. Gels were then imaged under UV light in a Gel Doc™ XR+ (Bio-Rad).

2.4 Protein Interaction Assays

2.4.1 Dual Luciferase Reporter Assay (DLRA)

GV3101 strains of *Agrobacterium tumefaciens* were co-transformed with pUBC-bHLH-YFP & pBIN61-p19 and pGREEN-MS2-LUC & pSOUP. These lines were separately cultured, resuspended to an OD600 of 0.4 in infiltration buffer (10mM $MgCl_2$, 10mM MES pH 5.6, 150µM Acetosyringone) and then combined in equal parts to co-infiltrate the leaves of 4-week-old *Nicotiana benthamiana* plants as in Hellens et al. (2005). On each leaf were four experimental tests, i.e. combinations of transcription factors (pUBC-bHLHX-YFP) co-transformed with pGREEN-pMS2-LUC, and both a negative (pUB:GFP & pMS2:LUC) and positive (pUB:GAL4-VP64 & p35s:5xUAS:LUC) control.

After a 2-4 day incubation, 2cm leaf discs were harvested from infiltrated region and flash-frozen in liquid nitrogen and stored -80°C. Frozen leaf discs were homogenized, mixed into 200µl Passive Lysis Buffer (Dual-Luciferase® Reporter Assay System, Promega) and centrifuged at max speed for 5 minutes at room temperature. 20µl of the supernatant was added to 50µl Luciferase Assay Reagent II and chemiluminescence of the Firefly luciferase was directly measured in a Biotek Synergy LX multi-mode reader. 50µl Stop & Glo® Reagent was then added and luminescence of the Renilla luciferase measured.

Relative luminescence (RLU) of the target promoter was ascertained with respect to internal p35s driven Renilla luciferase expression:

$$RLU = \left(10{,}000 \times \frac{pMS2{:}\,LUC - blank}{p35S{:}\,REN - blank}\right)$$

Experimental RLU (Exp) was then normalised to negative (Neg) and positive (Pos) control RLUs on the same leaf using the following equation, where RRR is the Relative Response Ratio:

$$RRR = \frac{Exp\ -\ Neg}{Pos - Neg}$$

Graphpad Prism was used plot individual RRR values, with bars representing the median and 95% confidence intervals.

2.4.2 Bimolecular Fluorescence Complementation (BiFC)

Transcription factors CDSs were cloned into ubiquitin-driven split-YFP constructs (pUBC-bHLH-nYFP and pUBC-DELLA/MYB-cYFP) by LR Gateway Cloning as in Section 2.3.3 and transformed into GV3101 Agrobacteria. These were cultured separately and combined in equal parts with pBIN61-p19 cultures to infiltrate tobacco leaves as in Section 2.4.1. After 2 days, YFP expression was imaged on the Leica TCS SP5 microscope using the 514nm laser, with detection at 523-575nm.

2.4.3 Yeast Two Hybrid (Y2H)

Tapetal bHLH CDSs (DYT1, AMS, bHLH89, bHLH91, bHLH10) in pDEST32-BD and pDEST22-AD vectors were provided by Dr Wenzhe Yin. Transformed yeast cultures were mated on Yeast Peptone Dextrose Adenine (YPDA) media (1% Bacto Yeast Extract, 2% Bacto Peptone, 2% Dextrose, 0.01% Adenine Hemisulfate, 2% Bacto Agar) and then screened on SD –leu –trp –his –ade + 25mM/ 50mM/ 100mM 3-amino-1,2,4-triazole (3AT) media.

2.5 MICROSCOPY

2.5.1 Laser Confocal Microscopy

Freshly dissected anthers were mounted in 50% Glycerol and analysed using the Leica TCS SP5 microscope with a 20x objective. GFP was detected using the 488 nm Argon laser with a transmission detected from 499 to 538nm and YFP was detected at 523-575nm using the 514nm laser. Chlorophyll autofluorescence was detected from 597 to 601nm. Z-stack images were taken every 1µm through the anther and fluorescence intensity was assessed in Image J using the maximum projection of these Z-stacks.

2.5.2 Transmission Electron Microscopy (TEM)

Inflorescences from Col-0 and various *bhlh* mutants were fixed overnight at 4°C in 3% (v/v) Glutaraldehyde in 0.1M Cacodylate buffer then washed and stored in 0.1M Cacodylate buffer. Samples were stained for 1hr in 1% (v/v) Osmium Tetroxide, washed twice in dH_2O and soaked for 1hr in the dark at 4°C in 2% (v/v) aqueous Uranyl Acetate. Dehydration was carried out by an Ethanol series (2 x 10 mins in 50%, 70%, 90% and 100% v/v) and 2 x 10 mins in 100% Propylene Oxide. The buds were then soaked for 30mins in 3:1, Propylene Oxide: Resin solution before leaving overnight in 1:1, Propylene Oxide: Resin solution. Samples were transferred into pure Resin and left for 2.5hrs before Resin was changed. After a further 2.5hrs, samples were embedded in fresh Resin and left to

polymerise at 60°C for 2 days. A Leica EM UC6 Ultramicrotome fitted with a diamond knife was then used to cut Semi-thin (500nm) and Ultra-thin (90nm) sections. Semi-thin sections were stained with Toluidine Blue in 1% (v/v) Sodium Borate to assess quality and placement of the sample. Ultra-thin sections were then flattened using a heated element, or by exposure to chloroform vapours, and collected onto 200-mesh carbon-coated copper grids (EM Resolutions Ltd) and left to dry. Sample matrices were placed on a droplet of Saturated Uranyl Acetate in 50% ethanol for 5 minutes then vigorously washed twice in 50% (v/V) ethanol and once in dH_2O. Grids were then placed on a droplet of Reynold's Lead Citrate, surrounded by Sodium Hydroxide Pellets, for at least 5 minutes and then washed twice in dH_2O. Samples were imaged using an FEI Tecnai 12 BioTwin TEM.

2.5.3 Scanning Electron Microscopy (SEM)

Freshly harvested flowers were imaged by Dr Elisabeth Steer at University of Nottingham's Nanoscale and Microscale Research Centre using the FEI Quanta 650 ESEM.

2.5.4 GUS Staining

Inflorescences were stained overnight in 50 mM Phosphate buffer pH 7.2 containing 0.5 mg/ml X-Gluc in Dimethyl Formamide, 0.5 mM $K_3Fe(Cn)_6$, 0.5 mM $K_4Fe(Cn)_6$ and 0.1% Triton X-100. Stained samples were incubated at 50°C in acidified methanol (4% HCL, 20% MeOH) for 15 minutes, transferred to 7% NaOH in 60% EtOH for 15mins at room temperature and then cleared overnight in 60% EtOH. Samples were rehydrated through a decreasing ethanol series (40%, 20%, and 10% each for 20 minutes) and stored in 50% glycerol at 4°C. GUS expression in the whole inflorescence was imaged using a Stemi SV6 stereomicroscope (Zeiss) and then the isolated anthers viewed with bright-field microscopy using the Leica DM5000b.

2.5.5 DAPI staining

Isolated anthers were stained in 3µg/ml 4'.6-diamidino-2-phenylindole (DAPI) in 50% (v/v) Glycerol, squashed to release microspores and left for 16+ hours in darkness at 4°C to allow the stain to infiltrate the microspores. Stages of meiosis were observed using the A4 fluorescence cube of a Leica DM5000b microscope.

2.5.6 Alexander staining

Mature buds were fixed in 3:1 ethanol: acetic acid and kept at 4°C. Pollen was then expelled from fixed anthers before staining for 30mins+ in 1:50 Alexander solution diluted in water (Alexander, 1969). Pollen viability was observed using with bright-field microscopy with the Leica DM5000b.

2.6 PHENOTYPING

2.6.1 Silique lengths and seed set analysis

Fully developed siliques were measured from the point of contact with the pedicel to their tip. Lengths were recorded over developmental time from the earliest silique to develop (position 1) to the most recent. Silique filling was assessed by manual counting of seed within bisected siliques using a Stemi SV6 stereomicroscope (Zeiss).

2.6.2 GA profiles

Freshly harvested inflorescences were separated into pre- and post-mitosis I stage buds by size, and then freeze-dried for 24hrs. Samples were then processed by Dr Danuše Tarkowská at Palacký University,CZ and quantified by ultra-performance liquid chromatography–tandem mass spectrometry (Urbanová et al., 2013).

2.6.3 Seedling root vs shoot growth

Arabidopsis seed was sterilised and plated on ½ MS + Sucrose Agar plates as in Section 2.1.2 and stratified for 2 days at 4°C. Plates were moved to a Conviron growth cabinet set at 100 µmol/m^2/s light intensity to germinate for 4 days whereupon root growth was marked and half of the plates were moved to 40 µmol/m^2/s light condition. After 8 more days plates were imaged and these images were processed in Image J to assess root growth and shoot area.

3 *BHLH089 BHLH091* AND *BHLH010* MUTANTS EXHIBIT LIGHT-SENSITIVE STERILITY

3.1 INTRODUCTION

3.1.1 bHLHs in tapetum development

Development of viable pollen relies upon the secretion of proteins, lipids, polysaccharides and other molecules into the anther locule from the surrounding tapetum tissue (Piffanelli et al., 1998). Genetic control of tapetum development is immensely complex with interacting regulatory networks containing feedback and feedforward loops (Ferguson et al., 2017; Zhu et al., 2011; Figure 3.1) in which several transcription factors are known to play key roles. These include the pivotal basic Helix Loop Helix (bHLH) transcription factors DYSFUNCTIONAL TAPETUM1 (DYT1; Zhang *et al.*, 2006) and ABORTED MICROSPORES (AMS; Sorensen *et al.*, 2003), which interact with three additional bHLH proteins: bHLH010 (AT2G31220), bHLH089 (AT1G06170) and bHLH091 (AT2G31210) (Xu et al., 2010; Feng et al., 2012). *DYT1* regulates *AMS* via *DEFECTIVE IN TAPETAL DEVELOPMENT AND FUNCTION 1* (*TDF1*), a putative R2R3 MYB transcription factor (Gu et al., 2014; Zhu et al., 2008) and AMS in turn influences expression of the PHD-finger motif protein *MALE STERILE1* (*MS1*; Wilson et al., 2001) through *MYB80*, another R2R3 MYB (Zhang et al., 2007).

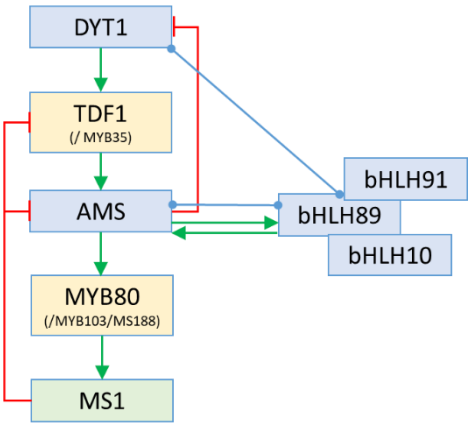

Figure 3.1. Regulatory model for the tapetum development pathway in Arabidopsis. Blue boxes show bHLH transcription factors, yellow MYBs and green PHD-finger proteins. Based on Ferguson et al. (2016)

3.1.2 Male Fertility depends on redundant bHLH010, -089 and -091

In *Arabidopsis thaliana* bHLH010, bHLH089 and bHLH091 are highly conserved (Appendix II) and thought to be redundant in their regulation of tapetum and pollen development, as demonstrated by the varying degrees of phenotypic abnormalities seen in the *bhlh* mutants (Zhu *et al*., 2015). The *bhlh* single mutants are morphologically indistinguishable from Wild Type (WT), whilst double and triple *bhlh* mutants have increasingly defective anthers with abnormal tapetum morphology, delayed callose degeneration and aborted pollen. The mutant defects reported by Zhu *et al.* (2015) not only suggest redundancy of the bHLHs in the tapetum development pathway but also that bHLH010, -089 & -091 are important in control of callose deposition and pollen wall formation.

Unpublished data from Dr Steve Thomas' group at Rothamsted Research (pers. comms) suggested that fertility of the *bhlh089 bhlh091* mutant is light-sensitive, which led us to carry out more in-depth characterisation of the response of the *bhlh* mutants to light. Recent studies have also shown that *bhlh89,91* and *bhlh89,10* double mutants exhibit male sterility in response to high temperatures (Fu et al., 2020), leading to the hypothesis that bHLH89, 91 and 10 function as hubs integrating varying environmental cues into the reproductive development pathway.

Much has been published on the effect of temperature on male reproductive development in *Arabidopsis* (Rieu et al., 2017), with high temperature leading to abnormal stamen development, reduced production of viable pollen, defective meiosis, abnormal ploidy in mature pollen and defective anther dehiscence (De Storme and Geelen, 2020; Nguyen et al., 2019). However, less is known about the effects of light on male reproductive development, although there are a few reports of light-sensitive male sterility linked to Gibberellin (GA) signalling. The sterile GAMYB-like *myb33 myb65* double mutant exhibits restored fertility under high light and low temperature (Millar and Gubler, 2005). HEAT SHOCK PROTEIN-RELATED (AtHSPR) was also shown to be involved in GA- and light intensity mediated regulation of flowering and seed set, with *hspr* mutants male sterile at low light intensity (20 µmol/m^2/s) but pollen developing as WT at 150 µmol/m^2/s (Yang et al., 2020). Outside of GA pathways, the *yet another kinase1 (yak1)* mutant also shows increased fertility under higher light intensity that may be linked to ABA signalling (Huang *et al*., 2017).

Whilst little is known about the effects of light on fertility itself, there have been many studies on light-mediated initiation of flowering. A low Red: Far Red (R:FR) ratio of light is an indicator of shading and activates floral transition via phytochrome-mediated pathways involving PHYTOCHROME INTERACTING FACTORS (PIFs), a class of bHLH proteins (Franklin, 2008; Wit et al., 2016). Under normal light conditions the photoreceptors phyA and phyB interact with PIFs leading to their inactivation or degradation (Pham et al., 2018). In shaded conditions, or low R:FR light, the interaction between the PIFs and the photoreceptors ceases enabling the PIFs to bind to downstream targets and regulate a wide number of pathways including skotomorphogenesis (hypocotyl elongation in the dark) and floral transition. Beyond floral transitioning very little is known about the effects of light on fertility.

3.1.3 Chapter Aims

In this chapter an in-depth characterisation of the light-sensitive sterile phenotype of the *bhlh* double mutants was carried out, focusing on the effect of light on the development of tapetum, microspores and overall fertility. Localisation of bHLH transcripts and proteins in reproductive tissue

in response to low light and the effect of light on vegetative development of the *bhlh* mutants was further examined.

3.2 RESULTS

3.2.1 Fertility of *bhlh* double mutants is reduced in low light

T-DNA insert lines of *bhlh010* (GK-055H02-012479), *bhlh089* (SALK-123106) and *bhlh091* (GK345C06-016233) were crossed by colleagues at Rothamsted Research to obtain double knockout *bhlh* mutants. These lines differed from those previously published by Zhu *et al.* (2015); in the case of the *bhlh091* mutant the T-DNA insert used in this thesis was located towards the end of the first exon as opposed to upstream of the 5' UTR. However the SALK insert used here for bHLH089 was located near to the previously reported GABI-KAT site in the first exon of bHLH089 (Figure 3.2 A). Due to the close proximity of bHLH010 and bHLH091 loci, and resulting difficulties in crossing, the original *bhlh089 bhlh010* amiR-bHLH091 line developed by Zhu *et al.* (2015) was used as the triple mutant in our studies, retaining the original *bhlh089* GK insertion and incomplete miRNA knockdown of bHLH091. Line homozygosity was confirmed by PCR with gene specific and T-DNA specific primers and bHLH expression levels were assessed by qRT-PCR, verifying that bHLH089 and bHLH091 levels are knocked down to 12-15% and 0.2% respectively of WT levels in the new *bhlh* double mutant backgrounds (Figure 3.2 B).

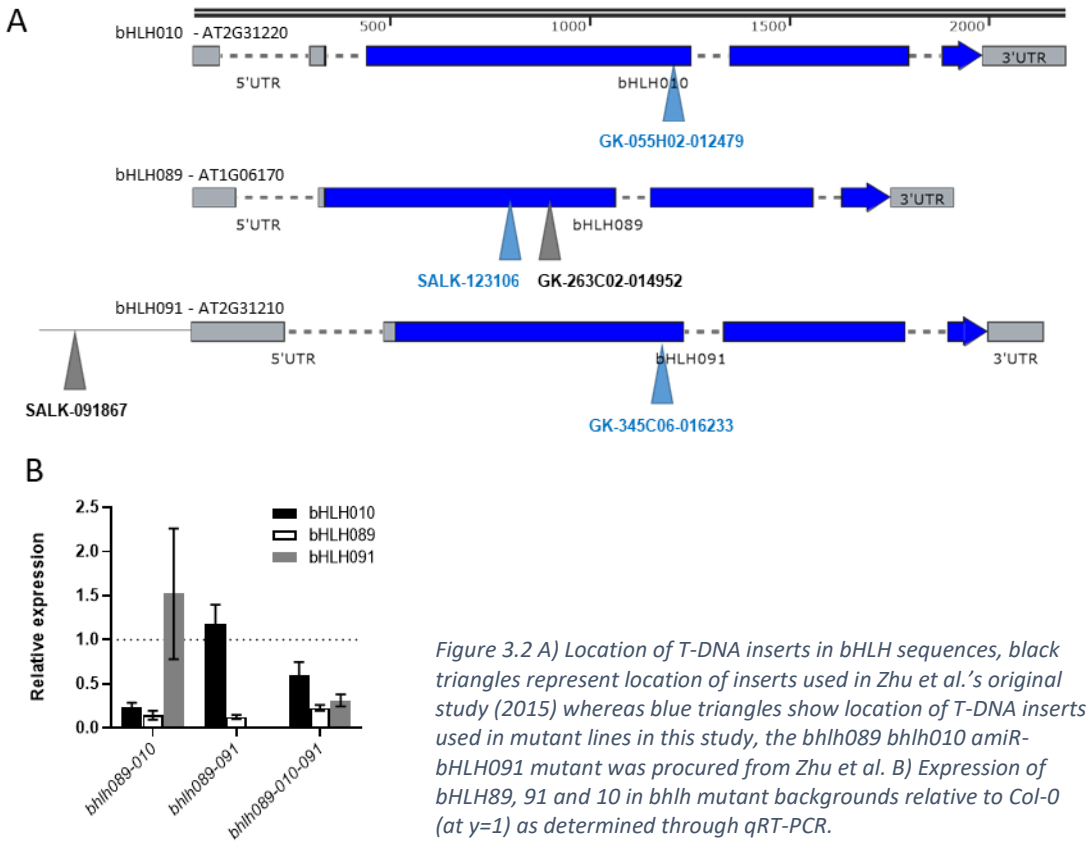

Figure 3.2 A) Location of T-DNA inserts in bHLH sequences, black triangles represent location of inserts used in Zhu et al.'s original study (2015) whereas blue triangles show location of T-DNA inserts used in mutant lines in this study, the bhlh089 bhlh010 amiR-bHLH091 mutant was procured from Zhu et al. B) Expression of bHLH89, 91 and 10 in bhlh mutant backgrounds relative to Col-0 (at y=1) as determined through qRT-PCR.

In their original study, Zhu *et al.* (2015) reported that *bhlh* single mutants develop as WT throughout development whilst the *bhlh089 bhlh091* double mutant has smaller anthers and a reduced number of mature pollen grains but is otherwise fertile. Pollen is not produced in early flowers of the *bhlh089 bhlh010* double mutant, although a small amount is produced in the anthers of later flowers. The triple mutants have even smaller anthers and shorter filaments than the double mutants, abnormal tapetum morphology and total abortion of pollen (Zhu *et al.,* 2015, Figure 3.3A). Whilst the *bhlh89,10* mutant used in our study showed initial sterility as reported by Zhu *et al.* (2015), prolonged sterility was also exhibited in the *bhlh89,91* double mutant under our normal growth conditions (Figure 3.3A).

To assess the effect of light on fertility, Col-0, *bhlh089 bhlh091* and *bhlh089 bhlh010* mutants were grown under standard conditions (with light levels of 200 µmol/m^2/s, Chapter 2.1) until bolting and then transferred to low light (50 µmol/m^2/s). In this study, silique length was used as measure of fertility as it correlates well with seed set across the different mutant backgrounds and light treatments (Figure 3.3B) and, since *Arabidopsis* is primarily self-pollinating, seed set is good indicator of pollen viability. Onset of fertility appeared to be consistent across primary and lateral flowering stems for each genotype in normal conditions (Figure 3.4), whereas in low light treated plants the primary stem fertility is confounded by the effect of higher light levels on flower development prior to transfer to the low light at bolting. Therefore in further experiments silique lengths were recorded only on the lateral stems to ensure that all developing buds received consistent light treatment. It also appears that initial fertility was higher on secondary stems in both light conditions, with the first couple of siliques 3-4mm longer than on primary and lateral stems (Figure 3.4).

Under normal light conditions the first 3-4 siliques in Col-0 show reduced length and seed set, but full fertility was established after this point. In the *bhlh* double mutants initial silique lengths are shorter, with reduced seed set, reaching maximum fertility at approximately position 10-12, suggesting a fertility defect that restores later in development (Figure 3.3C).

Under low light conditions the fertility of WT and all lines tested was reduced, with a maximum silique length of 12mm observed in Col-0, compared with 17mm in normal light conditions (Figure 3.3C). In low light, the *bhlh089 bhlh010* mutant was initially sterile but fertility was eventually restored to WT levels by flower position 20. However the *bhlh089 bhlh091* mutant remained partially sterile across development, with minimal rescue of fertility. The triple *bhlh089 bhlh010* amiR-bHLH091 mutant was sterile under both light conditions.

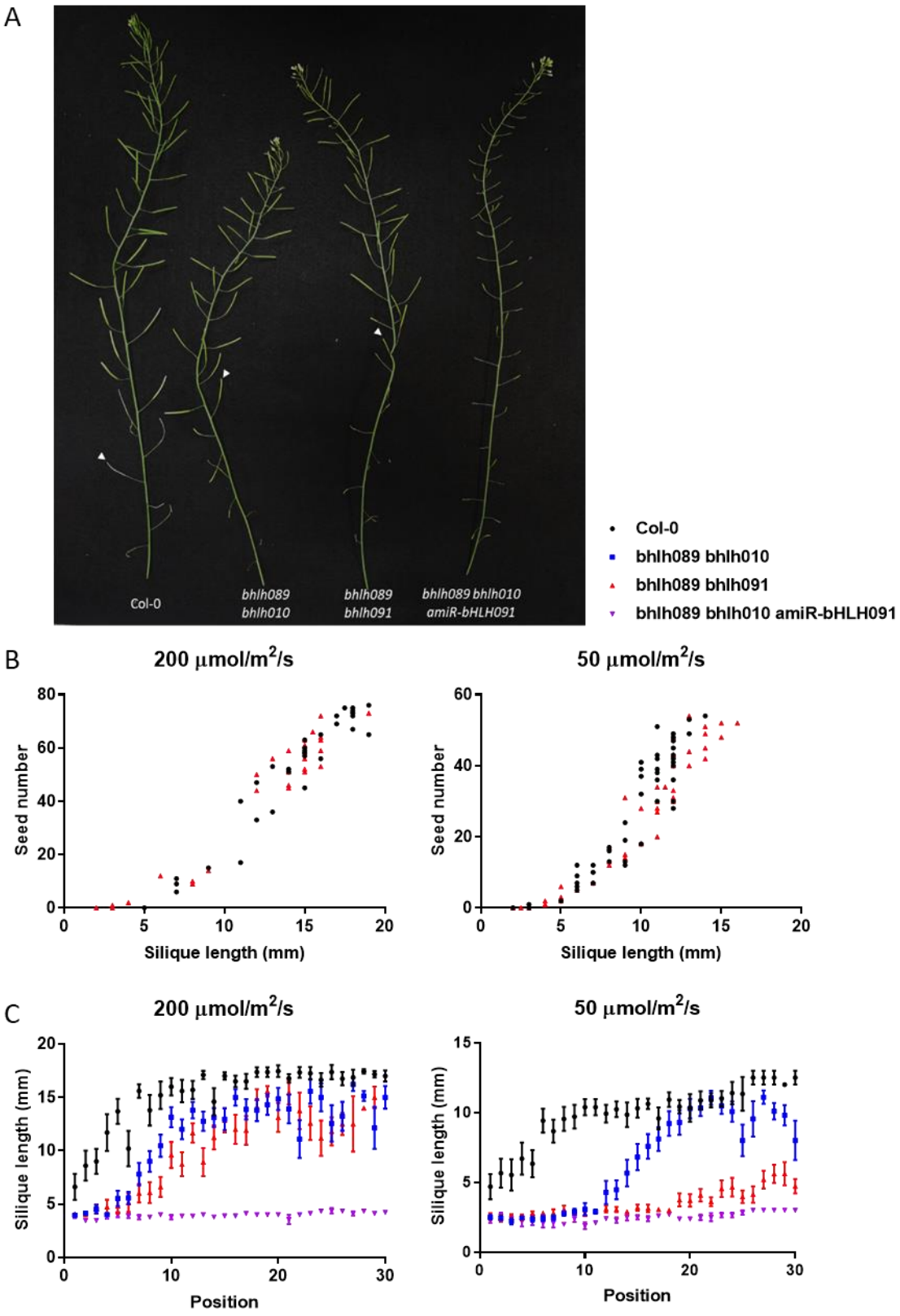

Figure 3.3 Fertility phenotypes of bhlh mutants. A) Delayed onset of fertility in bhlh double mutants compared to Col-0 grown in normal conditions is highlighted by a white arrow at the first fertile silique, the triple bhlh mutant remains completely sterile throughout development. B) Seed number and silique length strongly correlate between Col-0 and bhlh mutants in each light condition, enabling silique length to be used as a proxy measure for fertility. C) The effect of light on fertility across the flowering stem, showing a heightened delay in onset of fertility in low light treated bhlh double mutants

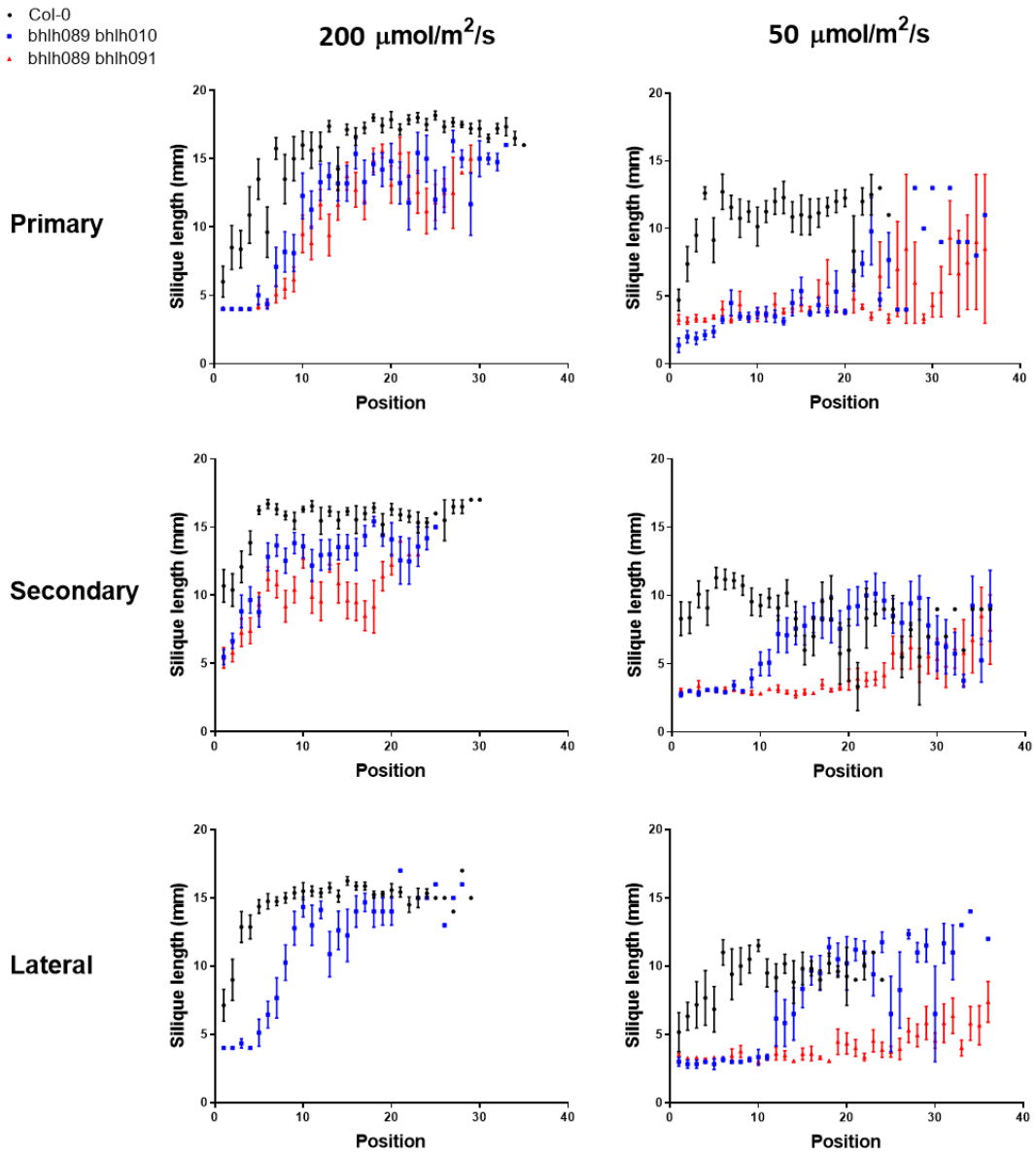

Figure 3.4. Pilot study of fertility of bhlh double mutants vs Col-0 across different flowering stems using silique length as a proxy for fertility. Mean silique length is plotted against position on Primary, Secondary and Lateral (Primary) stems. Primary stems exhibit varied fertility under low light due to confounding effects of higher light intensities prior to transfer. Thus as the later developing lateral stems show similar onset of fertility to the primary, and are exposed only to the light treatment intended, these were used in further studies. Error bars represent SEM.

3.2.2 Microspore development in the *bhlh* mutants

Microspore development was examined to elucidate the cause of the fertility defects. Fresh buds were harvested from plants growing in normal and low light conditions, measured and their anthers extracted and stained with DAPI to assess the stage of microspore development (Chapter 2.5.5). Under normal light conditions, DAPI staging suggested that *bhlh089 bhlh010* buds start meiosis at a smaller bud size than Col-0, but buds were comparable in size from single microspore stage and beyond, however a Residual Maximum Likelihood (REML) mixed effects model revealed no significant difference between WT and *bhlh* mutant buds at any stage of development ($F=0.1$, $p>0.05$, Figure 3.5 A,B).

Col-0 plants grown under low light conditions appeared to undergo later stages of microspore development at a smaller bud size than those grown in normal light (Figure 3.5 C), however a student's T-test showed only a statistical significant difference at the Bicellular Microspore stage ($p=0.02$, $df=12$, $t=2.6$). Conversely, *bhlh* double mutants proceed through stages at the same bud size as they would in normal light conditions, and were unchanged from WT; however, microspore development is aborted after Bicellular Microspore stage in low-light treated *bhlh89,91* buds and after Single Microspore stage in early *bhlh89,10* buds (Figure 3.5 D, E).

Ethanol- acetate fixed mutant anthers, particularly from the low light conditions, proved extremely difficult to DAPI stage as mutant microspores stuck within the anther locule despite high levels of applied pressure. The microspores of fresh samples were more easily released however they often remained in large aggregations just outside the anther walls, suggesting stickier deposits than WT. Additionally, beyond the bicellular stage in low light *bhlh089 bhlh091* samples very few microspores were dislodged from within the locule and those that were expelled had completely collapsed and no DAPI staining was seen.

This suggested that light may affect the pollen development and wall deposition of *bhlh* mutants, therefore environmental Scanning Electron Microscopy (eSEM) was employed to look at structure of mature pollen. Dehisced flowers were collected from plants grown under different light intensities and analysed through eSEM by Dr Elisabeth Steer at the Nanoscale and Microscale Research Centre (NMRC, University of Nottingham). Normal pollen wall shape and patterning was maintained in Col-0 in low light conditions (Figure 3.6 A,B). However, whilst *bhlh* double mutant pollen develops as WT under normal light conditions (Figure 3.6 C,E), under low light conditions both *bhlh89,10* and *bhlh89,91* double mutants show defective pollen exine patterning: the *bhlh089,10* mutant showed highly irregular exine deposits and abnormal indentation whereas *bhlh089,91* pollen was misshapen and collapsed (Figure 3.6 D,F).

To further elucidate the differences in pollen development within the initial sterile period, pollen viability was assessed by Alexander staining of pollen sampled from 'early' flowers, ie those within the period of initial sterility (with between 1 and 6 opened flowers below in the stem), and 'late' flowers (with more than 20 flowers/siliques below sample). Col-0 pollen appeared to be viable in early and late flowers (Figure 3.6 G-J), with perhaps some reduction in pollen number in early flowers although this wasn't quantified. This suggests that initial fertility is reduced in WT flowers through means other than pollen development, possibly reduced stamen elongation relative to the pistil prevents pollination.

Under normal light conditions, early flowers from the *bhlh089,91* mutant contained an aggregated mixture of viable and distorted, collapsed pollen whereas pollen from late flowers was fully viable (Figure 3.6 K,L). In low light, what little pollen was expelled from the *bhlh089,91* anther was clumped together and non-viable (Figure 3.6 M,N). Taken together this suggests that initial and prolonged sterility of the *bhlh* double mutants is directly linked to development of non-viable pollen.

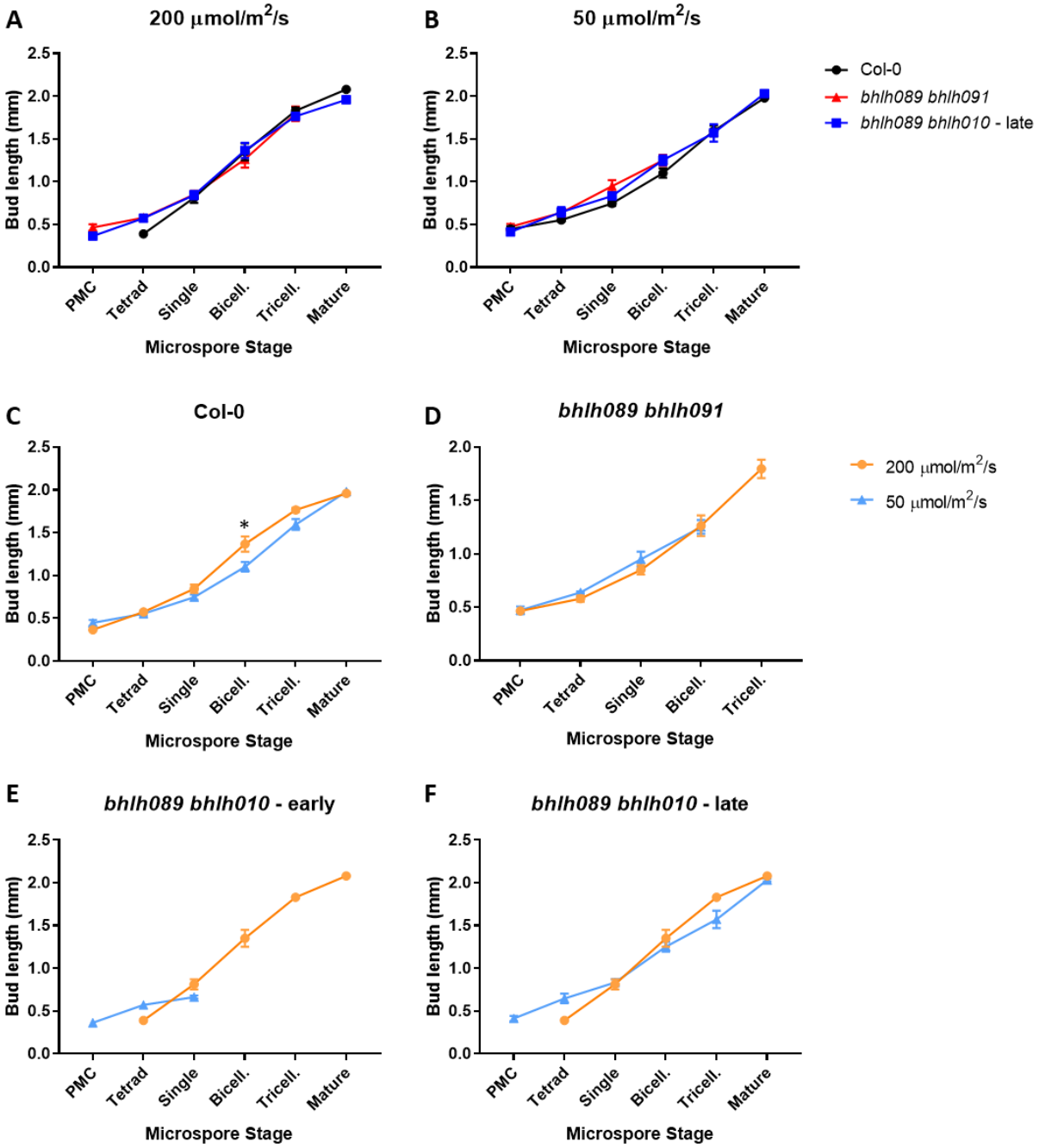

Figure 3.5. Comparison of bud sizes at each stage of microspore development in Col-0 vs bhlh mutant inflorescences grown under 200 (A) and 50 (B) µmol/m²/s light. The effect of light on bud size at different developmental stages is shown for Col-0 (C), bhlh089 bhlh091 (D) and bhlh089 bhlh010 (E, F). A-D and F represent 'late' inflorescences, harvested after 20+ flowers have already opened, whereas E is from 'early' inflorescences at the beginning of the flowering stem with less than 3 open flowers below the harvested inflorescence. Mean and SEM plotted. Asterisk indicates significant difference according to a student's T-test ($p<0.05$).

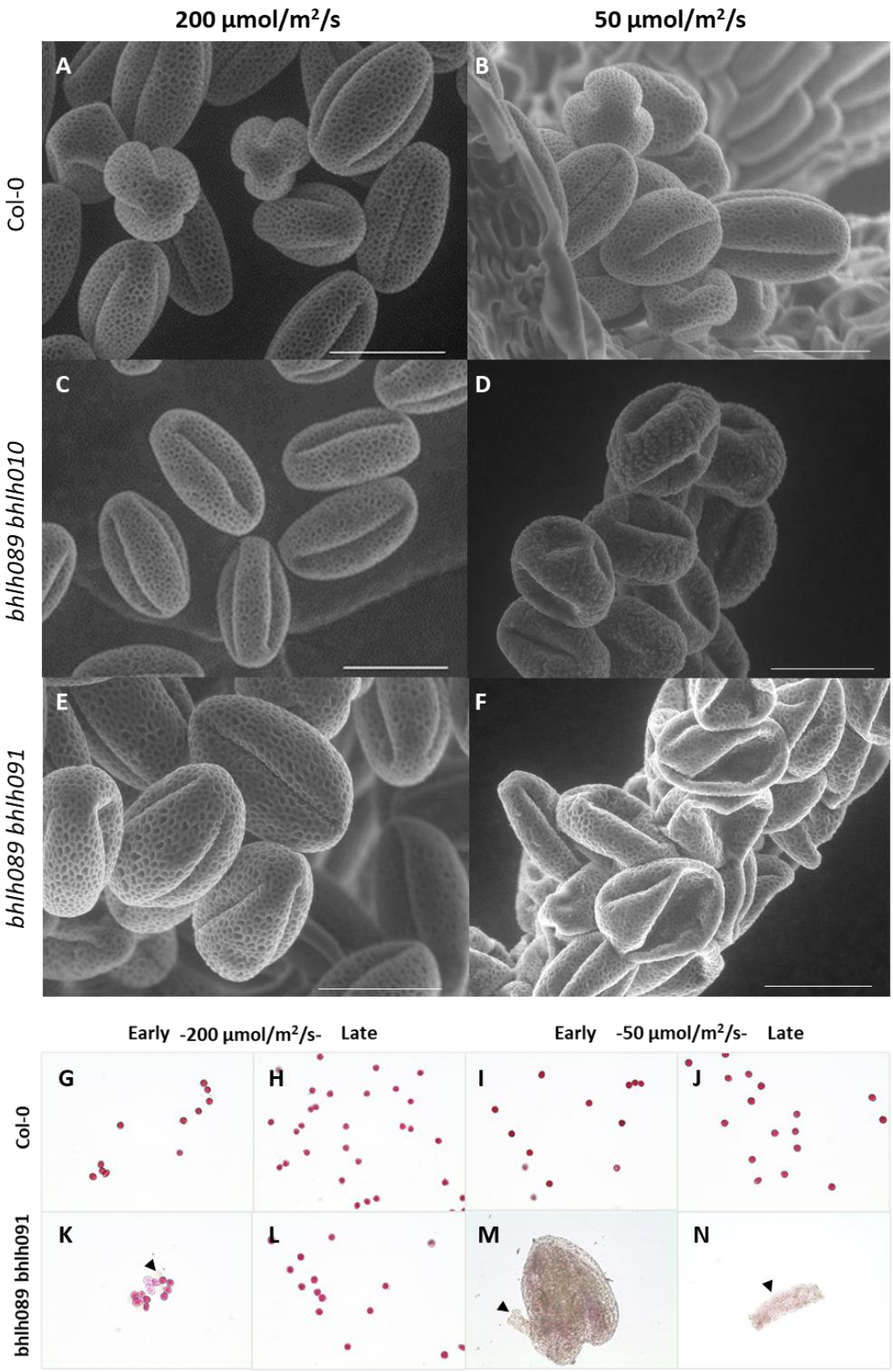

Figure 3.6. Characteristics of Col-0 and bhlh double mutant pollen grown under normal (200 µmol/m²/s) and low (50 µmol/m²/s) light conditions. A-F) Scanning Electron Micrographs of exine patterning and pollen shape, scale bar 20 µm. G-N) Alexander staining of Col-0 and bhlh089-091 mature pollen sampled from early (<6 dehisced flowers below on the stem) and late (>20 flowers/siliques below sample) flowers. Black arrows highlight unstained, non-viable pollen.

3.2.3 Low light affects development of *bhlh* mutant tapetum

Given that bHLH89, 91 and 10 are expressed in the tapetum, and the maternal role of the tapetum in development of viable pollen, microspore developmental defects observed in the *bhlh* double mutants in low light might be expected to originate from defects in the tapetum tissue.

In their study of the original *bhlh89/91/10* mutants, Zhu *et al.* (2015) recorded that triple mutant anthers and the early anthers of the *bhlh010 bhlh089* double mutant showed abnormally large and disorganised tapetal cells with increased vacuolation at stage 6 (PMC) and notably thinner callose walls which showed delayed degradation. In *bhlh089 bhlh091* and late *bhlh010 bhlh089* anthers the tapetal cell size was uneven and the tapetum layer less organised than WT. Given that the initial sterility of *bhlh89,10* mutant, reported originally by Zhu *et al.* (2015), was prolonged under low light treatment, similar tapetum defects might be expected in *bhlh* mutant tissue under low light conditions.

Transmission Electron Microscopy (TEM) was initially undertaken to elucidate the differences in anther development at single microspore stage (Figure 3.7). This showed normal exine structure in WT microspores in both light conditions and in the *bhlh089 bhlh091* mutant under normal light conditions, however in low light conditions the *bhlh089,91* exine layer appears to be thinner, with reduced electron dense baculae, and the callose wall had not fully degraded (Figure 3.7 M,O,P red arrows). The *bhlh089 bhlh010* mutant also showed defective exine deposition under low light, with irregular deposition of baculae and no visible tecta (Figure 3.7 V red arrows). TEM images further suggest that the tapetum is disorganised/ multi-layered (pink arrows) with larger vacuoles (yellow arrows) in *bhlh* double mutants under low light (Figure 3.7 K-V). Unfortunately, micrographs could not be obtained for the *bhlh089,010* mutant under normal light at a comparable developmental stage.

To provide a broader picture of changes in the anther tissues throughout development, a greater number of developmental stages were observed using semi-thin sections stained with Toluidine Blue (Figure 3.8). This highlighted differences in *bhlh89,91* vs Col-0 developmental response to low light. At tetrad stage, the tapetum of *bhhlh89,91* appeared to be more vacuolated and pulled away from cell walls in comparison to Col-0 in low light (Figure 3.8 I,J). There were also increased numbers of lipid/ oil bodies in the tapetum of the *bhlh* mutant at single microspore stage, and within the *bhlh* mutant microspores themselves in later stages of development, especially within mature pollen of low light *bhlh89,91* (Figure 3.8 H). Not only are there more lipid deposits, but a significant amount of the mature pollen was completely collapsed in the *bhlh89,91* mutant in low light (Figure 3.8 H inset).

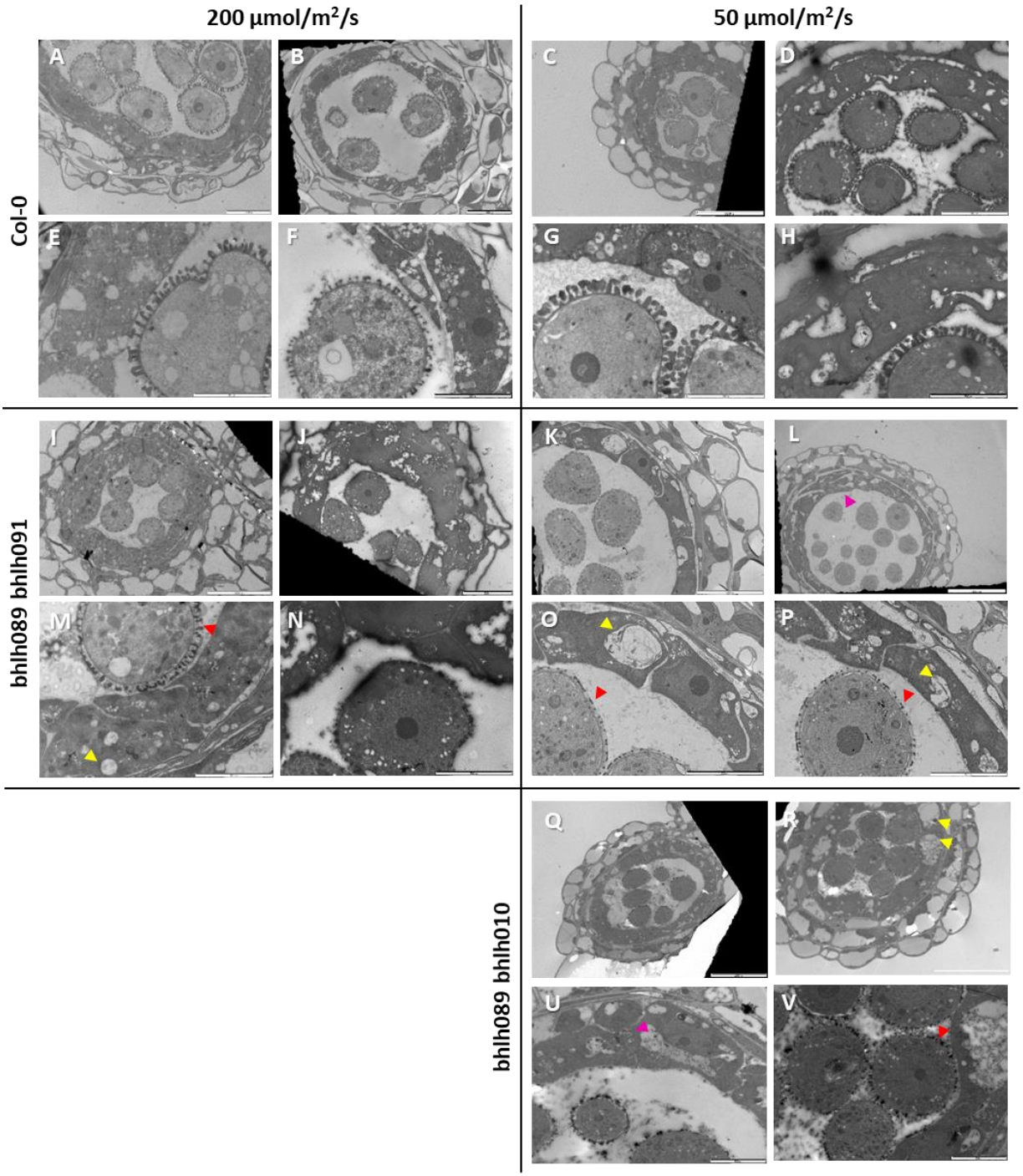

Figure 3.7. TEM sections of WT (A-H), bhlh089 bhlh091 (I-P) and bhlh089 bhlh010 (Q-V) single microspore stage anthers grown under normal and low light conditions with magnification showing structural differences in microspore exine (red arrow) and tapetum tissue (pink and yellow arrows). Scale bar: 1000µm for A,B,C,K,L; 2000µm for D,I,L,Q,R; 5000µm for E-H,M-P,U-V

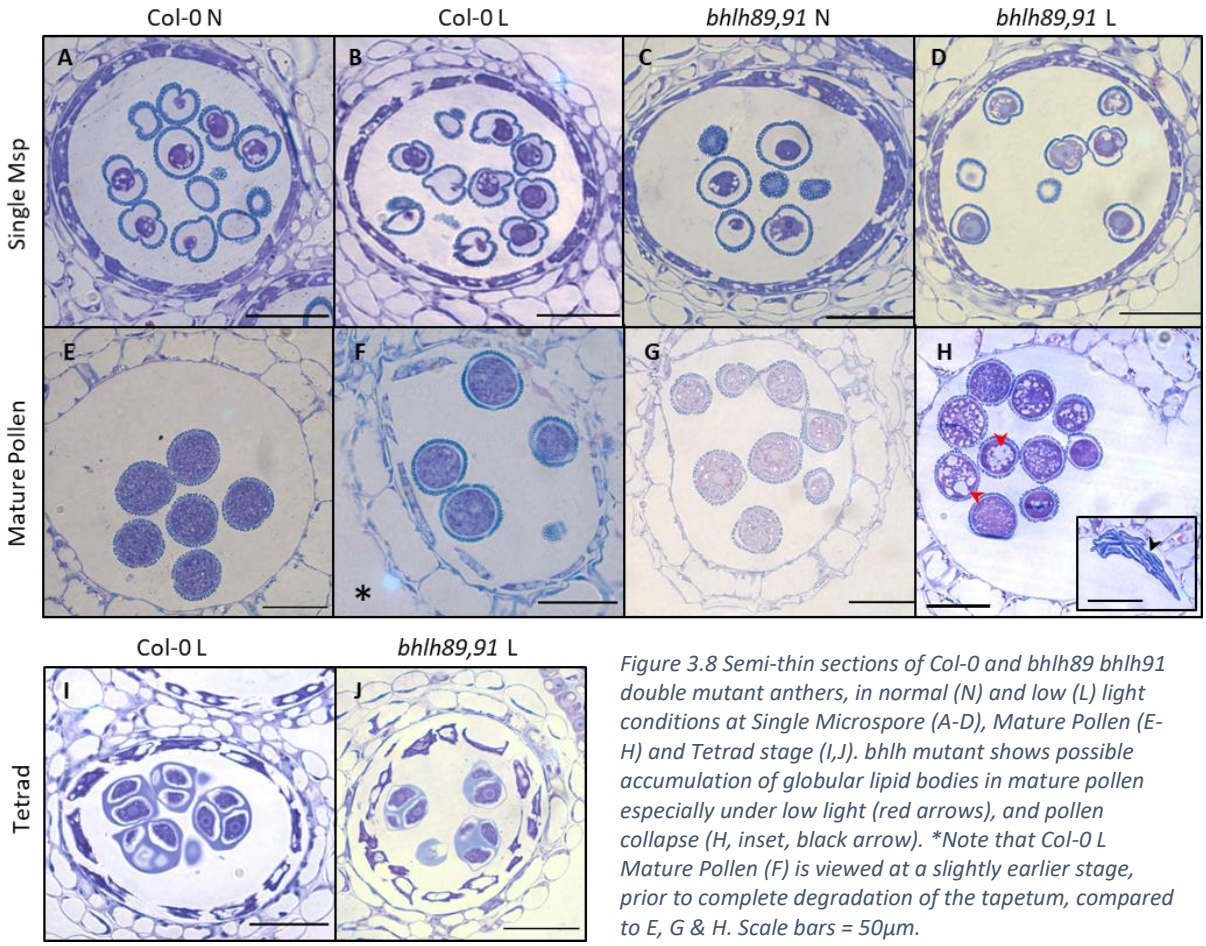

*Figure 3.8 Semi-thin sections of Col-0 and bhlh89 bhlh91 double mutant anthers, in normal (N) and low (L) light conditions at Single Microspore (A-D), Mature Pollen (E-H) and Tetrad stage (I,J). bhlh mutant shows possible accumulation of globular lipid bodies in mature pollen especially under low light (red arrows), and pollen collapse (H, inset, black arrow). *Note that Col-0 L Mature Pollen (F) is viewed at a slightly earlier stage, prior to complete degradation of the tapetum, compared to E, G & H. Scale bars = 50µm.*

3.2.4 Light affects transcript abundance of tapetal bHLH genes

Since bHLH89, -91 and -10 are reported to be functionally redundant (Zhu et al., 2015), expression changes of the bHLHs in low light could potentially cause the conditional sterility observed in the *bhlh* double mutants. Thus, qRT-PCR and subsequently RNASeq (Chapter 4) were used to assess the transcriptome dynamics of the bHLH genes in different backgrounds and light regimes.

RNA was extracted from staged buds (pre- and post- mitosis I) and whole inflorescences from Col-0 and *bhlh* double and triple mutants grown under normal and low light conditions. Non-parametric Kruskall-Wallis analysis of variance on ranks, with post-hoc Dunn tests, were carried out on the qRT-PCR dataset. This confirmed that *bHLH089* was knocked down in *bhlh89,91* and *bhlh89,10* double mutant whole buds compared to WT ($Z<-2$, $p<0.05$) and likewise *bHLH091* is downregulated in *bhlh89,91* compared to WT and *bhlh89,10* ($Z<-2$, $p<0.01$; Figure 3.9 A). The *bhlh089 bhlh010 amiR-bHLH091* mutant was also confirmed to be deficient in *bHLH091* ($Z=-2$, $p<0.05$) but the reduced expression of *bHLH89* and *-10* was not significant. *bHLH010* expression levels do not differ significantly from WT in the *bhlh089 bhlh091* mutant, nor does *bHLH091* in the *bhlh089 bhlh010* mutant ($p>0.05$).

qRT-PCR expression analysis of bHLH transcripts under different light conditions suggested that they were reduced, on average, in response to low light especially in whole inflorescences; but none of these differences were significant according to Kruskall-Wallis analysis of variance (Figure 3.9 A). However, according to RNASeq analysis of Col-0 pre-mitosis I stage buds, all of the bHLHs in the tapetum development pathway show a slight, but significant, reduction in transcript abundance when grown under low light conditions (log2FC<1, q<0.05, Figure 3.9 B). *bHLH010* levels decreased from 83 to 56 Transcripts Per Million (TPM) kilobases, bHLH089 decreased from 46 to 30 TPM, *bHLH091* fell from 30 to 22 TPM, AMS reduced from 226 to 144 and DYT1 levels also reduced from 10 to 6 TPM. In the *bhlh89,91* mutant this reduction in *bHLH* expression under low light was maintained for all bHLHs apart from *AMS*; *bHLH010* expression falls from 78 to 60 TPM, *bHLH089* goes from 25 to 16 and *bHLH091* and *DYT1* expression is also slightly reduced from 23 to 17 TPM and 15 to 11 TPM respectively.

Whereas *AMS* and *DYT1* were upregulated in the *bhlh89,91* mutant compared to WT, there was no differential expression of bHLH010, MS1, MYB80 or TDF1 in the *bhlh089 bhlh091* mutant compared to WT in normal light conditions according to RNAseq (Figure 3.9 B). In terms of light response in the latter three genes, TDF1 exhibits a large reduction in expression in response to low light in Col-0 but this is reduced in the *bhlh089 bhlh091* mutant, MYB80 only shows a drop in expression in low light in WT and MS1 expression doesn't respond to light in either background.

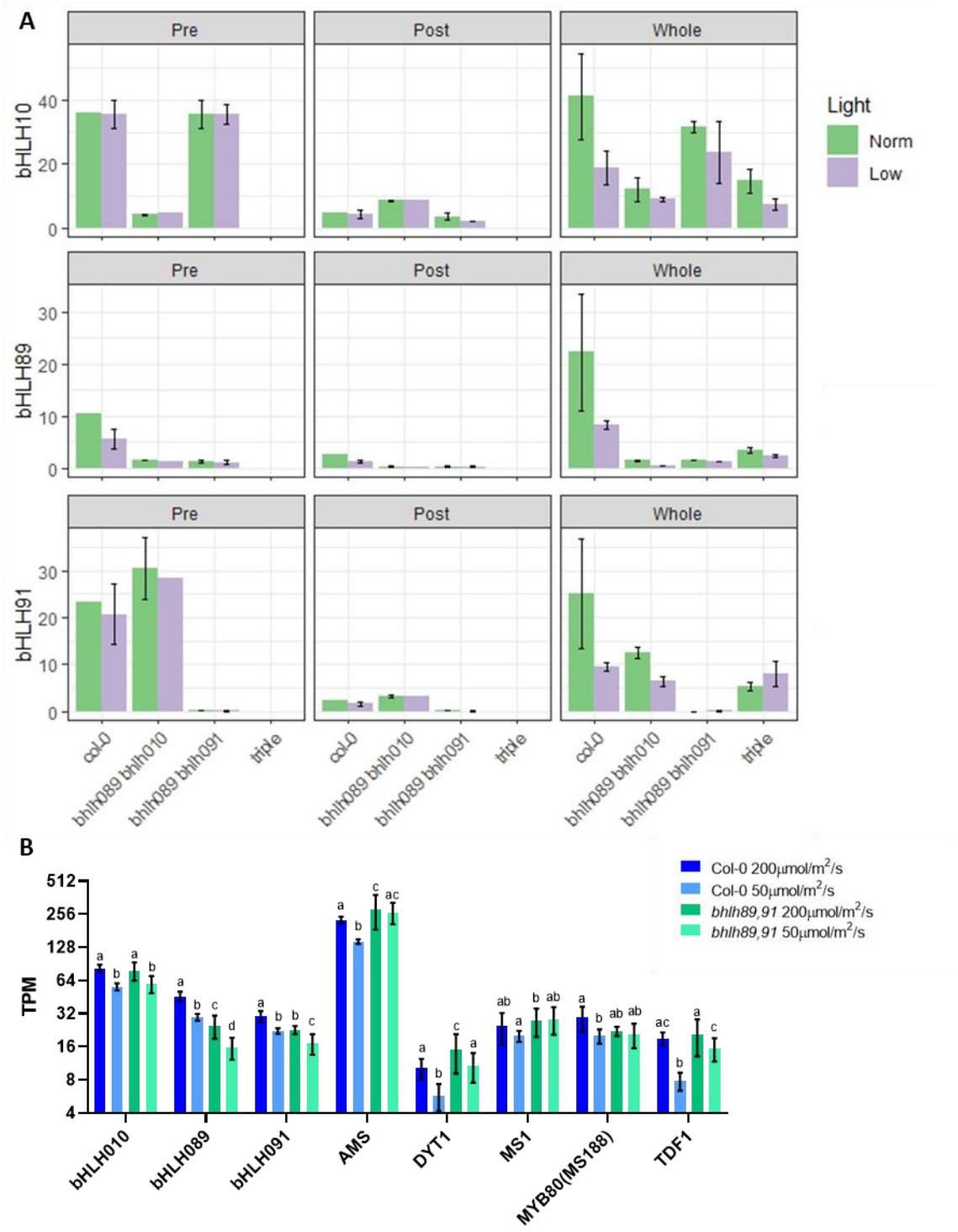

Figure 3.9. The effect of low intensity light treatment (50 compared to 200µmol/m²/s) on bHLH expression in Col-0, bhlh089 bhlh010, bhlh089 bhlh091 and bhlh089 bhlh010 amiR-bHLH091 triple mutant backgrounds. A) Mean expression of bHLH transcripts in and pre- and post- Pollen Mitosis I (PMI) staged buds and whole inflorescences as determined by qRT-PCR. All expression values have been normalised to the expression of the housekeeping gene PP2A3. Data is missing for triple mutant in Pre- and Post-PMI plots. B) Mean Transcript Per Million (TPM) expression of key tapetum transcription factors according to RNASeq. Letters represent significant differences q<0.05 within each gene. Error bars represent standard error of the mean of 2-3 (A) and 4 (B) biological replicates.

3.2.5 Expression of bHLH transcript and proteins

Transcriptional and translational bHLH reporter lines were generated to determine the effect of various environmental and genetic factors on bHLH expression patterns.

Transcriptional bHLH-GUS reporter lines in a Col-0 background showed prolonged expression of bHLH010, -089 and -091 in the tapetum from Pollen Mother Cell (PMC) until Bicellular Microspore stage of anther development (Figure 3.10 F-H). Some GUS expression was also seen in Tricellular Microspores of *pbHLH091:GUS*. GUS expression in the transcriptional reporters grown under low light conditions shows that the bHLH89 and -91 expression patterns persist in low light (Figure 3.10 C, E).

Translational fusions suggest that bHLH protein expression is more limited, with nuclear-localised fluorescent signals seen in the tapetum of *pbHLH091:bHLH091-YFP* and *pbHLH089:bHLH089-GFP* translational reporter lines in Pollen Mother Cell (PMC) and Tetrad stage anthers. Weaker cytoplasmic bHLH91-YFP expression was also seen in the tapetum at early Single Microspore (Msp) stage (Figure 3.12). According to fluorescence intensity analysis (Chapter 2.5.1), it appears that low light treatment increases the fluorescent activity of bHLH-FPs on average, however this was not significant ($p>0.05$), and the expression patterns were the same as in normal growth conditions.

To determine the extent of which bHLH expression depends upon other genes within the tapetum development gene network, transcriptional and translational bHLH reporters were crossed into various male sterile mutant backgrounds. Unfortunately integration was unconfirmed for several male sterile combinations but, in those that were successful, both bHLH89 and -91 GUS expression patterns were maintained in the *ams* background, bHLH91 expression persisted in the *myb80* background and bHLH89 continues in the *tdf1* background (Figure 3.11). However, no pbHLH89:GUS expression was seen in the *dyt1* background. bHLH89-GFP fluorescence was confirmed in the tapetum in *ams, tdf1* and *dyt1* mutant backgrounds and bHLH91-YFP fluorescence in the *ams* mutant tapetum (Figure 3.12). Translational fusion expression patterns in *ams* and *tdf1* mutant backgrounds were the same as in WT, however expression of bHLH89-GFP persisted at low levels in the *dyt1* mutant throughout single microspore development until the tapetum degraded.

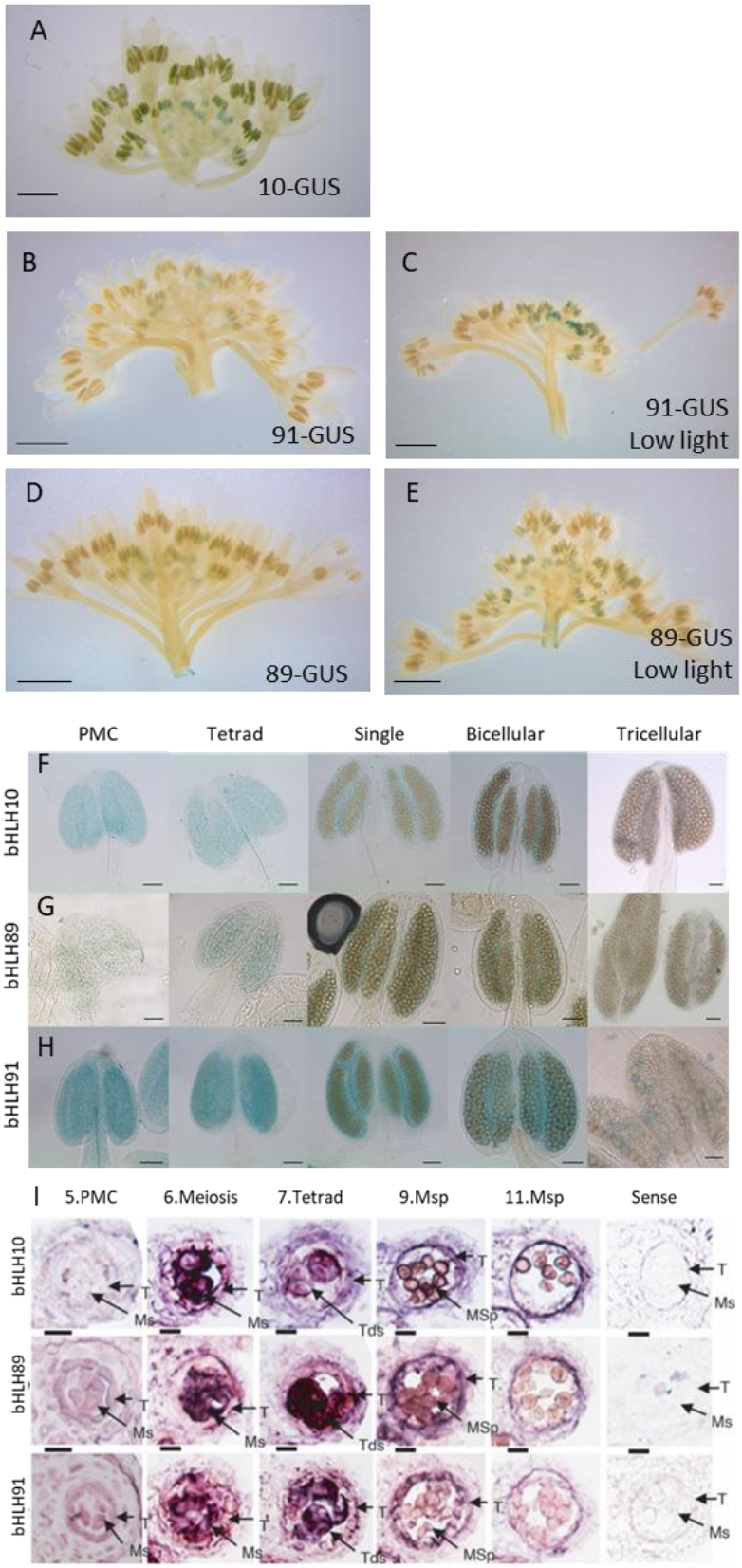

Figure 3.10. X-Gluc staining of bHLH transcriptional reporter inflorescences (A-E) and dissected anthers (F-H) showing spatial-temporal patterns of bHLH gene expression. pbHLH::GUS expression is prolonged from Pollen Mother Cell Stage to Bicellular Microspore stage in the tapetum with some GUS expression also seen in Tricellular Microspores of pbHLH91:GUS (H). pbHLH:GUS expression patterns persist under low light treatment (C, E) RNA in situ hybridisation from Zhu et al., 2015 (I) confirms bHLH transcript expression patterns in WT anthers at stages 5, 6, 7, 9 & 11. Controls use a sense probe on WT stage 6 anthers. T, tapetum; Ms, microsporocytes; Tds, tetrads; MSp, microspores Scale Bars represent 1mm in A- E, 50µm in F- G and 10µm in I.

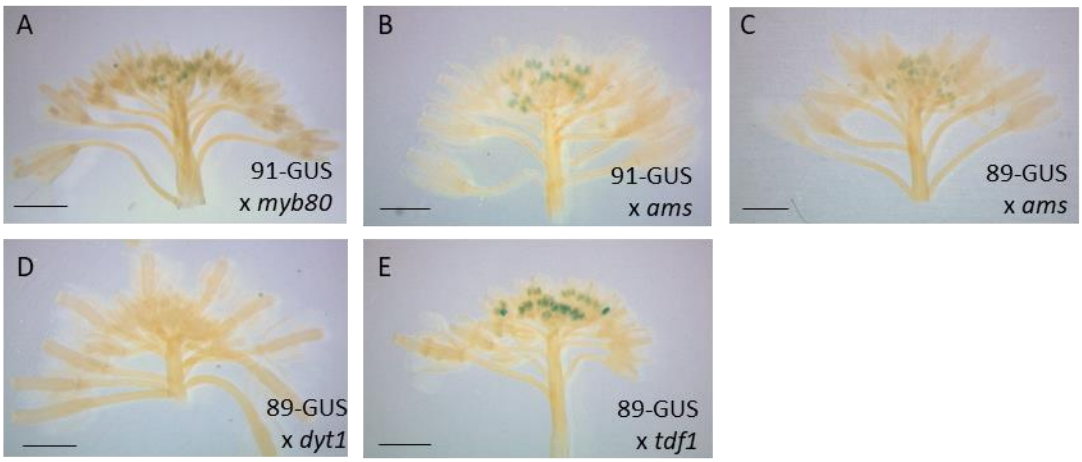

Figure 3.11 X-Gluc staining of bHLH transcriptional reporters in male sterile backgrounds showing GUS expression in ams, myb80 and tdf1 mutant backgrounds but no bHLH89:GUS expression was observed in the dyt1 mutant background. Scale Bars represent 1mm.

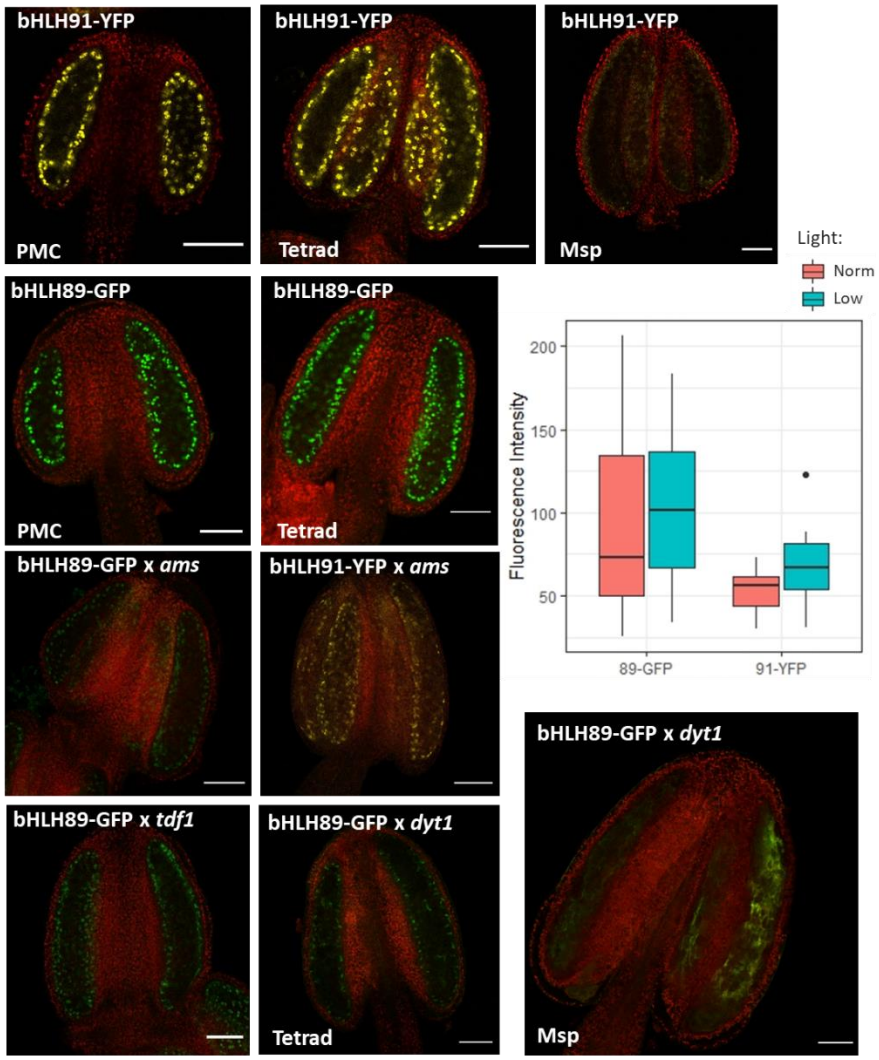

Figure 3.12. Expression of translational bHLH-fluorescent reporter proteins in WT and male sterile mutant backgrounds. Showing bHLH89-GFP and bHLH91-YFP expression in the nuclei of tapetum tissue at Pollen Mother Cell (PMC) and Tetrad stages of anther development and cytoplasmic bHLH91-YFP expression in single microspore (Msp) stage tapetum. This expression pattern persisted in ams and tdf1 mutant backgrounds but bHLH89-GFP expression was also seen in the dyt1 mutant anther locule at Msp stage. Fluorescence Intensity plot showing bHLH- fluorophore response to low light suggests bHLH protein expression was elevated in low light conditionswithin tetrad stage anthers, but this was non-significant ($p>0.01$). Scale bars represent 50μM.

3.2.6 Seedling growth

According to developmental expression atlas data (Klepikova et al., 2016; Schmid et al., 2005), bHLH089, 091 and 010 are expressed at low levels in the root tissue. To determine whether bHLHs have any effect on root development, seedlings were grown on ½ MS Agar plates under a light intensity of either 100 or 40 µmol/m^2/s, and root length and shoot area was assessed after 12 days.

There was no significant change in Col-0 root length in response to different light intensities (Figure 3.13 A). Although average shoot area appeared to be decreased in the low light condition this was not significant, and as such there was no significant change in Root/Shoot Ratio in Col-0 (Figure 3.13 B,C). *bhlh089 bhlh091* roots were significantly longer than WT when grown at 100 µmol/m^2/s. Under low light conditions root lengths were decreased in both *bhlh* double mutants, although the changes in *bhlh89,10* roots fell just beyond the significance threshold (q=0.059). Shoot area was significantly decreased in both *bhlh* mutants in low light and thus root to shoot ratio was significantly increased in *bhlh* double mutants in response to low light. However, aside from the increased length of *bhlh89,91* roots at 100 µmol/m^2/s, there were no other significant differences between Col-0 and *bhlh* double mutants within each light condition in any of seedling growth parameters (Figure 3.13).

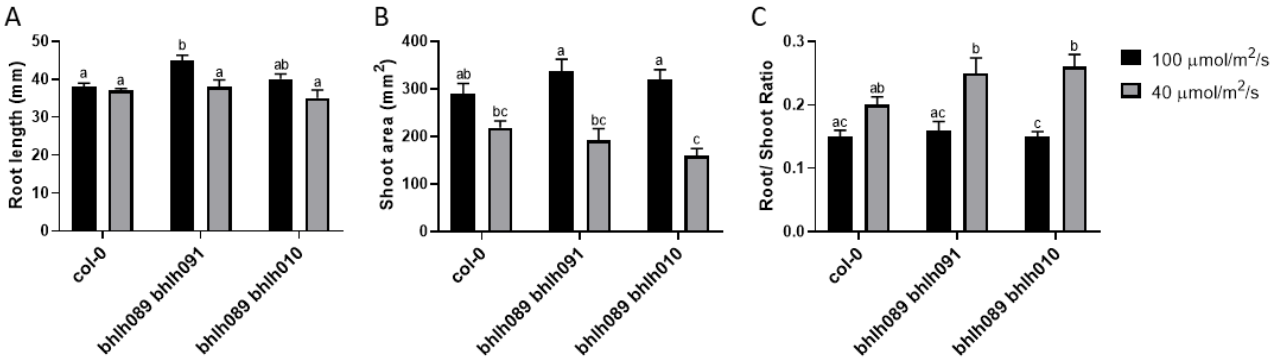

Figure 3.13. Seedling growth of bhlh double mutants in comparison to Col-0 at 100 and 40 µmol/m^2/s light intensity. Differences in A) Root lengths B) Shoot area and C) Root to Shoot Ratio of seedlings was determined by ANOVA with Tukey multiple comparisons test (q<0.05), n= 10-22.

3.3 DISCUSSION

3.3.1 Conditional sterility is more severe in *bhlh089 bhlh091* mutant

In this chapter, a novel light-sensitive conditional sterility phenotype for *bhlh89,10* and *bhlh89,91* double mutants has been presented and characterised.

Under normal light conditions, initial sterility of both for *bhlh89,10* and *bhlh89,91* double mutants is prolonged compared to WT Col-0. This extended period of sterility is consistent with Zhu *et al.* (2015)'s observation that the first flowers to develop on the *bhlh89,10* mutant were male sterile. However, whereas Zhu *et al.*'s study reported no such phenotypic abnormalities in *bhlh89,91*

developing flowers, our data suggests that initial sterility is more prolonged in the *bhlh89,91* mutant. This phenotype may have not been observed by Zhu *et al.*, because the location of the T-DNA insert in the bHLH91 CDS in our study may be more disruptive to bHLH91 function than the previous mutant, or possibly their growth conditions had a higher light intensity than 200 µmol/m^2/s. Given the flexibility of *bhlh89,91* fertility in response to light, the fertility defects observed in the *bhlh89,91* mutant may be totally masked if the light levels were higher, as is the case in the conditional sterility of the *myb33 myb65* double mutant (Millar and Gubler, 2005). Further study at increased light intensities would be valuable in elucidating the effect of light on fertility of *bhlh* double mutants.

Silique length was used as a proxy measure of fertility in this chapter as it is easily measured across a large dataset and closely correlates with seed number and flower fertility, as *Arabidopsis thaliana* is primarily self-pollinating. Silique lengths of all genotypes were reduced in low light but the seed-set relative to length remained consistent (Figure 3.3 E). Thus it seems that light directly affects fertility rather than silique elongation.

Whilst fertility of all lines were reduced in response to low light, with prolonged sterility and shorter siliques, the greatest effect was observed in the *bhlh89,91* mutant. Whereas Col-0 is fertile by position 6 and *bhlh89,10* exhibits recovery of fertility by position 20, there was minimal rescue in *bhlh89,91* (Figure 3.3D). Likewise, whilst pollen wall patterning is defective in the *bhlh89,10* mutant under low light, the pollen appears intact, whereas *bhlh89,91* pollen is misshapen, collapsed and non-viable (Figure 3.6). Thus it seems that, although previously thought to be functionally redundant, the bHLHs have a differential response to the light environment and bHLH91 in particular might be key to maintaining fertility in response to low light.

A key question is what causes the recovery of fertility, both in normal and low light conditions? Since there appears to be differences in initial fertility on secondary stems compared to primary and lateral stems (Figure 3.4) this may suggest a localised effect of light. As light intensity increases the closer the plants grow to the bulb (Chapter 2.1), and the secondary stems start growth at a greater height, it may be that increased light availability causes greater fertility higher up the plant. This could account for some of the fertility recovery seen.

The pollen wall is made up of two main components: the exine (the outermost and thickest layer of sculpture-like columella and tecta structures, containing sporopollenin) and the intine (made up of pectin, cellulose and proteins) (Shi et al., 2015). Lipid precursors to sporopollenin are secreted from the tapetum into the anther locule and are deposited between the plasma membrane and callose wall of microspores, forming the primexine matrix. Sporopollenin is then deposited and polymerized on this primary scaffold to form the exine wall with its sculptural tecta and baculae.

Whilst pollen autofluoresces due to phenols in the pollen exine in mature WT anthers (Roshchina, 2003), Zhu *et al.* (2015) reported no such autofluorescence in stage 11 triple and early *bhlh089 bhlh010* mutant anthers, indicating that bHLH089 and -010 may be involved in the regulation of pollen wall formation. In this chapter, observations of microspore stickiness and defective exine development in *bhlh* double mutants suggest defects in microspore wall development are aggravated in low light conditions. The early arrested development of double *bhlh* mutant microspores at single and bicellular stages in low light (Figure 3.5 D,E) further supports the hypothesis that microspore development is dependent on light-mediation of bHLH activity. Preceding this however, microspore development appears to progress at the same rate as WT, with microspore stages at comparable bud sizes in normal and low light conditions (Figure 3.5). In all lines tested pollen mother cells were present from ~0.4mm buds and meiosis was completed to leave tetrads by ~0.6mm just as previously reported (Chen et al., 2011b). Single microspore stage buds were all 1mm long or less, and buds undergo a sharp increase in size after pollen mitosis I.

Commonly microspore defects originate in abnormal tapetum development. Zhu *et al.* (2015) previously identified that the triple *bhlh089 bhlh010 amiR-bHLH091* mutant and early anthers of the *bhlh089 bhlh010* double mutant had an abnormally large, disorganised tapetum with increased vacuolation with respect to WT tissue and the *bhlh089 bhlh091* mutant. In this chapter Transmission Electron and Bright-field Microscopy of anther sections suggests that tapetum development was largely unaffected by light in Col-0. Conversely, the *bhlh89,91* tapetum becomes vacuolated and disorganised in response to low light conditions and shows increased lipid body accumulation within the tapetum and mature pollen (Figure 3.7 & Figure 3.8). This suggests a possible role for bHLHs in modulating lipid export from the tapetum into the locule and developing microspores in response to environmental signals.

Root and shoot growth in seedlings was unaltered compared to WT under different light conditions, suggesting that bHLH action in mediating light-responses is limited to reproductive processes.

3.3.2 bHLH expression at the transcript and protein level, what causes conditional sterility?

The *bhlh* double mutant fertility defects were aggravated in low light; therefore it can be hypothesised that bHLHs maintain fertility in response to changing light environments and that in order to do this there may be differential regulation of either transcription or translation of the bHLHs in response to light.

Orthologous bHLHs are known to be light-sensitive; pepper (*Capsicum annuum*) AMS expression is light responsive, with significantly higher *CaAMS* expression levels recorded by qRT-PCR in tetrad stage buds of dark-treated plants (Guo *et al*., 2018). In *Arabidopsis*, our RNAseq data shows that

bHLH transcripts are slightly reduced in response to low light, with *bHLH89*, *-91* and *-10* expressed at approximately 2/3 of normal levels. However, whilst *AMS* and *DYT1* were both downregulated in response to low light in Col-0 buds, this response was reduced in the *bhlh89,91* mutant for *DYT1* and lost completely for *AMS.* As for other transcription factors acting with tapetum development: *TDF1* was downregulated in response to low light in both WT and *bhlh89,91* mutant backgrounds but response was reduced in the latter, *MYB80* was downregulated in low light only in WT buds and *MS1* exhibited no change in response to light in either background. This suggests that low light modulates the *DYT1-TDF1-AMS-MYB80* transcriptional cascade, with bHLH89/91 activity involved in maintaining transcriptional response of *AMS* and *MYB80.*

Given that bHLH89, -91 and -10 have some degree of functional redundancy (Zhu et al., 2015), it is possible that within *bhlh* double mutants the reduced expression of the remaining functional bHLH91 or -10 in low light causes reduced fertility. However, the expression changes are relatively small, and there are no obvious differences in bHLH expression patterns in low light conditions (Figure 3.10), making it unlikely that minor transcriptional regulation would have such large effects on the fertility. Cui *et al.* (2016) previously demonstrated that bHLH89, -91 and -10 have distinct functions in regulating downstream genes. Therefore the different levels of conditional sterility seen within the two *bhlh* double mutants could also be indicative of bHLH10 and -91 fulfilling distinct roles in tapetum development, with bHLH91 playing a more important role in activation of downstream targets than bHLH10.

It is also likely that post-translational control may play a role in regulating bHLH activity, and this has been explored further in Chapters 5 & 6. In this chapter however, striking differences were demonstrated in the temporal expression of bHLH transcripts vs proteins, with bHLH-YFP translational reporters showing strict expression primarily in PMC and tetrad stages of anther development (Figure 3.12) whereas bHLH-GUS transcriptional reporter expression was more prolonged (Figure 3.10). This could suggest that bHLH proteins are more tightly regulated than their transcripts, or it may simply be that GUS activity is more stable.

Published RNA *in situ* hybridisation patterns of bHLH89/91/10 expression (Figure 3.10 I) show a weak signal in the tapetum and developing microspores at stage 5, increasing to peak at stage 7 (when the microspores are at the tetrad stage of development) and then falling back to background levels by stage 9 in microspores and stage 11 in the tapetum (Zhu *et al*., 2015). Our transcriptional reporters showed a similar expression pattern however bHLH-GUS expression was not observed at any point in the developing microspores at stages 5-11, although some pbHLH91-GUS expression was observed in mature pollen (Figure 3.10 H). Interestingly, expression atlas data suggests there is no expression

of bHLH091 in the mature pollen (RMA<4; Klepikova *et al.*, 2016). Endogenous GUS activity has been reported in the tapetum and pollen at later stages of anther development in untransformed tomato, potato and tobacco plants (Plegt and Bino, 1989; Alwen et al., 1992) and in WT Arabidopsis tissues, including pollen, under acidic conditions (Eudes et al., 2008). However, GUS expression was not seen in Col-0, *pbHLH10:GUS* or *pbHLH89:GUS* pollen and it is unlikely that the acidity of the *pbHLH091:GUS* samples differed from the other lines so consistently, as the same growth conditions and staining solution was used.

High protein turnover through Post-Translational Modification (PTM) may explain the temporal difference in transcript and protein expression patterns, and this was therefore explored further (Chapter 5 & 6). A number of PTMs are known to affect bHLH proteins including ubiquitination, phosphorylation, lysine acetylation, redox-dependant regulation and SUMOylation (Pireyre and Burow, 2015). Prolonged expression bHLH89-GFP signals in the *dyt1* mutant background (Figure 3.12) might indicate a role for DYT1 in regulating genes that contribute to post-translational regulation of bHLH levels.

Besides protein stability, differences in translational and transcriptional expression patterns of genes could also be due to transcriptional regulation, transcript stability and translation efficiency.

Interestingly, light levels have been reported to generally affect every level of regulation from transcript to protein. There have been multiple reports of bHLH transcript abundance being affected by light (Buti et al., 2020). PIF1 transcription, for example, has long been known to reduce upon exposure to light (Huq et al., 2004). Light has also been shown to induce expression of the non-DNA-binding bHLH PACLOBUTRAZOL RESISTANCE 3 (PRE3/bHLH135) and reduce the expression of its close homolog KIDARI (KDR/PRE6/bHLH163; Castelain, Le Hir and Bellini, 2012). CRYPTOCHROME INTERACTING BHLH 1 (CIB1) and another bHLH transcription factor are also upregulated by at least 2-fold in seedlings in response to white-light (Ma et al., 2001). Low R:FR light ratio of light has also been shown to induce rapid increases in multiple bHLH transcripts in hypocotyl and cotyledons (Kohnen et al., 2016).

Overall translational activity has also been shown to increase in light (Liu et al., 2012). Light intensity also has an effect on translation efficiency, with low light (25 µmol/m^2/s) causing a reduction in polysome abundance and dissociation of ribosomal subunits (Floris et al., 2013).

In terms of protein stability, rapid light-induced degradation of PIF1 protein is a prime example of how light quality and quantity affects bHLH protein stability: under red and far red light PIF1 is phosphorylated and ubiquitinated and thus targeted for degradation (Shen et al., 2008). Likewise,

phytochrome activation by light causes rapid ubiquitination and degradation of PIF1, -3,- 4 & -5 (Leivar and Quail, 2011). phyA, phyB, CRY1 and CRY2 photoreceptors have been shown to stabilise three partially redundant bHLH proteins MYC2, 3 & 4 in light, whereas in darkness they are targeted for proteasomal degradation through the E3 ubiquitin ligase CONSTITUTIVE PHOTOMORPHOGENIC1 (COP1) (Chico et al., 2014). Similarly, the floral transition master regulators CRY2- INTERACTING bHLH (CIB)1, -2 , -4 & -5 are degraded by the 26S proteasome in darkness, but stabilised in blue light (Liu et al., 2013).

As bHLH-FP expression appears to be increased in anthers in response to low light according to fluorescence intensity analysis, it is possible that bHLH proteins are stabilised in low light conditions. However this need to be investigated further using alternative methods of assessing protein levels, such as Western Blots.

3.4 CONCLUSIONS

Our results show that *bhlh089 bhlh010* and *bhlh089 bhlh091* double mutants exhibit conditional sterility in response to a low light environment (50 µmol/m^2/s), with microspore development halting just after pollen mitosis I and defects in pollen wall formation. This phenotype is more severe in *bhlh89,91* than *bhlh89,10*, with a prolonged sterility, thus demonstrating that the three bHLHs are not fully redundant as previously thought and instead have distinct roles in maintaining fertility in response to environmental variation.

Differences in bHLH transcript vs protein expression patterns suggest that post-translational modifications may play a key role in regulating bHLH function in response to light, and this will be explored further in subsequent chapters.

4 TRANSCRIPTIONAL RESPONSE OF *BHLH089 BHLH091* TO LOW LIGHT

4.1 INTRODUCTION

As sessile photoautotrophs, the ability to adapt growth to the availability of light is essential to the survival of plants. In nature, shade is characterised not only by low-light intensities but also by the spectral quality of the light. In direct sunlight, plants receive equal amounts of blue, red and far-red (FR) light as well as some UV-B. However, a leafy plant canopy will absorb UV-B, red and blue, transmitting only FR light to the plants shaded below. This high proportion of FR light and reduction in blue light is sensed by photoreceptors (phytochromes and cryptochromes respectively) and activates what is known as the shade-avoidance response, comprised of major changes to plant growth and development: notably elongation growth and accelerated flowering.

bHLH proteins are intrinsically involved in the shade-avoidance responses, often directly interacting with various photoreceptors (Buti et al., 2020; Figure 4.1B). Although the PHYTOCHROME INTERACTING FACTORS (PIFs) are perhaps the most well-known in terms of their light-response, many other bHLH sub-families such as ATB1-INTERACTING FACTOR (AIF), BR ENHANCED EXPRESSION (BEE), BES1-INTERACTING MYC-LIKE (BIM), PACLOBUTRAZOL RESISTANCE (PRE) and PHYTOCHROME RAPIDLY REGULATED (PAR) proteins play equally important roles in shade-induced hypocotyl elongation and even, in the case of the BEEs, light-mediated control of floral transition (Buti et al., 2020; Figure 4.1A).

Shade-avoidance is associated with considerable phytohormonal changes, with major roles played by auxin, gibberellic acid (GA), brassinosteroids and ethylene in shade-induced elongation and secondary responses governed by cytokinins, abscisic-, salicylic- and jasmonic- acids (ABA, SA, JA) (Yang and Li, 2017; Figure 4.1C). Often these hormonal responses to shade are dependent on bHLH proteins (Buti et al., 2020).

GA is a prime example of the intrinsic link between shade, phytohormones and bHLHs. Under normal light conditions PIFs are bound by DELLA proteins, preventing them from interacting with E-box motifs on target DNA. In shaded conditions expression of GIBBERELLIN20-OXIDASE1 (GA20ox1) and -2 is induced (Hisamatsu et al., 2005), catalysing the biosynthesis of bioactive GA, increasing GA levels which in turn lead to degradation of DELLA proteins. This derepression of the PIFs under low-light conditions enables them to activate transcription of target DNA and induce many of the changes associated with shade avoidance (De Lucas et al., 2008).

The PIFs also play a vital role in mediating auxin levels, promoting auxin biosynthesis through upregulation of YUCCA8 and 9 (Hornitschek et al., 2012; Li et al., 2012), which catalyse the conversion of IPA (indole-3-pyruvic acid) to IAA (indole-3-acetic acid). In addition to biosynthesis, auxin sensitivity is conferred through Auxin Response Factors (ARFs) which have been found to be important regulators of bHLH action, through heterodimerisation and promoter-binding (Oh et al., 2014).

Many transcriptome studies have been carried out on the effect of shade on seedlings, leaves and axillary buds (Sellaro et al., 2017). However, to my knowledge, none of these studies have looked at transcriptional changes in the inflorescence if shading occurs after floral transition during reproductive development.

As reported in the previous chapter, low light has a significant effect on fertility of the *bhlh089 bhlh091* mutant. In this chapter, an RNAseq study is presented with the aim of understanding the transcriptional changes in low light grown inflorescences in order to underpin the role that the bHLHs play in flower development under sub-optimal conditions.

Since the transcriptome changes associated with a number of the male sterile mutants have been well characterised, with microarray data available for *dyt1* (Feng et al., 2012), *tdf1* (Lou et al., 2017), *ams* (Xu et al., 2010; Ma et al., 2012), *myb80* (Phan et al., 2011), *ms1* (Yang et al., 2007) and *bhlh089 bhlh010 amiR-bHLH091* (Zhu et al., 2015) mutants, differential gene expression within the partially sterile *bhlh089 bhlh091* mutant was compared to transcriptomic data from other fully male sterile mutants.

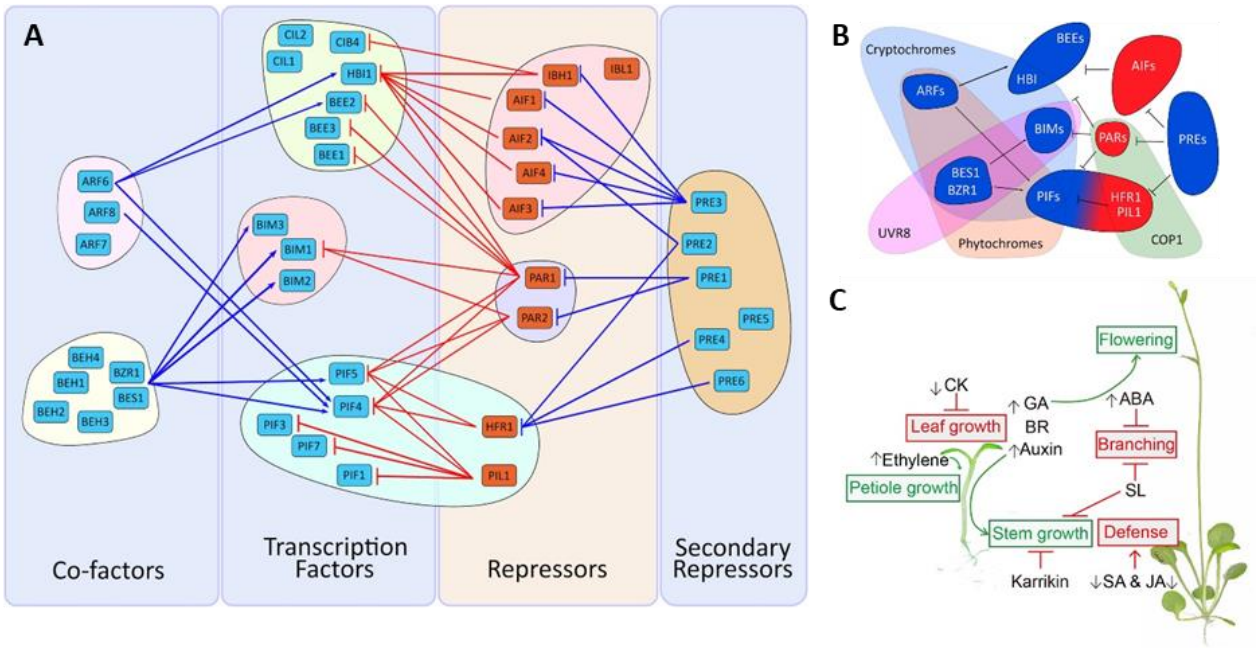

Figure 4.1. Mechanisms underlying the shade-avoidance response. A) bHLH transcription factors and their co-factors involved in shade-avoidance response. B) Interaction between photoreceptors and bHLH proteins. C) Hormonal regulation in shade-avoidance. A & B from Buti et al. (2020), C from Yang & Li (2017).

4.2 RESULTS

4.2.1 Low light treatment leads to major transcriptional changes in wild-type Col-0 that are absent in the *bhlh089 bhlh091* mutant

Expression analysis was conducted using the *bhlh089 bhlh091* double mutant since it showed the strongest conditional sterility in response to low light in comparison to WT (Section 3.2.1, 3.2.2), RNA was isolated from pre-mitosis I stage buds from Col-0 and *bhlh089 bhlh091* plants grown under normal and low light conditions (200 and 50 µmol/m^2/s respectively). RNA quality was assessed using an Agilent 2100 Bioanalyzer, all samples were of high quality and sufficient concentrations, absorbance and integrity (RNA Integrity Number (RIN) ≥ 9). Thus these 4 factor groups (*bhlh089 bhlh091* Low, *bhlh089 bhlh091* Norm, Col-0 Low, Col-0 Norm), each with 4 biological replicates, were sequenced using the BGISEQ-500 platform (BGI). Cleaned reads were mapped to *Arabidopsis thaliana* Reference Transcript Dataset 2 (AtRTD2; Zhang *et al.*, 2017) and then read counts and transcript per million reads (TPMs) were generated using tximport in R and normalised by the TMM method (Bullard et al., 2010).

Principal Component Analysis (PCA) of RNAseq data showed that under normal light conditions Col-0 and the *bhlh089 bhlh091* mutant exhibit minimal variation, and cluster in the PCA plot (Figure 4.2 A). Both Col-0 and the *bhlh089 bhlh091* mutant show separation of principal components between light treatments, into distinct principal component space. This is reflected in the number of Differentially Expressed Genes (DEGs). A total of 2492 genes were identified as differentially expressed under

different light conditions and between the lines, with log_2 Fold Change (log_2FC)≥1, and Benjamini-Hochberg FDR-adjusted p value (q)≤0.01 (Figure 4.2 B). In keeping with the PCA plot, there are only 289 DEGs showing differential expression under normal light conditions between the *bhlh089 bhlh091* double mutant and Col-0 (*bhlh089 bhlh091* Norm- Col-0 Norm), compared to 1300 DEGs changing between the two lines under low light conditions (*bhlh089 bhlh091* Low- Col-0 Low).

The *bhlh* mutant shows reduced transcriptional response to low light than WT, with 1853 and 634 DEGs in Col-0 and *bhlh089 bhlh091* respectively (Figure 4.2 D). Only 396 DEGs are common between Col-0 and *bhlh089 bhlh091* at 50 µmol/m^2/s compared to 200 µmol/m^2/s (Figure 4.2 E). This is further echoed at the transcript level where there are 1914 light-responsive DE transcripts in Col-0 compared to 406 in *bhlh089 bhlh091* (Figure 4.2 F), of which only 263 are common. Differential Alternative Splicing (DAS) and Differential Transcript Usage (DTU) of transcripts also fall drastically in the *bhlh* mutant compared to WT (Figure 4.2 G, H).

According to hierarchical clustering, DEGs can be arranged into 10 clades (Figure 4.2 C). Generally clusters 2 & 9 contain genes with very similar responses to light in both Col-0 and the *bhlh089 bhlh091* mutant whereas clusters 5, 6 & 8 show transcriptional changes in low light Col-0 that are absent or reduced in *bhlh089 bhlh091*. Clusters 1 & 7 contains DEGs that seemingly are most responsive in *bhlh089 bhlh091* low and normal light treatments respectively. Clusters 3 & 10 contains DEGs that are differentially regulated between Col-0 and *bhlh089 bhlh091*, regardless of light.

Initial Gene Ontology (GO) enrichment analysis revealed that processes such as response to stimulus and stress and phenylpropanoid biosynthesis and metabolism were enriched in the 2492 DEGs (Figure 4.3). Focusing in on GO enrichment per cluster an overrepresentation of some key GO terms were seen, including a large number related to stress and phytohormone responses and signalling (Figure 4.4). There is significant enrichment of response to cold, water deprivation, osmotic stress, chitin and abscisic acid (ABA) in cluster 2, and enrichment of flavonoid biosynthetic process in cluster 9, suggesting that DEGs related to these terms are functioning the same in *bhlh089 bhlh091* and WT light-response. However, a significant enrichment of GO terms such as circadian rhythm, SCF-dependent proteasomal ubiquitin-dependent catabolic process, sexual reproduction, lipid storage, oxidation-reduction process and glucose import were observed in clusters 5, 6 & 8 suggesting that DEGs related to these terms differentially respond to light in *bhlh089 bhlh091*.

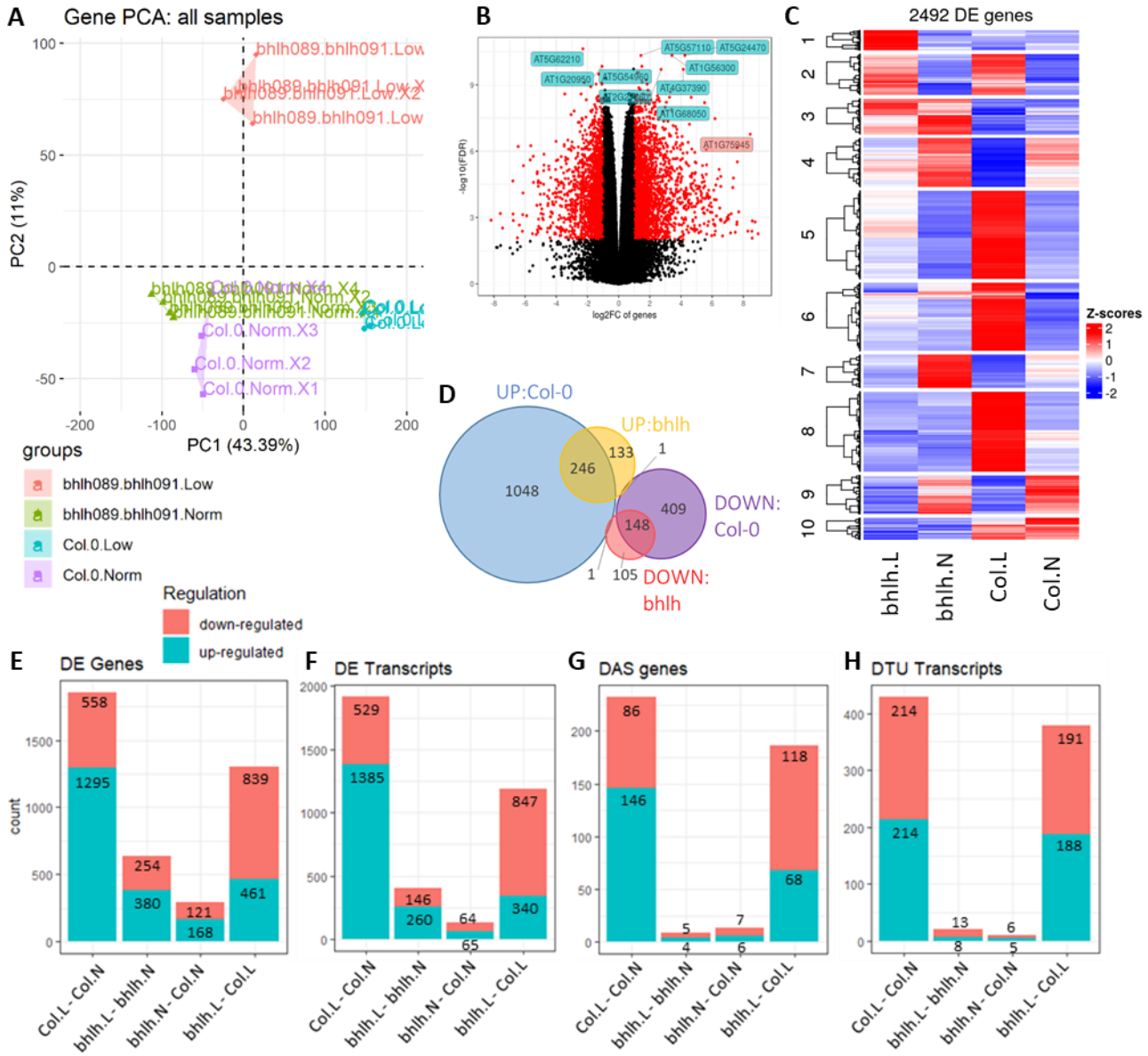

Figure 4.2. Differentially Expressed Genes (DEGs) in Col-0 and the bhlh089 bhlh091 mutant under normal and low light conditions as determined by RNAseq. A) PCA plot showing variance of samples within the RNAseq dataset. Aggregation of Col-0 and bhlh089 bhlh091 mutant samples grown in normal light conditions (purple and green respectively) shows high similarities in gene expression whereas major differences are suggested in the segregation of low light Col-0 (blue) and bhlh089 bhlh091 (red). Crucially each sample group shows a tight distribution, indicating that there are no big outliers in the dataset. B) Volcano plot showing log_2FC of genes against –log10(FDR adjusted P values), red dots indicate significant DEGs with $|log_2FC|>1$ ($q \leq 0.01$) and black dots represent non-DEGs. C) Heatmap of DEG expression, within each factor group, partitioned by hierarchical clustering with Ward's algorithm and Euclidean distance. D) Overlap of up- and down-regulated DEGs in response to light in Col-0 (Col.L-Col.N) and bhlh089 bhlh091 (bhlh.L-bhlh.N). E-H) For each contrast group, number of up- and down-regulated DEGs (E), DE transcripts (F), Differential Alternative Splicing (DAS) genes (G) and Differential Transcript Usage (DTU) transcripts (H). DAS and DTU were identified with a Δ Percent Spliced (ΔPS) ratio ≥ 0.1, $q<0.01$.

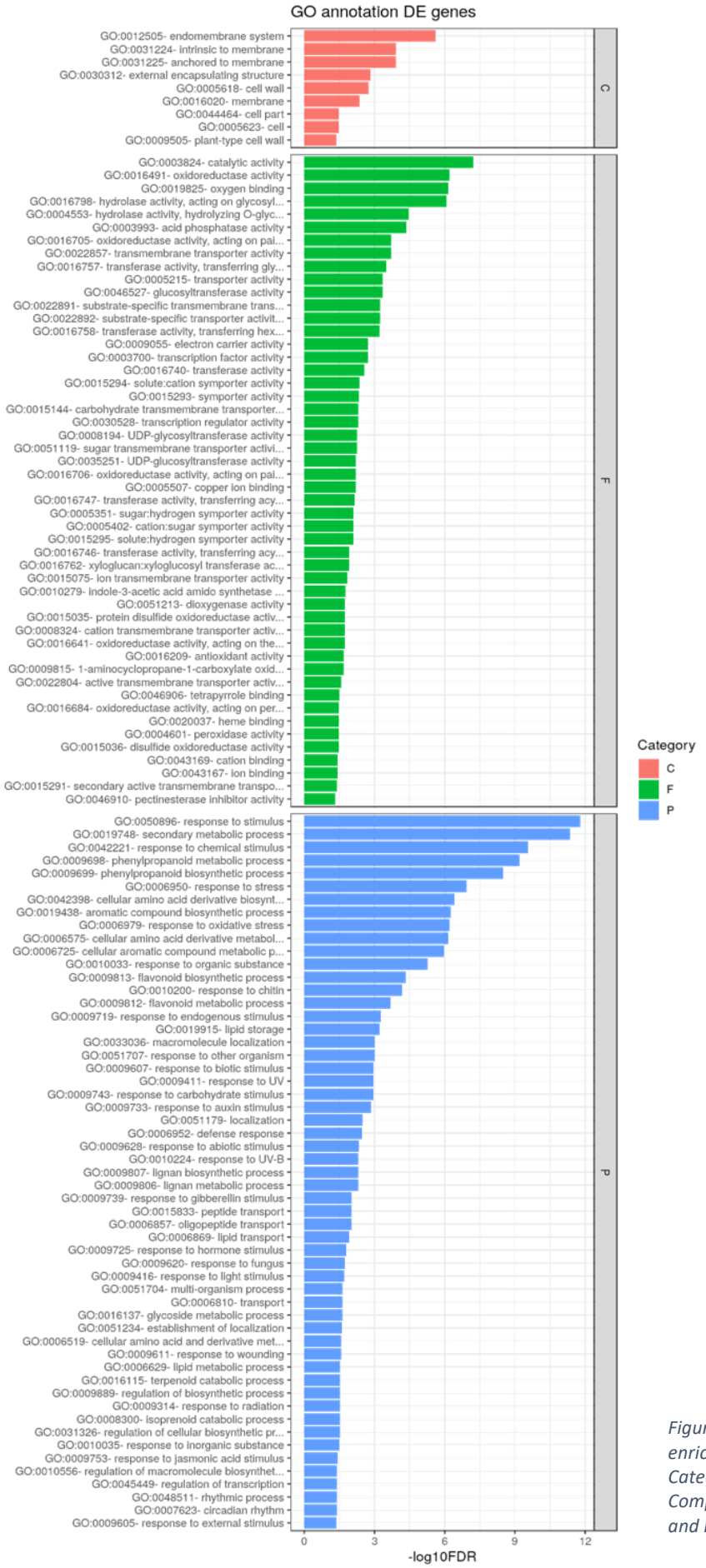

Figure 4.3. Gene Ontology (GO) enrichment analysis of all DEGs. Categories represent Cellular Component (C), Molecular Function (F) and Biological Process (P)

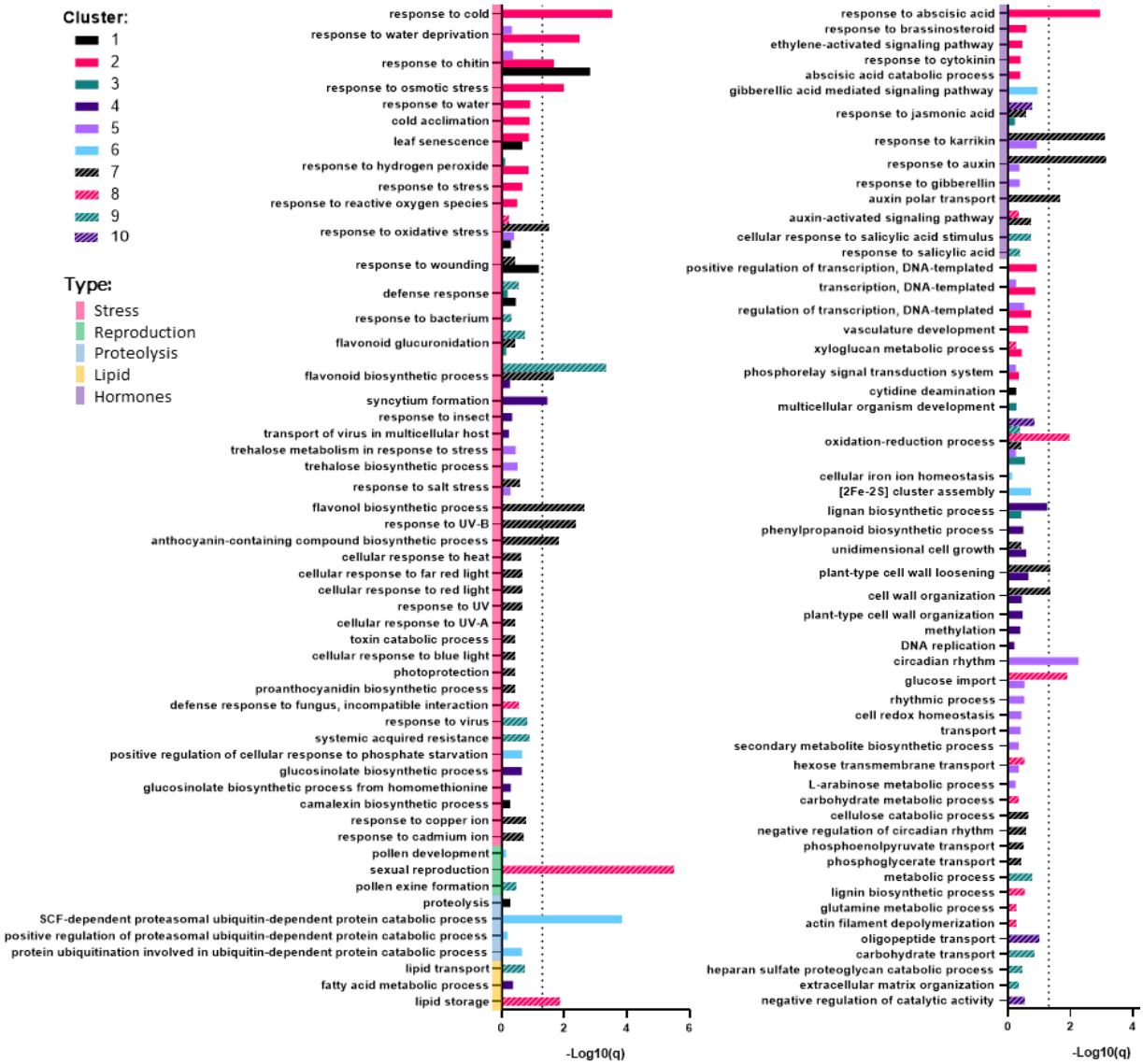

Figure 4.4. Significant GO terms per cluster identified in Figure 4.2C (p<0.05), q is the p-value adjustment by Benjamini method and dotted line at q=0.05 represents the stricter significance threshold.

Closer analysis of light-sensitive DEGs, i.e. those with a $log_2FC>2$ between normal and low light in Col-0 (543 DEGs), was undertaken to further investigate the WT response to light in pre-mitotic buds. This found highly significant (Benjamini-adjusted p-value (q)<0.05) GO term enrichment of biological processes such as sexual reproduction, lipid storage & metabolism, circadian rhythm, response to oxidative stress, oxidation-reduction process and response to auxin (Figure 4.5). The DEGs show significant enrichment in the cellular compartments: monolayer-surrounded lipid storage body, extracellular region, membrane, integral component of plasma membrane and pollen coat. Significant enrichment of acid phosphatase activity, lipid binding and monooxygenase activity molecular functions are also seen in WT.

Comparing WT with $log_2FC>2$ changes in the *bhlh089 bhlh091* mutant (187 DEGs), there is differential enrichment of GO terms (Figure 4.5). Interestingly, many of biological processes highlighted in Col-0 are not enriched in *bhlh089 bhlh091* mutant in response to low light. Notably sexual reproduction, lipid storage & metabolism, spermidine biosynthesis and responses to hormones such as auxin, jasmonic acid, ethylene and gibberellin lose significant enrichment in the *bhlh* mutant light response. Instead there is significant enrichment of biological processes such as response to cold, karrikin, bacterium and cellular response to heat in *bhlh089 bhlh091* (q<0.05).

The total 2492 DEGs, identified in the RNAseq as differentially expressed in at least one of the 4 contrast groupings, map to a number of different KEGG pathways, with the most significant being phenylpropanoid biosynthesis, biosynthesis of secondary metabolites and flavonoid biosynthesis (Table 4.1). Many of these KEGG pathways show big differences in light-responsive transcriptional changes between Col-0 and *bhlh089 bhlh091*. The Phenylpropanoid biosynthetic pathway is a prime example of this (Figure 4.6) with multiple pathways, for example biosynthesis of spermidine, exhibiting differential gene expression in Col-0 low-light but are unchanged in low-light in the *bhlh* mutants. Likewise, the *bhlh* mutant shows losses of differential regulation in Cutin, Suberine and Wax biosynthesis pathways (Figure 4.7).

Figure 4.5. GO enrichment of biological processes in Col-0 and bhlh089 bhlh091 normal vs low light DEGs (p<0.01). Colour scale represents -log10(q) where q is the p-value adjusted by the Benjamini method.

Table 4.1. KEGG pathway enrichment of total DEGs shown in order of significance. % refers to involved genes (count)/total DEGs, the q value is the p-value adjustment by the Benjamini method. Pathways considered significant according to p<0.05 are highlighted in yellow, whereas green highlights the stricter significance threshold of q<0.05.

KEGG pathway	Count	%	p value	q value
Phenylpropanoid biosynthesis	38	1.55	0.000	0.000
Biosynthesis of secondary metabolites	125	5.11	0.000	0.000
Flavonoid biosynthesis	11	0.45	0.000	0.000
Starch and sucrose metabolism	25	1.02	0.000	0.002
Plant hormone signal transduction	40	1.63	0.000	0.005
Metabolic pathways	185	7.56	0.000	0.005
Cutin, suberine and wax biosynthesis	9	0.37	0.001	0.017
Galactose metabolism	12	0.49	0.005	0.061
Diterpenoid biosynthesis	7	0.29	0.007	0.086
Circadian rhythm - plant	9	0.37	0.008	0.082
Amino sugar and nucleotide sugar metabolism	20	0.82	0.014	0.134
Tyrosine metabolism	9	0.37	0.015	0.128
Alanine, aspartate and glutamate metabolism	10	0.41	0.015	0.121
Phenylalanine metabolism	9	0.37	0.019	0.145
Nitrogen metabolism	9	0.37	0.019	0.145
Cyanoamino acid metabolism	10	0.41	0.055	0.344
Fructose and mannose metabolism	10	0.41	0.066	0.377
Zeatin biosynthesis	5	0.20	0.077	0.407
Carotenoid biosynthesis	6	0.25	0.086	0.424

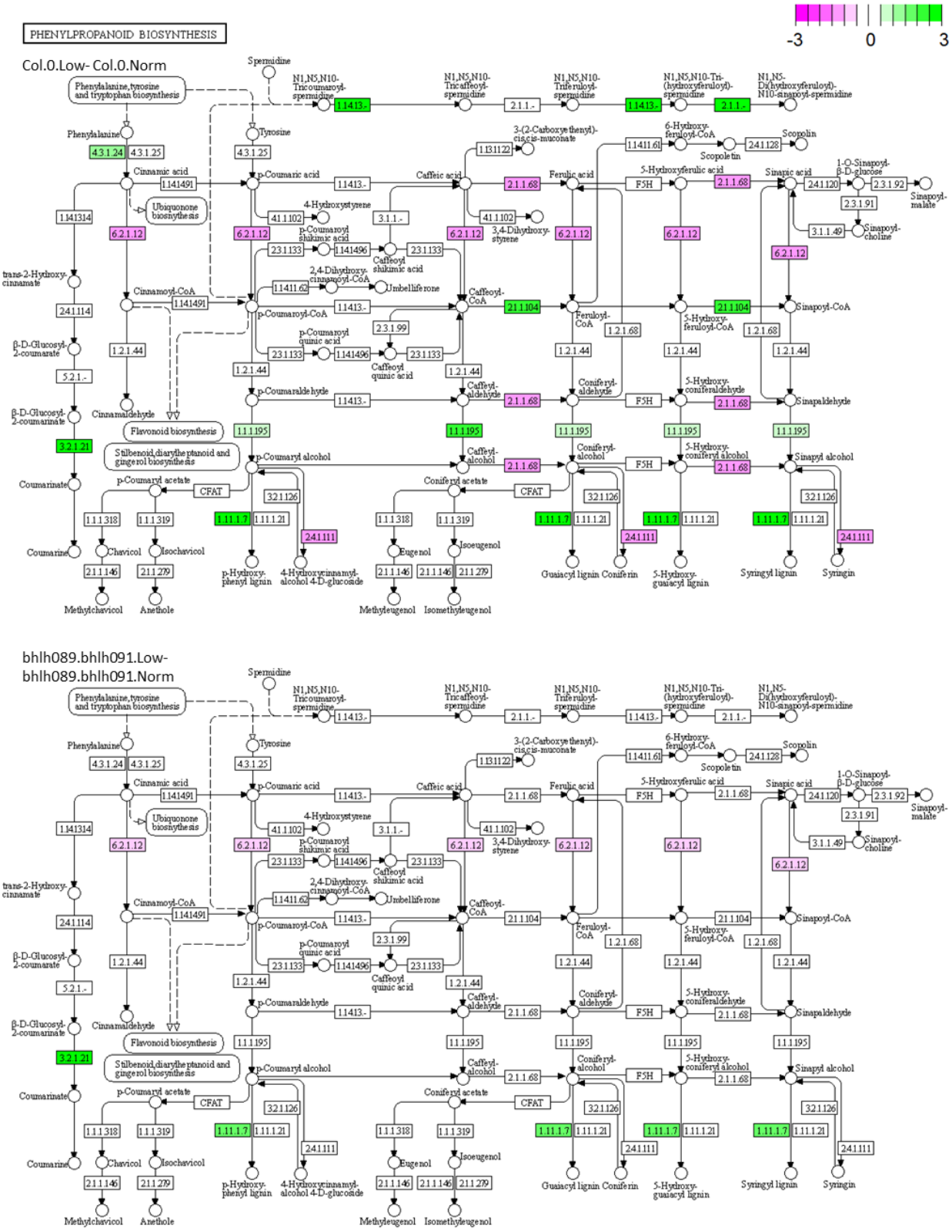

Figure 4.6. Phenylpropanoid biosynthesis KEGG pathway with fill colour showing log_2FC of low-light upregulated (green) and downregulated (magenta) DEGs in Col-0 (top) and bhlh89,91 mutant (bottom). Cut-off for significant DEGs $log_2FC>1$, $q<0.01$. Plot created using Pathview in R.

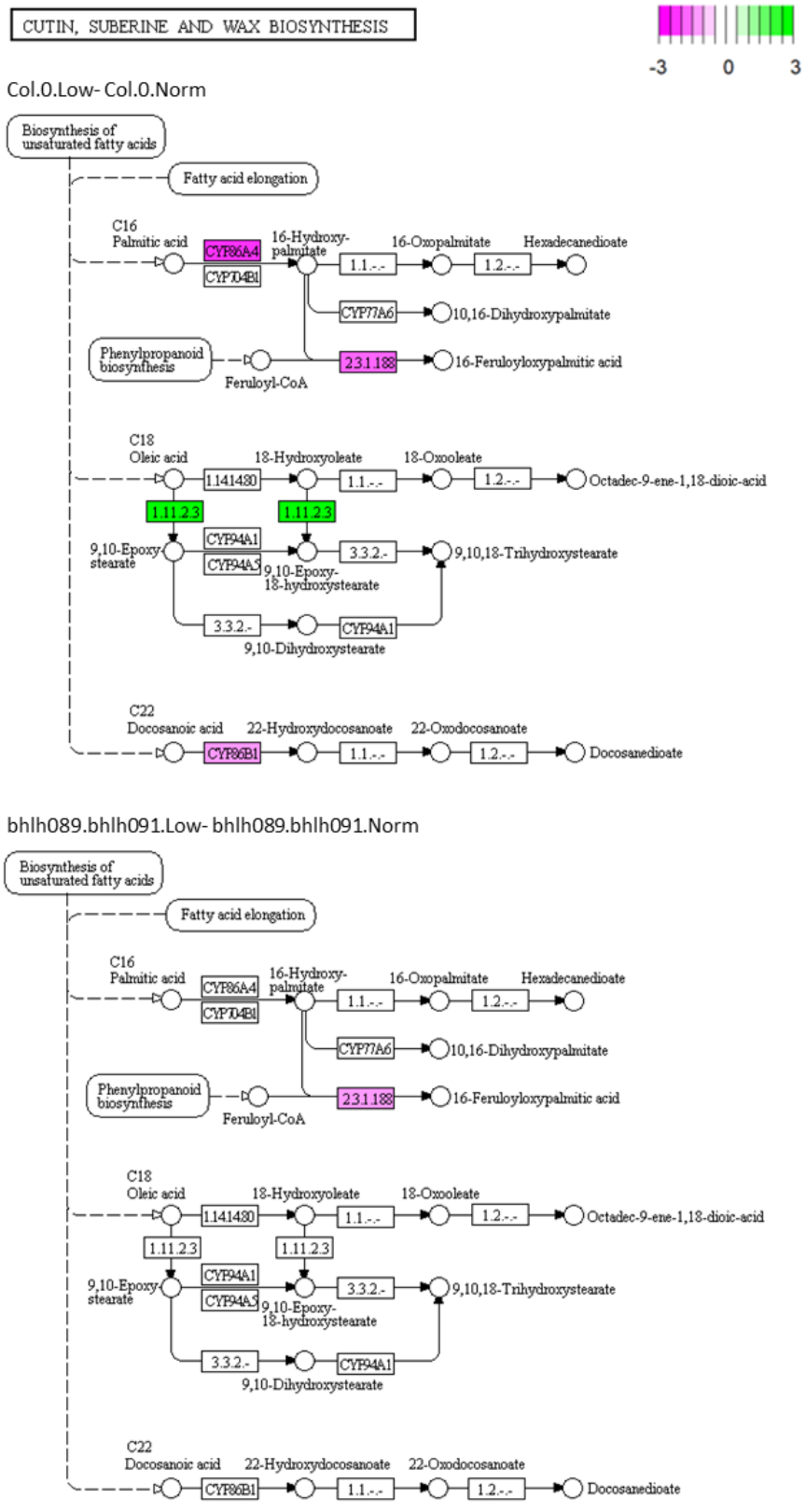

Figure 4.7. Cutin, Suberine and Wax biosynthesis KEGG pathway with fill colour showing log_2FC of low-light upregulated (green) and downregulated (magenta) DEGs in Col-0 (top) and bhlh89,91 mutant (bottom). Cut-off for significant DEGs $log_2FC>1$, $q<0.01$. Plot created using Pathview in R.

4.2.2 Phytohormone signal transduction is reduced in the *bhlh089 bhlh091* mutant

The Plant Hormone Signal Transduction KEGG pathway shows upregulation of genes involved in auxin, cytokinin and ABA signalling in Col-0 in low light that are altered, or absent, in the *bhlh089 bhlh091* mutant (Figure 4.8). The auxin signalling components AUXIN/INDOLE-3-ACETIC ACID (AUX/IAA)s are upregulated in response to low light in Col-0, but downregulated in *bhlh089 bhlh091*. WT upregulation of Small Auxin Upregulated RNAs (SAURs) appears to be absent in the *bhlh89,91* mutant according to Figure 4.8. However, if you look at the differential expression of all SAUR genes in the RNAseq dataset (Table 4.2) there is in fact some downregulation of specific SAURs in *bhlh089 bhlh091* low light that is not seen in Col-0. There is also differential regulation of Gretchen Hagen3 family proteins, which are crucial to IAA-conjugation and thus inactivation of auxin response.

The Pathview plots also imply a major reduction in ABA signal transduction in the *bhlh* mutant (Figure 4.8), starting with downregulation of the ABA sensors PYRABACTIN RESISTANCE 1 (PYR1)-LIKE 2 (PYL2) & -11 under low light conditions in Col-0, however there is upregulation of PYL5 in the transcriptome (Table 4.2). Further upregulation is seen within the PP2Cs, ABA INSENSITIVE 2 (ABI2) and ABI5, and SUCROSE NON-FERMENTING 1 (SNF1)-RELATED PROTEIN KINASE 2.3 (SNRK2.3) & SNRK2.9. Outside of the signal transduction pathway there is differential regulation of ABSCISIC ALDEHYDE OXIDASE 3 (AAO3).

It also appears from Figure 4.8 that Ethylene response is differentially regulated in Col-0 and *bhlh089 bhlh091*, with upregulation of ETHYLENE RESPONSIVE FACTOR 2 (ERF2) in low light only highlighted in the *bhlh089 bhlh091* mutant. However, looking on an individual gene basis (Table 4.2), the situation is far more complex with differential expression of multiple ERFs.

Small changes are seen in the signal transduction pathways of JA and Cytokinin. With the latter upregulation of type-A and type-B ARABIDOPSIS RESPONSE REGULATORS (ARRs) was observed in Col-0 under low light, whereas ARRs are unchanged in the *bhlh* mutant. There was also upregulation of JAR1 only in the WT JA signalling pathway.

The KEGG pathview plots show no significant differences in GA signalling in response to light in WT or mutant inflorescences. However, further analysis revealed changes at the level of Diterpenoid biosynthesis (Figure 4.9). These differences between Col-0 and *bhlh089 bhlh091* arise from the start of the GA biosythesis pathway, with the upregulation of GA REQUIRING 1 (GA1) in Col-0 low light, which is absent in *bhlh089 bhlh091*. Later in the same pathway there is differential regulation of various GIBBERELLIN 2- & 20-OXIDASES (GA2OX / GA20OXs; Table 4.2). Differential expression is also seen in the GA transporters: *NITRATE TRANSPORTER 1/PEPTIDE* (*NPF*) and *SUGARS WILL EVENTUALLY BE EXPORTED TRANSPORTER (SWEET)* genes.

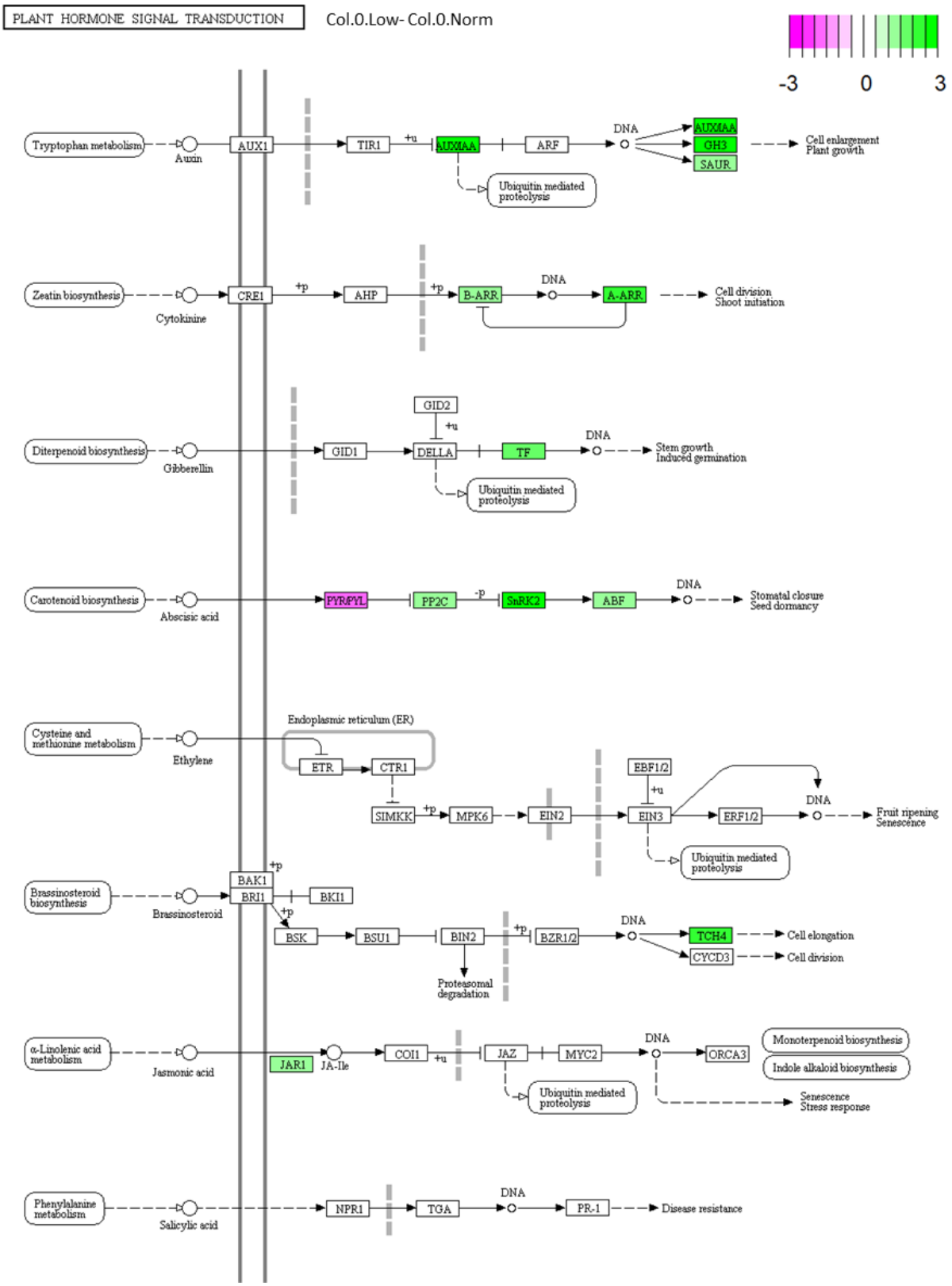
PLANT HORMONE SIGNAL TRANSDUCTION
Col.0.Low- Col.0.Norm
-3
0
3
Tryptophan metabolism
Auxin
AUX1
TIR1
+u
AUXIAA
ARF
DNA
AUXIAA
GH3
SAUR
Cell enlargement
Plant growth
Ubiquitin mediated proteolysis
Zeatin biosynthesis
Cytokinine
CRE1
+p
AHP
+p
B-ARR
DNA
A-ARR
Cell division
Shoot initiation
Diterpenoid biosynthesis
Gibberellin
GID2
+u
GID1
DELLA
TF
DNA
Stem growth
Induced germination
Ubiquitin mediated proteolysis
Carotenoid biosynthesis
Abscisic acid
PYR/PYL
PP2C
-p
SnRK2
ABF
DNA
Stomatal closure
Seed dormancy
Cysteine and methionine metabolism
Ethylene
Endoplasmic reticulum (ER)
ETR
CTR1
SIMKK
+p
MPK6
EIN2
EBF1/2
+u
EIN3
ERF1/2
DNA
Fruit ripening
Senescence
Ubiquitin mediated proteolysis
Brassinosteroid biosynthesis
Brassinosteroid
+p
BAK1
BRI1
BKI1
+p
BSK
BSU1
BIN2
+p
BZR1/2
DNA
TCH4
Cell elongation
CYCD3
Cell division
Proteasomal degradation
α-Linolenic acid metabolism
Jasmonic acid
JAR1
JA-Ile
COI1
+u
JAZ
MYC2
DNA
ORCA3
Monoterpenoid biosynthesis
Indole alkaloid biosynthesis
Ubiquitin mediated proteolysis
Senescence
Stress response
Phenylalanine metabolism
Salicylic acid
NPR1
TGA
DNA
PR-1
Disease resistance

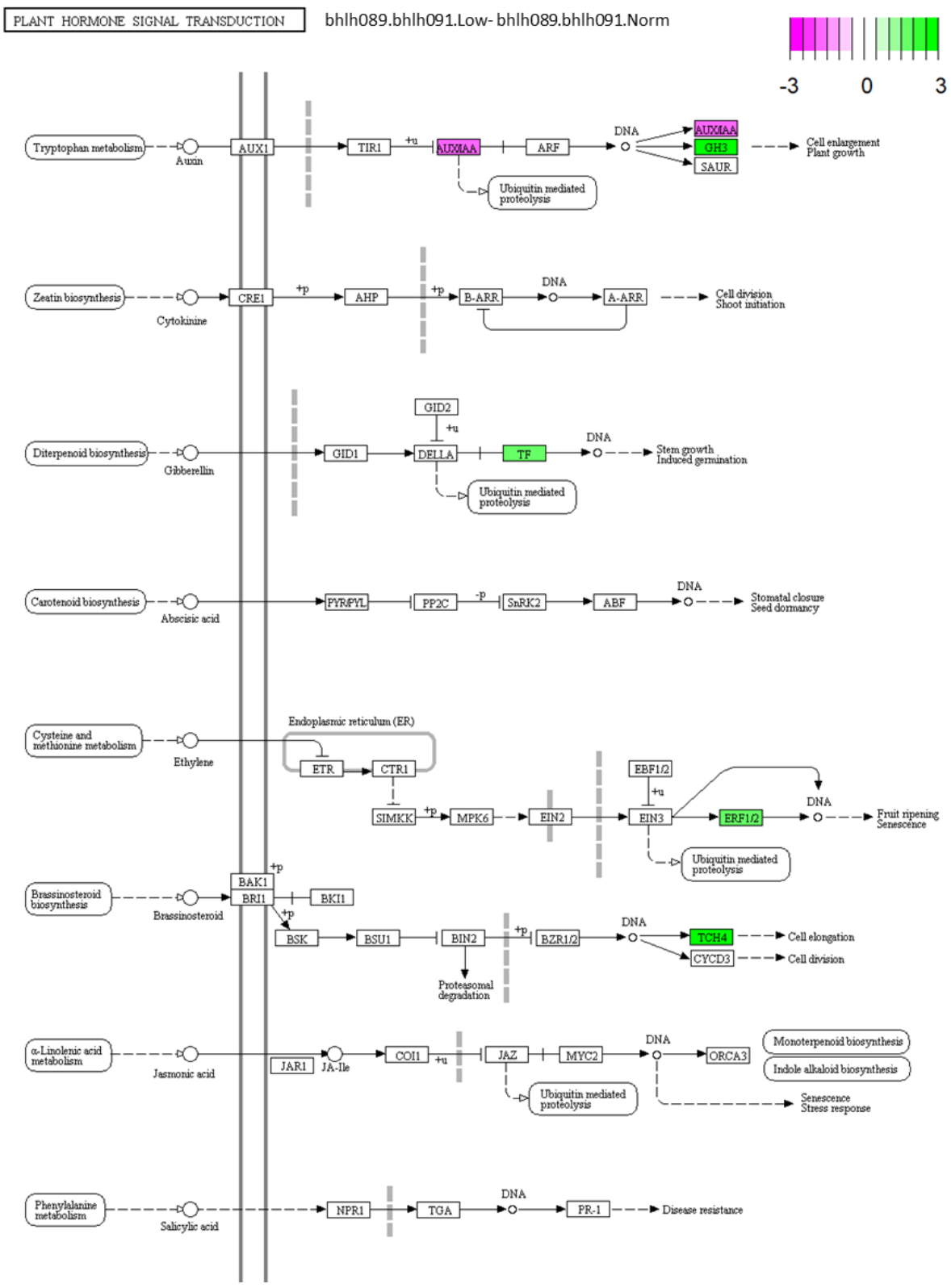

Figure 4.8, continued from previous page. Plant Hormonal Signal Transduction KEGG pathway showing changes in DEGs involved in Auxin, Cytokinin, ABA and JA signalling pathways in low light in Col-0 that are absent or altered in the bhlh089 bhlh091 mutant. Fill colour intensity is indicative of low-light upregulated (green) and downregulated (magenta) DEGs in Col-0 (top) and bhlh89,91 mutant (bottom). Cut-off for significant DEGs $log_2FC>1$, $q<0.01$. Plot created using Pathview in R.

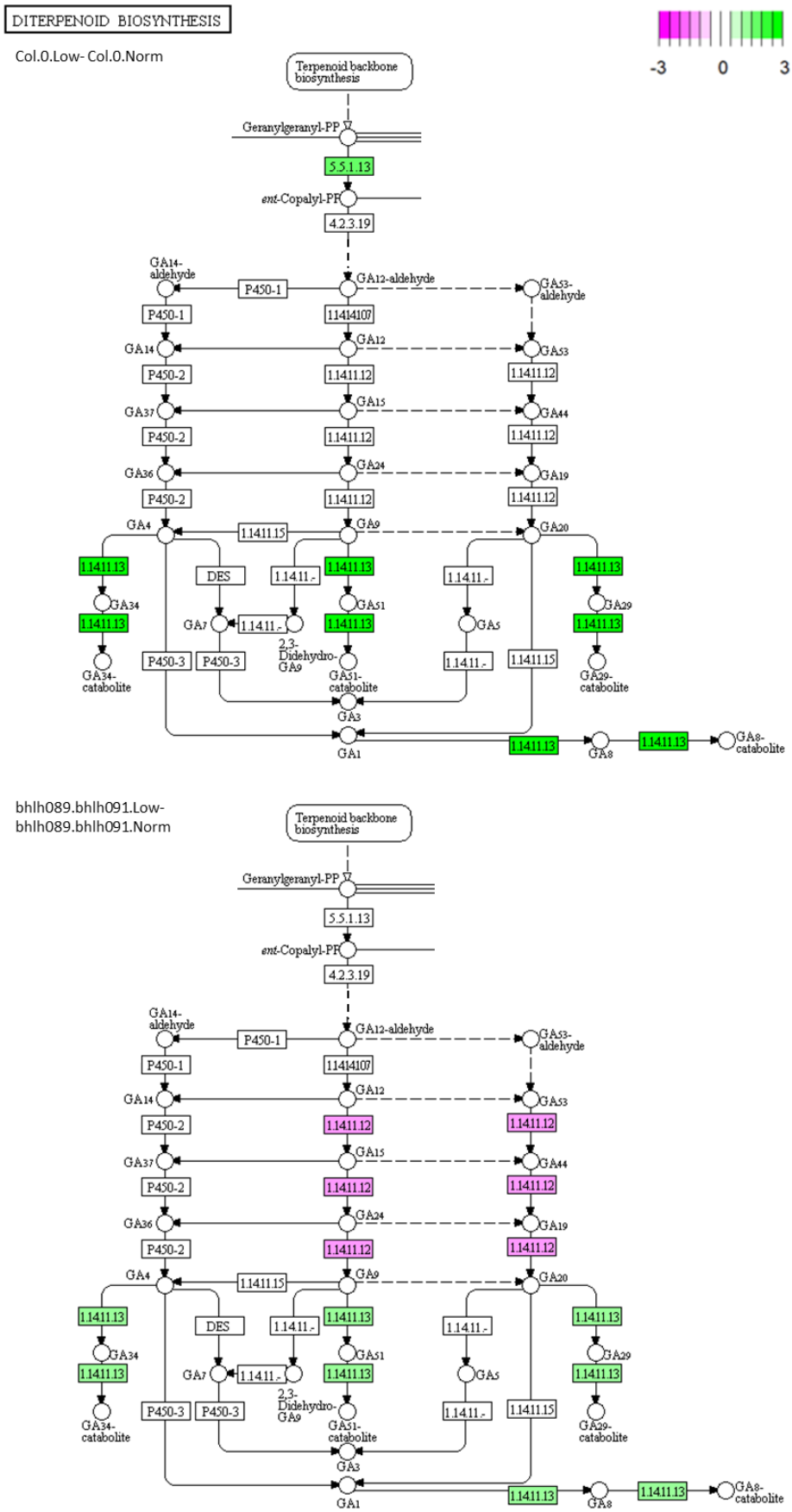

Figure 4.9. Diterpenoid biosynthesis KEGG pathway, fill colour represents log_2FC of low-light upregulated (green) and downregulated (magenta) DEGs in Col-0 (top) and bhlh89,91 mutant (bottom). Cut-off for significant DEGs $log_2FC>1$, $q<0.01$. Plot created using Pathview in R.

Table 4.2. Log$_2$FC of hormone responsive and biosynthetic genes under low vs. normal light conditions in Col-0 and bhlh089 bhlh091 mutant buds. Red indicates upregulation, in low light or bhlh mutant, blue shows downregulation and blank indicates no significant changes (q>0.01)

Hormone	Loci	Gene	col.L_col.N	bhlh.L_bhlh.N	bhlh.N_col.N	bhlh.L_col.L
Auxin	AT2G23170	GH3.3	2.3			-2.9
	AT4G27260	GH3.5	2.3	1.6	-0.8	-1.5
	AT5G54510	GH3.6	1.3	0.9		
	AT2G47750	GH3.9	1.1			-1.0
	AT1G28130	GH3.17	1.2			-0.9
	AT1G48670	GH3 family	-2.8			2.0
	AT5G13380	GH3 family	1.8			-3.7
	AT2G46370	JAR1	1.2			-1.2
	AT4G37390	YDK1	4.1	1.5		-3.5
	AT4G14560	IAA1	1.1			-1.2
	AT3G23030	IAA2	2.2			-1.9
	AT5G43700	IAA4	1.8			-1.5
	AT4G14550	IAA14	2.0			-1.5
	AT1G04250	IAA17	-1.3	-1.7	0.8	
	AT3G15540	IAA19	1.4			-1.0
	AT2G46990	IAA20	1.1			
	AT2G01200	IAA32	1.7			-1.3
	AT5G57420	IAA33	-2.2	-1.4		1.9
	AT2G17500	PILS5	-1.2	-1.2	0.5	0.5
	AT5G16530	PIN5	-0.9	-1.2	0.9	
	AT4G34790	SAUR3	1.4			
	AT2G16580	SAUR8	-1.5	-0.8		0.8
	AT2G46690	SAUR32	1.8			-1.5
	AT1G16510	SAUR41				-1.1
	AT5G03310	SAUR44	3.3			-2.4
	AT3G09870	SAUR48				3.0
	AT4G34750	SAUR49	1.1			-0.7
	AT1G19840	SAUR53	-1.6	-0.8		0.9
	AT1G29430	SAUR62		-1.0	1.0	
	AT1G29440	SAUR63		-1.1		
	AT4G13260	YUC2	2.0			-1.2
Cytokinin	AT5G61380	APRR1	1.8	1.2		-0.9
	AT5G60100	APRR3	2.6	1.6		-0.9
	AT5G49240	APRR4	1.2			
	AT5G24470	APRR5	4.2	4.7	-1.2	-0.8
	AT1G67710	ARR11	1.0			-1.1
	AT2G40670	ARR16	1.3		1.4	
	AT3G57040	ARR9	1.0			
	AT2G19500	CKX2	6.2			-2.6
	AT5G56970	CKX3	2.3	1.2		-1.3
	AT3G63440	CKX6	0.8			-1.0
	AT5G38450	CYP735A1	4.2			-4.2
	AT1G67110	CYP735A2	4.2			-3.0
	AT1G80440	KMD1	2.3	3.4	-3.3	-2.2
	AT1G15670	KMD2	1.6	1.1	-1.1	-1.6
	AT3G59940	KMD4	1.3	1.2		-0.6
	AT1G19770	PUP14		1.7		

Hormone	Loci	Gene	col.L_col.N	bhlh.L_bhlh.N	bhlh.N_col.N	bhlh.L_col.L
ABA	AT2G27150	AAO3	1.1			-0.6
	AT5G57050	ABI2	1.2			
	AT2G36270	ABI5	1.4	1.0		-0.2
	AT2G29090	CYP707A2	2.9	1.5		
	AT5G45340	CYP707A3	1.2	1.6		
	AT3G19270	CYP707A4		1.0		1.1
	AT2G26040	PYL2	-1.6			1.0
	AT2G38310	PYL4				-1.0
	AT5G05440	PYL5	1.3			-1.7
	AT5G45860	PYL11	-1.5			1.4
	AT5G66880	SNRK2.3	1.1	0.8	-0.3	-0.5
	AT2G23030	SNRK2.9	1.8			
Ethylene	AT4G27950	CRF4	1.2			-0.6
	AT4G17500	ERF1A		2.1		
	AT5G47220	ERF2		1.9		
	AT4G17490	ERF6		3.6		
	AT5G67190	ERF010	1.3	1.0		-0.9
	AT2G31230	ERF15	-2.4	-1.5		
	AT1G01250	ERF023	-2.2	-1.4	1.1	2.0
	AT4G28140	ERF054	2.1			
	AT2G22200	ERF056	1.9			
	AT4G13620	ERF062		5.8		5.8
	AT5G61600	ERF104		3.0		
	AT5G61590	ERF107	2.1	1.8		-2.0
	AT5G13330	ERF113				1.1
	AT3G54990	SMZ	0.5		-1.8	-1.7
GA	AT4G02780	GA1	1.7			-0.7
	AT4G25420	GA20OX1	-1.3	-1.2		
	AT5G51810	GA20OX2	1.0			-0.7
	AT1G78440	GA2OX1	1.5	0.8		-0.7
	AT1G30040	GA2OX2	1.0	1.2		
	AT2G34555	GA2OX3				-1.4
	AT1G47990	GA2OX4				-1.4
	AT1G75750	GASA1	1.0			-1.1
	AT5G59845	GASA10	2.0		2.0	
	AT2G18420	GASA11	7.3			-4.4
	AT5G14920	GASA14	0.9			-1.1
	AT1G15550	GA3OX1		-0.9		
	AT3G25260	NPF4.1	-1.1	-0.6	-1.1	-0.6
	AT1G69850	NPF4.6	2.3			-2.3
	AT5G46050	NPF5.2	-0.8		-1.9	-1.5
	AT5G01180	NPF8.2	-0.7	-0.8	1.2	1.1
	AT5G50800	SWEET13			1.3	1.7
	AT4G25010	SWEET14		-1.4		-1.3

4.2.3 Identifying new targets of the bHLHs

To narrow down bHLH and light-responsive targets, the 2492 DEGs were filtered to 383 genes that exhibit a $log_2FC \geq 2$ in Col-0 under different light conditions and a $log_2FC \leq 1$ in the *bhlh089 bhlh091* mutant in response to light. 121 of these are expressed in the anther according to anther laser capture expression data (Wilson group, unpublished) and only 80 of these are annotated (Table 4.3). All of the 80 anther-expressed DEGs are upregulated in Col-0 in low light, are not significantly changed in the *bhlh89,91* mutant, and fall in Clusters 5, 6 & 8 (Figure 4.2C). The majority exhibit a peak in expression in stage 10-12 flowers according to developmental RMA data (Table 4.3; Schmid et al., 2005).

A literature search revealed that 25 of these genes have a known reproductive phenotype of some kind; including a number of genes that have previously been shown to impact on male fertility: *ABGC9, ATA27, EXL4, EXL6, FST1, GASA10, GRDP2, GRP17, LBD27, MYB101, NIP4;1, SBT5.4, SHT, SWEET8, TOL8, TSM1* and *YSL3*. Expression patterns of notable pre-studied genes from Table 4.3 are shown in transcript abundance plots (Figure 4.10). Notably these all show upregulated expression in Col-0 in response to low light. Furthermore, most are expressed at the lower 'normal' WT level in the *bhlh89,91* mutant; suggesting that bHLH89 and 91 are required to activate transcription of these genes under low light conditions. The exception is *GIBBERELLIN-REGULATED PROTEIN10* (*GASA10*) which is expressed at the higher level of Col-0 low light in the *bhlh* mutant.

Table 4.3 (next page) Expression and annotations of anther-expressed DEGs which exhibit a low-light induced $log_2FC>2$ in Col-0 and $log_2FC<1$ in the bhlh089 bhlh091 mutant ($q<0.01$). A) Log_2FCs are shown for each contrast group of this RNAseq study, and from dyt1, bhlh089 bhlh010 amiR-bHLH091 triple, tdf1, ams, myb80 and ms1 mutant microarray data (Feng et al., 2012; Zhu et al., 2015; Lou et al., 2017; Ma et al., 2012; Phan et al., 2011; Yang et al., 2007). B) Log_2FCs at various different stages of microspore development in the ams mutant (Meiosis, Pollen Mitosis (PM) 1, Bicellular (BC) and PM2; Xu et al., 2010) and expression levels (RMA, purple) are also indicated various stages of flower development in Col-0. Red shows strength of upregulation in low light or mutant, with blue showing downregulation. Blank cells indicate non-significant differential expression.

A

Locus	Name	Description	Col-0, L-N	8991, L-N	Norm 8991-Col-0	Low 8991-Col-0	dyt1	bhlh tripl	tdf1	ams	myb 80	ms1
AT4G27420	ABCG9	ABC transporter G 9	2.0			-1.4	-4.6			-4.5		-2.3
AT5G59370	ACT4	Actin-4	2.8			-3.7	-3.5					
AT3G57690	AGP23	Arabinogalactan peptide 23	4.5			-2.4	-4.8			-4.8		
AT4G28700	AMT1-4	Ammonium transporter 1 member 4	2.0			-1.3	-2.8			-2.4		
AT4G04460	APA3	Aspartic proteinase A3	2.1			-1.0	-1.4		-1.2	-1.8		-3.5
AT3G42850	ARA2	Arabinokinase 2	2.2			-1.8	-2.5		-1.9	-2.1		
AT1G75940	ATA27 / BGLU20	Beta-glucosidase 20	4.5			-3.8	-6.2	-3.0		-6.2		
AT5G44400	BBE26	Berberine bridge enzyme-like 26	4.9			-6.4	-4.7		-5.0	-5.0		-5.3
AT5G20230	BCB / SAG14	Blue Copper Binding / Senescence Associated Gene 14	2.5				-3.0	-5.5		-2.1	-2.5	
AT5G20710	BGAL7	Beta-galactosidase 7	3.3			-3.0	-4.0	-4.2		-3.3	-1.8	
AT3G26940	CDG1	Constitutive Differential Growth 1	2.9			-2.2	-2.9			-2.7		
AT5G24090	CHIA / LYS1	Chitinase A, Lysozyme 1	5.5			-1.8	-1.9			-4.9		
AT5G59040	COPT3	Copper transporter 3	2.9			-1.8	-3.5			-3.2		
AT3G21910	CRRSP17	Putative cysteine-rich repeat secretory protein 17	2.4			-4.4	-4.3		-4.4	-4.1		
AT1G28430	CYP705A24	Cytochrome P450, family 705, subfamily A, polypeptide 24	4.4			-3.7	-5.0			-4.0		
AT5G38450	CYP735A1	Cytokinin hydroxylase	4.2			-4.2	-3.4			-4.0		
AT1G67110	CYP735A2	Cytokinin hydroxylase	4.2			-3.0	-2.7			-3.3		
AT1G13150	CYP86C4	Cytochrome P450, family 86, subfamily C, polypeptide 4	2.6			-2.4	-4.7			-4.8		-4.0
AT1G74540	CYP98A8	Cytochrome P450 98A8	3.2			-5.2	-4.3			-4.4		-4.5
AT1G74550	CYP98A9	Cytochrome P450 98A9	4.6			-3.7	-4.8			-4.6		-3.4
AT2G31980	CYS2	Cysteine proteinase inhibitor	2.2			-2.3	-4.1	-2.1		-4.4		-4.5
AT3G18590	ENODL5	Early nodulin-like protein 5	7.7			-3.3	-2.4			-2.1		
AT1G48940	ENODL6	Early nodulin-like protein 6	6.6			-2.2	-3.4			-2.8		
AT1G75910	EXL4	GDSL esterase/lipase EXL4	8.5			-6.8	-5.2			-5.3		-6.3
AT1G75930	EXL6	GDSL esterase/lipase EXL6	7.2			-4.2	-5.8			-6.1		-5.6
AT3G59480	FRK4	Fructokinase 4	3.0			-1.6	-2.6			-2.5		
AT4G10260	FRK5	Fructokinase 5	3.7			-3.8	-4.7		-4.3	-5.5		-1.7
AT5G59845	GASA10	Gibberellin-regulated protein 10	2.0		2.0		-2.6		-2.2	-2.6		-2.6
AT2G18420	GASA11	Gibberellin-regulated protein 11	7.3			-4.4						-2.6
AT5G08030	GPD6	glycerophosphodiester phosphodiesterase 6	3.5			-1.7	-5.5			-4.6		
AT4G37900	GRDP2	Glycine-rich domain-containing protein 2	4.5			-4.0	-3.8	-2.2	-3.6	-4.2		-5.1
AT5G07510	GRP14	Glycine-rich protein 14	6.2			-2.1	-2.8			-2.8		
AT5G07540	GRP16	Glycine-rich protein 16	6.7			-6.5	-4.4			-4.5		-4.8
AT5G07530	GRP17	Glycine-rich protein 17	5.3				-4.3	-1.9		-4.6		-6.1
AT5G07520	GRP18	Glycine-rich protein 18	3.6			-1.6	-3.9			-4.0		-4.7
AT5G07550	GRP19	Glycine-rich protein 19	5.1			-3.8	-4.4	-7.1		-4.7		-7.3
AT5G07560	GRP20	Glycine-rich protein 20	6.0			-3.6	-4.3			-4.6		-7.1
AT1G52120	JAL12	Jacalin-related lectin 12	3.9			-1.9	-2.4		-2.1	-2.2		
AT3G19090	LARP6C	LA-related protein 6C	2.3			-2.8	-4.4			-4.3		
AT3G47870	LBD27 / SCP	LOB domain-containing protein 27 / Sidecar Pollen	3.1			-1.7	-5.0			-4.5		
AT2G03740	LEA11	Late embryogenesis abundant 11	3.7		1.9	-1.5	-5.5	-2.5	-5.5	-5.8		
AT1G24400	LHT2	Lysine histidine transporter 2	2.8			-2.0	-4.8			-4.0		
AT3G51590	LTP12	Non-specific lipid-transfer protein 12	2.5			-1.5	-5.2	-9.9		-5.4		-6.8
AT1G18280	LTPG3	Glycosylphosphatidylinositol-anchored lipid protein transfer 3	5.3			-3.0	-3.7		-3.6	-3.8		
AT4G08670	LTPG4	Glycosylphosphatidylinositol-anchored lipid protein transfer 4	4.8			-2.4	-4.0		-3.5	-3.8		
AT3G62860	MAGL12	Alpha/beta-hydrolases superfamily protein	2.4			-1.5	-1.8		-1.7	-1.5		
AT2G32510	MAPKKK17	Mitogen-activated protein kinase kinase kinase 17	2.9				-1.5	-4.0			-1.4	
AT4G20080	MCTP11	Multiple C2 domain and transmembrane region protein 11	4.0			-2.2	-2.9		-1.9	-2.6		
AT1G23060	MDP40	Microtubule destabilizing protein 40	2.4									
AT2G11810	MGD3	Monogalactosyldiacylglycerol synthase 3, chloroplastic	2.5			-1.4	-3.1			-3.3		
AT2G32460	MYB101	Transcription factor MYB101	2.8			-2.0	-2.7	-6.3		-2.9		
AT1G61110	NAC025	NAC transcription factor 25	3.3		1.8	-2.3	-5.9			-3.6		-4.1
AT3G15510	NAC056	NAC transcription factor 56	2.7			-2.8	-2.1			-2.8		
AT5G37810	NIP4;1	NOD26-like intrinsic protein 4;1	4.5			-4.3	-5.1			-4.8		
AT1G59740	NPF4.3	Protein NRT1/ PTR family 4.3	3.1			-3.4	-1.8			-2.9		-2.5
AT1G69850	NPF4.6	Protein NRT1/ PTR family 4.6	2.3			-2.3	-1.8	-1.6		-1.7		-1.7
AT5G28470	NPF4.8 / FST1	Flavonol sophoroside transporter 1	4.3			-4.5	-5.8		-5.0	-5.9		
AT5G19640	NPF7.1	Protein NRT1/ PTR family 7.1	3.4			-1.5	-3.1		-2.2	-2.6		
AT1G73220	OCT1	Organic cation/carnitine transporter 1	2.4			-3.1	-1.3			-3.0		
AT5G53510	OPT9	Oligopeptide transporter 9	3.1			-1.6	-3.0	-5.4		-2.5		
AT5G57240	ORP4C	OSBP(oxysterol binding protein)-related protein 4C	3.4			-2.0						
AT2G46880	PAP14	Probable inactive purple acid phosphatase 14	3.7			-1.3	-6.5			-5.6		
AT3G52810	PAP21	Purple acid phosphatase 21	6.8			-7.4	-6.3			-6.7		-3.2
AT1G62760	PMEI10	Pectinesterase inhibitor 10	3.3			-2.3	-2.4		-2.1			
AT5G09500	RPS15C	40S ribosomal protein S15-3	2.4			-1.2	-2.7		-2.1	-2.6		
AT5G59810	SBT5.4	Subtilisin-like protease SBT5.4	2.7			-1.9	-1.7	-5.9		-1.9		
AT4G35770	SEN1	Senescence 1/ Dark Inducible 1	3.8			-3.3	-2.5	-5.0				
AT2G19070	SHT	Spermidine hydroxycinnamoyl transferase	2.2			-2.9	-4.7	-6.3		-4.8		-5.1
AT5G22270	SIED1	Salt-induced and EIN3/EIL1-dependent 1	2.2		2.3							
AT4G28090	sks10	Multi-copper oxidase type I family protein	3.1			-2.1	-4.6			-4.6		
AT2G45130	SPX3	SPX domain-containing protein 3	2.9			-2.0	-3.2			-2.4		
AT2G41290	SSL2	Strictosidine Synthase-Like 2	2.6			-2.5	-3.0			-3.2		
AT1G07340	STP2	Sugar Transporter 2	3.8			-2.1	-3.9	-7.3		-4.3		
AT5G40260	SWEET8/ RPG1	Bidirectional sugar transporter SWEET8/ Ruptured Pollen Grain 1	2.2			-1.5	-2.9			-2.6		
AT1G18520	TET11	Tetraspanin-11	5.0			-4.6	-4.3			-3.3		-2.0
AT3G08790	TOL8	TOM1-like protein 8	3.5			-2.4	-4.7		-4.1	-4.5		
AT5G62240	TPXL8	Cell cycle regulated microtubule associated protein	2.8			-1.8	-3.9		-3.6	-2.9		
AT1G67990	TSM1	Tapetum-Specific Methyltransferase 1	2.7			-2.6	-6.3	-5.7		-6.6		-6.8
AT3G25050	XTH3	Xyloglucan endotransglucosylase/hydrolase protein 3	8.8			-7.6	-7.2			-7.5		-6.0
AT5G53550	YSL3	Yellow Stripe Like 3	2.2			-2.4	-1.5	-3.3				

B

Name	ams - meosis	PM1	BC	PM2	Flower stage 9	10/11	12	15	Stamen stage 12	15	Pollen	Flowers
ABCG9					6	8	6	2	7	3	6	8
ACT4	0.0	0.0	-0.6	-0.2	4	5	8	7	11	10	12	6
AGP23					7	10	13	13	14	14	14	11
AMT1-4	0.2	-1.5	-1.0	0.0	4	6	5	4	9	4	9	7
APA3	-0.2	-2.1	-2.8	-1.4	9	12	13	11	14	8	5	12
ARA2	-0.9	-1.8	-2.2	0.0	5	8	9	4	11	5	8	8
ATA27 / BGLU20	-3.9	-4.5	-3.9	0.6	11	13	12	3	12	3	5	13
BBE26	-1.1	-2.7	-3.1	0.0	5	10	9	6	8	4	6	10
BCB / SAG14	0.3	-0.2	-0.7	-0.9	5	7	11	12	14	12	14	9
BGAL7	-0.3	-2.8	-3.3	-1.5	6	9	10	4	12	3	12	10
CDG1					3	3	4	3	6	3	5	3
CHIA / LYS1	0.0	0.9	0.0	0.0	3	5	6	3	8	3	5	5
COPT3	-1.9	-2.5	-1.1	0.0	4	6	4	3	6	3	7	6
CRRSP17												
CYP705A24	-0.7	-1.9	-3.4	-1.0	3	8	10	3	11	3	5	8
CYP735A1					3	3	3	2	4	3	8	3
CYP735A2					3	4	3	3	3	3	3	4
CYP86C4	-1.0	-1.4	-1.3	-0.5	6	10	8	3	7	4	5	10
CYP98A8	-3.4	-3.3	-1.8	0.0	8	11	7	2	7	3	3	10
CYP98A9	-2.8	-3.1	-0.8	0.0	6	9	7	4	7	5	7	9
CYS2	-2.1	-3.1	-3.4	-2.7	9	12	14	9	14	8	7	12
ENODL5												
ENODL6	-2.0	-2.8	-2.9	0.0	4	8	3	3	3	3	8	8
EXL4	-0.7	-2.9	-4.2	0.0	8	12	12	4	11	4	6	12
EXL6	0.0	-4.8	0.0	-1.1	7	11	12	2	12	3	4	12
FRK4	-0.7	-1.3	0.2	0.0	7	8	5	5	6	4	9	8
FRK5	-1.0	-3.4	-3.2	0.0	3	7	8	3	9	3	9	8
GASA10	-1.7	-2.2	-1.7	-0.3	9	11	10	7	11	5	6	11
GASA11	0.0	-1.8	0.0	0.0	4	8	5	3	4	3	4	8
GPD6	0.5	0.0	0.0	0.0	5	7	4	3	5	4	8	8
GRDP2	-1.0	-1.7	0.0	0.0	9	11	9	4	8	4	5	11
GRP14	-1.9	-3.2	-2.9	-2.7	7	11	11	5	12	6	7	11
GRP16	-2.4	-3.0	-2.6	-2.6	4	11	13	3	14	4	5	12
GRP17	-3.2	-3.7	-2.6	-3.2	9	13	14	5	14	7	7	13
GRP18	-2.9	-3.9	-3.3	-2.5	7	10	10	3	12	4	6	10
GRP19	-3.1	-3.6	-2.5	-3.7	10	13	14	2	14	4	4	13
GRP20	-2.9	-3.4	-2.8	-3.2	6	10	11	1	12	2	2	11
JAL12												
LARP6C					4	5	8	3	11	5	10	6
LBD27 / SCP												
LEA11	0.0	0.0	-1.5	0.0	9	11	9	4	9	4	6	11
LHT2	-1.5	-1.4	-2.0	-1.0	6	8	9	3	12	3	10	9
LTP12	-3.7	-3.0	-4.2	0.0	12	13	10	2	9	2	3	13
LTPG3	-1.0	-2.8	-2.6	-1.9	4	9	11	3	13	4	11	10
LTPG4					3	7	10	2	12	3	11	9
MAGL12					5	7	7	7	7	7	6	6
MAPKKK17					4	5	4	5	6	9	5	5
MCTP11					2	3	2	2	3	2	4	2
MDP40	0.0	-0.6	0.7	-0.4	4	7	8	9	10	10	5	6
MGD3					3	4	4	5	5	5	7	4
MYB101					3	5	4	6	9	9	12	4
NAC025	-2.1	-3.4	-1.6	-0.9	8	11	9	4	12	7	5	10
NAC056	0.0	0.0	0.0	-0.4	4	8	8	6	11	7	6	8
NIP4;1					2	5	8	2	11	3	10	6
NPF4.3	-1.2	-2.2	-2.3	-0.9	5	9	8	6	9	3	3	9
NPF4.6					5	7	6	8	7	9	4	7
NPF4.8 / FST1	0.0	-1.0	0.2	0.0	3	7	3	2	6	3	10	6
NPF7.1					3	3	4	3	7	3	6	4
OCT1	-1.7	-3.1	-2.1	-1.6	5	9	9	10	12	8	2	8
OPT9	0.3	-1.2	0.0	0.0	5	6	3	2	3	2	8	6
ORP4C					4	7	7	3	5	4	9	7
PAP14					4	5	3	3	3	3	6	5
PAP21					3	8	9	2	10	3	4	8
PMEI10	0.1	0.2	0.3	0.4	3	4	4	4	5	5	6	3
RPS15C	-2.0	-1.9	-2.0	0.0	6	7	7	4	9	5	10	7
SBT5.4	-0.2	-1.4	-0.3	0.2	4	6	6	6	5	2	8	7
SEN1					7	7	6	8	7	10	5	5
SHT	-3.5	-3.9	-3.4	0.0	8	10	5	2	3	2	4	10
SIED1					6	8	8	9	8	8	6	7
sks10					4	6	5	3	7	3	5	6
SPX3					3	3	3	4	3	3	5	3
SSL2	0.0	-2.1	0.2	0.0	8	10	7	5	6	4	6	9
STP2	-0.3	-1.1	0.3	0.0	6	8	5	2	6	2	10	7
SWEET8/ RPG1	-1.9	-2.0	-2.7	0.0	9	9	8	3	9	3	11	10
TET11	0.6	-0.8	0.9	0.0	3	7	6	2	8	3	9	7
TOL8												
TPXL8												
TSM1	-4.2	-3.9	-3.9	0.0	11	12	5	2	3	3	4	12
XTH3	-4.3	-2.8	-4.2	0.0	5	12	12	3	11	3	3	12
YSL3	0.0	0.0	0.0	0.1	6	7	7	9	6	9	5	7

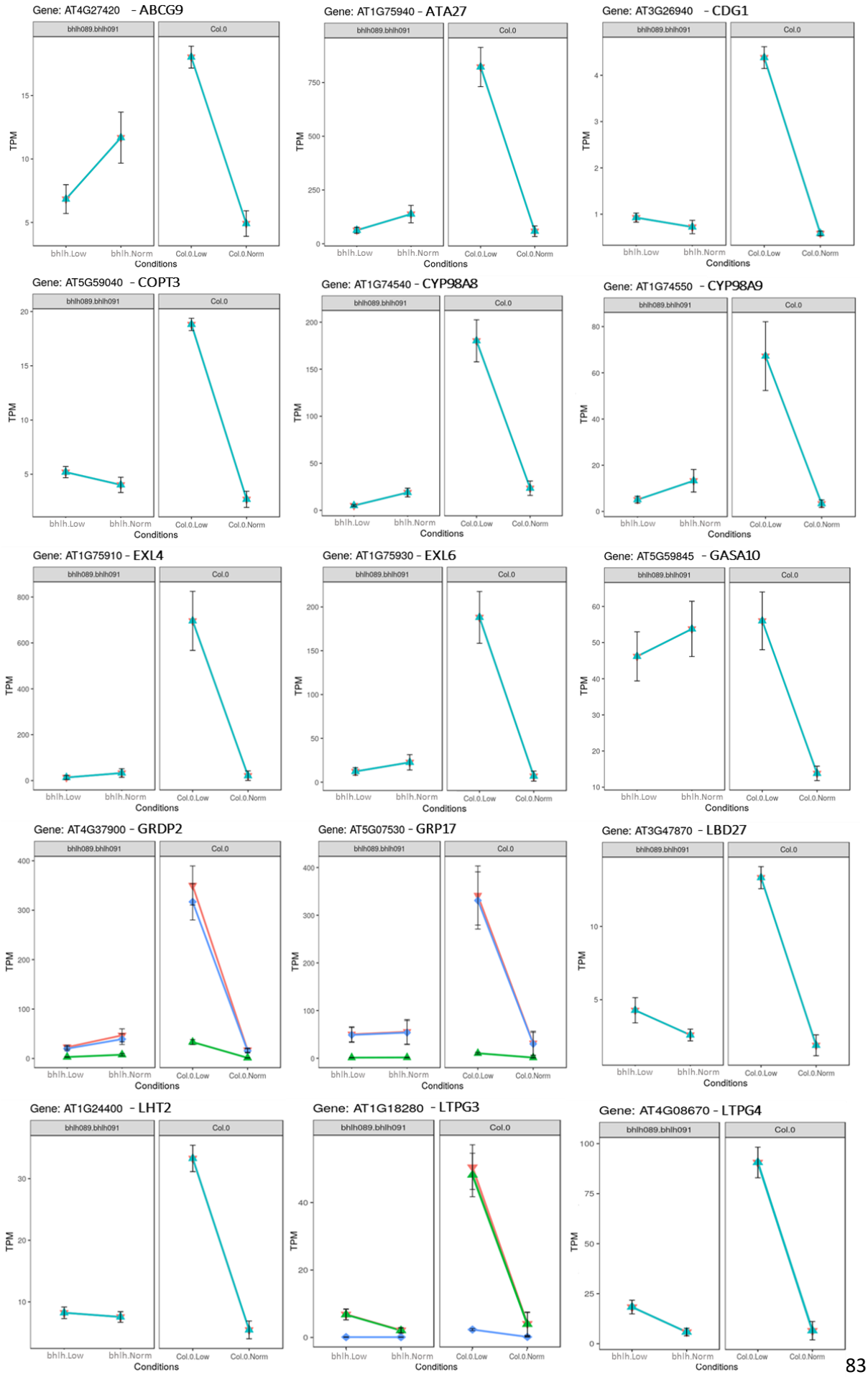
Gene: AT4G27420 - ABCG9
Gene: AT1G75940 - ATA27
Gene: AT3G26940 - CDG1
Gene: AT5G59040 - COPT3
Gene: AT1G74540 - CYP98A8
Gene: AT1G74550 - CYP98A9
Gene: AT1G75910 - EXL4
Gene: AT1G75930 - EXL6
Gene: AT5G59845 - GASA10
Gene: AT4G37900 - GRDP2
Gene: AT5G07530 - GRP17
Gene: AT3G47870 - LBD27
Gene: AT1G24400 - LHT2
Gene: AT1G18280 - LTPG3
Gene: AT4G08670 - LTPG4
bhlh089.bhlh091
Col.0
TPM
bhlh.Low
bhlh.Norm
Col.0.Low
Col.0.Norm
Conditions

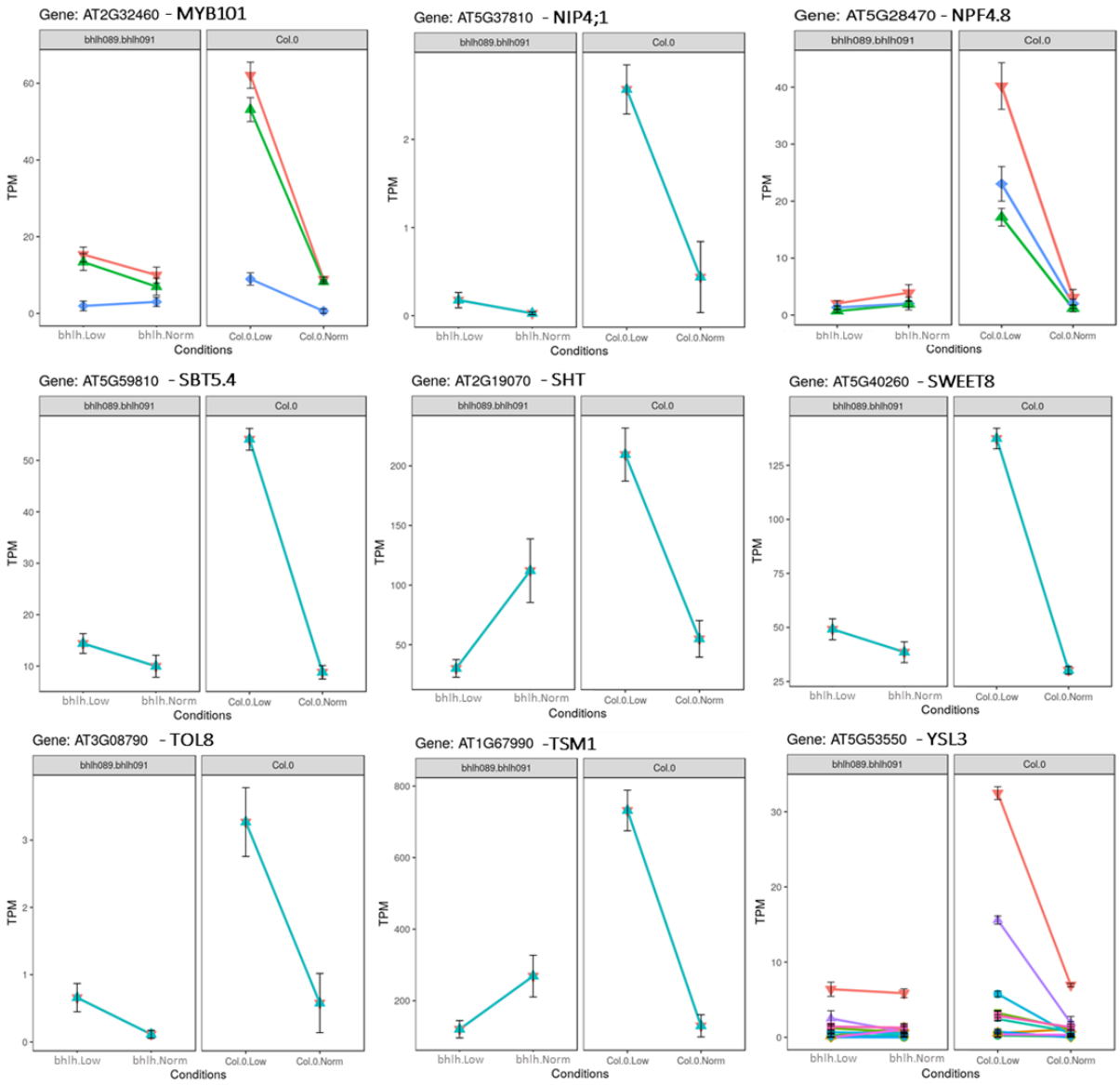

Figure 4.10, continued from previous page. Abundance plots showing differential expression of genes and transcripts implicated in male reproductive development, coloured lines represent different transcript numbers.

4.2.4 Overlap with other tapetal bHLH mutant transcriptomes

Published transcriptomic data from the *dyt1, ams* and *bhlh089 bhlh010 amiR-bHLH091* mutants was accessed and filtered to include DEGs of $\log_2$FC≥1 (q≤0.01) in order to be directly comparable to the RNAseq study outlined above (Feng et al., 2012; Ma et al., 2012; Zhu et al., 2015; Figure 4.11 A).

Out of the 289 genes that are differentially expressed between *bhlh089 bhlh091* and Col-0 under normal growth conditions, there was an overlap of 126 with *dyt1* (44%), 63 with *ams* (22%) and 42 with *bhlh089 bhlh010* amiR-bHLH091 (15%, Figure 4.11 B). A more detailed analysis of how this is split across up- and down-regulated genes is shown in Figure 4.11 D-F.

When you consider only the DEGs that are expressed in the tapetum according to unpublished laser capture transcriptome data, there is a much higher degree of overlap among the transcriptomes

(Figure 4.11 C). *bhlh089 bhlh091* shares 115 out of 122 anther DEGs with *dyt1* (94%), 105 with *ams* (86%) but only 12 with the *bhlh089 bhlh010* amiR-bHLH091 mutant (10%).

Focusing in on the filtered light-sensitive tapetal genes in Table 4.3, 76 out of 80 were also downregulated in the *dyt1* dataset, and 71/80 were downregulated in the *ams* microarray (q<0.01). However, only 19 were also differentially expressed (q<0.05) when compared to our re-analysis of the *bhlh089 bhlh010 amiR-bHLH091* triple mutant transcriptome (Table 4.3A).

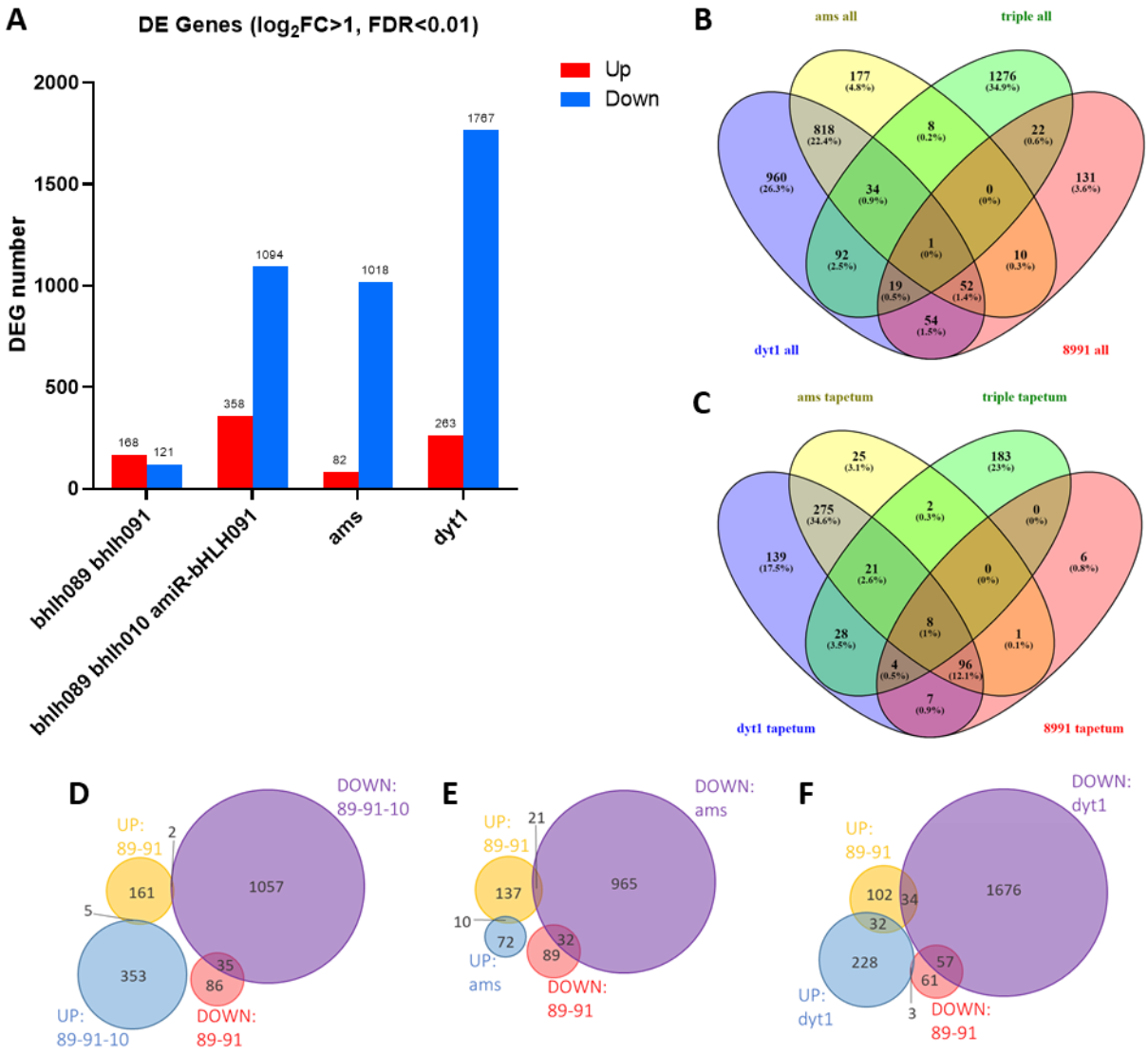

Figure 4.11. A) Comparison of col-0 vs bhlh mutant DEGs from our RNAseq dataset of bhlh089 bhlh091 and existing microarrays of the ams, dyt1 and bhlh089 bhlh010 amiR-bHLH091 mutants (Xu et al., 2010; Zhu et al., 2015). Venn diagrams showing overlap in all four microarray datasets of total (B) and anther-expressed DEGs (C). Proportional Venn diagrams show levels of up- and down-regulation in bhlh089 bhlh091 vs bhlh089 bhlh010 amiR-bHLH091 (D), ams (E) and dyt1 (F) DEGs.

18 of the 29 direct AMS-targets identified from Chromatin Immunoprecipitation (ChIP) and EMSA binding assays (Xu et al., 2010, 2014) are induced in response to low light in Col-0 ($log_2FC>1$) but are unresponsive to light in the *bhlh89,91* mutant and differentially expressed compared to WT (Table 4.4). This suggests that light input through bHLH89 and -91 is essential to the regulation of AMS targets. Three additional AMS targets are downregulated in response to light in Col-0 but these are not differentially expressed in the *bhlh89,91* mutant so are likely to be independently regulated.

Table 4.4. Differential expression (log_2FC, $q<0.01$) of direct AMS-targets, identified by Xu et al. (2010, 2014), in response to low (L) light and in the bhlh89,91 mutant according to RNASeq data.

Gene	Loci	Col-0, L-N	8991, L-N	Norm, 8991-Col-0	Low, 8991-Col-0	Description
AT1G06990	AT1G06990	4.86			-5.20	GDSL esterase/lipase
AT1G66850	AT1G66850	1.86			-2.33	Bifunctional inhibitor/lipid-transfer protein/seed storage 2S albumin superfamily protein
CHS	AT4G00040	1.98			-1.94	Chalcone synthase
CYP86C3	AT1G13140	1.23			-2.89	Cytochrome P450 86C3
CYP98A8	AT1G74540	3.22			-5.17	Cytochrome P450 98A8
CYP98A9	AT1G74550	4.60			-3.74	Cytochrome P450 98A9
EXL4	AT1G75910	8.55			-6.77	GDSL esterase/lipase EXL4
EXL5	AT1G75920	4.46			-4.06	GDSL esterase/lipase EXL5
EXL6	AT1G75930	7.19			-4.25	GDSL esterase/lipase EXL6
GRP14	AT5G07510	6.15			-2.09	Glycine-rich protein 14
GRP18	AT5G07520	3.57			-1.64	Glycine-rich protein 18
GRP19	AT5G07550	5.14			-3.78	Glycine-rich protein 19
KCS15	AT3G52160	1.60			-2.58	3-ketoacyl-CoA synthase 15
KCS21	AT5G49070	1.98			-2.41	Probable 3-ketoacyl-CoA synthase 21
LTP12	AT3G51590	2.50			-1.53	Non-specific lipid-transfer protein 12
NPF4.3	AT1G59740	3.11			-3.41	Protein NRT1/ PTR FAMILY 4.3
OCT1	AT1G73220	2.37			-3.11	Organic cation/carnitine transporter 1
TSM1	AT1G67990	2.67			-2.65	Tapetum-specific methyltransferase 1
AT5G62080	AT5G62080	-1.08				Bifunctional inhibitor/lipid-transfer protein/seed storage 2S albumin superfamily protein
PKSB	AT4G34850	-1.05				Polyketide synthase B/Less adhesive pollen 5
TKPR1	AT4G35420	-1.04	-0.69			Tetraketide alpha-pyrone reductase 1

4.2.5 Overlap with shade microarrays

Microarray data from Leivar *et al.* (2012), which shows shade-induced changes in the Col-0 seedling transcriptome after exposure to FR light for 1-24hrs ($log_2FC>1$, $q<0.05$), was compared to our RNAseq dataset. Out of the 1853 genes differentially expressed ($log_2FC>1$, $q<0.01$) in Col-0 low-light conditions in our RNAseq dataset 202 DEGs overlap with the seedling microarray (11%). A GO enrichment analysis revealed that this gene set was significantly enriched in response to auxin and regulation of cytokinin- and auxin-activated signalling pathways. Response to sugars such as sucrose, fructose and glucose was also enriched. In terms of light response, there is overrepresentation of responses to Far Red (FR), Red, Blue, UV-A, UV-B and complete absence of light and enrichment of phenylpropanoid metabolism, flavonoid biosynthesis and proteolysis (Table 4.5).

Of these 202 overlapping DEGs, 42 are expressed in the anther according to unpublished laser capture data (Table 4.6). These include six of the filtered genes highlighted in Table 4.3 which respond to low light in Col-0 but not in the *bhlh89,91* mutant (CYS2, GPD6, MDP40, ORP4C, SEN1, SIED1), four hormone responsive genes from Table 4.2 (ARR16, GH3.9, KMD1 & -4) and two Heat Shock Proteins (HSPs).

Table 4.5. GO term enrichment of Biological Processes in 202 overlapping DEGs of shade-response in Col-0 seedlings (Leivar et al. 2012) and pre-mitotic buds. Terms considered significant according to p<0.05 are highlighted in yellow, whereas green highlights the stricter significance threshold of q<0.05.

GO term	Count	%	p value	q value
response to auxin	16	7.9	0.000	0.000
response to karrikin	10	5.0	0.000	0.000
response to sucrose	5	2.5	0.001	0.092
negative regulation of cytokinin-activated signalling pathway	3	1.5	0.001	0.075
auxin-activated signalling pathway	8	4.0	0.001	0.068
regulation of phenylpropanoid metabolic process	3	1.5	0.001	0.070
flavonoid biosynthetic process	7	3.5	0.001	0.061
L-phenylalanine catabolic process	3	1.5	0.002	0.070
response to oxidative stress	9	4.5	0.003	0.105
regulation of proteolysis	4	2.0	0.003	0.098
response to fructose	3	1.5	0.010	0.238
response to cold	8	4.0	0.014	0.290
response to toxic substance	4	2.0	0.015	0.292
response to UV-B	4	2.0	0.015	0.292
cellular response to far red light	2	1.0	0.017	0.305
cellular response to red light	2	1.0	0.017	0.305
response to absence of light	3	1.5	0.020	0.335
response to glucose	3	1.5	0.030	0.433
tyrosine catabolic process	2	1.0	0.033	0.451
cellular response to sucrose starvation	2	1.0	0.033	0.451
cellular response to UV-A	2	1.0	0.041	0.507
leaf senescence	4	2.0	0.043	0.500
hexose transmembrane transport	3	1.5	0.047	0.514
cellular response to blue light	2	1.0	0.050	0.517
leucine catabolic process	2	1.0	0.050	0.517
cell wall organization	7	3.5	0.050	0.507
regulation of transcription, DNA-templated	26	12.9	0.052	0.502
toxin catabolic process	3	1.5	0.057	0.524
glucose import	3	1.5	0.057	0.524
photoprotection	2	1.0	0.058	0.510
protein ubiquitination involved in ubiquitin-dependent protein catabolic process	5	2.5	0.063	0.529
response to far red light	3	1.5	0.064	0.523
cellular response to high light intensity	2	1.0	0.066	0.517
flavonol biosynthetic process	2	1.0	0.073	0.547
response to hydrogen peroxide	3	1.5	0.076	0.548
response to wounding	5	2.5	0.088	0.591
de-etiolation	2	1.0	0.089	0.584
cell wall biogenesis	3	1.5	0.091	0.582
protein folding	6	3.0	0.097	0.595

Table 4.6. Anther-expressed overlapping DEGs, with log_2FC expression, in Leivar et al. (2012)'s seedling response to 1-24h of FR light and low-light response pre-mitotic Col-0 and bhlh mutant buds grown under low light. Red indicates upregulation, in shade/low light, blue shows downregulation and blank indicates no significant changes (q>0.01)

Loci	Gene	Description	1h FR	3h FR	24h FR	col.L_col.N	bhlh.L_bhlh.N
AT2G40670	ARR16	response regulator 16		-1.9	-2.7	1.3	
AT3G47340	ASN1	glutamine-dependent asparagine synthase 1	1.7	2.5	1.7	2.2	1.7
AT1G13990	AT1G13990	plant/protein	0.4	0.9	1.1	1.6	0.7
AT1G54120	AT1G54120	hypothetical protein	1	0.8	-1.2	-1.8	-0.9
AT1G54740	AT1G54740	FANTASTIC four-like protein	0.9	1.2	2.4	1.7	0.8
AT1G56220	AT1G56220	Dormancy/auxin associated family protein	0.7	1.4	1.2	1.4	1.5
AT1G80180	AT1G80180	hypothetical protein	0.9	1.1	1.9	2.2	1.4
AT2G05540	AT2G05540	Glycine-rich protein family	0.7	1.2	1.8	4.5	4.3
AT2G32150	AT2G32150	Haloacid dehalogenase-like hydrolase (HAD) family	0.9	1.4	1.3	2.9	1.8
AT3G15450	AT3G15450	aluminium induced protein with YGL and LRDR motifs	0.7	1.2	1.2	2.2	3.2
AT3G51000	AT3G51000	alpha/beta-Hydrolases superfamily protein	0.6	1.3	0.7	2.5	
AT5G19120	AT5G19120	Eukaryotic aspartyl protease family protein	0.7	1.1	0.9	1.5	1.9
AT1G10070	BCAT2	branched-chain amino acid transaminase 2	2.2	4.2	3	3.7	1.2
AT3G55120	CHI1	Chalcone-flavanone isomerase family protein	-1.1	-1.4	-0.7	-1.1	-1.2
AT5G07990	CYP75B1	Cytochrome P450 superfamily protein	-1	-1.6	-1.1	-2.4	-2.2
AT2G31980	CYS2	Phytocystatin 2	1.7	2.8	2.7	2.2	
AT1G65870	DIR21	Disease resistance-responsive (dirigent-like) family	-0.8	-1	1.1	-2	-1.3
AT4G28250	EXPB3	expansin B3	-0.5	-1.2	-1.7	-1.6	-0.8
AT3G51240	F3H	flavanone 3-hydroxylase	-1.2	-2.2	-0.6	-1.2	-1.6
AT5G08640	FLS1	flavonol synthase 1	-1.2	-2.6	-0.9	-1.3	-1.3
AT2G47750	GH3.9	putative indole-3-acetic acid-amid synthetase	-0.3	-1.5	-1.8	2	
AT5G08030	GPD6	glycerophosphodiester phosphodiesterase 6	-0.3	-1.6	-1.8	3.5	
AT5G17220	GSTF12	glutathione S-transferase phi 12	-0.8	-2.8	-2.6	-1.8	-1.2
AT5G51440	HSP23.5	HSP20-like chaperones superfamily protein	0.6		1.1	-1.3	
AT5G02490	HSP70-2	Heat shock protein 70	-0.4	-1	-1	-1.7	-0.7
AT3G45300	IVD	isovaleryl-CoA-dehydrogenase	0.8	1.8	1.7	1.4	
AT5G48880	KAT5	peroxisomal 3-keto-acyl-CoA thiolase 2	-1.3	-1.8	-1.3	-1.1	-1.1
AT1G80440	KMD1	galactose oxidase/kelch repeat superfamily protein	0.8	1.3	1.8	2.3	3.4
AT3G59940	KMD4	Galactose oxidase/kelch repeat superfamily protein	0.4	1	0.9	1.3	1.2
AT2G40100	LHCB4.3	light harvesting complex photosystem II	-0.5	-1.2	0.7	-1.1	-1.3
AT1G23060	MDP40	Microtubule destabilizing protein 40	0.5	1.4	-0.9	2.4	
AT1G24020	MLP423	MLP-like protein 423	-0.6	-1.4	-3	-1.3	-0.4
AT5G39610	NAC92	NAC domain containing protein 6	0.7	1.5	1.3	1.1	1.1
AT5G57240	ORP4C	OSBP (oxysterol binding protein)-related protein 4C	0.5	1.3	-0.8	3.4	
AT2G37040	PAL1	PHE ammonia lyase 1	-1	-1.5		1.5	
AT2G43010	PIF4	phytochrome interacting factor 4	0.6	1.8	2.3	1.8	1.5
AT3G05880	RCI2A	low temperature and salt responsive protein	0.4	1	1.1	1.1	1.5
AT4G35770	SEN1	Senescence 1	1	2.1	1.4	3.8	
AT5G22270	SIED1	Salt-induced and EIN3/EIL1-dependent 1	0.8	1.5	2	2.2	
AT1G11260	STP1	sugar transporter 1	0.8	1.3	1.6	2.7	1.1
AT4G05070	WIP2	Wound-induced Polypeptide 2	0.7	1.2	1.3	1.6	1.5
AT5G57655	XYLA	xylose isomerase family protein	0.4	1.1	0.8	1.3	0.6

4.3 DISCUSSION

4.3.1 The *bhlh089 bhlh091* mutant has a reduced transcriptional response to light

The WT response to low light involves major transcriptional changes in pre-mitotic buds with highly significant enrichment (q<0.05) of genes related to sexual reproduction, lipid storage & metabolism, circadian rhythm, response to oxidative stress, oxidation-reduction process and response to auxin (Figure 4.5).

Under normal light conditions there are minimal differences between Col-0 and the *bhlh089 bhlh091* mutant transcriptomes, as indicated by their close proximity in the PCA plot and the relatively low

number of DEGs in the *bhlh089 bhlh091* vs Col-0 contrast group (Figure 4.2 A,D). However, these differences are more than quadrupled under low light stress, primarily due to changes in transcription in low light in Col-0 that are absent in the *bhlh089 bhlh091* mutant. For the most part these DEGs are represented in clusters 5, 6 & 8 of the heatmap (Figure 4.2C). Overrepresented terms in these clusters (Figure 4.4) suggest that genes related to sexual reproduction, SCF-dependent proteasomal ubiquitin-dependent catabolic process, circadian rhythm, lipid storage, oxidation-reduction process and glucose import are upregulated in response to low light in Col-0, but are unresponsive under the same conditions in the *bhlh089 bhlh091* mutant. The fact that bHLH10 alone cannot maintain the WT transcriptional response to light strongly suggests that bHLH89, 91 and 10 are not fully redundant.

GO analysis of clusters 1 & 7 (Figure 4.2C) also suggests that the *bhlh89,91* mutant exhibits changes indicative of general stress responses, which are not seen in Col-0. With genes involved in response to auxin, karrikin and UV-B as well as flavonoid, flavonol and anthocyanin biosynthesis showing strong downregulation in the *bhlh* mutant in response to low light (Figure 4.4). This suggest a possible role for bHLH89 and -91 in buffering stress responses in floral tissue through auxin mediated pathways.

The flavonoid biosynthesis is also enriched in cluster 9 which suggests some stress responses are maintained in the *bhlh* mutant as in WT, as genes in clusters 2 & 9 show the same patterns of regulation between the two genotypes in response to light (Figure 4.2C, Figure 4.4). Thus it seems that responses to ABA, cold, water deprivation and osmotic stress are unaffected by bHLH89 and -91. This could mean that they are only involved in certain stress responses.

If we look at differential enrichment of the most light-sensitive DEGs, i.e. those that have a $\log_2$FC>2, in Col-0 vs *bhlh089 bhlh091,* sexual reproduction and lipid storage GO terms are still enriched in Col-0 light response only (Figure 4.5), however whilst glucose import is enriched only in the Col-0 transcriptome, this is not significant ($p>0.05$). Whilst oxidation-reduction processes remain enriched in both genotypes, this is only significant in Col-0 ($q<0.05$), thus it appears that the *bhlh089 bhlh091* mutant has an impaired oxidation-reduction response. Since circadian rhythm biological processes are enriched in both the light responses of Col-0 ($q<0.01$) and *bhlh089 bhlh091* ($q<0.05$, Figure 4.5) it seems that the light-sensitivity of bHLH089 and bHLH091 is not linked to the circadian clock.

The enrichment of SCF-dependent proteasomal ubiquitin-dependent catabolic processes seen in cluster 6 is lost within the $\log_2$FC>2 dataset, primarily because all but 1 of the 12 F-box genes in this cluster have a $\log_2$FC<2. Regardless, the fact that these genes are differentially expressed only in the WT response to light is still likely to be important and it suggests that ignoring $\log_2$FCs between 1

and 2 may be too stringent. A quick search of F-box proteins within the whole RNAseq dataset revealed that 80 are differentially expressed ($log_2FC>1$), and of these 63 are upregulated in response to low light in Col-0 but not *bhlh89,91*. F-box proteins are a key component of the SCF ubiquitin-ligase (E3) complexes, involved in binding target proteins. The huge variety of different F-box proteins, each with different target specificity, contributes to post-translational regulation of many different processes in Arabidopsis (Callis and Vierstra, 2000). The observed loss in light-sensitive regulation of F-box genes in the *bhlh089 bhlh091* mutant could implicate bHLH089 and -091 in control of ubiquitin-mediated proteolysis of multiple genes in response to abiotic stress.

4.3.2 Enrichment of genes related to Sexual Reproduction is lost in the *bhlh* mutant

Crucially, there is no enrichment (significant or otherwise) of genes related to sexual reproduction in the light-response of the *bhlh089 bhlh091* mutant (Figure 4.5). bHLH010, -089 & -091 had been previously reported as having a functionally redundant role in male reproductive development (Zhu et al., 2015) and ordinarily the remaining functional bHLH rescues fertility defects in the *bhlh* double mutants. Since transcription of all the core tapetal bHLH transcription factors are reduced in low light (Figure 3.9) it may be that the levels of bHLH010 transcript are not sufficient to support the roles of the lost bHLH089 and bHLH091 and activate downstream reproductive genes in low light treated *bhlh089 bhlh091*. However, given the enrichment of the SCF-dependent proteasomal ubiquitin-dependent catabolic process in cluster 6 it is also possible that bHLH10 has a distinct function from bHLH89 and -91 and that lack of bHLH89/91-dependent proteolysis of other genes within the reproductive development pathway is causing widespread transcriptional changes.

Curiously, all of the anther genes which respond to light in Col-0 ($log_2FC>2$) but not *bhlh089 bhlh091* ($log_2FC<1$; Table 4.3) show upregulation in response to low light in WT, suggesting that the bHLHs play an activating role under low light conditions. A large proportion of this filtered set in Table 4.3 have a confirmed role in male reproductive development and many of the published mutant phenotypes of these genes mimic the *bhlh* mutant phenotypes (Table 4.7). For example, reduced silique lengths and/or seed set are recorded in p35S::GASA10, *ltpg4*, *myb97-myb101-myb120, nip4;1,* p35S::SBT5.4, *sweet8* and *tsm1* mutants (Trapalis et al., 2017; Edstam and Edqvist, 2014; Liang et al., 2013; Di Giorgio et al., 2016; Liu et al., 2009; Guan et al., 2008; Fellenberg et al., 2008) and the delayed onset of fertility shown in the *bhlh* double mutants is also very clearly echoed in the *nip4;1* mutant (Di Giorgio et al., 2016).

The pollen coat consists of vast number of waxes, lipids, sterols, sugars, proteins and phenylpropanoids such as spermidine conjugates and flavonols (Shi et al., 2015). Spermidine biosynthesis & metabolism GO terms were enriched in Col-0 but not *bhlh089 bhlh091* and this was

also reflected in the Pathview comparison of the phenylpropanoid biosynthesis KEGG pathway (Figure 4.5, Figure 4.6). Polyamines, such as spermidine, are involved in abiotic and biotic stress adaptations as well as normal plant growth and reproductive development, with losses of biosynthetic enzymes resulting in decreased pollen viability (Chen et al., 2014). Four of the DEGs in our filtered list are known to affect the levels of spermidine in the pollen coat: TAPETUM-SPECIFIC METHYLTRANSFERASE 1 (TSM1), an O-methyltransferase belonging to the CCoAOMT gene family, the BAHD acyltransferase SPERMIDINE HYDROXYCINNAMOYL TRANSFERASE (SHT) and two partially redundant cytochrome P450 enzymes CYP98A8 and CYP98A9 (Fellenberg et al., 2008; Grienenberger et al., 2009; Matsuno et al., 2009), all of which act together in a single spermidine biosynthetic pathway in pollen development (Fellenberg et al., 2009). Grienenberger *et al.* (2009) hypothesised that the location of these spermidines in the outer layer of the pollen coat may protect the pollen grain against environmental stresses. Since differential regulation of these four crucial enzymes in response to low light stress are observed in the *bhlh089 bhlh091* mutant one might expect significant changes in spermidine derivatives in the pollen coat compared to WT, leading to reduced protection of the pollen from environmental stresses.

Additionally, a recent study by Grunewald et al. (2020) showed that the tapetum-specific major facilitator protein NPF4.8, also known as FLAVONOL SOPHOROSIDE TRANSPORTER 1 (FST1), is required for transport and accumulation of flavonol sophorosides on the pollen surface. Although loss of *fst1* affects deposition of flavonols, no dramatic effect on pollen structure was seen and mutant plants showed only a 10% reduction on pollen viability. However, our data showed that alongside FST1, a number of other NPF proteins are differentially regulated in the anther in response to light. Indeed, NPF4.3 was identified as direct target of AMS and is thus likely to also play a key role in pollen development (Xu et al., 2010). FST1 could be acting redundantly with other family members to control pollen coat development, it would therefore be interesting to develop combinations of *npf* knockout lines to assess pollen coat phenotypes.

Many of these genes will of course act much downstream of the bHLHs. Whilst there has been no differentiation between direct or indirect targets here, the expression profiles may provide clues as to what genes may be directly regulated, focussing on those that are expressed in the same stages as bHLH89/91 (tetrad stage, aka. flower stage 9, Table 4.3 B). In this way potential targets can be narrowed down and Chromatin Immunoprecipitation (ChIP)-qPCR can be carried out in future to assess bHLH binding.

Table 4.7. Published reproductive phenotypes and floral expression of DEGs from Table 4.3. Papers which show only expression patterns are shown in brackets. Key: Ant- anther, C- filament-anther contact, F- flower, Msp- Microspore, Si- Silique, St- stamen, Tpm- tapetum.

Gene	Reference	Expression	Mutant Phenotype
ABCG9	Choi et al. 2014	Tpm	*abcg9 abcg31* pollen shrivelled, clumped and collapsed, 50% loss pollen viability. Humidity and temperature dependant
AGP23	(Pereira et al., 2014)	Msp	
AMT1-4	(Yuan et al., 2009)	Msp	no phenotype (single KO), role in ammonium uptake
ATA27 / BGLU20	Dong et al., 2019 (Rubinelli et al., 1998)	Tpm	KO 35-65% reduction in pollen viability
CDG1	Kim et al., 2011		OE flattened siliques
COPT3	Andrés-Colás et al., 2010 (Honys et al., 2006)	Tpm & Msp	OE short stamens
CYP98A8	Matsuno et al., 2009	Tpm	KO altered spermidine levels
CYP98A9	Matsuno et al. 2009	Tpm	KO altered spermidine levels
CYS2	(Hwang et al., 2010)	C	
ENODL5	(Mashiguchi et al., 2009)	Msp	no phenotype (single & double KO)
ENODL6	(Mashiguchi et al., 2009)	Msp	no phenotype (single & double KO)
EXL4	Updegraff et al., 2009		KO slow hydrating pollen after stigma contact (worsened in *exl4 grp17*)
EXL6	Dong et al., 2016	Msp	KO severe pollen defect, cytoplasm degeneration after tetrad stage
GASA10	Trapalis et al. 2017	Tpm & Msp	OE reduced silique length & seed number, KO no phenotype
GPD6	(Cheng et al., 2011)	Ant	
GRDP2	Ortega-Amaro et al., 2015	F	KO late flowering, OE early flowering, auxin accumulation and salt stress
GRP17	Mayfield and Preuss, 2000	St	KO delay in pollen hydration after stigma contact
LBD27 / SCP	Chen and McCormick, 1996; Oh et al., 2010; Kim et al., 2015	Msp	KO 53% pollen abortion & extra-celled microspores, delayed mitosis, *lbd27 lbd10* shrivelled unviable pollen
LHT2	Lee and Tegeder, 2004	Tpm & Msp	no phenotype (single KO), amino acid transport / pollen nutrition
LTP12	(Ariizumi et al., 2002)	Tpm	
LTPG3	Edstam & Edqvist, 2014		sterile, deformed/collapsed pollen
LTPG4	Edstam & Edqvist, 2014		sterile, deformed/collapsed pollen, reduced seed set in early siliques
MCTP11	(Liu et al., 2018)	Msp	
MGD3	(Kobayashi et al., 2004)	Msp & Ant	
MYB101	Alonso-Peral et al., 2010; Leydon et al., 2013; Liang et al., 2013	Msp	*myb33 myb65 myb101* male sterile; *myb97 myb101 myb120* shorter siliques, reduced seed set (fail to discharge sperm); GA responsive
NIP4;1	Di Giorgio et al. 2016	Msp & Ant	KO collapsed pollen, delayed onset of fertility (smaller siliques) and reduced seed set; worsened in *nip4;1 nip4;2*amiR line
NPF4.8 / FST1	Grunewald et al., 2020	Tpm	reduced accumulation of flavonol sophorosides on the pollen surface, slight reduction in pollen viability, otherwise normal pollen structure
NPF7.1	(Babst et al., 2019)	Msp & Ant	increased flower stalk branching and size, response to Nitrogen
SBT5.4	Liu et al. 2009	F & Si	OE stunted misshapen siliques, KO no phenotype
SHT	Grienenberger et al., 2009	Tpm	KO reduced spermidines, pollen coat irregularities and depressions, less autofluorescence, reduced silique number and seed set; OE more pollen autofluorescence
STP2	(Truernit et al., 1999)	Msp	
SWEET8/ RPG1	Guan et al. 2008; Zhu et al., 2020	Tpm & Msp	KO delayed fertility, 90% reduced seed set, post-meiotic microspore abortion, defective exine development from tetrad stage. Fertility restored at low temperature and by slowing development.
TET11	(Wang et al., 2015)	Msp	
TOL8	Korbei et al., 2013		*tol5 tol8* & *tol7 tol8* double KOs aborted seed; quintuple KO mutant delayed flowering, reduced fecundity
TSM1	Fellenberg et al. 2008	Tpm	KO reduced spermidines and short, misshapen siliques
XTH3	(Ariizumi et al. 2002)	Tpm	
YSL3	Waters et al., 2006	Ant	*ysl1 ysl3* reduced pollen viability

4.3.3 Lipid storage, metabolism & transport is impaired in *bhlh089 bhlh091*

In the previous chapter it was demonstrated that tapetum and pollen of the *bhlh89,91* mutant seemingly have a higher number of lipid bodies. Enrichment of DEGs related to lipid storage, metabolic process and transport between light conditions in WT is lost in the *bhlh089 bhlh091* mutant. Looking at the genes involved in these processes, this is largely because of a loss of upregulation in low light of the previously highlighted tapetal genes (Table 4.3): GLYCINE RICH PROTEIN14 (GRP14), GRP16- 20, EXTRACELLULAR LIPASE4 (EXL4) & 6, NPF4.6, ORP4C, LIPID TRANSFER PROTEIN 12 (LTP12), -11 & -13 and ASPARTIC PROTEINASE A3 (APA3).

EXLs 4 & 6 and GRPs 14, 16-19 proteins are highly abundant in the pollen coat (Mayfield et al., 2001) and a recent study by Lu *et al.* (2020) showed that they are downstream of MS1 in anther development. AMS was also found to directly bind to the promoters of EXL4-6 and GRP14, 18 & 19 thus suggesting that their expression is partially controlled by AMS (Xu et al., 2010, 2014). In terms of function, EXL4 and GRP17 have both been shown to play a prominent role in pollen hydration whilst *exl6* plants show defective microspore development (Updegraff et al., 2009; Mayfield and Preuss, 2000; Dong et al., 2016). Although the other genes haven't yet been characterised it is possible that the remaining genes are also involved in lipid deposits on the pollen coat. Since the *bhlh89,91* mutant is sterile in low light and the vast majority of these genes are also differentially regulated in the male sterile *dyt1, ams* and *ms1* mutants this may reflect general changes that occur in male sterile backgrounds rather than specifically light-responsive changes. Of course, given that bHLH89, 91 and 10 are known to interact with DYT1 and AMS to co-regulate targets this could also explain the overlap (and the fact that relatively few of the DEGs change in *ms1* background).

Other abiotic stresses, such as heat, are known to impact the composition of lipid species within the pollen. Studies of pea cultivars (*Psium sativum* L.) showed that lipid content on the pollen surface changes in response to heat stress (Lahlali et al., 2014; Jiang et al., 2015). Likewise the phospholipid content of pollen grains is significantly altered in heat-stressed Sorghum (*Sorghum bicolor* L.) (Prasad and Djanaguiraman, 2011). It may be that similar changes in pollen coat composition occur during low light stress.

Reproductive development is highly energy intensive, and photosynthesis is essential in providing the carbohydrates to fuel respiration to meet this energy requirement (Ferguson et al., 2021). Rates of photosynthesis of course depends largely on light availability, thus under low light conditions photosynthesis is slowed, fewer carbohydrates are produced and the flowers cannot develop properly. Carbon status in the floral tissue is therefore correlated with fertility, with low light availability leading to defective pollen development (Lauxmann et al., 2016).

4.3.4 Overlap among tapetal bHLH transcriptomes

By comparing differential genes expression in the *bhlh89,91* mutant to other male sterile transcriptomic data we can gain a sense of downstream targets that may be co-regulated by an interaction of AMS and DYT1 with bHLH89, -91 and -10. DYT1 has been shown to require either bHLH89, -91 or -10 for nuclear localisation and therefore transactivation (Cui et al., 2016), therefore significant overlaps are expected.

A significant level of overlap between *bhlh089 bhlh091* DEGs and the *dyt1* and *ams* microarrays was observed, at 94% and 86% respectively (Figure 4.11). Curiously, however, there is very little overlap between these and the *bhlh089 bhlh010 amiR-bHLH091* triple mutant RNAseq that was re-analysed to fit the statistical parameters of our RNAseq study. This is very surprising given the high degree of overlap between *dyt1* and the *bhlh* triple mutant reported by Zhu *et al.* (2015). However comparing the list of triple *bhlh* DEGs from Zhu *et al.* (2015) with our re-analysed set there is very little consensus between the two, most likely due to our more stringent analysis parameters, there were much fewer DEGs highlighted from the 2 biological replicates.

A large proportion of the genes assumed to be direct targets of AMS (Xu et al., 2010, 2014) were upregulated in low light in Col-0 but unchanged in the *bhlh89,91* mutant suggesting that bHLH action is crucial to the integration of light signals into AMS-regulated reproductive development. Given that bHLH89 and 91 interact with AMS (Xu et al., 2010) it seems likely that the bHLHs are regulated in response to environmental signals, thus affecting this interaction and impacting on expression of AMS targets. Since these targets (e.g. EXLs and GRPs, CYP98A8 & A9 and NPFs) all appear to play a crucial role in pollen development, as discussed in previous sections, it seems likely that loss of the bHLH- environmental signal 'hub' at this point is what causes the huge changes to pollen morphology reported in Chapter 3.

4.3.5 Light sensing is unaffected by bHLH89/91

Whilst many biological processes highlighted in the GO term enrichment analysis exhibit changes in enrichment in the *bhlh* mutant, responses to red light, far-red light, UV-B and UV-A are unaffected, if not more enriched in *bhlh089 bhlh091*. Thus, the reduced transcriptional response of the *bhlh89,91* does not appear to be due to impaired light sensing.

Comparing the transcriptome response of a Col-0 seedling to simulated shade (Leivar et al., 2012) to pre-mitotic Col-0 buds in this RNAseq study, 11% of seedling shade-responsive DEGs were found to be conserved.

Not only would we expect big differences in the genes involved in development of seedlings vs floral tissue, but Leivar *et al.* (2012)' seedlings were grown on agar with FR supplemented light to simulate shaded conditions, whereas our plants were grown on soil under shade-netting. As the experimental set-ups were vastly different between Leivar *et al.* (2012)'s investigation and our own study it is impossible to directly compare the two. With these growth differences in mind it's perhaps surprising that there are any commonalities in the datasets at all, let alone an 11% overlap.

From GO enrichment analysis, there seems to be conservation of genes related to auxin response and signalling in the Col-0 buds as well as stress-indicative terms such as phenylpropanoid metabolism and flavonoid biosynthesis. Notably early light-sensitive genes, such as *PIF4,* respond in much the same way to shade in seedlings as they do in response to low light in flowers (Table 4.5). However, more downstream genes are differentially regulated in floral tissue, such as those involved in hormonal responses: *ARABIDOPSIS RESPONSE REGULATOR 16 (ARR16)* and *GRETCHEN HAGEN3.9 (GH3.9)*. These show upregulation in response to low light in flowers but downregulation in response to shade in seedlings; suggesting that whilst there is overlap in pathways vegetative and reproductive tissues could be responding very differently to light.

4.3.6 *bhlh089 bhlh091* hormone signal transduction & biosynthesis differs from WT

GO term enrichment analysis suggested that genes related to response to Auxin ($q<0.05$), Jasmonic Acid (JA), Ethylene stimulus and Gibberellic Acid (GA) ($p<0.05$) are significantly enriched in Col-0 buds in response to changes in light intensity. This enrichment was absent in the *bhlh089 bhlh091* mutant suggesting that the bHLHs might have a regulatory role in hormone response. These differences in hormone signal transduction in WT vs the *bhlh* mutant were further highlighted in the Pathview plots (Figure 4.8).

4.3.6.1 Auxin

According to Figure 4.8, AUX/IAAs were upregulated in WT and downregulated in *bhlh089 bhlh091*. However, if you look at the RNASeq dataset, only INDOLEACETIC ACID-INDUCIBLE17 (IAA17) and IAA32 are downregulated in response to low light and this hold true for both the *bhlh* mutant and WT (Table 4.2). Despite this, there is a net upregulation in WT as seven additional IAAs are upregulated under low light solely in Col-0. Generally, upregulation of IAA genes results in a lower response to auxin, since AUX/IAAs dimerize with ARFs and repress their activity (Tiwari et al., 2001).

Many ARFs are known to interact with other bHLHs through heterodimerization, for example ARF6 binds PIF4 proteins, and has also been shown to bind to the promoters of multiple bHLHs involved in shade-avoidance including *PRE*s, *BIM1* and *BEE1* (Oh et al., 2014). It may be that bHLH089 & -091

regulate auxin signalling through dimerization with ARFs and activating some form of positive feedback loop.

In this study there is also a general upregulatory trend in WT of the Gretchen Hagen 3 (GH3) family proteins including YADOKARI1 (YDK1), which is largely lost or reduced in the *bhlh089 bhlh091* mutant. GH3 proteins conjugate amino-acids to free IAAs, inactivating the IAA and decreasing auxin response (Staswick et al., 2005; LeClere et al., 2002). Several of the GH3 proteins differentially expressed in our study have been previously shown to be regulated by light. YDK1 is upregulated in darkness and red light (Takase et al., 2004), GH3.5 expression is increased by FR light (Tanaka et al., 2002) and GH3.6 otherwise know as DWARF IN LIGHT1 (DFL1), was shown to act within the light signal transduction pathway in seedlings (Nakazawa et al., 2001).

This all points towards differential auxin signalling responses in low-light-treated Col-0 buds that are missing in the *bhlh089 bhlh091* mutant, suggesting that these tapetal bHLHs are involved in regulating multiple components of the auxin signalling pathway.

The PIFs, in addition to their role in auxin signalling, have been shown to increase auxin biosynthesis in response to shade through upregulation of YUCCA8 and 9 (Hornitschek et al., 2012; Li et al., 2012). In our data, there was a 4-fold upregulation of the close relative YUC2 in low-light treated Col-0 buds but no differential regulation in the *bhlh* mutant in response to light. Since YUC2 is strongly expressed in the tapetum and developing microspores prior to pollen mitosis I (Cecchetti et al., 2008), and therefore overlaps with bHLH expression, this implies that auxin biosynthesis, as well as signalling, may be influenced by bHLH089 & -091 just like their distant PIF cousins.

Auxin appears to be important in anther development, particularly at Tetrad to Single Microspore stages, with auxin synthesis playing a major role in control of stamen and pollen development (Cecchetti et al., 2008; Cheng et al., 2006). Pollen development was found to be accelerated in later stages in the *tir1 afb1 afb2 afb3* mutant, which is defective in auxin-perception (Cecchetti et al., 2008); both this line and the auxin transporter *mdr1 pgp1* mutant exhibited stunted stamen elongation. Interestingly, male sterility was obsereved upon treatment with the auxin transport inhbitor NPA and in the Middle Layer (ML)-deficient *receptor-like protein kinase2 (rpk2)* mutants (Cecchetti et al., 2017), suggesting that auxin transport from the tapetum in to the ML is vital in maintaining fertility. With decreased expression *of AMS, MS1* and *MYB80 (MS188)* in *rpk2* mutants and upon NPA-treatment, this suggests that core tapetum development transcription factors are highly sensitive to changes in auxin levels.

In summary, it appears that auxin biosynthesis may increase in Col-0 flowers, but not in *bhlh89,91*, in response to low light. Conversely it seems that auxin signalling may be increased in *bhlh89,91* since there is loss of WT net upregulation of inactivating GH3 and IAA family proteins. Therefore one could speculate that subsequent changes to auxin levels and signalling may be contributing to the male sterile defects observed under low light in the *bhlh89,91* mutant. Future study into auxin changes within the floral tissue in Col-0 and *bhlh* mutant backgrounds will thus be intensely valuable. Alongside global hormone profiling by mass spectrometry, the use of auxin reporter lines in Col-0 vs *bhlh* mutant floral tissue under different light treatments would be of interest.

4.3.6.2 Jasmonic Acid (JA)

In terms of core JA signalling transduction, there is differential expression of the GH3 gene JASMONATE RESISTANT 1 (JAR1). Whereas in auxin signalling the conjugation of amino acids to IAA largely inactivates them, the JA-Ile conjugate promoted by JAR1 is the bioactive form, thus the lack of upregulation of JAR1 in *bhlh089 bhlh091* low-light suggests that JA signalling is not induced in the *bhlh* mutant. However, responses to JA are enriched in clusters 3, 7 and 10 which represents genes that are either differentially regulated in the *bhlh89,91* mutant compared to Col-0 in both light conditions and do not strongly respond to light, or are more strongly regulated in response to light in *bhlh89,91* (Figure 4.2C, Figure 4.4). Therefore it seems that JA signalling is unlikely to be critical in the light-sensitive sterility of the *bhlh89,91* mutant.

4.3.6.3 Cytokinin

There is upregulation of CYTOCHROME P450 FAMILY 735A1 (CYP735A1), CYP735A2 and CYTOKININ DEHYDROGENASE 2 (CKX2) in response to low light in Col-0 that is absent in the *bhlh* mutant. CYP735A1 and –A2 encode cytokinin hydroxylases that catalyse trans-Zeatin biosynthesis (Takei et al., 2004) whereas CKX2 has sequence similarity with cytokinin oxidase/dehydrogenases, which degrade cytokinins. Thus there is upregulation of enzymes related to both cytokinin biosynthesis and degradation in Col-0 low light, that is absent in the *bhlh* mutant, suggesting that bHLH89/91 may be involved in increasing cytokinin biosynthetic flow in low light.

Figure 4.8 implies that WT differential regulation of type A- and B-ARRs in Cytokinin signalling in low light is absent in the *bhlh089 bhlh091* mutant. However, whilst there is a loss of upregulation of the type-A ARRs (ARR9 & -16) in low-light treated Col-0, there is no differental regulation of the type-B ARR11 in light (Table 4.2). And although the differentially expressed APRR4 groups with the type-B ARRs hence the highlighted Pathview box, it is in fact a pseudo-response regulator and is not considered a part of the family due to the lack of a conserved D-D-K motif (Maxwell and Keiber, 2010). Since type-A ARRs are negative regulators of cytokinin sigalling and are upregulated in

response to cytokinin, loss of differential expression in the *bhlh* mutant may be an artefect of the aforementioned changes to cytokinin biosynthesis.

4.3.6.4 Abscisic Acid (ABA)

In terms of ABA signalling components there are big differences in light-responsive regulation in Col-0 vs *bhlh089 bhlh091* in the Pathview plots (Figure 4.8) which indicated downregulation of the PYR/PYL ABA sensors in Col-0 low light. However, focussing in on the individual gene responses, not only is there downregulation of *PYL2* and *PYL11* but there's also upregulation of *PYL5* (Table 4.2). These ABA receptors have functionally diverse roles, with PYL2 showing ABA-dependent inhibition of PP2Cs whereas PYL5 is ABA-independent, thus its been suggested that that PYL5 may be involved in processes other than ABA signalling (Hao et al., 2011).

Downstream of the PYLs in ABA signalling: ABI2, SnRK2.3 and 2.9, show upregulation in Col-0 low-light but no change in the *bhlh89,91* mutant (Table 4.2). ABI2 encodes a protein phosphatase 2C (PP2C) which act as negative regulators of ABA signalling and also co-receptors of ABA signalling with PYR/PYL. In the absence of ABA, PP2Cs are free to repress SnRK2 activity, however when ABA is present PYR/PYL receptors interact with PP2Cs allowing derepression of SnRK2s and phosphorylation of ABA-RESPONSIVE ELEMENT BINDING FACTORS (ABFs). Thus the differential regulation of these genes under low light in Col-0 suggests that ABA sensitivity might be increased, but since this does not occur in the *bhlh* mutant this implicates bHLHs in regulation of ABA signalling.

There is additional evidence for ABA playing an important role in light-sensitive sterility since ABI5 levels are elevated in the light-sensitive sterile mutant *yet another kinase1* (*yak1,* Huang et al., 2017). ABI5, a basic leucine zipper (bZIP) transcription factor, is highly conserved with the ABFs and has been shown to bind to PP2C promoters including *ABI2*, thus forming a negative feedback loop (Wang et al., 2019). ABI5 was upregulated in response to light in both Col-0 and *bhlh89,91*, although to a slightly lesser degree in the latter which suggests a minimal role for bHLHs in regulating ABI5 levels. But changes in upstream signalling components as outlined above suggests that ABA signalling may be important in conditional sterility.

A link between light, bHLHs and ABA signalling has been previously shown in seed germination where PIF1 directly induces *ABI3* and *ABI5* expression (Oh et al., 2009) and activates *SOMNUS* (*SOM*), which in turn activates genes involved in ABA biosynthesis and supresses catabolism by *CYP707A2*, increasing ABA levels (Kim et al., 2008).

Much like the previously mentioned phytohormones, not only are there changes in ABA signal transduction in the RNASeq dataset but there is also differential regulation of biosynthetic genes. In

this case there is a 2-fold change in WT expression of *AAO3* that is absent in the *bhlh89,91* mutant. Since AAO3 catalyses the final step of ABA biosynthesis one might expect ABA levels to reduced in the *bhlh89,91* mutant. As ABA induces expression of PP2Cs (Wang et al., 2019) it follows that this may be the cause of some of the differences in expression changes just discussed. Thus its possible that, like their PIF cousins, tapetal bHLHs regulate ABA signalling either through regulation of biosynthesisis or downsteam transcription factors.

4.3.6.5 Gibberellin (GA)

bHLHs and GA signalling have long been linked in shade-avoidance reponse, and according to the hormone signal transduction KEGG pathway there appears to be upregulation of GA responsive transcription factors in low light in both WT and *bhlh89,91* mutant inflorescences (Figure 4.8). However, genes related to gibberelic acid signalling pathway and response to gibberellin are enriched in clusters 5 & 6 (Figure 4.2C, Figure 4.4) suggesting that these processes are regulated in response to light in Col-0, but not in *bhlh89,91*. This is supported by the particularly strong upregulation of GA-regulated transcription factors GASA11 and -10 under low light in Col-0 that is absent in the *bhlh* mutant (Table 4.2).

Crucially, it seems that regulation of GA biosynthesis is altered in the *bhlh* mutant (Figure 4.9). *GA1*, an ent-kaurane synthetase, is upregulated under low-light in WT, but not in the *bhlh* mutant. GA1 is highly active in anthers of developing flowers (Silverstone et al., 1997) and catalyses the first step in GA biosynthesis. With lower GA1 activity in *bhlh89,91* there is likely to be decreased GA biosynthesis on the whole compared to Col-0. Furthermore there is differential regulation in enzymes involved in the later steps of the biosynthetic pathway but once again the situation is not as clear-cut as the Pathview plots suggest. *GA20OX1* is apparently unaffected by bHLH expression and remains downregulated in both genotypes in low light whereas there is upregulation of *GA20OX2* only in Col-0. Since GA20OX1 & -2 occupy the same space in the pathway, the upregulation of *GA20OX2* in Col-0 presumably negates the net downregulation seen in the *bhlh089 bhlh091* KEGG pathway.

GA20OX1, 2 and 3 are functionally redundant and expression levels are important in the establishment of plant fertility, with increasingly defective sterile phenotypes in double and triple mutants that echo those of *bhlh010, -089 and -091* mutants. The *ga20ox1 ga20ox2* double mutant for example has a semi-fertile phenotype with impaired seed set in early flowers and reduced silique elongation throughout development (Rieu et al., 2008b) whilst the *ga20ox1 ga20ox2 ga20ox3* triple mutant was completely sterile due to defective tapetum degeneration and a post-meiotic arrest in

stamen development (Plackett et al., 2012). It follows then that impaired upregulation of just one of these genes in the *bhlh* mutant may have a significant effect on GA biosynthesis and fertility.

GA2OX genes on the other hand mediates the degradation of bioactive GA (Rieu et al., 2008a). The *ga2ox1 -2 -3 -4 -6* quintuple mutant had a number of phenotypes including reduced fertility, characterised by reduced silique lengths and seed number. Our RNAseq data showed low-light upregulation of *GA2OX1* only in Col-0, whereas upregulation of *GA2OX2* was maintained in both genotypes and no significant expression changes were observed in *GA2OX3, -4* or *-6* in response to low light. It's possible that differential regulation of 1 out of the 5 *GA2OX* genes may have an effect on GA degradation, but given the high functional redundancy it's unlikely. Thus one might expect degradation of bioactive GA to not be significantly altered in the *bhlh089 bhlh091* mutant.

Four *NPF*s and two *SWEET* genes with confirmed GA transporter activity (Chiba et al., 2015; Kanno et al., 2016) are differentially expressed in the *bhlh89,91* mutant compared to WT, suggesting that bHLHs may impact on GA transport in addition to biosynthesis. Taken together one might expect to see big changes in GA levels in *bhlh* mutant flowers in comparison to Col-0 under different light conditions, therefore this will be explored further in Chapter 5.

Table 4.8 Summary of changes to phytohormone biosynthesis and response according to RNAseq data. Increased activity highlighted in red and decreases highlighted in blue.

Hormone	Biosynthesis	WT	bhlh89,91	Signalling/Response	WT	bhlh89,91
Auxin	May increase in Col-0 in response to low light, but not *bhlh89,91,* as *YUC2* is only upregulated in Col-0			Appears to decrease in Col-0 in low light, but not in *bhlh89,91*, as *IAA*s and *GH3*s mostly upregulated only in Col-0		
Cytokinin	Likely increases in WT through upregulation of *CKX2* and *CYP73*s, but is unchanged in *bhlh89,91*			Uncertain		
ABA	Possibly increased in Col-0 response to low light, but unchanged in *bhlh89,91*, as *AAO3* is upregulated only in Col-0			Appears to increase in Col-0 in response to low light, as *ABI2* and *SnRK*s are upregulated and *PYL* receptors are differentially expressed, but are unaltered in *bhlh89,91* mutant		
GA	Probably increased in Col-0 low light response with respect to *bhlh89,91*			Likely induced in Col-0 low light response but not *bhlh89,91.*		

4.4 CONCLUSIONS

Our results show that low-light induces huge transcriptional changes in the early stages of flower development in Col-0 that are absent in the *bhlh089 bhlh091* mutant. This suggests that bHLH089 and bHLH091 are critical in floral-response to low light stimulus, through regulation of genes related to sexual reproduction, lipid storage and metabolism, and hormonal responses. In the next chapter the effect of bHLHs and low light on GA levels shall be explored. However, as it seems that other hormonal responses may be greatly affected by the bHLHs (Table 4.8), additional study of other hormones in low-light treated *bhlh* mutants could provide valuable insight into the mechanisms behind light responses. A number of genes have also been identified which exhibit light-sensitive regulation reliant on bHLH activity. Further analysis of the control and function of these genes will help to elucidate the role of the bHLHs in male reproductive development.

5 bHLHs and Gibberellin (GA) signalling

5.1 Introduction

Gibberellin (GA) is an essential phytohormone in plant growth and development, regulating vegetative and reproductive development alike in everything from seed germination to stem elongation, leaf expansion and floral transition (Fleet and Sun, 2005). GA is also necessary for normal reproductive development, controlling amongst other things filament elongation and pollen development in *Arabidopsis* and Rice *Oryza Sativa* (Plackett et al., 2014). Studies in these two species have led to the identification GA signalling components from the point of perception at the GID1 GA receptor (Ueguchi-Tanaka et al., 2005; Griffiths et al., 2006) through to control of anther development by the GAMYB transcription factor, which controls the majority of GA-regulated genes within the rice anther and is essential to tapetum and pollen exine development (Aya et al., 2009).

DELLA proteins are repressors of GA responsive growth and development, bioactive GA stimulates rapid degradation of the DELLAs and thus relieves this repression. DELLAs belong to the GRAS family of transcriptional regulators (so named for GAI, REPRESSOR OF GA1-3 [RGA], and SCARECROW [SCR]) and are structurally characterised by a GRAS domain at the C-terminus and a conserved DELLA (aspartate (D), glutamate (E), leucine (L), leucine (L), alanine (A)) domain at the N-terminus. GFP fusion reporters show that the DELLAs localise to the nucleus (Silverstone et al., 2001) where they interact with transcription factors to regulate expression of GA-responsive genes (Fleet and Sun, 2005; Zentella et al., 2007). GA, when present, binds to the GID1 receptor causing it to interact with the DELLA protein and recruiting the SCF/SLY1 ubiquitin E3 ligase complex. This causes polyubiquitination of the DELLA, which is subsequently targeted to the 26S proteasome and degraded, thus de-repressing GA responses (Figure 5.1).

The anther is very sensitive to changes in levels of GA. An excess of GA, simulated by exogenous GA treatment and/or DELLA loss of function, causes male sterility through defective male meiotic cytokinesis and callose wall formation (Plackett et al., 2014; Liu et al., 2017a). Conversely, GA-deficiency or insensitivity, through loss of GA biosynthesis genes or receptors, also affects fertility through impaired floral organ development (Koornneef and van der Veen, 1980; Rieu et al., 2008b; Plackett et al., 2017; Hu et al., 2008; Griffiths et al., 2006). Studies in rice suggest that within anther development GA has the greatest effect on the tapetum tissue, with GA-deficient or GA-insensitive lines all showing enlarged tapetums with defective Programmed Cell Death (PCD) (Aya et al., 2009). Overexpression of SPINDLY (SPY), an *Arabidopsis* protein involved in repression of GA signal

transduction, was also shown to inhibit post-meiotic anther development in Petunia (Izhaki et al., 2002). A delicate balance in GA levels thus shapes male reproductive development.

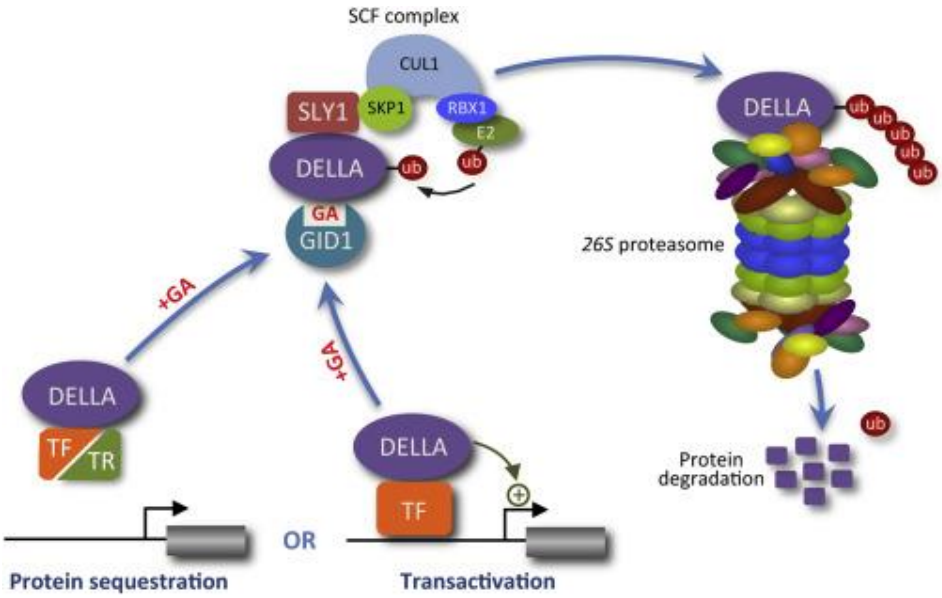

Figure 5.1. DELLA-mediation of GA responses. In the absence of GA, DELLA proteins repress GA responses by interacting with Transcription Factors (TF) or regulatory proteins (TR), inhibiting their activity or activating transcription of TF-targets. When GA level increase, GA binding to the GID1 receptor enables an interaction with DELLAs which results in recognition by the SCF/SLY complex. DELLA proteins are subsequently ubiquitinated and targeted for degradation through the 26S proteasome, de-repressing GA responsive genes. Figure from Davière and Achard (2016)

Many monocot crops contain a single DELLA protein: REDUCED HEIGHT-1 in Wheat (RHT-1, Peng et al., 1999), SLENDER RICE 1 in Rice (SLR1, Ikeda et al., 2001) and also SLENDER 1 in Barley (SLN1, Chandler et al., 2002). However there are five paralogues of DELLA in Arabidopsis: REPRESSOR OF ga1-3 (RGA), GA INSENSITIVE (GAI) and RGA-LIKE 1, 2 and 3 (RGL1, RGL2 and RGL3) each with overlapping and distinct roles (Davière and Achard, 2016; Dill and Sun, 2001). GAI and RGA are expressed ubiquitously (Tyler et al., 2004), and regulate flowering time in response to GA-signalling, whereas RGL1 & 2 are relatively enriched in the inflorescence (Lee et al., 2002; Wen and Chang, 2002) and are involved in floral organ development. GA-deficiency seemingly blocks stamen and anther development through the interaction of RGA, RGL1 and RGL2 (Cheng et al., 2004).

The first observation of the 'release of DELLA restraint' model (Peng et al., 1997) in plants was in RGA-mediated regulation of PHYTOCHROME INTERACTING FACTOR 4 (PIF4) activity (De Lucas et al., 2008). PIF4, an Arabidopsis bHLH protein, plays a central role in shade avoidance responses through activation of genes involved in hypocotyl elongation. De Lucas *et al.* (2008) found that light not only destabilises the PIF4 protein through the light-activated phyB photoreceptor, but also that DELLAs repress the transcriptional activity of PIFs by interacting through the bHLH DNA-binding domain, sequestering them into an inactive DELLA-PIF complex that is unable to bind DNA. Upon exogenous GA treatment, or induction of higher levels of endogenous GA (for example in shaded conditions),

RGA is degraded and PIF4 is released from the inactive complex, enabling activation of genes in the shade avoidance response.

De Lucas *et al.* (2008) thus provided the first evidence for DELLA regulating activity of bHLH transcription factors through their bHLH domain. Since then, DELLAs have been found to regulate the action of many bHLH proteins including bHLH48 and bHLH60 which control floral transition in response to GA (Li et al., 2017a). In the tapetum development pathway, bHLH089 and bHLH091 have both been reported to interact with GAI and RGA in Yeast 2 Hybrid (Y2H) screens (Marín-de la Rosa et al., 2014; Lantzouni et al., 2020). ATTED-II data (http://atted.jp) shows that co-expression is particularly high between bHLH089/91 and RGL2 (Marín-de la Rosa et al., 2014), suggesting that they may have a role in co-regulating tapetum development, further study could reveal interaction between these proteins.

The phenotypes observed in various *bhlh089, bhlh091* and *bhlh010* mutants (Zhu et al., 2015) are similar to that of GA-deficient Arabidopsis mutants. The most severely deficient GA mutants fail to set seed, largely because of defective stamen development: reduced filament elongation, inhibition of anther dehiscence and reduced pollen production. Both the *ga1-3* mutant and the *ga20ox1 ga20ox2 ga20ox3-1* triple mutant are thus male sterile (Plackett et al., 2012; Koornneef and van der Veen, 1980), with anther development arresting prior to pollen mitosis II in the *ga1-3* mutant (Cheng et al., 2004) and the *ga20ox1 ga20ox2 ga20ox3-1* mutant showing defective tapetum degeneration (Plackett et al., 2012). According to Plackett *et al* (2012), these severe GA-deficient mutants exhibited some recovery of floral development later along the inflorescence stem, with occasional dehiscent anthers and Tricellular Pollen seen by position 25. The milder GA-deficient *ga20ox1 ga20ox2* and *ga3ox1 ga3ox3* double mutants showed greater recovery of fertility in later flowers (Rieu et al., 2008b; Plackett et al., 2017; Hu et al., 2008), with silique development initially stunted and then recovering from position 10, as observed in our *bhlh* double mutant data (Chapter 3.2.1). Restoration of fertility in later flowers was also observed in the transgenic DELLA line, YPet-rgl2Δ17, which expresses a RGL2 protein that cannot be degraded by GAs, thus showing that blocking RGL2-dependent GA signalling results in initially severe defects in flower development and impaired pollen development that attenuates in later flowers (Gómez et al., 2019). Whilst early flowers of these various GA mutants were indehiscent, in each case the recovery of fertility was largely assumed to be due to progressive elongation of the stamen filaments overcoming a physical barrier that had previously prevented pollination. Since it seems that later rescue of fertility is a common occurrence among GA mutants as the plant matures and the stem grows (Table 5.1), and given that the *bhlh* double mutants also show rescue of fertility in later flowers, this further supports our hypothesis that bHLH89/91/10 may be linked to GA signalling.

Table 5.1 GA mutant vegetative and reproductive phenotypes in comparison to bhlh mutants, with a focus on fertility defects and timing of restoration of male fertility. Traffic light colour system is indicative of phenotype with severe defects in red, lesser defects in orange and yellow and normal phenotypes highlighted in green.

Mutant	Stature	Male organs	Flower time	Male Sterility	Fertility Restoration	Citation
ga1-3	Dwarf	Shorter filaments	Delayed	Anther development arrests before PMII.	Minor, by position 25	Koornneef & van der Veen, 1980; Plackett *et al.,* 2012
gid1a gid1b gid1c	Dwarf	Shorter filaments	Delayed	Early stamen arrest	Not reported	Griffiths *et al.*, 2006
ga20ox1 ga20ox2 ga20ox3	Dwarf	Shorter filaments	Delayed	Defective tapetum degeneration. Reduced dehiscence	Minor, by position 25	Plackett *et al.,* 2012
ga20ox1 ga20ox2	Semi-dwarf	Shorter filaments	Delayed	Reduced dehiscence	By position 10	Rieu *et al.,* 2008; Plackett *et al.,* 2012, 2017
ga3ox1 ga3ox3	Dwarf	Shorter filaments	Delayed	Reduced dehiscence	Some, after positon 10. Most, by position 25	Hu *et al.,* 2008
YPet-rgl2Δ17	Normal	Shorter filaments	Normal	Reduced dehiscence	Some, by position 25	Gómez *et al.,* 2019
bhlh89 bhlh10	Normal	Smaller anthers	Delayed (but not quantified)	Early, aborted pollen development. Tapetum vacuolated in early flowers	Full, by position 10	Zhu *et al.,* 2015; Chapter 3
bhlh89 bhlh91	Normal	Smaller anthers	Normal	Early, aborted pollen development.	Full, by position 10	Zhu *et al.,* 2015; Chapter 3
bhlh89 bhlh10 amiR-bHLH91	Normal	Shorter filaments, Smaller anthers.	Not quantified	Aborted pollen development. Vacuolated tapetum	None	Zhu *et al.,* 2015

Additional to the later recovery of fertility, the *bhlh089 bhlh091* and *bhlh089 bhlh010* mutants exhibit conditional sterility in response to low light and high temperature (Chapter 3; Fu et al., 2020). Similarly, light- and heat-sensitive conditional sterility is also seen in the *myb33 myb65* double mutant, which is almost fully fertile when grown under high light (330 µmol/m^2/s) or low temperature (16°C) conditions but shows impaired anther development in lower light (95 µmol/m^2/s) or normal temperature (22°C) conditions, manifesting in an enlarged tapetum that fails to degrade and ultimately leads to degeneration of microspores (Millar and Gubler, 2005). Since MYB33 and -65 are closely related to HvGAMYB, a positive regulator of GA signal transduction in the Barley aleurone, and MYB33/65 are downregulated by miRNA which are in turn supressed by DELLA proteins (Achard et al., 2004) it has been speculated that MYB33 and MYB65 may play a similar role to HvGAMYB in the GA response in *Arabidopsis* and limit pollen development under stressful conditions (Millar and Gubler, 2005). bHLHs are known to form complexes with MYB and WD-40 proteins (Ramsay and Glover, 2005), and since the expression of *MYB33/65* and *bHLH10,89,91* overlaps, it is an interesting question as to whether bHLH010, -089 and -091 interact with MYB33/65 to regulate GA-dependent tapetum development.

5.1.1 Chapter Aims

Overlaps in GA and *bhlh* mutant phenotypes (Table 5.1) coupled with the known DELLA-bHLH interactions and differential expression of GA biosynthesis genes and GA-sensitive transcription factors in the *bhlh89,91* RNAseq (Chapter 4.2.2) led to two hypotheses. (1) bHLHs are required for the biosynthesis of GAs that ensure normal anther development, and in response to changing light environments. (2) DELLAs interact with bHLHs, sequestering them and thereby repressing transcriptional regulation of tapetum development.

This chapter addresses these hypotheses by first examining GA profiles and then expression of GA-regulated and GA-biosynthesis genes within *bhlh* mutant buds under different light conditions, to determine whether the bHLHs perturb the GA biosynthesis or signalling pathways. The molecular basis of this interaction was subsequently investigated through Bimolecular Fluorescence Complementation (BiFC) assays. To further ascertain whether the conditional sterility seen in the *bhlh* double mutants is related to GA deficiency, the effect of exogenous GA and Paclobutrazol (PAC) treatments, an inhibitor of GA, on reproductive development was also investigated.

5.2 RESULTS

5.2.1 GA hormone profiling

The prolonged sterility of the *bhlh* double mutants is reminiscent of various GA deficient mutants, and is further affected by light which is known to alter GA levels. Thus to test our hypothesis that bHLH89, -91 and -10 are required for GA biosynthesis in the anther, GA levels were analysed in Col-0 and *bhlh* double mutant inflorescences grown in normal and low light conditions. Buds were separated into pre- and post-mitosis I stage by size, freeze-dried and sent to Dr Danuše Tarkowská (Palacký University, CZ) whereupon GAs were extracted and quantified by ultra-performance liquid chromatography–tandem mass spectrometry.

For each GA, significant differences were analysed by a 2-way ANOVA with post-hoc TUKEY tests (Figure 5.2). In early (pre-mitosis I) stage buds light-induced changes in GA levels were negligible, the exception being that GA_{15} levels were significantly elevated in low light conditions in the *bhlh89,10* mutant (Figure 5.2 A). Conversely, many significant changes were seen in GA levels in late (post-mitosis I) stage buds (Figure 5.2, Figure 5.3).

GA_4, the main bioactive GA in *Arabidopsis,* was significantly reduced in response to low light in Col-0 (Figure 5.2 D). This reduction was maintained in the *bhlh89,91* mutant but the *bhlh89,10* mutant

shows no decrease in GA_4 levels in low light. Both *bhlh* double mutants further exhibited reduced GA_4 levels compared to Col-0 under normal conditions.

For the most part, light response of non-C13-hydroxylated GA metabolites (bioactive GA_4, its precursors GA_{15}, GA_{24} & GA_9 and derivative GA_{34}) are consistent across genotypes (Figure 5.2 A-E). In WT tissue, there is a significant decrease in GA_9, GA_4, and GA_{34} in response to low light whereas GA_{15} and GA_{24} levels were not significantly altered. The *bhlh89,10* mutant differs slightly from WT response in that it had significantly increased GA_{15} levels and no significant drop in GA_4 levels under low light conditions; whereas GA_9 showed a drop to undetectable levels in Col-0 under low light conditions, levels were unchanged in *bhlh89,10* and undetectable in *bhlh89,91*.

Nevertheless, C13-hydroxylated GA forms (bioactive GA_1, precursors GA_{53}, GA_{44}, GA_{19} & GA_{20} and derivative GA_8) showed notable differences in light-response between genotypes (Figure 5.2 G-M). Bioactive GA_1 levels did not change in response to low light in WT Col-0 but were significantly increased in both *bhlh* mutants (Figure 5.2 K). Similarly, two of GA_1's precursors GA_{44} and GA_{19} did not significantly change in WT but were respectively increased and decreased to varying degrees in the *bhlh* mutants (Figure 5.2 H,I). Conversely, GA_{53} levels were increased in low light in WT but exhibit no significant changes in the *bhlh* mutants and, whilst GA_{20} levels were increased in all lines in low-light, the response of the *bhlh* mutants was less than half that of WT (Figure 5.2 G,J).

Heatmaps of GA level changes in response to light (Figure 5.3) show that levels of C13-hydroxylated GA forms appear to reflect the severity of the light-sensitive sterility of WT and *bhlh* double mutants, with the strongest low-light induced changes in GA_1, GA_{44} & GA_{19} seen in the more severely sterile *bhlh89,91* mutant.

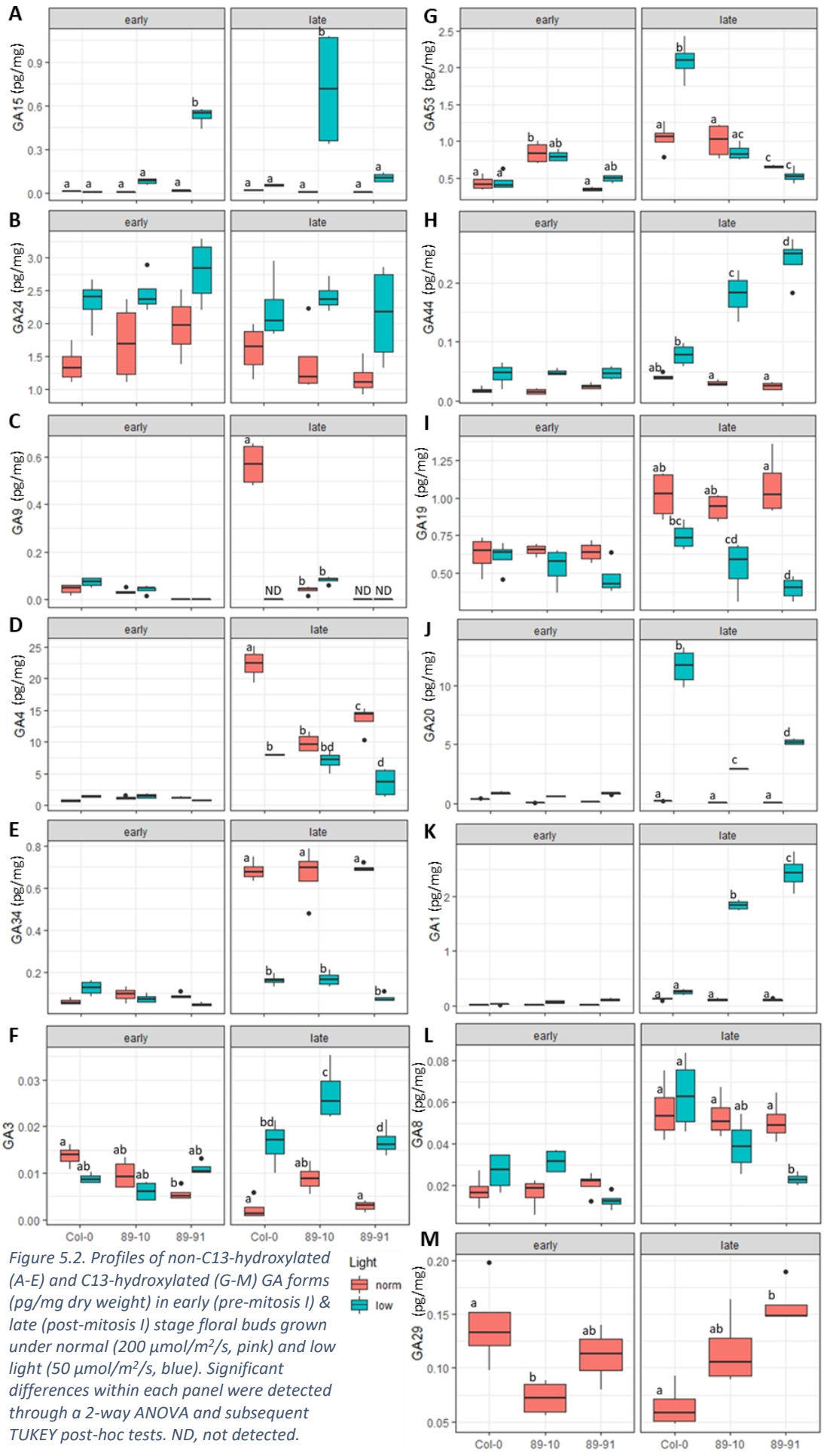

Figure 5.2. Profiles of non-C13-hydroxylated (A-E) and C13-hydroxylated (G-M) GA forms (pg/mg dry weight) in early (pre-mitosis I) & late (post-mitosis I) stage floral buds grown under normal (200 µmol/m²/s, pink) and low light (50 µmol/m²/s, blue). Significant differences within each panel were detected through a 2-way ANOVA and subsequent TUKEY post-hoc tests. ND, not detected.

5.2.2 Differential expression of GA-related genes

5.2.2.1 Expression of GA biosynthesis genes

Since the *bhlh89,91* and *bhlh89,10* double mutants have significant differences in their GA levels compared to WT, it's likely these bHLHs modulate GA biosynthesis. Therefore the RNAseq study of pre-mitosis I stage flowers (Chapter 4) was re-examined, focusing on differential expression of core enzymes within the GA biosynthesis pathway, revealing significant differences between *bhlh89,91* and Col-0 light responses (Figure 5.3). This suggests that bHLHs may be important in regulating GA biosynthesis in floral tissue. Both *ENT-COPALYL DIPHOSPHATE SYNTHETASE 1 (CPS1)* / *GA REQUIRING 1* (*GA1*) and *GA20ox2* were differentially regulated under low light only in Col-0 (log2FC>1) whilst log2FC of *GA2ox1* was halved in *bhlh89,91* and *GA3ox1* was slightly downregulated only in *bhlh89,91* samples. Regulation of GA biosynthesis mainly occurs transcriptionally at the GA20-, 3- and 2oxidase level, providing feedback and feedforward loops.

Since changes in GA levels primarily occurred in post-mitosis I stage buds, qRT-PCR of select GA biosynthesis genes was performed on whole inflorescences from Col-0 and *bhlh* double mutants grown under normal and low light conditions, to capture expression changes that may have been missed in the RNASeq of pre-mitosis I staged tissue. *bhlh89,10* was included alongside *bhlh89,91* due to significant differences in GA profiles (Figure 5.2). According to 2-way ANOVA analyis of qRT-PCR data, with TUKEY post-hoc tests, light has no effect on *GA2ox1* expression in Col-0 whole inflorescences, but levels drop in response to low light in *bhlh89,10* ($p<0.05$) and *bhlh89,91* ($p=0.065$, Figure 5.4 C), this starkly contrasts with the RNAseq data which shows that *GA2ox1* expression is increased in pre-mitotic tissue in response to low light in both Col-0 ($log_2FC=1.5$) and *bhlh89,91* ($log_2FC=0.8$, Figure 5.3). *GA3ox1* and *GA20ox2* levels were higher in the *bhlh* double mutants than in Col-0 in both light conditions however, this was only significant ($p<0.05$) for *bhlh89,10* vs Col-0, with *bhlh89,91* vs Col-0 differential expression of *GA3ox1* falling just beyond the threshold significance level ($p=0.0517$). Although there were no other significant differences, it appears that *GA3ox1* and *GA20ox2* levels slightly decrease in Col-0 inflorecences in response to low light whereas they are increased in *bhlh89,91* and *bhlh89,10* respectively (Figure 5.4 D-E). This qRT-PCR expression data contrasts with the RNAseq data for pre-mitosis I stage inflorescences, in which *GA3ox1* was not differentially expressed in the *bhlh89,91* mutant compared to WT and was slightly decreased in response to low light in the *bhlh89,91* background only ($log_2FC=-0.89$, Figure 5.3). GA20ox2 levels in the RNAseq were seen to increase only in Col-0 in response to low light ($log_2FC=1$) and were slightly reduced in the *bhlh89,91* mutant relative to WT in low light only ($log_2FC=-0.72$). No significant differences were found in either of the two GA 13-oxidases, *CYP72A9* or *CYP72A15*, within

the qRT-PCR analysis however *GA13ox* expression was slightly elevated in low light WT floral tissue (Figure 5.4 A-B).

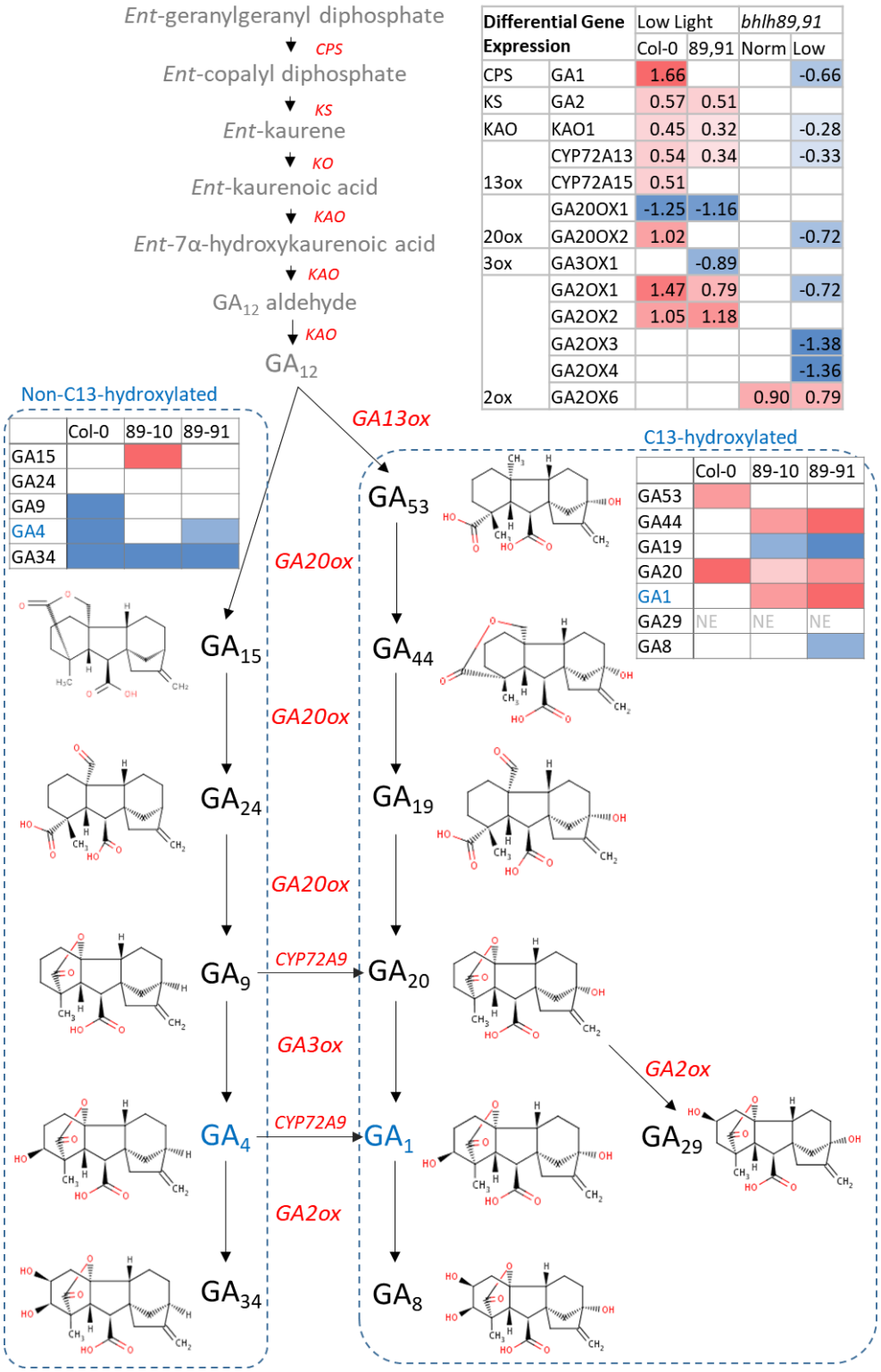

Differential Gene Expression		Low Light Col-0	Low Light 89,91	*bhlh89,91* Norm	*bhlh89,91* Low
CPS	GA1	1.66			-0.66
KS	GA2	0.57	0.51		
KAO	KAO1	0.45	0.32		-0.28
13ox	CYP72A13	0.54	0.34		-0.33
	CYP72A15	0.51			
20ox	GA20OX1	-1.25	-1.16		
	GA20OX2	1.02			-0.72
3ox	GA3OX1		-0.89		
2ox	GA2OX1	1.47	0.79		-0.72
	GA2OX2	1.05	1.18		
	GA2OX3				-1.38
	GA2OX4				-1.36
	GA2OX6			0.90	0.79

	Col-0	89-10	89-91
GA15			
GA24			
GA9			
GA4			
GA34			

	Col-0	89-10	89-91
GA53			
GA44			
GA19			
GA20			
GA1			
GA29	NE	NE	NE
GA8			

Figure 5.3. GA biosynthesis pathways in Arabidopsis: early GA precursors are coloured in grey whilst metabolites measured in our study have been marked in black, or blue in the case of bioactive forms. Key pathway enzymes (marked in red), show significant changes (q<0.01) in expression pre-mitosis I stage buds in response to low light (within Col-0 and bhlh89,91) according to RNAseq (top-right panel; Chapter 4), as well as differential expression in the bhlh89,91 mutant under normal and low light. Significant changes to levels of C13-hydroxylated or non-C13-hydroxylated GA metabolites in response to low light, within post-mitosis I stage buds as outlined in Figure 5.2, are summarised in heatmaps (blue showing a decrease, red an increase and white showing no-significant difference), NE= not estimated due to contamination.

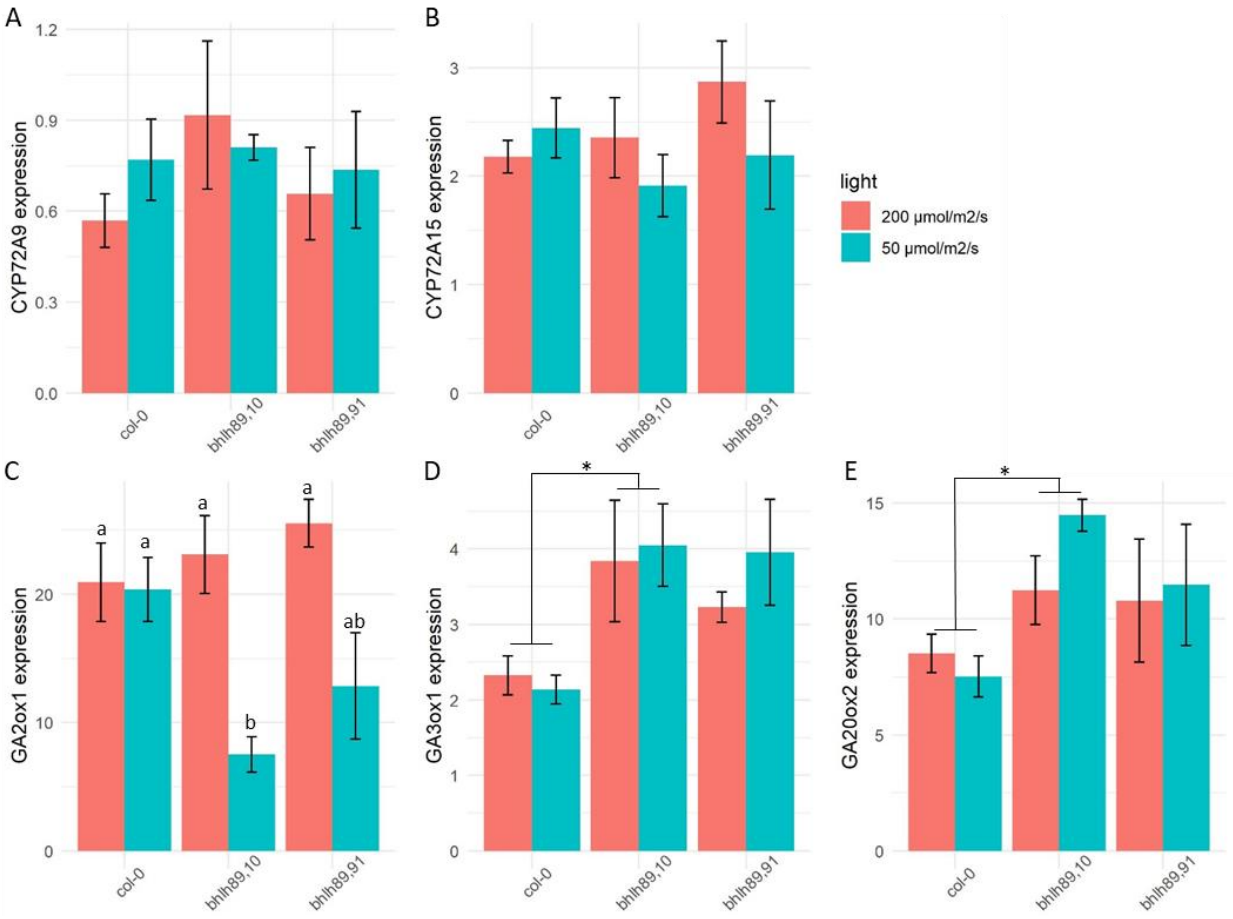

*Figure 5.4 qRT-PCR expression analysis of GA biosynthesis genes in normal and low light within whole inflorescences of Col-0, bhlh89,10 and bhlh89,91 double mutants. Bars represent mean and SEM of 3 biological replicates. Significant differences * ($p<0.05$) have been determined by 2-way ANOVA, with post-hoc TUKEY tests.*

5.2.2.2 *Expression of GA transporters*

Movement of GA into various tissues is essential for development, and this requires GA influx transporters: NITRATE TRANSPORTER 1/PEPTIDE (NPF) and SWEET sucrose efflux transporter family proteins (as reviewed in Binenbaum et al., 2018). 12 out of the 53 *Arabidopsis* NPFs, and 7 of the 17 SWEETs, were differentially expressed in response to low light and/or *bhlh89,91* loss of function mutant (Table 5.2). Five of the differentially expressed NPFs show no GA transport activity and activity of 8 NPF/ SWEET proteins has not yet been tested. However, GA transport activity has been confirmed for 6 of these transporter proteins: including NPF4.6 which is upregulated (Log2FC>1, q<0.01) in response to low light in Col-0, suggesting increased floral GA transport, but was not differentially expressed in the *bhlh89,91* mutant.

Table 5.2 Differential expression of GA transporter proteins in pre-mitosis I stage flowers according to RNASeq data (Chapter 4). Significant Log2FC (q<0.01) changes are shown in response to low light for Col-0 and bhlh89,91 alongside differential expression within bhlh89,91 mutant compared to Col-0 in normal and low light (blue shows downregulation, red upregulation and white indicates non-significant change). GA transport activity, as reviewed by Binenbaum et al. (2018), 1 tick shows transport of bioactive GA in the heterologous system, with additional tick if activity has been confirmed in planta, question mark indicates untested activity.

	Col-0	89-91	Norm	Low	Activity
NPF4.1	-1.05	-0.57	-1.05	-0.57	✓
NPF4.3	3.11			-3.41	***X***
NPF4.4	3.44			-2.84	***X***
NPF4.6	2.33			-2.31	✓
NPF5.2	-0.84		-1.94	-1.51	✓
NPF5.4	-3.09	-1.27	1.96	3.78	***?***
NPF5.8	1.19				***X***
NPF5.15	1.75	2.53			***?***
NPF7.1	3.35			-1.46	***X***
NPF7.3			-2.25	-2.19	***X***
NPF8.2	-0.69	-0.82	1.20	1.08	✓
NPF8.4	1.56			-0.94	***?***
SWEET7	-1.11	-0.64	-0.84		***?***
SWEET8	2.20			-1.48	***?***
SWEET11	1.07			-0.99	***?***
SWEET12	1.22			-1.39	***?***
SWEET13			1.35	1.67	✓✓
SWEET14		-1.42		-1.30	✓✓
SWEET15	-1.14				***?***

5.2.2.3 *Overlap in GA and bhlh mutant transcriptomes*

In Chapter 4 it was demonstrated that response to GA was differentially regulated in the *bhlh* and Col-0 low light responses. In order to determine the degree of overlap between GA signalling pathways and *bhlh* mutant and low light transcriptomic responses, microarray data of GA-regulated genes in *ga1-3* mutant flowers was examined (Cao et al., 2006) alongside RNAseq data from the *bhlh089 bhlh010 amiR-bHLH091* triple mutant (Zhu et al., 2015) and Col-0 and *bhlh089 bhlh091* pre-mitosis I stage buds, grown under normal (200 µmol/m^2/s) and low (50 µmol/m^2/s) light conditions

(Chapter 4). The extent to which the low light response in pre-mitosis I stage buds is likely to be DELLA-mediated was explored through a comparison of low-light RNASeq data with RGA-induced changes in pre-mitosis I stage flowers of the *ga1-3 rga-t2 rgl2-1 35S:RGA-GR* line (Hou et al., 2008).

Transcriptomic analysis of the GA-deficient *ga1-3* mutant found 1248 GA-responsive genes in flower buds, with 826 genes downregulated in the *ga1-3* mutant and thus deemed to be GA-upregulated and 422 GA-downregulated (Cao et al., 2006). *bHLH91* was the only key tapetal transcription factor that was differentially expressed in the *ga1-3* background (GA-upregulated). 87 out of the 422 (20%) GA-downregulated genes were also downregulated in the *bhlh089 bhlh010 amiR-bHLH091* triple mutant, whilst 10% of GA-upregulated genes were differentially expressed in the triple mutant (Figure 5.5A). This suggests a role for bHLH89, -91 and -10 in inducing the expression of genes which are negatively regulated by GA.

Fewer genes are differentially regulated in the *bhlh89,91* mutant compared to WT Col-0 under normal growth conditions, so as you might expect there is a much lower degree of overlap (41 genes in total). However in low light conditions there is overall a fair degree of overlap between the *bhlh89,91* mutant and *ga1-3*, with 218 (17%) of the 1248 GA-responsive genes differentially regulated in *bhlh89,91* compared to WT (Figure 5.5B). Some, but not all, of these GA-related expression changes in the *bhlh* mutants are most likely related to general fertility changes rather than the bHLH proteins themselves, since 28/87 GA-down x *bhlh* triple mutant downregulated genes and 145/218 GA x *bhlh89,91* (low) genes were found to be differentially expressed in one or more *dyt1, tdf1, ams, myb80* or *ms1* mutant microarrays.

WT response to low light (Chapter 4) was compared to GA-regulated genes in the *ga1-3* mutant (Cao et al., 2006); of the 1248 GA-regulated genes, 296 were differentially expressed in Col-0 in response to low light, suggesting that almost a quarter of the transcriptome changes in response to low light come from the GA pathway (Figure 5.5C).

Hou *et al.* (2008) identified 806 RGA regulated genes in pre-mitosis I stage flowers, from the RGA-inducible line *ga1-3 rga-t2 rgl2-1 35S:RGA-GR*. Comparing this to our own RNAseq data, to gain an idea of how important an interaction with DELLA proteins might be, 222 (28%) of RGA-regulated genes were identified as differentially expressed in Col-0 in response to low light (Figure 5.5D). Whilst there was a fairly equal split of RGA-repressed genes in up- and down-regulated genes in low-light; no RGA-induced genes were downregulated in response to low light. There is also a huge representation of RGA-induced genes in the triple *bhlh* downregulated set, representing 34% of the 413 RGA-induced genes (Figure 5.5E). Taken together this suggests that RGA is important in

upregulating genes in pre-mitosis I stage floral tissue in response to low light, and that an interaction with bHLH89, -91 and -10 may be significant in this.

Combining both the *ga1-3* and *ga1-3 rga-t2 rgl2-1 35S:RGA-GR* microarray data together, 586 out of the total 2492 DEGs in our RNAseq dataset are also differentially expressed in at least one of the GA/DELLA microarrays, suggesting a fairly strong overlap between GA signalling, light responses and bHLH regulation of reproduction. Genes that undergo the highest upregulation in response to low light in Col-0 are largely downregulated by RGA (Table 5.3). Furthermore, with all of these top DEGs expressed in the tapetum and none showing significant log2FCs in the *bhlh89,91* mutant, this implies RGA interacts with bHLHs in tapetum development to regulate light responses. A number of these genes, such as EXL4 & 6 and GRP16, were highlighted in the previous chapter as playing a significant role in reproductive development particularly in pollen exine development (Table 4.7). Therefore it seems that bHLH-RGA interactions may be crucial to maintaining pollen development under low light conditions. The GA downregulated EARLY LIGHT INDUCED PROTEIN 1 (ELIP1) and ELIP2 (Cao et al., 2006) showed the highest downregulation in Col-0 and the *bhlh89,91* mutant in response to low light. From this one might assume that perception of light signals and early signal transduction are not affected in the *bhlh89,91* mutant, instead changes are likely to be more downstream.

Table 5.3 Genes showing the highest differential expression in response to low light in Col-0 (Col L-N), are compared to the bhlh89,91 mutant light response (bhlh L-N) and differential expression of bhlh mutant from WT in Normal (N) and Low (L) light conditions according to RNASeq (Chapter 4). These are further compared to published male sterile mutant microarrays dyt1, tdf1, ams, bhlh089 bhlh010 amiR-bHLH091 (trip bhlh), myb80 and ms1 (Feng et al., 2012; Zhu et al., 2015; Lou et al., 2017; Ma et al., 2012; Phan et al., 2011; Yang et al., 2007); ga1-3 microarray data from Cao et al. (2006) and transcriptomic changes in the RGA inducible line (Hou et al., 2008). Red indicates upregulated genes, blue shows downregulation and white indicates no significant differential expression. Finally, genes expressed in the tapetum (Tpm) according to Laser Capture Microscopy data are identified.

Gene	Col L-N	*bhlh* L-N	L. *bhlh* -Col	N. *bhlh* -Col	*dyt1*	*tdf1*	*ams*	*tripl bhlh*	*myb 80*	*ms1*	GA	RGA	Tpm
XTH3	8.8		-7.6		-7.2	-6.0	-7.5			-6.0		-3.2	✓
AT1G23570	8.6		-8.2		-4.5	-3.9	-4.7					-2.5	✓
EXL4	8.5		-6.8		-5.2	-5.1	-5.3			-6.3		-2.5	✓
AT1G54860	7.4		-6.8		-3.8	-2.0	-3.8				1.2	-1.7	✓
GASA11	7.3		-4.4									-1.6	✓
EXL6	7.2		-4.2		-5.8	-4.8	-6.1					-2.2	✓
GRP16	6.7		-6.5		-4.4	-4.2	-4.5				1.2	-2.5	✓
APG	6.5		-4.2								2.7		
XTH7	-2.3	-1.1	2.3	1.1	1.5		1.0				-1.4		
CYP75B1	-2.4	-2.2	1.4	1.1	1.0			2.4				-1.5	✓
TAT3	-2.4					-3.5					-2.1		
CYP83A1	-2.4		1.9								2.3	-2.2	
LURP1	-2.4					-2.3					-2.1		
BAM5	-2.5	-1.1	2.3		2.2	2.5	2.1	4.7			1.5	-1.7	
EXPA8	-2.6		2.6		1.1						2.3		
AT5G44820	-2.7	-1.8				-2.1					-1.3		
GPT2	-2.8	-2.8	2.8	2.8	2.4	2.3	2.4				-1.3		
ELIP2	-4.1	-3.4		1.6	3.0	1.2					1.8		
ELIP1	-5.0	-4.8		3.0	4.0				1.8		1.2	-3.6	

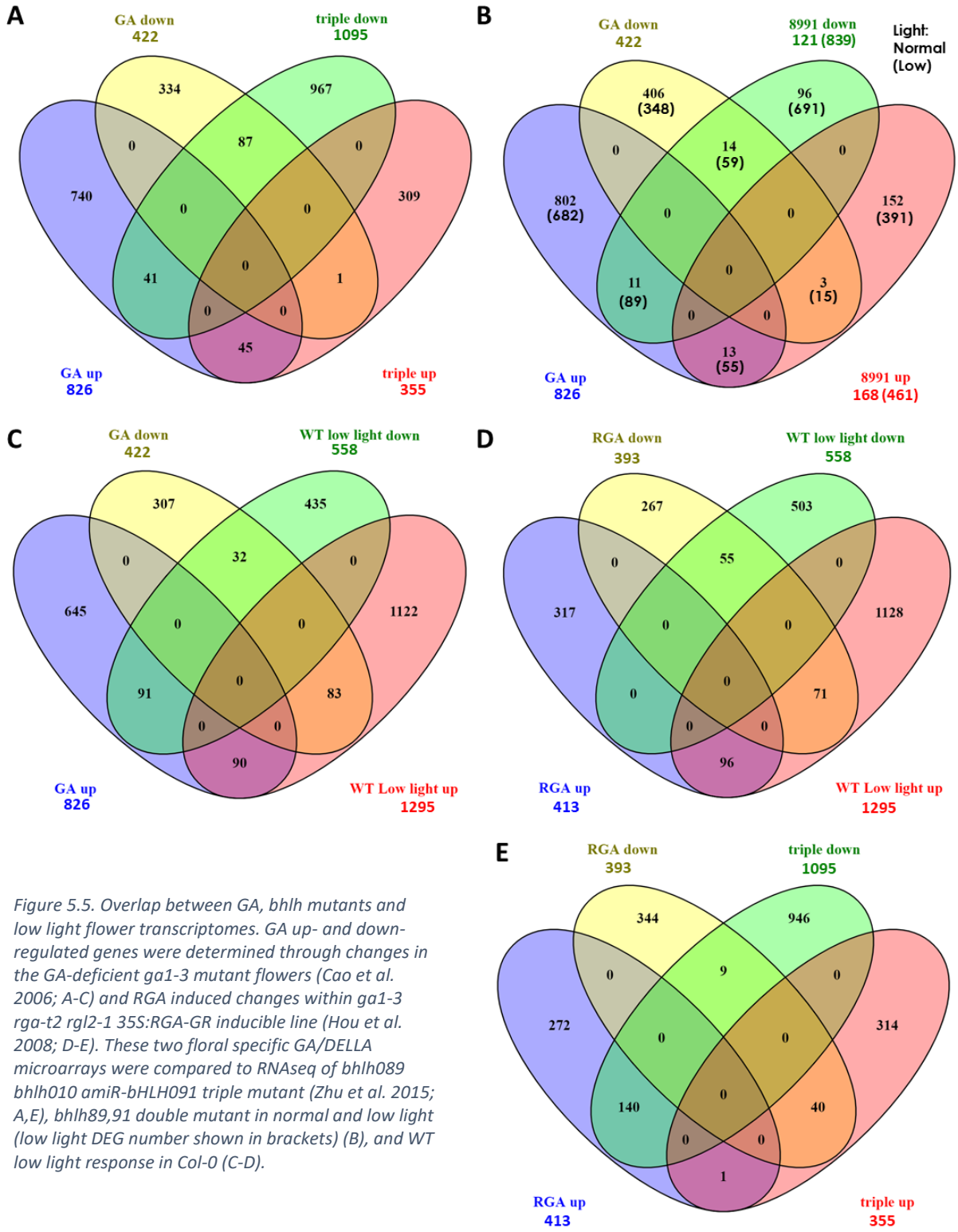

Figure 5.5. Overlap between GA, bhlh mutants and low light flower transcriptomes. GA up- and down-regulated genes were determined through changes in the GA-deficient ga1-3 mutant flowers (Cao et al. 2006; A-C) and RGA induced changes within ga1-3 rga-t2 rgl2-1 35S:RGA-GR inducible line (Hou et al. 2008; D-E). These two floral specific GA/DELLA microarrays were compared to RNAseq of bhlh089 bhlh010 amiR-bHLH091 triple mutant (Zhu et al. 2015; A,E), bhlh89,91 double mutant in normal and low light (low light DEG number shown in brackets) (B), and WT low light response in Col-0 (C-D).

5.2.3 bHLH protein interactions within GA signalling

To assess the molecular basis of bHLHs role in GA pathways, interactions of bHLH91/89/10 with selected DELLAs and MYB33/65 were assessed *in vivo* by a Bimolecular Fluorescence Complementation (BiFC) assay. The Arabidopsis CDS of these genes were cloned into ubiquitin-driven split-YFP constructs (pUBC-bHLH-nYFP and pUBC-DELLA/MYB-cYFP) and transiently expressed in tobacco leaves. Positive interactions were determined from visible nuclear YFP signals (Figure 5.6). These showed that bHLH89, -91 and -10 all interact with the DELLA proteins GAI, RGL2 and RGL3 *in planta.* Additionally, it seems that MYB33 and -65 both interact with bHLH10 and -91, although less nuclei fluoresced which may reflect lower infiltration of these cultures. Fluorescence was only observed in response to bHLH89-nYFP & MYB33-cYFP in 1 out of 3 replicates, possibly also in reflection of lower infiltration of MYB cultures. And no YFP signal was detected in response to infiltration with bHLH89-nYFP & MYB65-cYFP, which suggests that bHLH89 may not interact with MYB65.

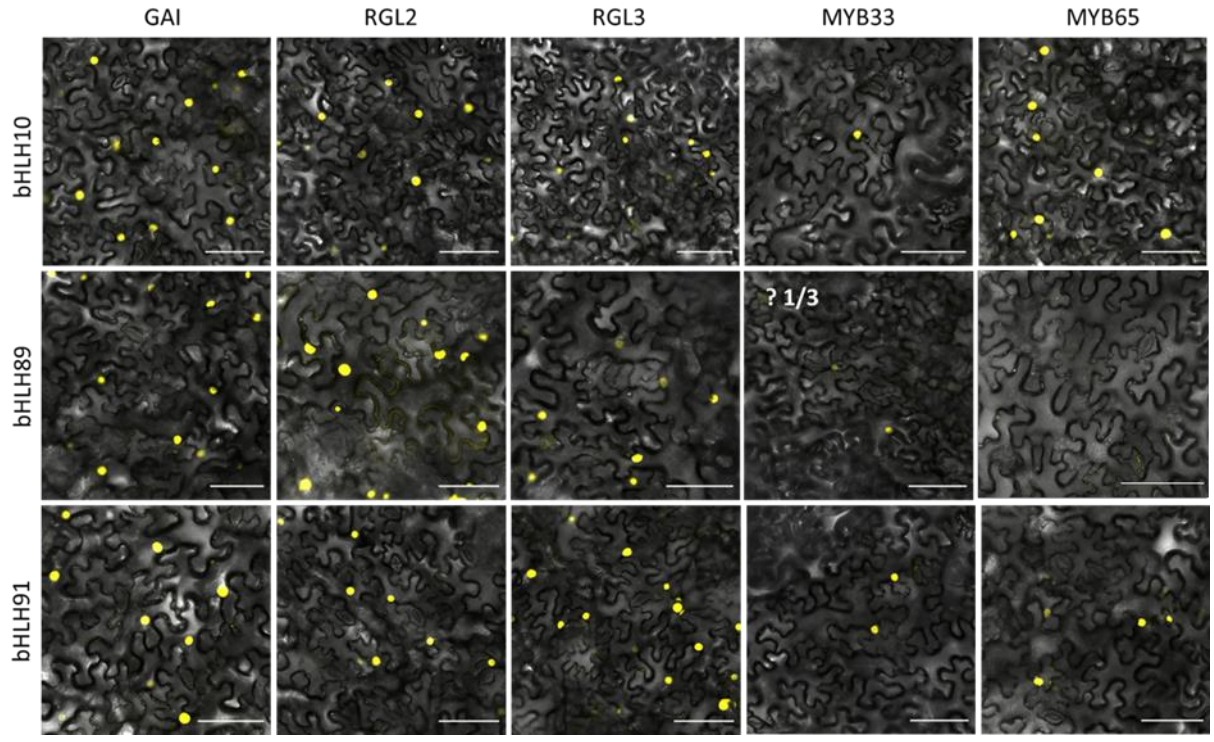

Figure 5.6. Bimolecular Fluorescence Complementation (BiFC) transient assay of bHLH protein interactions with DELLA and MYB proteins. Nuclear YFP expression shows that the three bHLH proteins interact with all three DELLAs tested (GAI, RGL2 and RGL3) and MYB33, although the bHLH89-MYB33 interaction was only identified in 1/3 replicates, whilst only bHLH10 and -91 interact with MYB65. bHLH89-nYFP and bHLH91-cYFP interaction was used a positive control whilst infiltration with just the bHLH-nYFP alone was used as a negative control (both not shown). Scale bar 100µm.

5.2.4 Exogenous GA_3 and PAC treatments impact on fertility of WT and *bhlh* mutants

The similarities in fertility of GA-deficient mutants and *bhlh* double mutant phenotypes led us to pose the question of whether the prolonged and conditional sterility of *bhlh* double mutants was due to GA levels. To address this, plants were grown under normal conditions until bolting and then transferred to normal (200 µmol/m^2/s) or low (50 µmol/m^2/s) light conditions and sprayed with 50µM GA_3, 50µM Paclobutrazol (PAC, a GA biosynthesis inhibitor) or a 0.5% (v/v) EtOH and 0.1% (v/v) Tween-20 control solution at 2-3 day intervals. As in Chapter 3.2.1, silique length was used as a measure of fertility.

Under normal light conditions, GA_3 treatment resulted in stunted silique development compared to control treatment in the first 4 positions of Col-0, after which point siliques develop as normal, suggesting that exogenous GA treatment causes initial silique development to be stunted as in low light conditions (Chapter 3). Silique development in the *bhlh89,10* mutant treated with 50µM GA_3 was not significantly changed from WT, however siliques developed to be on average 2mm shorter than those treated with the control solutions. Conversely, *bhlh89,91* plants exhibited reduced fertility in response to GA_3, with stunted silique development maintained across the flowering stem, mimicking low light treatment. According to analysis of silique lengths, treatment with PAC resulted in complete sterility, in WT and *bhlh* double mutants. However, since short (<5mm) siliques still set some seed this suggests that PAC treatment strongly impacted silique elongation rather than flower fertility (Figure 5.7 I).

Polynomial curves were fitted to the seedset data in order to demonstrate basic correlations however, as the number of datapoints was small (n=6- 33), none of the differences in trends were statistically significant. The relationship between silique length and seed number appears to be fairly constant between Col-0, *bhlh89-10* and *bhlh89-91* in mock-treated plants in both light conditions and GA_3-treated in normal light (Figure 5.7 G,H,J). However there appears to be some differences in seedset under normal light PAC and low light GA_3 treatment in the *bhlh* mutants compared to Col-0 (Figure 5.7 I,K).

This pilot study pointed to the necessity of more in depth characterisation, therefore PAC and GA_3 treatments were repeated in a dose response assay.

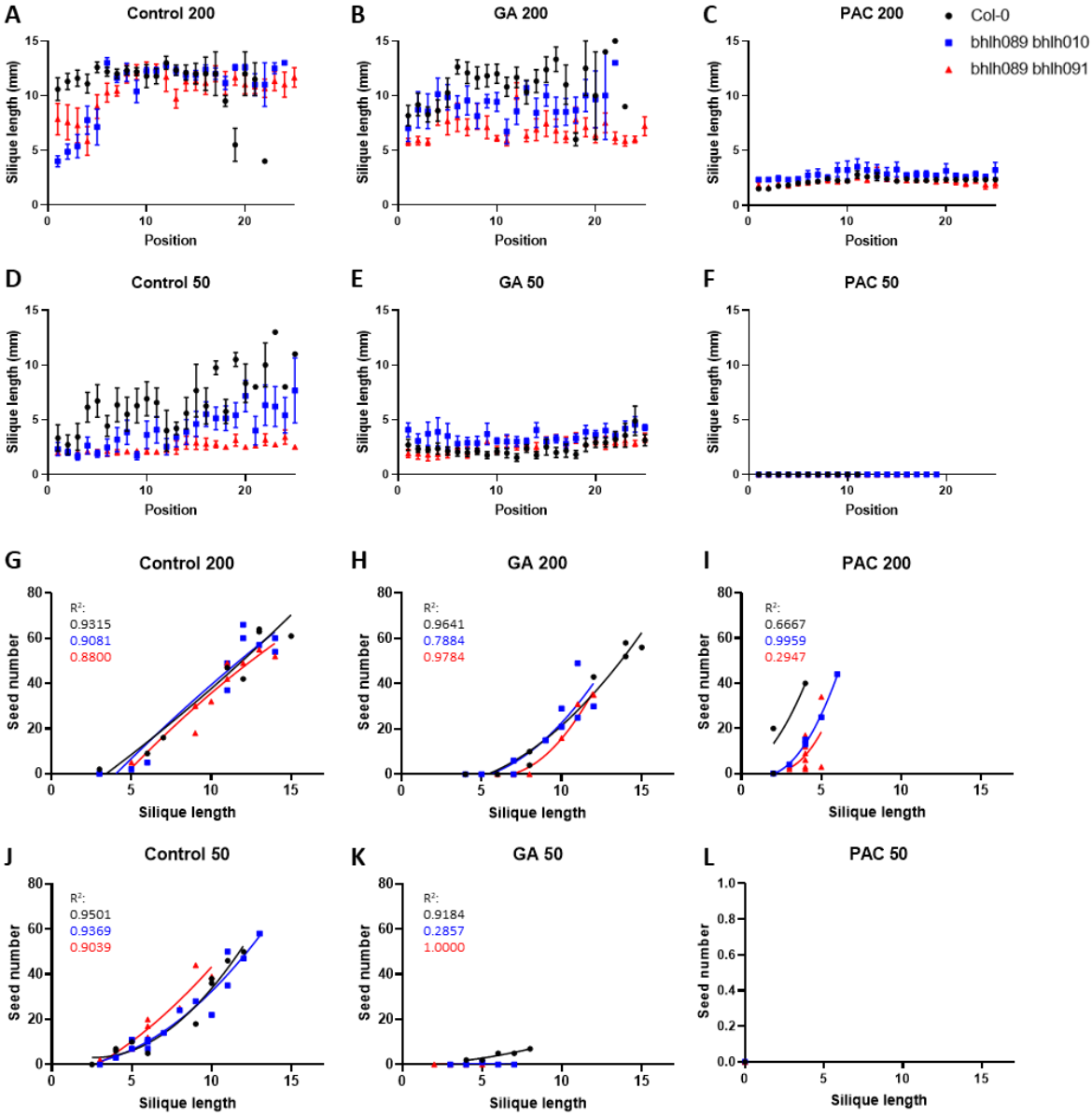

Figure 5.7. Effect of 50µM GA_3 or PAC treatment on fertility of Col-0, bhlh089 bhlh010 and bhlh089 bhlh091 plants in normal (200) and low (50 µmol/m²/s) light conditions. A-F) Mean and SEM of silique lengths across the length of the flowering stem. G-L) Correlation of seed number vs silique length, nonlinear regression analysis curve fitted with second order polynomial (quadratic) model. Col-0, black; bhlh89,10, blue; bhlh89,91, red for A-L.

5.2.4.1 GA_3 affects fertility in a dose-dependent manner

At onset of flowering, plants were either transferred to low light conditions or remained in normal light conditions and were sprayed with mock (0), 3.375, 6.75, 12.5, 25 or 50µM GA_3 solutions every 2-3 days. Silique lengths across the flowering stems were measured and 2-way ANOVA with Tukey Multiple Comparison Tests was performed to assess statistical differences between treatments at each position.

Under normal light conditions lower concentrations of GA_3 treatment had no effect on Col-0 fertility, whereas 50µM GA_3 treatment caused stunted silique development in the initial 5 positions (Figure 5.8 A), with significantly shorter siliques produced at positions 3-5 compared to other GA_3 concentrations ($q<0.01$). This suggests that higher GA levels prolong sterility in WT, as previously shown.

Fertility was further affected by GA_3 treatments when plants were grown under low light, with reduced sterility very much dose dependant. In Col-0, there is no significant difference between 0, 3 and 6µM GA_3 treatments at any point, but initial sterility is prolonged to flower position 4 in 12 and 25µM treated plants, and 50µM treated plants remain significantly shorter than the control until position 13/15 (Figure 5.8 B).

This prolonged sterility is very apparent in the *bhlh089 bhlh091* mutant in normal light conditions (Figure 5.8 E). After 50µM GA treatment *bhlh089 bhlh091* siliques were significantly shorter than 0 µM at positions 6-10 and shorter than 3, 12 and 25µM GA_3-treatments from positions 8-10. Curiously, the 6µM GA treatment caused prolonged sterility and was only significantly different from 50µm at position 10. *bhlh089 bhlh010* fertility was unaffected by any GA_3 treatment in normal light (Figure 5.8 C).

In low light, *bhlh089 bhlh091* GA_3 treatments cause total sterility across the flowering stem, whereas mock-treated (0µM GA_3) plants start to show some recovery of fertility by position 19 ($q<0.01$). GA_3-treated *bhlh089 bhlh010* have significantly shorter siliques than 0 µM controls from position 6, except 3µM GA_3 which do not differ significantly from the control at position 10, 16, 19 and 20, suggesting that 3µM GA_3 treated plants eventually return to fertility. There is no difference in silique lengths of 6 - 50 µM GA_3-treated plants, with all showing a prolonged sterility phenotype.

Thus it seems that GA levels affect fertility of all lines tested in a dose-dependent manner, with the strongest defects seen in *bhlh89,91* and then *bhlh89,10* then Col-0 in much the same way that they have differing severity of conditional sterility in response to light (Chapter 3). Thus it seems that *bhlh*

double mutants are more sensitive to GA. Crucially, this rules out GA deficiency causing the reduced fertility of the *bhlh* double mutants.

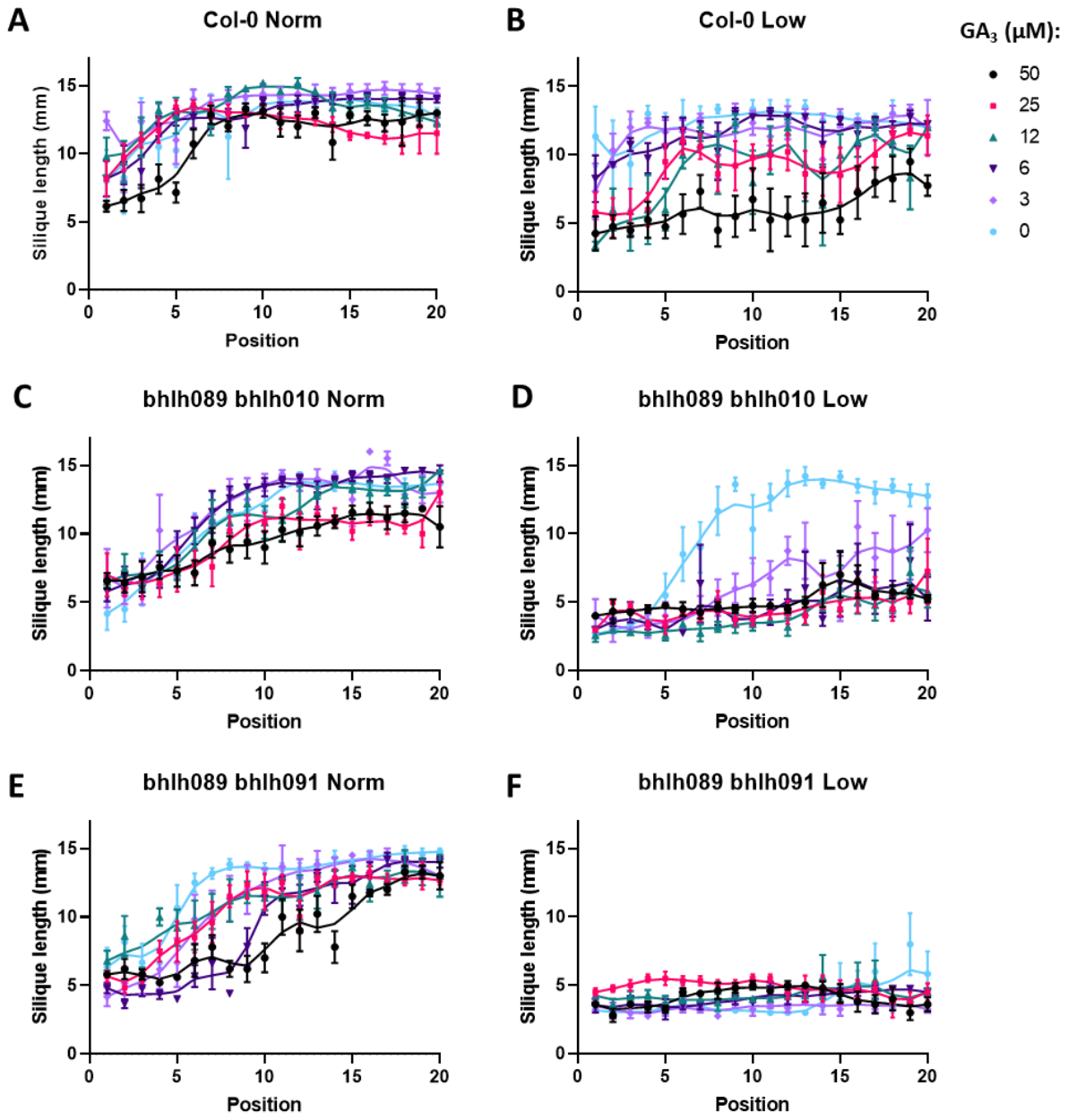

Figure 5.8. Effect of increasing exogenous GA_3 concentrations (0, 3, 6, 12, 25 and 50 µM) on the fertility of Col-0, bhlh089 bhlh010 and bhlh089 bhlh091 across development of lateral flowering stem (position). Datapoints represent Means and SEM of 4-7 biological replicates. LOWESS (Locally Weighted Scatterplot Smoothing) curves have been fitted to highlight data trends.

5.2.4.2 PAC dose responses suggest low concentrations mimic bhlh mutant phenotypes

A similar approach was used to identify the effect of blocking GA biosynthesis on fertility in plants grown under normal light conditions. Plants were sprayed with mock (0), 1, 5, 10, 25 or 50µM PAC solutions from the onset of flowering.

Due to work interruptions at the start of the Covid-19 pandemic, positional silique length measurements were not taken. However from images taken of the flowering stems (Figure 5.9) it appears that the lowest dose of PAC (1µM) reduced silique lengths of *bhlh089 bhlh010* and prolonged the sterility of *bhlh089 bhlh091* and 5µM PAC treatment stunted the development of siliques in all treated plants including Col-0. Stronger doses of PAC appeared to decrease silique lengths further and inhibit elongation of the flowering stem, resulting in progressively shorter plants. Stem elongation appears to be equally affected by PAC treatment in all lines. There appears to be little difference in the phenotype of plants treated with 25 and 50µM PAC.

Siliques were fixed in 3:1 ethanol: acetic acid for seedset analysis. Seed number was plotted against silique lengths and nonlinear models were fitted to the dataset to show trends using either a second order polynomial (quadratic) or exponential (malthusian) growth model depending on the comparison of fit. Accordingly, no difference in seedset among the genotypes was observed (Figure 5.10). Although, data suggests that *bhlh89,91* siliques reach a longer maximal length than Col-0 and *bhlh89,10* when treated with 10 µM PAC. In contrast to the pilot study, all fixed siliques in the 25 and 50 µM treatments were less than 3mm in length and did not contain any seeds.

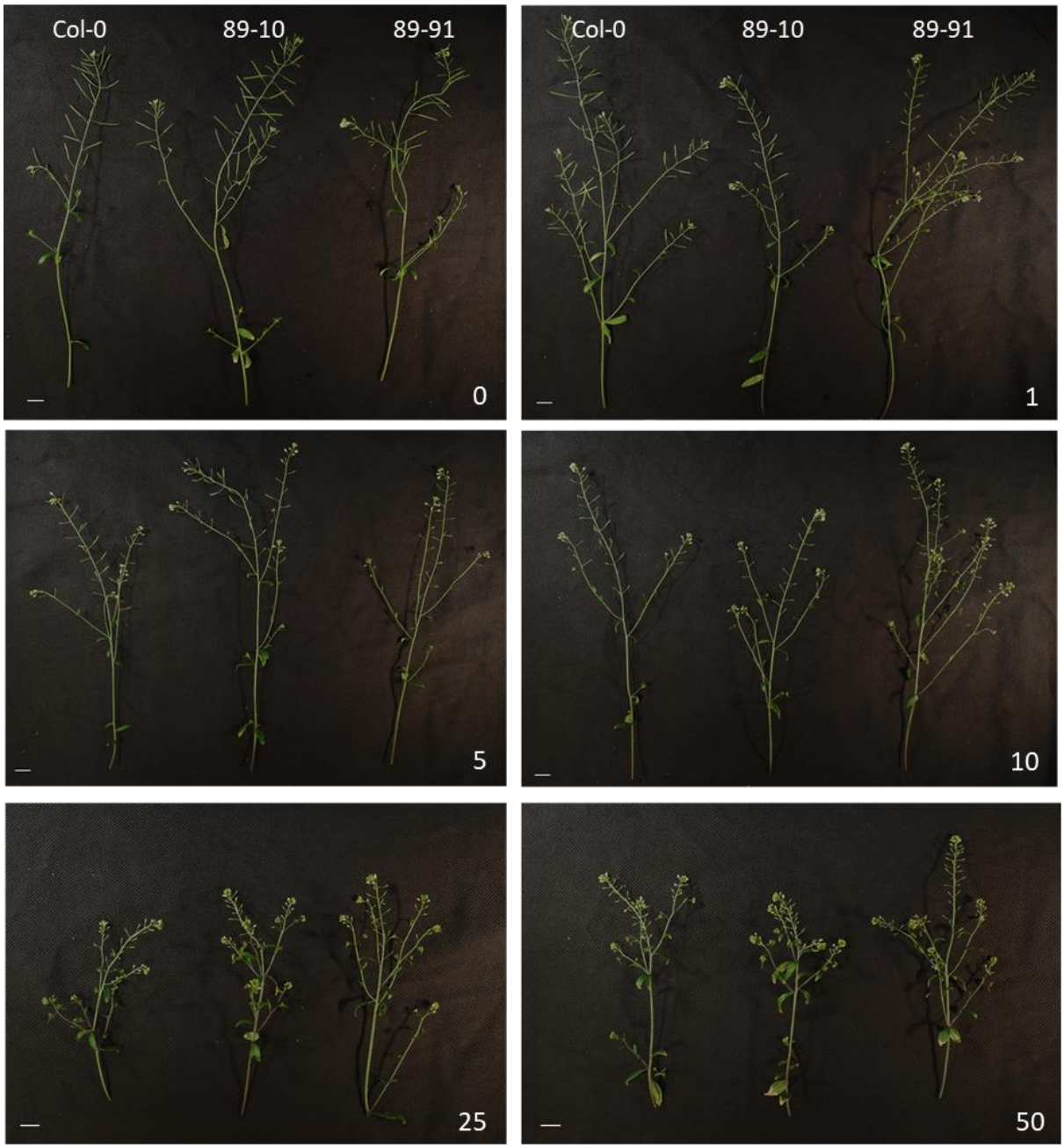

Figure 5.9 Effect of varying concentrations of Paclobutrazol (PAC) treatment (0-50µM) on fertility of lateral flowering stems of Col-0, bhlh089 bhlh010 and bhlh089 bhlh091 (from left to right in each panel). Reduced silique lengths are apparent in the bhlh mutants from 1µM PAC and Col-0 from 5µM PAC. Plant stature/ stem lengths are equally reduced in all treated plants with increasing PAC concentrations. Scale bar: 1mm.

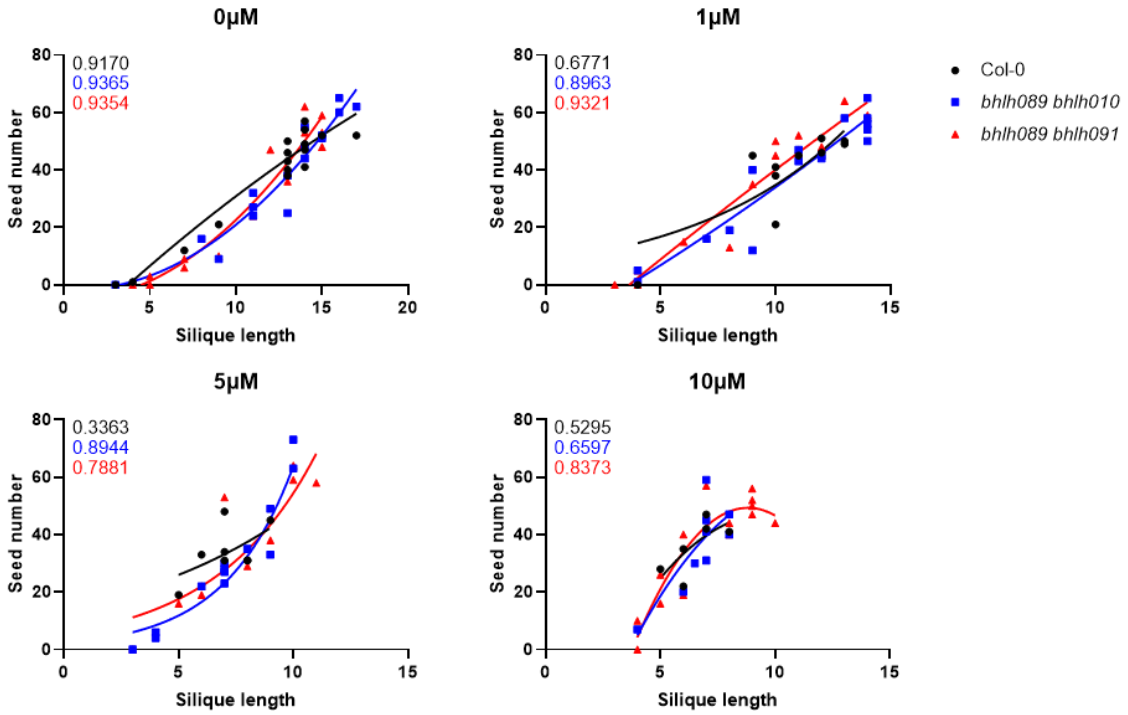

Figure 5.10 Seedset analysis of Col-0, bhlh89,10 and bhlh89,91 siliques in response to 0-10 µM PAC treatment, with correlation shown by nonlinear fit of a second order polynomial (quadratic) model (0-1µm) or Exponential (Malthusian) growth model (5-10µm), R^2 is reported for each model to show goodness of fit.

5.2.5 PAC treatment reduces the fluorescence of bHLH translational reporters

In order to determine the effect of GA on bHLH protein stability, the fluorescence intensity of bHLH translational reporters in response to 50µM PAC was analysed. As previously reported in Chapter 3, bHLH89 and -91 are both expressed in the tapetum of Pollen Mother Cell (PMC) and Tetrad stage anthers, as shown by strong nuclear-localised fluorescent signals of bHLH translational reporters *pbHLH091::bHLH091-YFP* and *pbHLH089::bHLH089-GFP* (Figure 5.11 C). A more diffuse, cytoplasmic bHLH91-YFP fluorescent signal was also seen in early Single Microspore (Msp) stage buds, showing on average between 9-50% of maximum fluorescent signal (Figure 5.11 A). bHLH89-GFP fluorescence was only reported in one Msp stage bud and this showed strong nuclear signal as in PMC and Tetrad stage anthers.

PAC-treated buds exhibited bHLH-FP expression at the same stages as untreated plants however this fluorescence occurred at a reduced bud size (Figure 5.11 A). For example, bHLH89-GFP fluorescence was recorded up until 1.1mm in untreated buds but was seen only in buds up to 0.8mm upon PAC treatment. Similarly, PAC treated bHLH91-YFP buds exhibit fluorescence at a maximum of 0.7mm compared to 0.9mm untreated. Disregarding buds with no fluorescence, the average fluorescence intensity was lower in PAC treated plants for both bHLH fluorescent fusion proteins (Figure 5.11 B), however this difference was not significant ($q>0.05$, ANOVA).

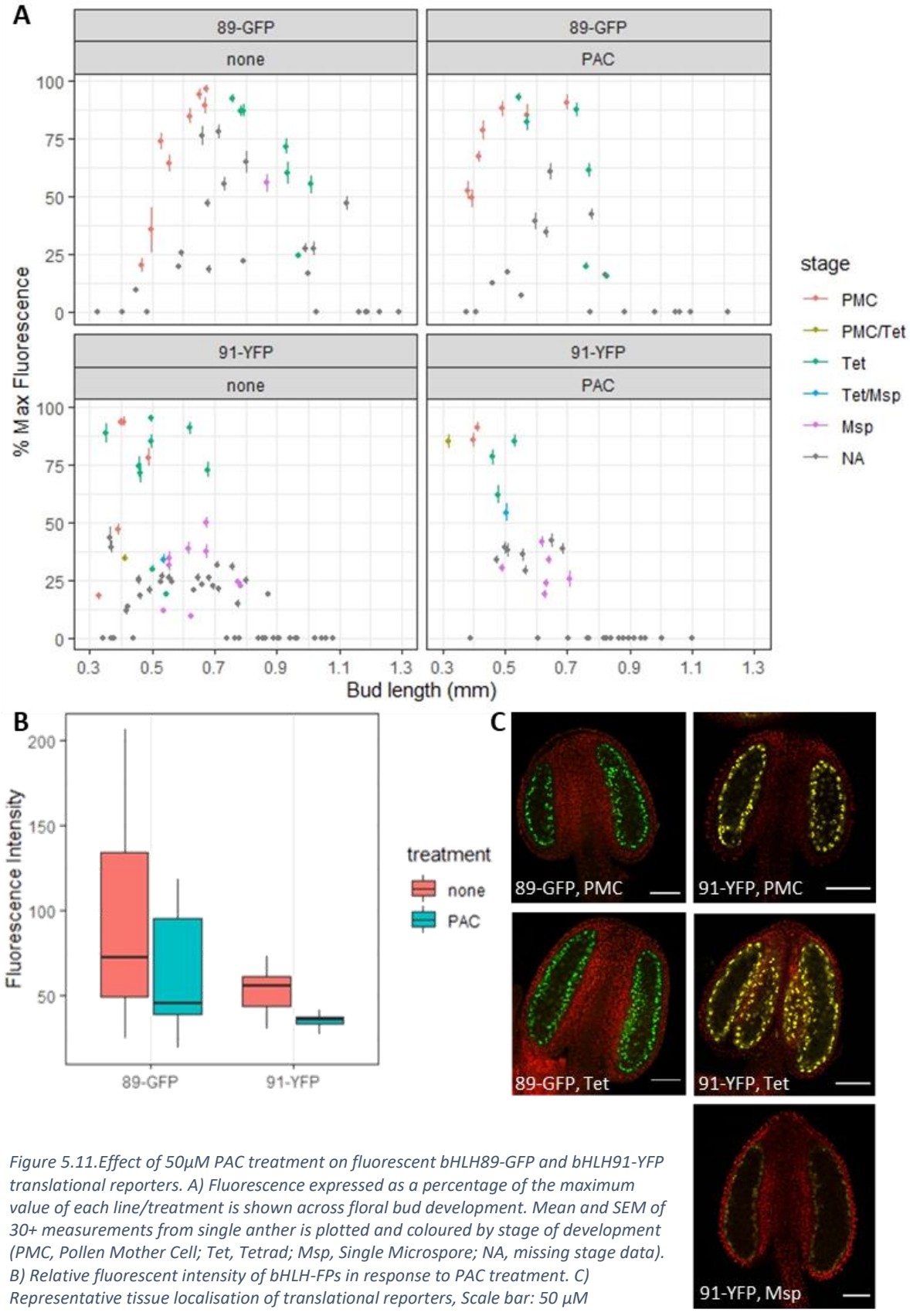

Figure 5.11.Effect of 50µM PAC treatment on fluorescent bHLH89-GFP and bHLH91-YFP translational reporters. A) Fluorescence expressed as a percentage of the maximum value of each line/treatment is shown across floral bud development. Mean and SEM of 30+ measurements from single anther is plotted and coloured by stage of development (PMC, Pollen Mother Cell; Tet, Tetrad; Msp, Single Microspore; NA, missing stage data). B) Relative fluorescent intensity of bHLH-FPs in response to PAC treatment. C) Representative tissue localisation of translational reporters, Scale bar: 50 µM

5.3 DISCUSSION

GA hormone profiles presented within this chapter suggest that bHLH89, -91 and -10 feedback into the GA biosynthesis pathway and contribute to changes in GA levels within the flower in response to different light intensities. Bimolecular Fluorescence Complementation (BiFC) assays further demonstrate that the bHLHs interact with DELLA and GAMYB-like proteins, crucial GA signalling components, thus potentially moderating downstream GA responses.

5.3.1 Floral GA biosynthesis in response to shade

Much of our previous knowledge on the effect of shade on GA levels comes from studies carried out in seedlings, using Far Red (FR) enriched light. Natural shade comprises of two key components: a low photosynthetic active radiation (PAR) and a reduced red to far-red ratio (R/FR). In our study, low light consists of reduced PAR but the spectral quality of the light remains constant between conditions (Figure 2.1).

In this chapter it's been demonstrated that decreasing the intensity of photosynthetically available light decreases bioactive GA_4 levels in flowers (Figure 5.2 D). In contrast, simulated shade (through FR enriched light) has been shown to increase bioactive GA_4 levels in Arabidopsis seedlings (Bou-Torrent et al., 2014). Decline of bioactive GAs in light is largely due to rapid repression of GA biosynthetic genes (GA 3-oxidases & GA 20-oxidases) and induction of catabolic genes (GA 2-oxidases) by light-activated phytochromes (Achard et al., 2007; Alabadí et al., 2008).

Less attention has been paid to the effects of low PAR on GA levels in Arabidopsis. A study in pea (*Pisum sativum*) seedlings showed that low irradiance increases bioactive GA_1 levels, alongside its precursors and derivatives (Gawronska et al., 1995). The combined effects of PAR and R/FR ratio were studied in sunflower (*Helianthus annuus*) seedlings, showing that low light intensities increase bioactive GA levels in leaves, but not significantly so, and the effect is milder than that of low R/FR alone or in combination (Kurepin et al., 2007).

GA_4 is well established as the predominant bioactive form of GA in Arabidopsis, with high levels in flowers (Hu et al., 2008). It has been shown to play a pivotal role during floral initiation and later male reproductive development (Eriksson et al., 2006 ; Plackett et al., 2011). GA_1 levels are much lower throughout the plant but appear to accumulate after floral initiation, and reach particularly high levels in developing seeds and siliques, suggesting an important role in later stages of development (Eriksson et al., 2006; Varbanova et al., 2007; Hu et al., 2018; Kanno et al., 2010). To my knowledge, no previous study has been made into the effects of shade on GA levels in Arabidopsis flowers.

In stark contrast to the shade-induced increases in bioactive GA levels recorded in seedlings, our hormone profiles show a reduction in GA_4 in response to low light in WT inflorescences (Figure 5.2 D). Although there is also a significant increase in bioactive GA_3, albeit still at incredibly low concentrations (Figure 5.2 F), since GA_3 doesn't appear to have a major role in Arabidopsis this is probably of less importance. Reduced GA levels are likely to be a result of reduced biosynthesis. Light has been shown to effect GA levels through phytochrome regulation of the GA biosynthetic genes: *GA3-oxidases* and *GA20-oxidases* (Kamiya and García-Martínez, 1999). *GA20ox1* and *GA20ox2* were differentially expressed in response to low light in Col-0 according to the RNASeq (Figure 5.3) but, since the changes in GA levels primarily occurred in post-mitosis I stage flowers, these changes are unlikely to be explained by differential expression in the pre-mitosis RNAseq dataset. According to qRT-PCR analysis of whole inflorescences there were no significant changes in expression of the biosynthetic enzymes *GA3ox1* and *GA20ox2* in response to low light in Col-0 (Figure 5.4 D,E). There are of course multiple homologs of GA3- and GA20- oxidases expressed in the floral tissue (Hu et al., 2008; Plackett et al., 2012) and given that *GA20ox1* was downregulated in pre-mitotic tissue it may be that this gene plays a greater role in GA biosynthesis in the floral tissue. The decrease in bioactive GA levels in the flower could also be the result of increased transport out of the flower and into vegetative tissues. *NPF4.6*, and other putative GA transporters were upregulated in response to low light according to out RNAseq study, suggesting increased transport.

GA_4 levels are significantly reduced in the *bhlh* double mutants compared to WT, which could be indicative of lower GA biosynthesis through bHLH-mediated reduction in expression of GA3- and GA20-oxidases. It seems that biosynthesis is at least partially independent of the bHLHs however since the *bhlh89,91* mutant still exhibits a drop in GA_4 in response to low light. Notably, both *bhlh* double mutants showed increased levels of the usually absent bioactive GA_1 in response to low light. Curiously, expression of *GA3ox1* and *GA20ox2* are increased relative to WT in the *bhlh* double mutants, suggesting an increased biosynthetic flux (Figure 5.4 D-E), indicative of WT bHLH proteins providing negative feedback into the GA biosynthesis pathway. GA3ox1 catalyses the final step in the biosynthesis of bioactive GA: the conversion of GA_9>GA_4 and GA_{20}>GA_1. In fitting with increased GA 3-oxidase activity, GA_9 and GA_{20} levels were greatly reduced or undetected in the *bhlh* mutants compared to WT (Figure 5.2 C, J). Whilst Col-0 shows no significant differences in expression of *GA2ox1*, which catabolises the breakdown of bioactive GA_4→GA_{34} and GA_1→GA_8, *GA2ox1* expression was significantly reduced in the *bhlh* double mutants in low light suggesting that catabolisis of bioactive GAs is reduced. These changes to GA biosynthesis and catabolisis are possibly an indirect effect of bHLH binding to DELLA proteins, which may inhibit DELLA upregulation of GA20- and GA3oxidases and downregulation of GA2oxidases (Zentella et al., 2007).

Despite the reduction in bioactive GA_4 levels in low light it appears that the reduced fertility of *bhlh* mutants is not caused by GA deficiency, since exogenous GA_3 treatments do not alleviate the fertility defects. Exogenous GA_3 applications were used here since it is not metabolised as rapidly as GA_4, levels of which are highly dependent on levels of GA2oxidases within the tissue. GA_3 is thus less influenced by tissue-specific expression of GA2oxidases, leading to a more reliable GA response.

Unfortunately, spatial information on the accumulation of GAs within the floral tissue is lacking; since whole flowers were used in the analysis of GA levels there is no resolution to what is happening in the anther. It may be that there are local changes to GA within anther tissues, through altered biosynthesis or transport, which are missed when looking at floral development as a whole. Future study GA accumulation in anthers, through GA reporters and biosensors, will be key to further understanding the role of bHLHs in low light GA responses.

5.3.2 DELLA control of bHLH activity

The fact that GA_4 levels in flowers seem to respond to light in a complete opposite manner to the way they do in seedlings complicates matters when it comes to the role of DELLA proteins. The degradation of DELLA proteins in shade has long been linked to GA signalling; binding of bioactive GA_4 to the GID1 receptor enables GID1 to associate with DELLA proteins, targeting them for degradation through the 26S proteasome (Figure 5.1). Thus when bioactive GA levels are low, the DELLAs are stable and can interact with other proteins; thus DELLAs accumulate in increased light in seedlings but from our data it could be that the DELLA proteins are stabilised in low light conditions in flowers.

Recent work has shown that GA levels are not quite as crucial as once thought in regulation of DELLA activity. Warmth and shade rapidly decrease RGA abundance through the E3 ubiquitin ligase, CONSTITUTIVELY PHOTOMORPHOGENIC 1 (COP1), independently of GA (Blanco-Touriñán et al., 2020). As the *bhlh* double mutants show conditional sterility in response to high temperature and low light intensity (Chapter 3, Fu et al., 2020) it is possible that DELLA degradation through the COP1 GA-independent pathway is key to this response. But future work will be crucial in determining how DELLA levels respond to low light intensities within the flower.

A comparison of transcriptomic data revealed a strong association between WT low light response and RGA regulated genes (Figure 5.5 D). All of the overlapping RGA-induced genes were upregulated in WT low light response, and whilst the split is not so clear cut when it comes to the RGA-repressed genes, the genes upregulated most strongly in response to low-light were entirely RGA-repressed (Table 5.3). All in all, this indicates that RGA plays a role in regulation of genes involved in low light response.

Our BiFC assay shows a strong *in planta* protein-protein interaction between bHLH89, -91 and -10 and the three DELLAs tested (GAI, RGL2 and RGL3; Figure 5.6). bHLH089 and -91 were also previously shown to interact with RGA in Y2H screens (Lantzouni et al., 2020). Of course, this interaction occurring in Arabidopsis is dependent on the proteins being present in the same tissues. Expression data suggests that all 5 *Arabidopsis* DELLA paralogues are expressed in flower buds (Tyler et al., 2004; Lee et al., 2002), although RGL3 expression appears much lower than the others, and developmental expression atlases imply that all of the DELLA proteins are expressed at corresponding developmental stages to the bHLHs (Klepikova et al., 2016; Schmid et al., 2005). The Rice DELLA homolog, SLR1, is expressed simultaneously in both the tapetum and pollen during flower development (Hirano et al., 2008; Tang et al., 2010). Tissue specific expression patterns of Arabidopsis DELLA proteins have not been fully resolved except in the case of RGL2. RGL2-GUS translational reporter expression was detected in most floral tissues including the filament but was absent from the anther itself (Lee et al., 2002) whereas a dominant fluorescent RGL2 translational fusion, YPet-rgl2Δ17, was detected in the nuclei of developing microspores, including Tetrads, and appears to have some expression in the anther as well as the filament (Gómez et al., 2019; although not acknowledged by the authors).

DELLAs largely play an inactivating role in Shade Avoidance Responses, sequestering PIFs and preventing activation of downstream targets (De Lucas et al., 2008). A similar situation might be expected when it comes to their interaction with bHLH89, -91 and -10, but since the DELLAs can play multiple roles, they could either be repressors (through sequestration and degradation of interactors) or enablers of bHLH function (through transactivation of downstream targets).

To gain some idea of the role of a DELLA-bHLH interaction the activity of bHLH fluorescent translational reporter proteins was observed in response to PAC treatment. PAC treatment is known to inhibit endogenous GA biosynthesis thus leading to stabilisation of DELLA proteins. Assuming that the DELLAs regulate bHLH activity by targeting them for degradation, as they would in the PIF model, this would mean that accumulation of DELLAs would increase turnover of the bHLH proteins. The slightly reduced fluorescence intensity of bHLH translational reporter proteins after PAC treatment (Figure 5.11) lends some support to this theory, but future work is necessary to confirm. YFP pulldown assays of pUB::bHLH-YFP proteins expressed in WT and *della* mutant backgrounds, grown in different light conditions, could be carried out to identify if the bHLH proteins are degraded in response to an altered light environment, and whether interactions with DELLAs mediates this.

If DELLAs are accumulating under low light conditions, when GA_4 levels are lower in WT flowers, this mechanism would mean that bHLHs would be degraded in response to low light. Coupled with the

high degree of functional redundancy reported among bHLH89, 91 and 10, DELLA-mediated protein degradation may explain the conditional sterility observed in the *bhlh* double mutants. Under normal light conditions both *bhlh* double mutants are mostly fertile because they have a single bHLH remaining functional. However, when the DELLAs accumulate under low light conditions they interact with the remaining bHLH, targeting it for degradation and thus preventing transcription of essential genes in the production of viable pollen.

Other inactivating roles for DELLA would explain this conditional sterility in much the same way. bHLHs are known to form complexes with MYB and WD proteins, to control genes involved in trichrome formation and anthocyanin biosynthesis; DELLA proteins have been shown to sequester components of theses complexes and inhibit their action (Qi et al., 2014; Xie et al., 2016). Here evidence has been presented that bHLH10 and 91 interact with MYB33 and MYB65 on a protein-protein level. It's possible that the bHLHs, in complex with MYB33/65 and perhaps also a WD40 protein, bind to promoters of transcription factors to activate genes essential in maintaining fertility. DELLAs may repress action through sequestration of bHLH89/91/10, inhibiting complex formation and downstream transcription. Identification of downstream targets genes, through Chromatin Immunoprecipitation (ChIP) would the first step to dissecting the roles of bHLH/DELLA/MYB interactions. Competitive binding assays should also be carried out to assess preferential dynamics in formation of bHLH-DELLA and bHLH-MYB dimers. Dual Luciferase Assays could further determine whether DELLAs sequester bHLHs and inhibit their promoter activation of targets, or on the contrary, whether their binding enhances activation capabilities.

The hypothesis that DELLAs may assume an inactivating role with regards to their interaction with the tapetal bHLHs is somewhat disputed by the transcriptomic data. A large subset of RGA-upregulated genes were found to be downregulated in the *bhlh089 bhlh010 amiR-bHLH091* triple mutant (Figure 5.5E), suggesting that the bHLHs ordinarily upregulate RGA-induced genes and lending support to the idea of transactivation. Numerous DELLA heterodimers have been shown to transcriptionally activate target genes, for examples enhancing the activation capabilities of ARABIDOPSIS RESPONSE REGULATORS (ARRs) and INDETERMINATE DOMAIN (IDD) proteins (Marín-de la Rosa et al., 2015; Yoshida et al., 2014). The transactivation mode-of-action would explain the conditional sterility of the *bhlh* double mutants if the DELLAs were indeed degraded in response to low light as they are in seedlings. In that case, increased DELLA stabilisation in normal light conditions would prove to enhance bHLH activity to support the mutant *bhlhs* and then there would be a reduction in activation abilities under low light with the loss of DELLAs. But as the dynamics of DELLAs in response to low light in flowers has not been confirmed, and GA levels suggest DELLA

accumulation in low light, this is probably an unlikely explanation for DELLA function at this point and future study will be key to resolve this question.

5.3.3 bHLHs are involved in GA biosynthetic pathway switch

There are two pathways of GA biosynthesis in Arabidopsis: the primary non-C13-hydroxylated (13-H) pathway results in bioactive GA_4, whereas an alternate C13-hydroxylated (13-OH) pathway produces the less abundant GA_1. In this study, GA_4 levels were reduced in the *bhlh* double mutants compared to WT under normal light and there was a clear induction of GA_1 in the *bhlh* mutants in low light that was absent in WT (Figure 5.2 D, K). Moreover it seems that the strength of light-response of the 13-OH GAs correlated with the severity of conditional sterility, with significant changes to 13-OH GA_1, GA_{44} & GA_{19} levels only in the partially-sterile *bhlh* double mutants, and the strongest changes seen in the more severe *bhlh89,91* mutant (Figure 5.3). This suggests a switch from the standard 13-H pathway (GA_{15}→GA_{24}→GA_9→GA_4→GA_{34}) to the 13-OH pathway (GA_{53}→GA_{44}→GA_{19}→GA_{20}→GA_1→GA_8).

GA 13-oxidases are likely to be responsible for this switch; CYP72A9, encoding a GA 13-oxidase, was found recently to catalyse the conversion of 13-H GAs to the corresponding 13-OH GAs (GA_{12} to GA_{53}, GA_9 to GA_{20} and GA_4 to GA_1) (He et al., 2019). GA_{20} and GA_1 were not detected in *cyp72a9* knockout mutants whereas GA_4 levels were increased, suggesting a major role for CYP72A9 in the formation of GA_1 and GA_{20}. However a closely related protein, CYP72A15, was also found to weakly catalyse the 13 hydroxylation of GA_{12} and GA_9, but not GA_4 (He et al., 2019).

There were no significant differences in expression of either *CYP72A9* or *CYP72A15* in either light condition or genotype, according to 2-way ANOVA of qRT-PCR data ($p>0.05$), however it appears that both are slightly upregulated in Col-0 in response to low light (Figure 5.4 A,B). Since CYP72A9 and CYP72A15 catalyse conversion of GA_{12} to GA_{53} and GA_9 to GA_{20}, this upregulation could explain the significant increases in GA_{53} and GA_{20} levels in Col-0 in low-light (Figure 5.2 F,J). Increased conversion of GA_9 to GA_{20} could also explain why GA_9 was undetectable in Col-0 in low light conditions (Figure 5.2 C). Under normal light conditions the average expression of both *CYP72A9* and *CYP72A15* is increased in the *bhlh* double mutant, although statistically insignificant, which might indicate a role of bHLH proteins in downregulating the 13-OH pathway under normal conditions. *CYP72A15* also appears to be downregulated in low light in the *bhlh* double mutants, however these differences are small and not statistically significant, but could nevertheless explain the observed slight decrease in GA_{53}.

Of course a simple explanation for increased GA_1 levels could be that the samples contained more mature floral tissues since GA_1 levels are known to be increased in developing seeds. However,

contamination of the samples is highly unlikely since studies have shown that activation of the GA_1 pathway occurs 6-12 days after flowering (/anthesis), and only at this point were increases in GA_1 and GA_{53} observed (Kanno et al., 2010). Thus the increased 13-OH GAs in low light and/or *bhlh* mutant backgrounds are unlikely to be due to inclusion of an extra post-anthesis flower.

5.3.4 Is GA responsible for the conditional sterility of *bhlh* double mutants?

A large number of GA-regulated genes were found to be differentially expressed in low light and *bhlh* mutant backgrounds, with transcriptomic studies revealing a strong link with regulation by the RGA DELLA protein (Figure 5.5). Our results thus suggest that the conditional sterility of *bhlh* mutants may be linked to GA signalling through their interaction with DELLA proteins.

With sterility of the double *bhlh* mutants increasing in low light conditions, when bioactive GA_4 levels are decreased, exogenous GA_3 and PAC treatments were expected to respectively alleviate or mimic this conditional sterile response. Low concentrations of PAC (1µM) effectively replicated the low-light induced prolonged sterility of *bhlh* double mutants (Figure 5.9). However, contrary to the initial hypothesis, exogenous GA_3 treatment mimics and enhances the light-sensitive sterility of *bhlh* double mutants in a dose-dependent manner (Figure 5.8).

The anther is incredibly sensitive to GA levels with deficiencies and excesses both leading to male sterility (Plackett et al., 2014; Koornneef and van der Veen, 1980). Since silique lengths of Col-0 are also reduced in response to the highest GA treatments in low light, one might hypothesise that this sterility is caused by an increased GA-response combined with reduced carbon resource availability in low light. Reduced light limits photosynthetic efficiency and thus the available carbon for respiration. Since male reproductive development is both highly-energy dependant and requires high amounts of carbohydrates, reduced light will limit available resources and impact on fertility (Ferguson et al., 2021). This coupled with GA-mediated regulation of genes involved in reproductive development will enhance sterility. Perhaps the bHLHs ordinarily act as a hub integrating environmental signals into reproductive development pathways through their interaction with DELLAs, reducing downstream GA signalling and thus enabling male reproductive development to continue is spite of adverse, carbon limiting, conditions. Therefore *bhlh* double mutants may show higher sterility in response to lower GA doses because, with only one working bHLH, male reproductive development is less buffered.

It seems that flowers treated with the GA inhibitor, PAC, progress through developmental stages at smaller bud sizes. This could either be an indication of development initiating earlier, progressing more rapidly, or less elongation of floral organs due to reduced GA availability. The latter explanation is probably the most likely since GA-deficiency is well known to reduce floral organ

growth (Plackett et al., 2017). Modelling of pistil and stamen elongation across floral development showed strong reduction in the elongation of floral organs in the severely GA-deficient *ga1-3* and *ga20ox1 -2 -3* triple mutant (Plackett et al., 2012), ultimately causing a spatial barrier to pollination in the mature flower. Whilst no obvious defects in stamen elongation were observed in the *bhlh* double mutants, no detailed study was taken of the ratio of pistil vs stamen lengths in early and late flowers and thus a mechanical barrier to pollination in early flowers that later corrects itself, as in the various *ga3ox* and *ga20ox* mutants, cannot be ruled out (Plackett et al., 2017). That said, pollen viability staining suggests that the differences in fertility of *bhlh* double mutants' early vs late flowers arise from pollen developmental defects (Chapter 3, Zhu et al., 2015).

Of course, despite the similarities in phenotypes of *bhlh* and various GA mutants, the role of GA signalling in this conditional sterility may be minor. Whilst primarily negative regulators of GA signalling, DELLA proteins have been shown to integrate signals from multiple hormonal pathways including abscisic acid (ABA), jasmonic acid (JA), auxin, cytokinin, ethylene, and brassinosteroids (BR) (Davière and Achard, 2016). Various studies have shown that JA, auxin and cytokinin regulate anther development (Qi et al., 2015; Aloni et al., 2006; Cecchetti et al., 2008; Kinoshita-Tsujimura and Kakimoto, 2011), and since there was significant differential regulation of many hormonal signalling and biosynthesis pathways in the RNAseq (Section 4.2.2) it may be that conditional sterility in *bhlh* mutants is caused by disruption to signalling of other phytohormones and future studies will be pivotal in unravelling this response.

5.4 CONCLUSIONS

Significant changes to the levels of various GA metabolites in *bhlh089, -91 and -10* double mutants, in particular the reduction in GA_4, suggests that the action of these bHLHs feed into the regulation of the GA biosynthetic pathway. Supporting this, key enzymes in GA biosynthesis are differentially expressed in *bhlh* mutant (especially under low light conditions). bHLHs are suggested to affect GA-signalling pathways through interactions with DELLA proteins, but future work is needed to elucidate the exact role of DELLA-bHLH interactions. First and foremost, *della x bhlh* mutants must be created to characterise light responses and determine whether the light-sensitive sterility of *bhlh* mutants is dependent on DELLA action. A clearer picture of the role of this interaction will then be gained through competitive binding, Dual Luciferase and GFP-pulldown assays.

Since initial sterility is common between the *bhlh, ga3ox* and *ga20ox* mutants GA biosynthesis might be expected to play a crucial role in later recovery of fertility. However, endogenous GA levels in floral tissues are fairly consistent between early vs late flowers in WT and *ga3ox* mutants (Hu et al., 2008), so it seems unlikely that the recovery is biosynthesis-linked. Plackett *et al.* (2017) suggest

instead that alteration of pathways downstream of GA signalling may enable reproductive development in spite of GA levels and it's possible that bHLH89, 91 and 10 through an interaction with DELLA proteins might be key in this.

6 bHLH PROTEIN INTERACTIONS

6.1 INTRODUCTION

6.1.1 bHLH protein interactions

bHLH proteins are characterised by a basic region at the amino (N)-terminus and a Helix Loop Helix (HLH) region at the carboxyl (C)-terminus. The basic region, consisting of around 15 amino acids, is involved in binding to 5'-CANNTG-3' E-box motifs on target sequences (Atchley et al., 1999; Toledo-Ortiz et al., 2003). The HLH region functions as a dimerization domain with hydrophobic residues forming two amphipathic α-helices separated by a variable length loop region (Murre et al., 1989; Ferré-D'Amaré et al., 1994).

Within the HLH region, leucine-zipper domains are considered essential for dimerization. Two Leucine residues, first identified in the helix regions of the human E47 and E12 bHLH proteins (Ferré-D'Amaré et al., 1994), are highly conserved in plant bHLHs (Carretero-Paulet et al., 2010). The Leu-27 residue, considered crucial to the structure of the mammalian bHLH Max protein (Brownlie et al., 1997), is found in all 147 of the AtbHLH proteins described by Toledo-Ortiz et al. (2003), suggesting that Leu-27 has a similar structural function in plant bHLH dimerization. A C-terminal bHLH protein interaction and function (BIF) domain, or ACT-like domain, is also considered essential for dimerization of several bHLH proteins and is found in more than a third of *AtbHLH* genes (Feller et al., 2006; Kong et al., 2012; Cui et al., 2016). bHLH proteins have been shown to form homodimers and heterodimers with varying specificity; some bHLH proteins restrict their dimerization to just one, often closely related, protein whilst others form heterodimers with multiple partners, enabling fine control of downstream processes (Toledo-Ortiz et al., 2003).

An example of this is found in the regulation of photomorphogenesis by the bHLH transcription factors LONG HYPOCOTYL IN FAR-RED1 (HFR1) and PHYTOCHROME INTERACTING FACTORS (PIFs). HFR1 forms a heterodimer with PIF4 and PIF5, inhibiting PIF action in the phytochrome signalling pathway. But HFR1 also interacts with KIDARI (KDR), a small HLH transcription factor, competitively forming non-functional HFR1- KDR heterodimers and releasing PIFs from the inactive HFR1-PIF complexes in shaded conditions (Hong et al., 2013). This phenomenon is common between species, in rice for example POSITIVE REGULATOR OF GRAIN LENGTH 1 (PGL1, a HLH protein) heterodimerises with ANTAGONIST OF PGL1 (APG, a bHLH protein) with an overall effect of increasing grain length and yield whereas the APG homodimer decreases it (Heang and Sassa, 2012).

Heterodimerisation of bHLHs within the *Arabidopsis* male reproductive development has been well-characterised. DYT1 has been shown to interact with bHLH089, -091 and -010 proteins in Yeast Two

Hybrid (Y2H) and Bimolecular Fluorescence Complementation (BiFC) assays (Zhu et al., 2015; Feng et al., 2012), with aforementioned BIF domain essential to dimerization (Cui et al., 2016). The authors further demonstrated that different DYT1-bHLH combinations show differential transcriptional activation. The DYT1-bHLH089 heterodimer, for example, binds to the MYB35 promoter and highly activates expression, whereas DYT1 or bHLH089 alone does not.

AMS has also been shown to interact with bHLH089 and bHLH091 in Y2H and Glutathione S-transferase (GST) pulldown assays (Xu et al., 2010). Although targets of AMS-bHLH complexes have yet to be determined, a comparison of *ams* mutant microarray data with the *bhlh089 bhlh010 amiR-bHLH091* RNASeq (Xu et al., 2010; Zhu et al., 2015) highlights some potential candidates to explore further. MALE STERILE 2 (MS2), also known as FATTY ACID REDUCTASE 2 (FAR2), is significantly downregulated in both mutants and is expressed in the tapetum at early single microspore stage (Aarts et al., 1997). MS2 encodes a fatty acyl-Acyl Carrier Protein (ACP) reductase necessary for producing the fatty alcohols essential to pollen wall formation, and the *ms2* mutant thus shows defective anther development from tetrad stage onwards with an enlarged vacuolated tapetum, unusual exine development and eventual collapse of microspores (Aar*ts et al*., 1993, 1997; Chen *et al*., 2011).

Models by Ferguson et al. (2016) suggest that due to competitive binding, bHLH089 & bHLH091 may associate earlier with DYT1 than AMS causing a delay in transcription of AMS-regulated genes such as MYB80 and MS1 until DYT1 levels are lower and the bHLHs are free to associate with AMS.

In addition to bHLH-bHLH dimerization, bHLHs are known to interact with a variety of other proteins, as previously indicated, with bHLH interactions with phytochrome and cryptochromes light receptors regulating diverse pathways in response to fluctuating light signals (Liu et al., 2013; Huq and Quail, 2002). Chapter 5 touched on the significance of bHLH interactions with MYB and WD-40 proteins, which form complexes to regulate diverse developmental pathways (Zhang et al., 2019), and evidence was presented for an interaction between bHLH10 & -91 and MYB33 & -65 (Chapter 5.2.3). Protein-protein interactions between DELLAs and bHLH89, -91 and -10 were further confirmed to occur *in planta* (Chapter 5.2.3). DELLA proteins have previously been shown to undergo a number of Post-Translational Modifications (PTM), including Small Ubiquitin-like Modifier (SUMO)-conjugation which acts to stabilise the protein and enable accumulation (Conti et al., 2014), ultimately leading to altered fertility (Campanaro et al., 2016).

6.1.2 SUMOylation in reproductive development

Like many PTMs, SUMOylation has multiple modes of action and, depending on its substrate, can alter protein-protein interactions (Figure 6.1 A,F), change protein localisation (Figure 6.1B), induce

conformational changes to activate proteins (Figure 6.1D), and both stabilise and destabilise a protein through inhibition or activation of ubiquitin-mediated degradation (Figure 6.1C,E; Morrell and Sadanandom, 2019).

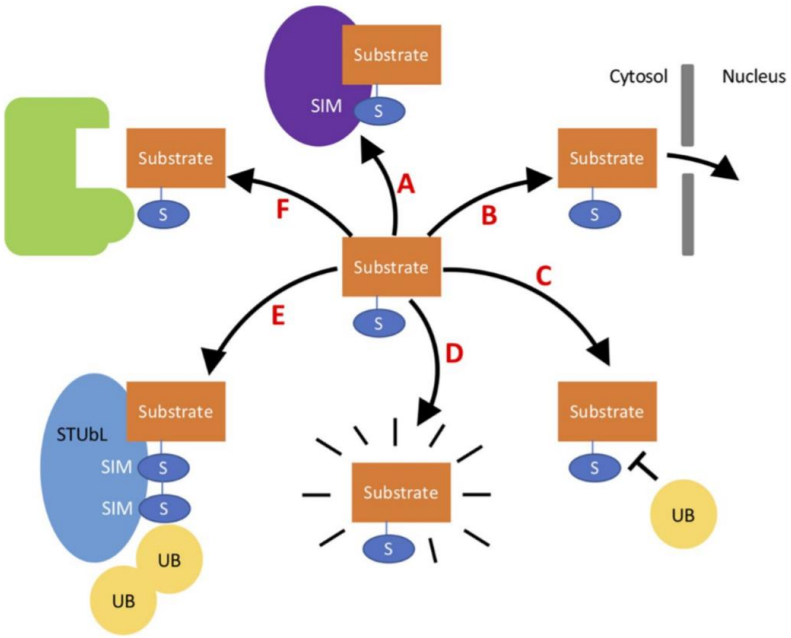

Figure 6.1. SUMO modes of action, from Morrell and Sadanandom (2019). SUMO conjugation to a protein can enable A) interaction with another protein through a SUMO interacting motif (SIM), B) localisation to the nucleus, C) inhibition of ubiquitin conjugation and subsequent protein degradation, D) conformational changes to activate the protein, E) interactions with SUMO-targeted Ubiquitin Ligases (STUbL) which lead to protein degradation, and F) inhibition of protein-protein interactions.

SUMOylation is a dynamic and reversible cycle that's heavily dependent on the activity of numerous enzymes: E1 activating enzymes, E2 & E3 conjugating enzymes, E4 ligases and SUMO proteases. SUMO proteases act to cleave SUMO from target substrates and also mature newly synthesized SUMO. Six SUMO proteases are expressed in *Arabidopsis* flowers: *EARLY IN SHORT DAYS 4 (ESD4), ESD4-LIKE SUMO PROTEASE 1 (ELS1), OVERLY TOLERANT TO SALT 1 (OTS1), OTS2, SUMO PROTEASE RELATED TO FERTILITY 1 (SPF1)* and *SPF2*. An early flowering phenotype is seen in *esd4-1* and *ots1 ots2 double* mutants (Reeves et al., 2002; Castro et al., 2016) and *spf1* mutants are late-flowering (Kong et al., 2017). Crucially, *spf1 spf2* and *ots1 ots2* mutants have been found to have male fertility defects. OTS1/2 facilitates the degradation of DELLAs through cleavage of the stabilising SUMO modification (Conti et al., 2014). Since DELLAs are key to maintaining normal male reproductive development disrupted regulation within the *ots1 ots2* mutants leads to reduced stamen elongation and seed production (Campanaro et al., 2016). Likewise, *spf1* and *spf1 spf2* mutants produce less pollen, and much of this is non-viable and misshapen (Liu et al., 2017b) but as of yet their targets within reproductive development are unknown.

6.1.3 Chapter Aims

In this chapter the role of protein-protein interactions between the tapetal bHLHs in regulating downstream targets was explored, focusing on the effect of homodimerization and heterodimerization. A new role for SUMOylation in reproductive development was further revealed and the SUMO proteases likely to be involved were identified.

6.2 RESULTS

6.2.1 Tapetal bHLHs interact to regulate downstream targets

A Yeast 2 Hybrid (Y2H) screen was performed to confirm the interactions between the tapetal bHLHs. This indicated that heterodimers could form between all combinations of AMS, bHLH89, -91 and -10, although the bHLH89-10 interaction appears to be weaker (Figure 6.2A).

Since different dimeric complexes have distinct functions in regulating downstream targets (Goossens et al., 2017) a Dual Luciferase Reporter Assay (DLRA) was set up to determine the roles of tapetal bHLHs in transcriptional activation of MS2. Here, tobacco leaves were co-transformed with pUBQ10 driven CDSs of various bHLH transcription factors and a Dual Luciferase construct carrying the promoter of MS2 was fused to a Firefly luciferase (LUC) reporter and a p35S driven *Renilla* luciferase (REN) reporter to act as an internal negative control. Transfection with a single bHLH transcription factor lead to negligible activation of pMS2:LUC expression, with an average Relative Response Ratio (RRR) of less than 0.3% of the positive control (Figure 6.2B). Weak pMS2:LUC reporter expression was seen in response to bHLH10 in 2 out of 5 replicates (10-15% of positive control) and whilst there was one instance of AMS inducing MS2:LUC expression at 79% of the positive control, the remaining 8 replicates showed no induction, with LUC activity largely below negative control levels. Taken together this suggests that bHLH89, -10, -91 and AMS do not activate the MS2 promoter in their homodimeric form.

MS2 activation increased in the DLRA when two bHLHs were co-transformed, thus enabling formation of heterodimers in the transient assay. Some LUC expression was reported in response to the bHLH91-10 dimer (9%), with a slightly stronger induction in response to AMS-bHLH91 (17%) and very strong activity in response to AMS-bHLH89 (55%, Figure 6.2B).

MS2 activation was also seen in response to combinations of AMS and two of bHLH89/91/10, with average RRRs of 14-36%. Whether or not they work in complex cannot be ascertained from this and it could that AMS is preferentially dimerising with one of the other bHLHs in this mix to activate MS2 expression. Addition of DYT1 to the 3-part AMS-bHLH mix lowers the induction of the MS2 promoter to 4-9% of the positive control.

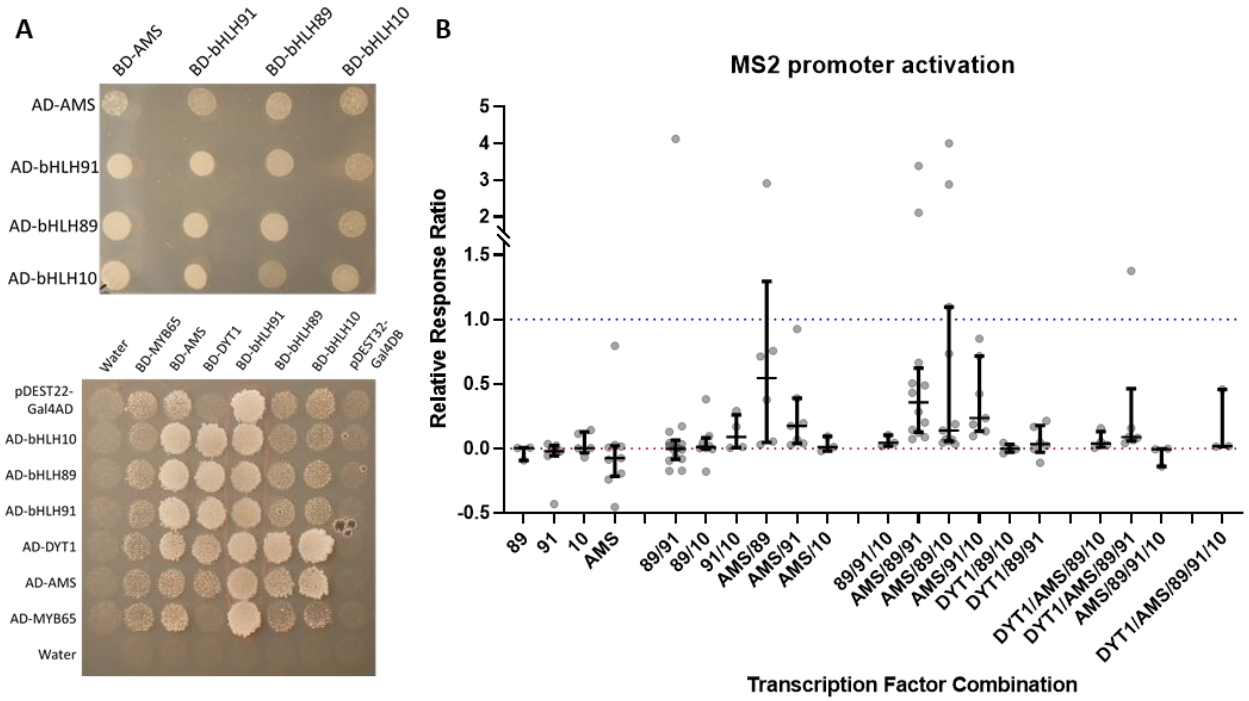

Figure 6.2 Different combinations of bHLH heterodimers affect transactivation of MS2 promoter.
A) Yeast 2 Hybrid showing bHLH protein interactions, in pDEST32-GAL4DBD Y187 yeast(α) and pDEST22-GAL4AD AH109 yeast(a). Mated colonies are plated on SD agar –leu –trp –his -ade to select for bait & prey plasmids and determine strength of interaction through activation of the Gal-responsive HIS3 and ADE2 genes. The bottom panel (image courtesy of W.Yin), illustrates controls of empty library plasmids (pDEST32-GAL4DB and pDEST22-GAL4AD) and water. Since colony growth was visible for the pDEST22-GAL4AD mated controls, suggesting varying degrees of autoactivation, 50mM 3-amino-1,2,4-triazole (3AT) was added to this minimal media in the top panel to minimise background growth of bait.
B) pMS2:LUC activity, as determined by Dual Luciferase Reporter Assay in Nicotiana tabacum, in response to co-transformation with various combinations of bHLH transcription factors (pUB:bHLH). pMS2:LUC expression has been normalised to internal p35s:REN control on the same construct and relative to controls on the same leaf: the positive control, co-transformed activator pUB:GAL4-VP64 & inducible p35s:5xUAS:LUC (y=1), and negative control, co-transformed pUB:GFP & pMS2:LUC (y=0). Individual replicates are plotted with bars representing the median and 95% confidence intervals.

6.2.2 bHLHs are SUMO-conjugated

SUMO site prediction software (Sadanandom, unpub.) identified four SUMO Interacting Motifs (SIM) on bHLH10 and -91 proteins, whilst bHLH89 contains one SUMO-binding and 2 SIM sites (Figure 6.3 A). Two of the SIM sites on each bHLH are upstream of the bHLH domain, with one SUMO/SIM site within the bHLH domain and a SIM site within the predicted BIF domain of bHLH010 and bHLH091. This suggested that these bHLHs have the potential to be SUMOylated. To confirm this, pUB:bHLH-YFP constructs were sent to Professor Sadanandom's lab, at the University of Durham, for transient SUMO pulldowns. Pulldown data revealed that bHLH89, -91 and -10 are SUMO-conjugated, with bHLH010 proteins showing particularly strong SUMOylation (Figure 6.3 B; Sadanandom, pers. comms.)

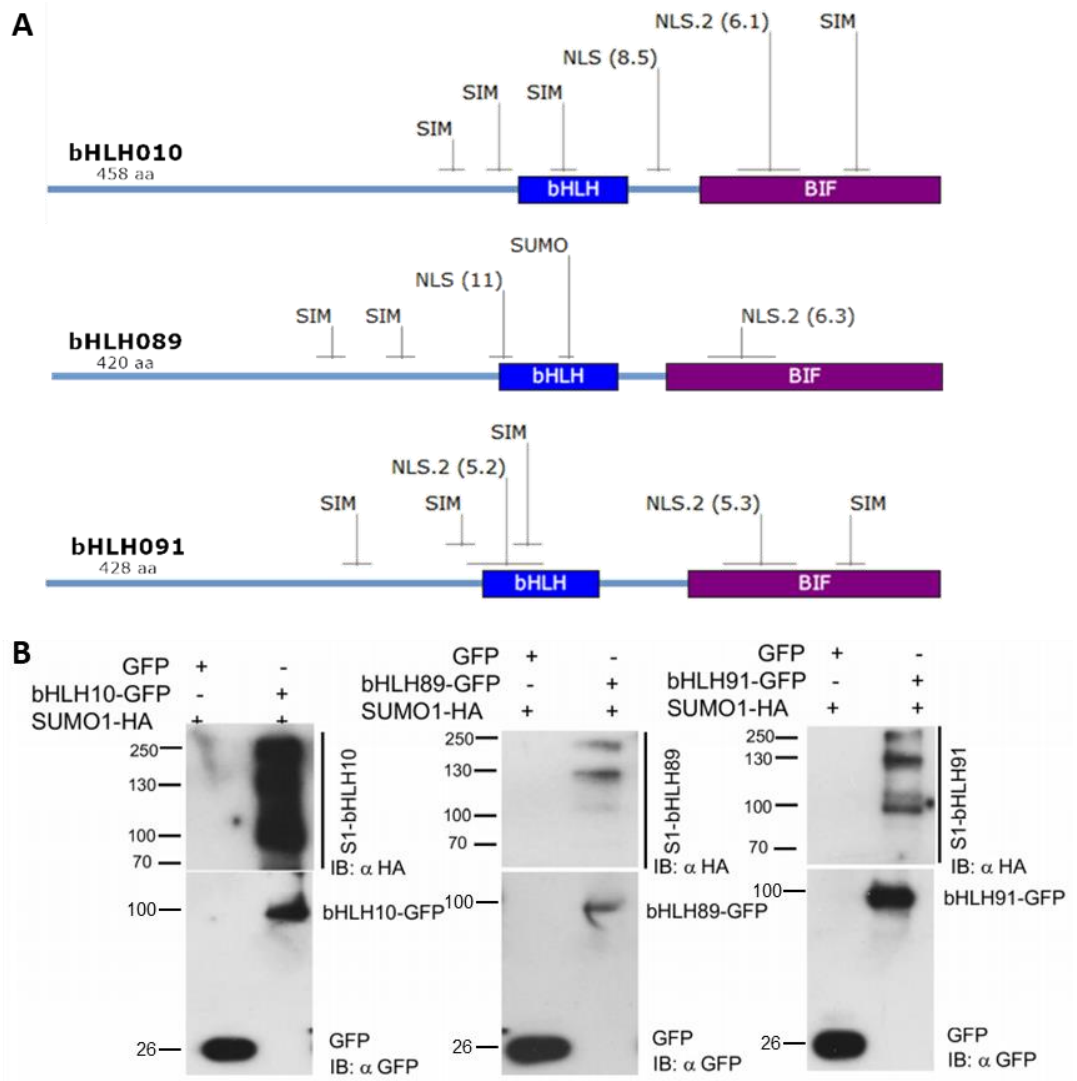

Figure 6.3 SUMOylation of bHLH89, -91 and -10. A) Predicted location of SUMO and SUMO Interacting Motif (SIM) sites on the bHLH proteins according to software developed by the Sadanandom lab (pers. comms). These are mapped alongside bHLH protein interaction and function (BIF) domains and predicted sites of monopartite and bipartite Nuclear Localisation Signals (NLS, NLS.2), with localisation strength in brackets, based on the cNLS mapper tool (http://nls-mapper.iab.keio.ac.jp). B) SUMO1-HA immuno-pulldowns: pUB::bHLH-GFP proteins were transiently expressed in tobacco, and immunoprecipitated by using GFP-Trap agarose beads. bHLH-GFP presence was detected by the anti-GFP antibody (IB:αGFP), whereas AtSUMO1-conjugated bHLH-GFP were visualized using anti-SUMO1-HA (IB:αHA). Image courtesy of A. Sadanandom.

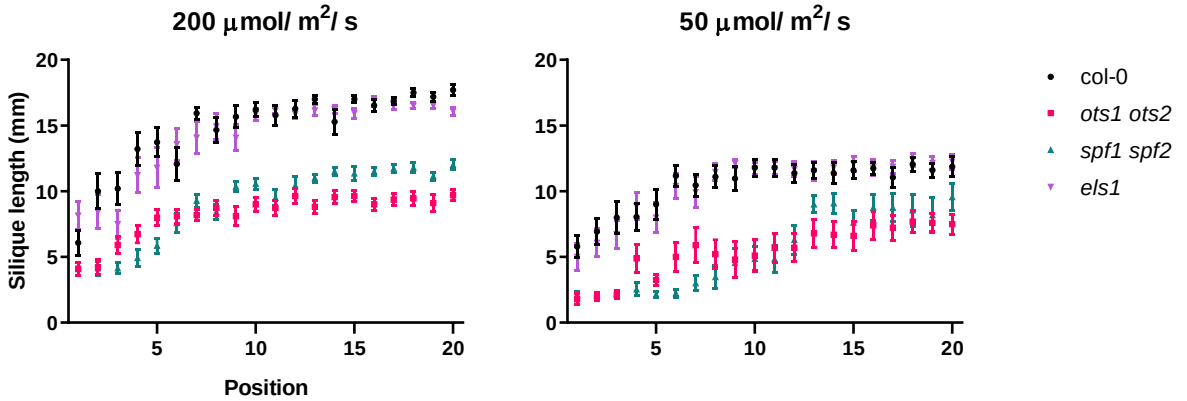

Figure 6.4. Fertility of SUMO protease mutants ots1 ots2, spf1 spf2 and els1 compared to WT Col-0, under normal (200 µmol/m²/s) and low (50 µmol/m²/s) light conditions, as determined by silique lengths at progressive positions across lateral flowering stems.

With a number of SUMO proteases linked to male fertility, the response of *ots1 ots2, spf1 spf2* and *els1* mutants to low light stress was assessed (Figure 6.4). Siliques of the *els1* mutant, which had no previously reported fertility defects (Hermkes et al., 2011) developed as WT. The *ots1 ots2* double mutant exhibits stunted siliques in normal and low light conditions and thus was not further affected by low light treatment. The characteristic delay in onset of fertility as reported in the *bhlh* double mutants was also observed in the *spf1 spf2* double mutant. Under normal light conditions (200 µmol/m^2/s), the initial 7 siliques of *spf1 spf2* double mutants showed reduced fertility, whilst recovery of fertility was delayed until position 14 under low light conditions (50 µmol/m^2/s). Thus the data suggest a role for SPF1 and 2 in regulating male fertility in response to light conditions.

No differential expression (log2FC>1, q<0.01) of any of the SUMO proteases, E4 ligases, E2/ E3 conjugating enzymes, or E1 activating enzymes was observed in our RNASeq analysis (Table 6.1). However, *SUMO4* was upregulated (log2FC=1.8) in low light in Col-0, but not differentially expressed in the *bhlh089 bhlh091* mutant, whilst SUMO3 was upregulated in low light (log2FC=1) in both Col-0 and the *bhlh* mutant.

6.3 DISCUSSION

6.3.1 bHLHs competitively form heterodimers to activate MS2 expression

Previous studies have demonstrated that DYT1 interacts with bHLH89, -91 and -10 and AMS interacts with bHLH89 and -91, although an interaction with bHLH10 was untested (Zhu et al., 2015; Feng et al., 2012; Xu et al., 2010) and Y2H in this chapter revealed that AMS also interacts with bHLH010 (Figure 6.2A). These data indicate that tapetal bHLHs are able to form both homodimers and heterodimers. Studies further suggested that DYT1-bHLH089 heterodimers were more transcriptionally active than homodimers in activating expression of MYB35/ TDF1 (Cui et al., 2016). Thus to assess the role of homo- and heterodimerization on transcriptional activity of AMS targets a DLRA approach was employed.

Analysis of *bhlh* and *ams* transcriptomes identified MS2 as a likely target of an AMS-bHLH complex. DLRA analysis revealed negligible pMS2:LUC expression in response to a single bHLH; however, strong luciferase expression was induced in response to co-transfection with multiple bHLHs. This suggests that single bHLHs, or as homodimers, are not able to induce MS2 expression whereas heterodimer complexes are transcriptionally active. Data further suggests that different bHLH heterodimers have distinct activation capabilities, with the AMS-bHLH89 heterodimer showing by far the strongest pMS2:LUC induction in our transient system. MS2 also appears to be induced in response to bHLH trimers, but it is impossible to tell if this is due to formation of trimeric complexes

with enhanced activation or preferential dimerization between two components. Since MS2 is essential for pollen wall development (Aar*ts et al*., 1993, 1997; Chen *et al*., 2011) it may be that post-translational regulation of bHLH-AMS dimerization allows for fine control of pollen development through targets such as MS2.

Future transcriptional activity analysis with the DLRA system should focus on other potential bHLH targets identified within this thesis to see if the same activity is seen in other bHLH targets. Given the known transactivating role of MYB proteins in bHLH complexes and the novel interactions reported between bHLH91 and -10 and MYB33 and -65 in the previous chapter, it would be valuable to co-transform MYBs into the DLRA system and assess how MYBs alter transcriptional activity of bHLHs.

Table 6.1. Expression (log2FC) of SUMO related genes in Col-0 and bhlh89,91 mutant in response to low (L) vs normal (N) light conditions (q<0.01), with red showing upregulation in low light/ bhlh mutant, blue showing downregulation and blanks indicating non-significant changes.

Function	Gene	Loci	Col-0, L-N	8991, L-N	Low, 8991-Col-0	Norm, 8991-Col-0
SUMO proteases	ESD4	AT4G15880	-0.2			0.2
	ELS1	AT3G06910				
	ELS2	AT4G00690				
	OTS1	AT1G60220				
	OTS2	AT1G10570	0.4			-0.4
	SPF1	AT1G09730	0.4	0.2		-0.4
	SPF2	AT4G33620				
	FUG1	AT3G48480	-0.6			0.4
	Desi 1	AT3G07090	-0.8	-0.7	0.3	0.5
	Desi 2A	AT4G25660				
	Desi 2B	AT4G25680				
	Desi 3A	AT1G47740				
	Desi 3B	AT2G25190				
	Desi 3C	AT5G25170				
	Desi 4A	AT4G17486				
	Desi 4B	AT5G47310				
E4 Ligases	PIAL1	AT1G08910				
	PIAL2	AT5G41580	0.3			-0.3
E3 conjugating enzymes	SIZ1	AT5G60410	0.4			-0.4
	HPY2	AT3G15150				
E2 conjugating	SCE1	AT3G57870	-0.4			0.3
E1 activating enzymes	SAE1A	AT4G24940	-0.4	-0.3		
	SAE1B	AT5G50680	0.4	0.3		
	SAE1B	AT5G50580				
	SAE2	AT2G21470				
SUMOs	SUMO1	AT4G26840	-0.4			0.3
	SUMO2	AT5G55160				
	SUMO3	AT5G55170	-1.0	-1.0		
	SUMO4	AT5G48710	1.8			-1.6
	SUMO5	AT2G32765	-0.2			
	SUMO6	AT5G48700				
	SUMO7	AT5G55855				
	SUMO8	AT5G55856				

6.3.2 SUMO regulation of bHLH89, 91 & 10 likely occurs through SPF1/2

A link between male reproductive development, GA signalling and SUMOylation was established through OTS1/2 destabilisation of DELLA proteins (Campanaro et al., 2016). Additionally, there is increasing evidence for the role of SUMO in light responses. The photoreceptor PHYB is SUMOylated in response to red light, with SUMOylation blocking protein-protein interactions with PIF5 and thus inhibiting hypocotyl elongation and cotyledon opening and expansion (Sadanandom et al., 2015). New data from the Sadanandom group suggests that SPF1/2 are degraded in response to blue light through regulation by CRY1/2 photoreceptors (Sadanandom, pers. comms.). Thus reduction of blue light could lead to enhanced stability of these SUMO proteases and subsequent cleavage of SUMO.

DeSUMOylation in response to light signals could be a rapid way of regulating transcriptional activity of the bHLHs in tapetum development as it was demonstrated that bHLH89, -91 and -10 are highly SUMO conjugated (Figure 6.3 B). Since bHLH89 contains a predicted SUMO site, it is likely to be directly SUMOylated, but further study will be necessary to elucidate the regulatory role of SUMOylation here. Work on the role of AUXIN REPSONSE FACTOR 7 (ARF7) in lateral root emergence in response to moisture (aka hydropatterning) demonstrated that SUMOylation inhibits DNA binding activity (Orosa-Puente et al., 2018). The authors created a non-SUMOylatable *ARF7* transgene by modifying the SUMO site, replacing the core SUMO binding Lysine (K) residue with Arginine (R), thereby abolishing SUMOylation of *ARF7*. This non-SUMOylatable *ARF7* transgene showed increased binding to target promoters and thus impaired lateral root hydropatterning. In this way, future studies of bHLH transgenes with mutagenized SUMO/SIM sites could be utilised to establish the role SUMO plays in tapetum gene regulation and male reproductive development.

bHLH10, -89 and -91 all contain multiple SIM sites that likely regulate SUMO dependent protein-protein interactions (Figure 6.3 A). There is a high degree of conservation of SIM sites between the three bHLHs (Appendix II). bHLH10 and -91 contain identical SIM sites (GGQIGEHYSFLFN) in their BIF domain, and have two well-aligned and highly similar SIM sites within, and immediately upstream of, the bHLH domain. The 2nd bHLH89 SIM site is also almost identical to the 1st bHLH91 SIM. This conservation suggests that the SIM sites are likely to be highly important in regulating downstream processes.

Previous work has shown that DELLA proteins are SUMOylated, particularly under salt stress, and are stabilised in their SUMO-conjugated form (Conti et al., 2014). Stabilised SUMOylated DELLAs sequester the GID1 GA-receptor, leading to the accumulation of non-SUMOylated DELLAs. Since the OTS proteases that control DELLA deSUMOylation are degraded in response to salt stress (Conti et al., 2008), this SUMO-mediated accumulation of DELLA proteins results in repression of growth

during stress. As highlighted in Chapter 5, DELLA proteins are crucial to male reproductive development, and thus unsurprisingly it has been shown that the *ots1 ots2* mutant has reduced fertility, although this appears to be due to reduced stamen elongation rather than defective pollen development (Campanaro et al., 2016). It is possible that SUMOylation of DELLA proteins enables the protein-protein interactions with bHLH89, -91 and -10, binding non-covalently through SIM sites on the bHLHs. It would be very interesting to see if DELLA-bHLH interactions still occur between non-SUMOylatable versions of DELLAs or bHLHs.

Since SIM sites are predicted in both the bHLH and BIF domains, which are considered essential for the dimerization of bHLH proteins, it is possible that SUMO-interactions through these sites prevent binding to their normal partners such as AMS and DYT1. Thus SUMO through preventing an interaction with these transactivating bHLHs, could potentially inhibit the transcriptional activity of bHLHs. Rapid cleavage of SUMO from the bHLHs by SUMO proteases in response to environmental changes may thus enable binding and rapid transcriptional responses.

The SUMO protease double mutant *spf1 spf2* has a similar light-sensitive fertility defect to *bhlh89,91* and *bhlh89,10* double mutants, with prolonged sterility under low light conditions (Figure 6.4). This suggests that accumulation of SPF proteases under low light conditions is important in maintaining fertility and potentially indicates a role for SPF1/2 mediated deSUMOylation of bHLHs in regulating reproductive development under adverse light conditions. If it's assumed that SUMO-conjugation of bHLHs inhibits their protein-protein interactions, deSUMOylation by SPF1/2 in low light would free the bHLHs to dimerise with AMS or other partners to activate target genes (Figure 6.5).

Light-mediated regulation of SUMO-machinery is likely to be largely post-transcriptional since there is no differential expression (log2FC>1) of any SUMO related genes in the RNAseq aside from SUMO4, which is differentially regulated in WT and *bhlh* light responses, with upregulation in low light only observed in Col-0. Whereas SUMO1 & -2 are important in stress response, the activity of SUMO 4 is largely unknown, although it seems that they may function in formation of poly-SUMO chains (Kurepa et al., 2003).

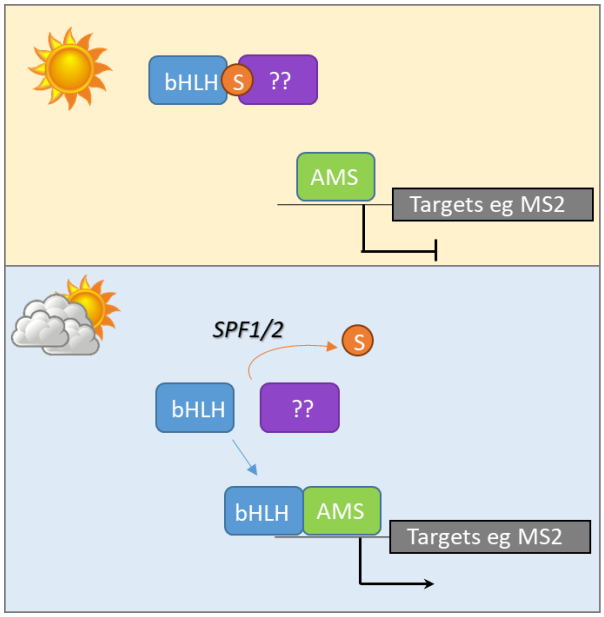

Figure 6.5. Proposed model for SUMO-regulation of bHLH activity in different light environments. In a normal light environment bHLHs may be sequestered by SUMOylated proteins through their SIM site and thus are unable to heterodimersise with AMS and activate transcription of target genes eg MS2. In low light conditions SPF1/2 proteases accumulate and cleave SUMO, freeing bHLHs to interact with AMS and activate target transcription.

6.4 CONCLUSIONS

Results from this chapter suggest that bHLH heterodimerisation is crucial in activating expression of downstream target genes within key male reproductive development pathways. Identification of bHLH-SUMO conjugation and a link with light-sensitive SUMO proteases leads us to speculate on the role of post-translational modifications in regulating these protein-protein interactions in response to a changing environment.

7 GENERAL DISCUSSION

An understanding of pollen development in an environmental context is essential for effective crop breeding. Hybrid crops have been long known to have increased 'vigour' compared to inbred lines, with increased yield and resilience to abiotic and biotic stresses (Brewbaker, 1964; Lippman and Zamir, 2007). Male sterile lines are inherently valuable in the creation of hybrids as they remove the need for labour-intensive emasculation of parental lines. Whilst traditionally Cytoplasmic Male Sterility (CMS) has been used in hybrid seed production, this system requires a third restorer line to propagate the male sterile parent. Thus breeders are now starting to take advantage of Environmentally-Sensitive Genetic Male Sterility (EGMS), in which lines are male sterile only under certain conditions and thus can be both easily crossed and propagated by altering growth conditions, simplifying breeding and reducing costs (Chen and Liu, 2014).

Microspore development is particularly vulnerable to abiotic stresses, such as heat and drought, especially at the tetrad stage of development (Parish et al., 2012). An understanding of the genetic mechanisms behind reproductive stress responses will enable breeders to harness this information for creation of new EGMS lines and can also be used to generate more climate resilient varieties that maintain pollen viability and therefore yield in spite of adverse conditions.

Fundamental research into the effects of environmental variation on pollen development is therefore absolutely crucial. Studies in the model species *Arabidopsis thaliana* have led to the characterisation of hundreds of genes that contribute to the development of viable pollen, however a small number of transcription factors acting within tapetum development appear to be largely responsible for regulation of downstream pollen development. The tapetum acts as a maternal tissue, secreting many of the precursors necessary to the pollen development (Shi et al., 2015). Tapetum development is regulated by a cascading transcriptional pathway *DYT1-TDF1-AMS-MYB80-MS1* with multiple feedback loops (Ferguson et al., 2017). Whilst loss of any of these genes leads to male sterility due to interruption of tapetum development (Sorensen et al., 2003; Zhu et al., 2008; Zhang et al., 2006; Higginson et al., 2003; Wilson et al., 2001), *AMS* and *MS1* in particular both appear to be master regulators of pollen wall formation (Xu et al., 2014; Lu et al., 2020).

Whilst the genetic basis of male reproductive development has been well characterised, less is known about how environmental signals are fed into these genetic networks. Multiple genes appear to be involved in maintaining pollen viability in adverse conditions including *MYB33/65* mutants which show conditional male sterility in response to high temperature and low light, that seemingly originates in tapetum defects (Millar and Gubler, 2005). In this thesis a new role for the tapetum transcription factors bHLH89, -91 and -10 in maintaining pollen viability in a low light environment

has been defined. These bHLHs were thought to function redundantly in tapetum development (Zhu et al., 2015), interacting with DYT1, to enhance nuclear localisation (Cui et al., 2016), and AMS (Xu et al., 2010; Ferguson et al., 2017), although the consequences of this latter interaction have not yet been fully established.

Dual Luciferase studies in Chapter 6.2 demonstrated that bHLH-AMS dimers exhibit higher transcriptional activation of MS2 than AMS alone, suggesting that bHLH89/91/10 may provide some control over processes regulated by AMS. Given that *bhlh89,10* and *bhlh89,91* double mutants demonstrate conditional sterility in response to high temperature (Fu et al., 2020) and low light intensity (Chapter 3.2), it's proposed that environmental signals may be fed into reproductive development pathways through modulation of AMS targets by bHLH89/91/10.

Work in this thesis suggests that bHLH89, -91 and -10 are likely to have distinct roles in maintaining fertility in response to a fluctuating environment. Whilst both *bhlh89,10* and *bhlh89,91* double mutants demonstrate conditional sterility in response to low light, the effect is more severe in *bhlh89,91* (Chapter 3.2). In the *bhlh89,10* double mutant low light causes a prolonged period of initial sterility with eventual recovery of fertility later in development, whereas partial sterility is maintained throughout development of the *bhlh89,91* double mutant. Both *bhlh* double mutants exhibited defective pollen exine development in low light conditions (Figure 3.6), but in the more severely sterile *bhlh89,91* mutant the majority of pollen was collapsed and non-viable, with abnormal lipid deposition (Figure 3.6, 3.8).

Transcriptionally, a large number of changes to low light response were seen in the *bhlh89,91* mutant flowers compared to WT, with loss of differential regulation of genes crucial to sexual reproduction, lipid storage, lipid metabolic process and lipid transport in the *bhlh89,91* mutant (Chapter 4). Notably, spermidine synthesis genes such as *TAPETUM-SPECIFIC METHYLTRANSFERASE 1 (TSM1)*, *SPERMIDINE HYDROXYCINNAMOYL TRANSFERASE (SHT)*, *CYP98A8* and *CYP98A9,* which are ordinarily upregulated in response to low light in Col-0 buds, were not induced in the *bhlh89,91* mutant in low light conditions (Chapter 4.2.3). The pollen coat proteins EXTRACELLULAR LIPASE4 (EXL4), -5 & -6 and GLYCINE RICH PROTEIN14 (GRP14), -16, -17, -18, -19, & -20, some of which are direct targets of AMS (Xu et al., 2014), all show loss of low-light induction in the *bhlh89,91* mutant. Thus it appears there would be major changes to pollen coat composition in WT in response to low light, ensuring that the pollen remains viable, that are absent in the *bhlh89,91* mutant. Since spermidine is crucial to pollen wall development and protection from environmental stresses this could mean that the *bhlh89,91* pollen is less adapted to the stressful environment it finds itself in and account for the reduced pollen viability.

7.1 WHAT CAUSES FERTILITY RESTORATION IN CONDITIONALLY STERILE LINES?

Our knowledge of the basis of fertility restoration in conditional sterility, or at least in Thermosensitive Genetic Male Sterile (TGMS) lines, has advanced significantly over the past year. Recent work by Zhu *et al.* (2020) isolated a new TGMS line, *reversibly male sterile (rvms)*, which disrupts the function of GDSL-TYPE ESTERASE/LIPASE 77 (GELP77). They found that lower temperatures restores fertility by slowing microspore development and pollen formation, probably enabling sufficient materials to accumulate and form a functional pollen wall. Thus it is possible that slower microspore development under low temperatures may be responsible for the fertility restoration of *myb33 myb65, callose synthase 5 (cals5), ruptured pollen grain1 (rpg1), acyl-coa synthetase 5 (acos5), cytochrome p450 703a2 (cyp703a2), atp-binding cassette g26 (abcg26)* and *plant u-box 4 (pub4)* TGMS mutants (Millar and Gubler, 2005; Zhu et al., 2020; Wang et al., 2013).

Whilst *bhlh89,10 and bhlh89,91* double mutants also exhibit TGMS (Fu et al., 2020), and restoration of this may be explained by the slowing down of development as described by Zhu *et al.* (2020), arguably the same mechanism would not explain the light-sensitive sterility reported in this thesis (Chapter 3.2). Low light is expected to slow development and restore fertility of the *bhlh* double mutants, as is the case with the temperature and light-sensitive *cals5* mutant which is sterile when grown at 100 µmol/m^2/s but fertile at 45 µmol/m^2/s (Zhang et al., 2020). However, the complete opposite effect of light is seen in the *bhlh* double mutants, with fertility restored at higher light intensities (Section 3.2). Nevertheless such fertility responses are not unexpected, with the *hspr, yak1* and *myb33 myb65* mutants all showing increased fertility at higher light intensities (Yang et al., 2020; Huang et al., 2017; Millar and Gubler, 2005), but this does suggest that slower rates of development cannot compensate for the defects associated with light-sensitive conditional sterility.

Many of the TGMS described by Zhu *et al.* (2020) encode transporters and enzymes, whilst bHLH89/91/10 and MYB33/65 are transcription factors and therefore control expression of networks of genes involved in male reproductive development. Thus knockouts of these genes disrupt many downstream processes and recovery of fertility is not an issue of simply slowing down development to allow one protein to accumulate. Interestingly *RPG1,* one of the TGMS targets identified by Zhu *et al.* (2020), was induced in response to low light in Col-0 but not in the *bhlh89,91* mutant (Chapter 4.2.3) thus it's possible that the environmental sensitivity of RPG1 is conferred, at least in part, through regulation by bHLH89/91.

A key question is what causes the *bhlh89,91* and *bhlh89,10* mutant to be sterile at low light intensities but largely fertile under normal light intensities? Possibly it is a simple case of carbon availability for reproductive processes and reallocation of resources. Reproductive processes are

highly dependent on photosynthesis providing sufficient energy and carbohydrates (Ferguson et al., 2021). Under low light conditions, photosynthesis rates are lower and thus less carbon is fixed and transported to floral tissues. When carbon demand outstrips availability this leads to defective pollen development (Lauxmann et al., 2016), and this is frequently observed in CMS (Kaul, 1988). Under normal environmental conditions it may be that bHLH action provides a genetic switch to limit other processes and enable key reproductive development to continue in carbon limiting conditions. It is also possible that local light sensing by the reproductive tissue accounts for restoration of fertility in later flowers (Chapter 3.2.1); a lower light intensity close to the rosette (Figure 2.2) may limit early reproductive development but, as the inflorescence grows upwards toward the light source, increases in light intensity enable normal reproductive development to resume.

Recovery of fertility might also be linked to GA signalling, as multiple GA-deficient mutants show male sterility that spontaneously recovers later in development (Rieu et al., 2008b; Plackett et al., 2017; Hu et al., 2008), bHLH89/91/10 interact with DELLA proteins, the negative regulators of GA signalling, and also appear to modify GA biosynthesis (Chapter 5.2). Whilst GA levels are reduced in floral tissues in low light, the *bhlh89,91* and *bhlh89,10* mutant defects don't appear to be caused by GA deficiency since exogenous GA treatments did not restore the low light phenotype, or decrease the period of sterility, but had rather the opposite effect of adding to it.

DELLAs act as a hub integrating multiple hormonal signals (Davière and Achard, 2016); and since various phytohormone signal transduction pathways are differentially regulated at a transcriptional level in response to light in *bhlh89,91* compared to WT (Chapter 4.2.2) one might speculate that bHLH interactions with DELLAs serve to modify responses to other hormones. Auxin signalling, for example, was particularly disrupted in the *bhlh89,91* mutant light response. Auxin levels in the tapetum have been shown to play an important role in maintaining pollen development, through regulation of *AMS, MS1* and *MYB80* expression (Cecchetti et al., 2017). Low light causes downregulation of *DYT1, TDF1, bHLH89, bHLH91, bHLH10, AMS* and *MYB80* in Col-0 pre-mitosis stage buds, however, this *AMS* and *MYB80* transcriptional response is lost in the *bhlh89,91* mutant (Chapter 3.2.4). Taken together this provides compelling evidence that bHLH interactions might coordinate auxin responses to low light through AMS and that disrupted auxin signalling in the *bhlh89,91* mutant may form the basis of it's conditional sterility. However, exploration into levels of auxin, and other phytohormones, within *bhlh89,91* flowers in response to low light through mass spectrometry will be key in elucidating these mechanisms. An understanding of hormone localisation within the anther in response to light would be also be crucial. Thus analysis of reporter lines, such as DR5 for auxin (Heisler et al., 2005), and biosensors, such as the Gibberellin Perception Sensor 1

(GPS1; Rizza et al., 2017), in the different *bhlh* mutant backgrounds should be undertaken to define potential roles of the tapetal bHLHs in hormonal responses.

7.2 DELLA-bHLH INTERACTION MAY INTEGRATE ENVIRONMENTAL CUES INTO REPRODUCTIVE DEVELOPMENT

Protein-protein interactions between bHLH89/91/10 and the DELLA proteins GAI/RGA/RGL2/RGL3 have been demonstrated by Yeast 2 Hybrid (Y2H; Marín-de la Rosa et al., 2014; Lantzouni et al., 2020) and Bimolecular Fluorescence Complementation (BiFC; Chapter 5.2.3). DELLAs are degraded upon increases in bioactive GA, through the SCF/SLY1 ubiquitin E3 ligase complex, and in response to warmth and shade, through the GA-independent COP1/SPA ubiquitin E3 ligase complex (Blanco-Touriñán et al., 2020). Since *bhlh89,91* and *bhlh89,10* show conditional fertility in response to high temperature (Fu et al., 2020) and low light (Chapter 3.2) it seems that DELLA interactions with bHLH89/91/10 could act as a hub integrating environmental signals into reproductive development (Figure 7.1).

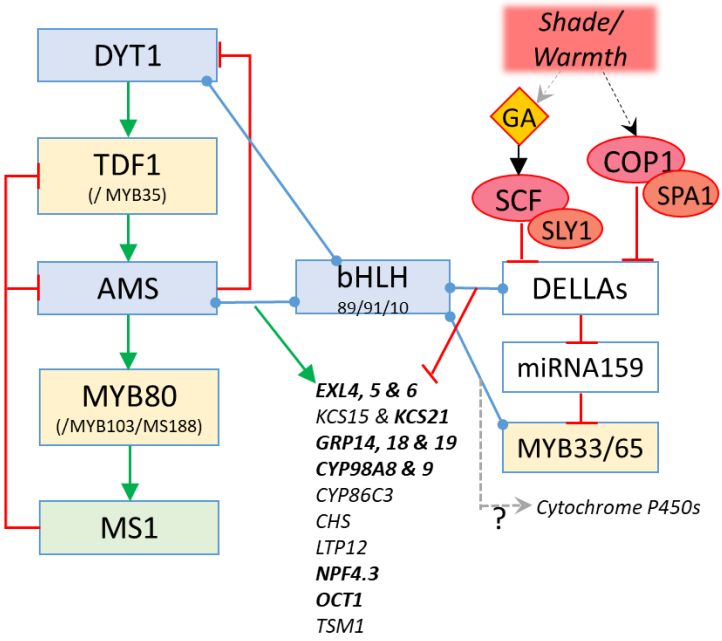

Figure 7.1 Proposed model for integration of environmental signals into reproductive development through bHLH89/91/10 interactions with DELLA and MYB33/65 GAMYB-like proteins. DELLA degradation in response to shade and warmth is modulated through COP1 E3 ubiquitin ligase, and in response to GA increases. Direct AMS-targets show bHLH89/91-dependent upregulation in response to low light and those in bold also show downregulation in response to RGA DELLA suggesting that light signals are integrated through bHLH-DELLA interactions. Green arrows show direct activation whilst red blunt-ended arrows indicate inhibition and blue circle-ended lines show protein-protein interactions.

bHLH89/91/10 are known to interact with AMS and DYT1 to regulate reproductive development (Xu et al., 2010; Feng et al., 2012; Cui et al., 2016). Since DELLAs are also well known to sequester bHLH proteins and inhibit their action (De Lucas et al., 2008), it is possible that DELLA proteins bind bHLHs competitively, inhibiting formation of AMS-bHLH and DYT1-bHLH heterodimeric complexes. AMS-

bHLH heterodimers were shown to have stronger activation capabilities, at least with respect to *MS2* induction (Chapter 6.2.1), thus DELLA inhibition of bHLH-AMS complex formation may reduce transcriptional activation of AMS targets.

Since bioactive GA levels increase in response to shade in vegetative tissues, ordinarily DELLAs will be degraded in low light environments through both GA-dependent SCF/SLY1 and GA-independent COP1/SPA1 pathways (Bou-Torrent et al., 2014), However, in contrast to vegetative tissues, bioactive GA_4 levels drop in response to low light in flowers (Chapter 5.2.1) therefore it is difficult to determine how DELLA might respond to reduced light in floral tissue.

Eighteen direct targets of AMS (Xu et al., 2014) were found to be upregulated in response to low light in Col-0 but not in the *bhlh89,91* mutant (Chapter 4.2.4) suggesting that bHLH89/91 are essential providing regulation of these genes in response to changing light intensities. Eleven of these AMS targets were also downregulated in response to RGA induction in *ga1-3 rga-t2 rgl2-1 35S:RGA-GR* buds (Hou et al., 2008) suggesting that they are repressed by RGA action. Only 2 out of these 11 were upregulated in response to GA (Cao et al., 2006), indicating that DELLA-repression of these genes may be GA-independent. Thus one might assume, from the induction of these targets in low light, that DELLAs are degraded through the GA-independent COP1/SPA ubiquitin E3 ligase pathway (Figure 7.1), releasing bHLHs from inactive DELLA-bHLH complexes to bind AMS and induce activation of targets such as EXL4-6 and GRPs in low light.

If you also consider that there are slight increases in fluorescent activity in bHLH89/91 translational reporter lines under low light (Chapter 3.2.5), compared to decreases in bHLH-FP fluorescence in response to stabilisation of DELLA-activity through PAC treatment (Chapter 5.2.5), this further suggests that DELLA degradation under low light conditions may regulate bHLH protein stability.

Of course, DELLA-bHLH interactions may affect reproductive development through DELLA control of bHLH function, but it could also be the other way around with bHLHs controlling DELLA function too, inhibiting or enhancing their interactions with other proteins. It may be that bHLHs inhibit the ability of DELLAs to regulate expression of *GA20-*, *GA3-* and *GA2-oxidases* (Zentella et al., 2007), and this could account for the changes to GA levels and biosynthesis genes in the *bhlh* double mutants (Chapter 5.2.1 & 5.2.2). *GA20ox*, *GA3ox* and *GA2ox* promoter activation in response to bHLH-DELLA interactions could possibly be explored through the Dual Luciferase assay in future studies.

Interactions between bHLH91/10 and MYB33/65 were also demonstrated through BiFC (Chapter 5.2.3). MYB33 and -65, as GAMYB-like transcription factors, act within GA signalling pathways and their abundance is regulated by GA through miRNA159 (Gocal et al., 2001; Millar and Gubler, 2005).

Since the *myb33 myb65* double mutant, like the *bhlh89,91* and *bhlh89,10* double mutants, exhibits conditional sterility in response to low light and high temperature it seems that a bHLH-MYB interaction may provide further regulation of reproductive development in response to environmental signals. Unfortunately, although there is microarray data available for the *myb33 myb65* double mutant (Alonso-Peral et al., 2010) this was performed on vegetative shoot tissue and will therefore provide no insight into MYB33/65 targets within the flower. It is thus hard to predict what genes may be co-regulated by bHLHs. However, OsGAMYB was found to regulate the majority of GA responsive genes within anther development in rice, with direct activation of the cytochrome P450 hydroxylase *CYP703A3* which is essential in exine development (Aya et al., 2009). It seems that *OsCYP703A3* expression is also directly regulated by the AMS homolog TAPETUM DEGENERATION RETARDATION 1 (TDR1) (Yang et al., 2014). If some functionality is conserved within Arabidopsis, bHLHs in combination with MYB33/65 may regulate pollen exine development through cytochrome P450 hydroxylases (Figure 7.1). However, future transcriptomic studies will be valuable in determining the role of MYB33/65 in Arabidopsis reproductive development.

7.3 PROPOSED MODEL FOR BHLH REGULATION OF REPRODUCTIVE DEVELOPMENT IN LOW LIGHT

It seems that dynamic deSUMOylation mediated potentially by SPF1/2 may be important in regulating bHLH action; this is supported by data indicating that bHLH89, 91 and 10 are SUMO targets, and the *spf1 spf2* SUMO protease mutant showed prolonged sterility in response to low light as seen in the *bhlh89,10* mutant (Chapter 6.2.2).

SPF1/2 proteases are stabilised in reduced light environments and degraded in response to blue light (Sadanandom, pers. comms.), therefore bHLHs are expected to be SUMO-conjugated only under normal light conditions, or non-stress environmental conditions (Figure 7.2). Given that bHLH91 and -10 both have SUMO Interacting Motif (SIM) sites within their HLH and BIF domains, which are essential to dimerization, SUMO-conjugation may affect protein-protein interactions. Thus in normal light, SUMOylated bHLHs may be unable to bind AMS, DYT1 and MYB33/65, or they may be sequestered by unknown proteins. In low light, bHLH89/91/10 are likely to be deSUMOylated through increased SPF1/2 activity, enabling these previously inhibited protein-interactions to occur and enhancing transcription of AMS targets (Figure 7.2).

This proposed SUMO-sequestration model fits in with DELLA-bHLH action if it's assumed that DELLAs accumulate in normal light conditions, sequestering bHLHs or targeting them for degradation (Figure 7.2). SUMOylation could even mediate DELLA interactions, as DELLA proteins are also SUMO-conjugated (Conti et al., 2014), but this would need to be explored further through binding assays with bHLH with mutated SUMO sites.

Through a combination of SUMO and DELLA interactions, it may be that there are fewer free bHLHs in the tapetum under normal conditions and thus other protein-protein interactions are limited. Competitive binding, as suggested by mathematical modelling (Ferguson et al., 2017), could mean that if limited amounts of bHLHs are present they will preferentially associate with DYT1 over AMS. In low light, accumulation of bHLHs as they are released from SUMO/ DELLA complexes will increase binding to AMS and enhance transactivation of targets such as EXL4 (Figure 7.2).

Given the differing severity of conditional sterility of *bhlh89,10* and *bhlh89,91* double mutants it seems that bHLH89, -91 and -10 are not as redundant as previously thought in their ability to maintain fertility in response to environmental stress. This may be due to different transactivation capabilities, AMS-bHLH89 and AMS-bHLH91 heterodimers were demonstrated to increase activation of the MS2 promoter in Dual Luciferase Assays compared to homodimers, whereas AMS-bHLH10 showed very little induction of MS2 (Chapter 6.2.1). Thus if this remains true for other AMS targets, it may be that only accumulation of bHLH89 and bHLH91 will increase transcription of AMS regulated genes in low light conditions.

Different levels of SUMOylation may also play a role in environmental sensitivity. bHLH10 shows the strongest SUMOylation, and therefore may be more strictly regulated by SUMO. It could be that SUMO blocks or enhances bHLH10 protein interactions or even prevents ubiquitination of bHLH10 and subsequent degradation by the 26S proteasome. Thus bHLH10 may accumulate and bind DYT1 in normal conditions, enabling DYT1 nuclear localisation and activation of downstream male reproductive development pathways. Unfortunately bHLH10 translational reporter lines were not constructed so fluorescence intensity changes have not been explored with respect to protein stability in response to low light and DELLA stabilisation. Further study into protein stability of SUMOylatable and non-SUMOylatable bHLHs in different light conditions and *della* mutant backgrounds through pulldowns and Western Blots will be enable us to test some of these new hypotheses.

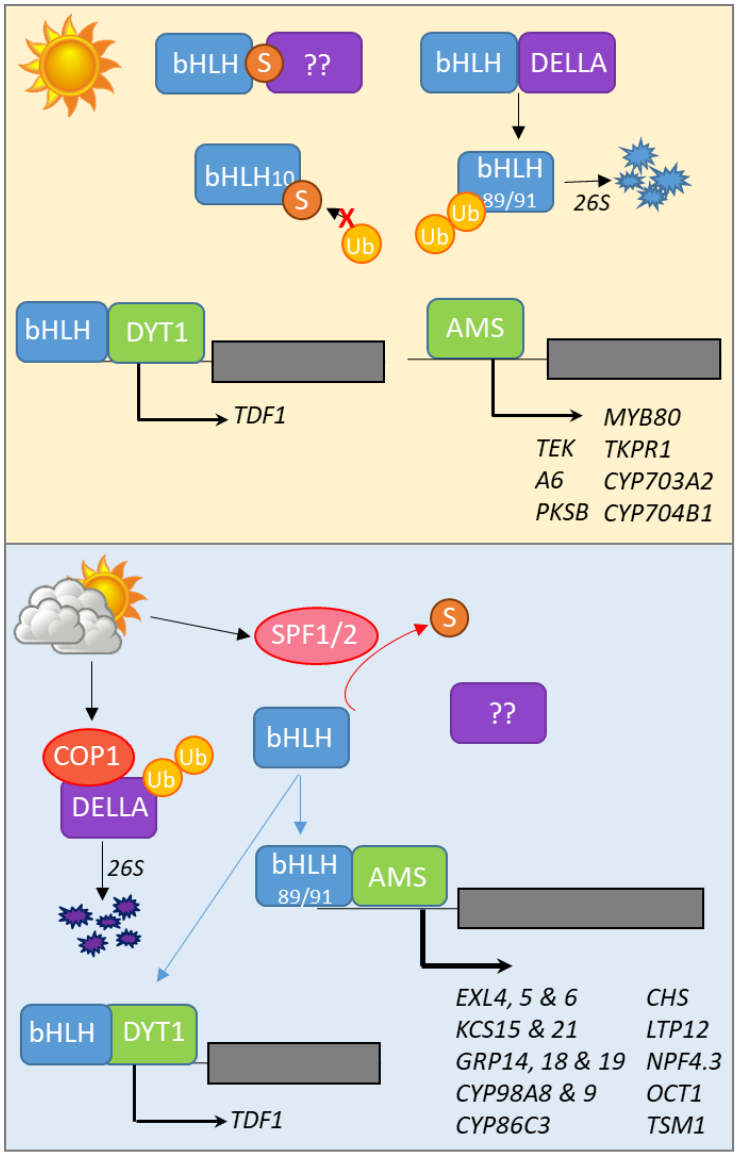

Figure 7.2. Proposed model for bHLH regulation by DELLA and SUMO interactions. Under normal light conditions, interactions with DELLA or SUMO (S) may sequester the bHLHs into inactive complexes. DELLA could also cause the bHLHs to be ubiquitinated (Ub) and targeted for degradation via the 26S proteasome pathway. This ubiquitination and subsequent degradation of bHLH10 may be prevented by strong SUMOylation. Thus low levels of bHLHs may persist and preferentially dimerise with DYT1, maintaining transcription of reproductive pathways, whilst AMS homodimers induce downstream targets that do not depend on bHLH89/91, and minimally induce bHLH-dependent genes. In low light, SUMO is removed by increased SPF1/2 SUMO protease activity and DELLAs are degraded through the COP1-mediated proteasomal degradation pathways. Together this enable accumulation of free bHLHs to interact with AMS and more strongly induce expression of downstream targets.

7.4 Conclusions and Future Perspectives

This thesis has outlined a potential role for bHLH89, -91 and -10 in integrating environmental signals such as light and heat into core reproductive processes, possibly through competitive interactions with DELLA proteins and AMS. Loss of fertility in response to low light in the *bhlh89,10* and *bhlh89,91* double mutants was characterised by defective microspore development and linked to a reduced transcriptional response to low light, perturbing not only genes related to sexual reproduction but also hormonal signal transduction pathways. Whilst the mechanisms behind this

conditionally sterile response are speculative, work in this thesis has attempted to shed some light on the role of bHLHs in tapetum development and provide insight into male reproductive development in an environmental context.

A number of studies can now be undertaken to answer some of the questions that have arisen within this thesis. Firstly, study of the *bhlh* mutant phenotypes at higher light intensities and different spectral qualities would demonstrate whether fertility recovery is linked to light intensity and whether fertility responses are dependent on specific wavelengths. Secondly, bHLH protein stability under different light conditions, in *della* mutant backgrounds, and using mutated non-SUMOylatable versions of bHLHs, should be assessed through methods such as Western Blots to gain an understanding of the role of DELLA and SUMO regulation of bHLHs. Additionally, identification of direct bHLH targets should be undertaken by Chromatin Immunoprecipitation and verified by an Electrophoretic Mobility Shift Assay (EMSA), with further identification of core binding sites through mutagenesis. EMSA, and other competitive binding assays, could then be used to assess preferential binding between tapetal bHLHs, DELLAs and MYBs; with the effect of these interactions on target activation explored through GFP-pulldown and Dual Luciferase assays. Finally, a full analysis of hormone levels and localisation in the anthers of WT and *bhlh* mutant lines under different light conditions, using mass spectrometry, reporter lines and biosensors, would further our understanding of the role of tapetal bHLHs in hormonal signalling and biosynthesis.

REFERENCES

Aarts, M.G.M., Dirkse, W.G., Stiekema, W.J., and Pereira, A. (1993). Transposon tagging of a male sterility gene in Arabidopsis. Nature **363**: 715–717.

Aarts, M.G.M., Hodge, R., Kalantidis, K., Florack, D., Wilson, Z.A., Mulligan, B.J., Stiekema, W.J., Scott, R., and Pereira, A. (1997). The Arabidopsis MALE STERILITY 2 protein shares similarity with reductases in elongation/condensation complexes. Plant J. **12**: 615–623.

Achard, P., Herr, A., Baulcombe, D.C., and Harberd, N.P. (2004). Modulation of floral development by a gibberellin-regulatedmicroRNA. Development **131**: 3357–3365.

Achard, P., Liao, L., Jiang, C., Desnos, T., Bartlett, J., Fu, X., and Harberd, N.P. (2007). DELLAs contribute to plant photomorphogenesis. Plant Physiol. **143**: 1163–1172.

Alabadí, D., Gallego-Bartolomé, J., Orlando, L., García-Cárcel, L., Rubio, V., Martínez, C., Frigerio, M., Iglesias-Pedraz, J.M., Espinosa, A., Deng, X.W., and Blázquez, M.A. (2008). Gibberellins modulate light signaling pathways to prevent Arabidopsis seedling de-etiolation in darkness. Plant J. **53**: 324–335.

Albrecht, C., Russinova, E., Hecht, V., Baaijens, E., and De Vries, S. (2005). The Arabidopsis thaliana SOMATIC EMBRYOGENESIS RECEPTOR-LIKE KINASES1 and 2 control male sporogenesis. Plant Cell **17**: 3337–3349.

Alexander, M.P. (1969). Differential staining of aborted and nonaborted pollen. Biotech. Histochem. **44**: 117–122.

Aloni, R., Aloni, E., Langhans, M., and Ullrich, C.I. (2006). Role of auxin in regulating Arabidopsis flower development. Planta **223**: 315–328.

Alonso-Peral, M.M., Li, J., Li, Y., Allen, R.S., Schnippenkoetter, W., Ohms, S., White, R.G., and Millar, A.A. (2010). The MicroRNA159-Regulated GAMYB-like genes inhibit growth and promote programmed Cell Death in Arabidopsis. Plant Physiol. **154**: 757–771.

Alwen, A., Moreno, R.M.B., Vicente, O., and Heberle-Bors, E. (1992). Plant endogenous β-glucuronidase activity: how to avoid interference with the use of the E. coli β-glucuronidase as a reporter gene in transgenic plants. Transgenic Res. **1**: 63–70.

Andrés-Colás, N., Perea-García, A., Puig, S., and Peñarrubia, L. (2010). Deregulated copper transport affects Arabidopsis development especially in the absence of environmental cycles. Plant Physiol. **153**: 170–184.

Ariizumi, T., Amagai, M., Shibata, D., Hatakeyama, K., Watanabe, M., and Toriyama, K. (2002). Comparative study of promoter activity of three anther-specific genes encoding lipid transfer protein, xyloglucan endotransglucosylase/hydrolase and polygalacturonase in transgenic Arabidopsis thaliana. Plant Cell Rep. **21**: 90–96.

Atchley, W.R., Terhalle, W., and Dress, A. (1999). Positional dependence, cliques, and predictive motifs in the bHLH protein domain. J. Mol. Evol. **48**: 501–516.

Aya, K., Tanaka, M.U., Kondo, M., Hamada, K., Yano, K., Nishimura, M., and Matsuoka, M. (2009). Gibberellin modulates anther development in rice via the transcriptional regulation of GAMYB. Plant Cell **21**: 1453–1472.

Babst, B.A., Gao, F., Acosta-Gamboa, L.M., Karve, A., Schueller, M.J., and Lorence, A. (2019). Three NPF genes in Arabidopsis are necessary for normal nitrogen cycling under low nitrogen stress. Plant Physiol. Biochem. **143**: 1–10.

Begcy, K., Nosenko, T., Zhou, L.Z., Fragner, L., Weckwerth, W., and Dresselhaus, T. (2019). Male Sterility in Maize after Transient Heat Stress during the Tetrad Stage of Pollen Development. Plant Physiol. **181**: 683–700.

Benjamini, Y. and Yekutieli, D. (2001). The control of the false discovery rate in multiple testing under dependency. Ann. Stat. **29**: 1165–1188.

Binenbaum, J., Weinstain, R., and Shani, E. (2018). Gibberellin Localization and Transport in Plants. Trends Plant Sci. **23**: 410–421.

Blanco-Touriñán, N. et al. (2020). COP1 destabilizes DELLA proteins in Arabidopsis. Proc. Natl. Acad. Sci. **117**: 13792–13799.

Borg, M., Brownfield, L., and Twell, D. (2009). Male gametophyte development: A molecular perspective. J. Exp. Bot. **60**: 1465–1478.

Bou-Torrent, J., Galstyan, A., Gallemí, M., Cifuentes-Esquivel, N., Molina-Contreras, M.J., Salla-Martret, M., Jikumaru, Y., Yamaguchi, S., Kamiya, Y., and Martínez-García, J.F. (2014). Plant proximity perception dynamically modulates hormone levels and sensitivity in Arabidopsis. J. Exp. Bot. **65**: 2937–2947.

Brewbaker, J.L. (1964). Agricultural Genetics (Prentice-Hall, Inc.).

Brownlie, P., Ceska, T.., Lamers, M., Romier, C., Stier, G., and Teo, H. (1997). The crystal structure of an intact human Max-DNA complex: New insights into mechanisms of transcriptional control. Structure **5**: 509–520.

Bullard, J.H., Purdom, E., Hansen, K.D., and Dudoit, S. (2010). Evaluation of statistical methods for normalization and differential expression in mRNA-Seq experiments. BMC Bioinformatics **11**.

Buti, S., Hayes, S., and Pierik, R. (2020). The bHLH network underlying plant shade-avoidance. Physiol. Plant.: 1–13.

Cai, C.F., Zhu, J., Lou, Y., Guo, Z.L., Xiong, S.X., Wang, K., and Yang, Z.N. (2015). The functional analysis of OsTDF1 reveals a conserved genetic pathway for tapetal development between rice and Arabidopsis. Sci. Bull. **60**: 1073–1082.

Calixto, C.P.G., Guo, W., James, A.B., Tzioutziou, N.A., Entizne, J.C., Panter, P.E., Knight, H., Nimmo, H.G., Zhang, R., and Brown, J.W.S. (2018). Rapid and dynamic alternative splicing impacts the arabidopsis cold response transcriptome[CC-BY]. Plant Cell **30**: 1424–1444.

Callis, J. and Vierstra, R.D. (2000). Protein degradation in signaling. Curr. Opin. Plant Biol. **3**: 381–386.

Campanaro, A., Battaglia, R., Galbiati, M., Sadanandom, A., Tonelli, C., and Conti, L. (2016). SUMO proteases OTS1 and 2 control filament elongation through a DELLA-dependent mechanism. Plant Reprod. **29**: 287–290.

Canales, C., Bhatt, A.M., Scott, R., and Dickinson, H. (2002). EXS, a putative LRR receptor kinase, regulates male germline cell number and tapetal identity and promotes seed development in Arabidopsis. Curr. Biol. **12**: 1718–1727.

Cao, D., Cheng, H., Wu, W., Soo, H.M., and Peng, J. (2006). Gibberellin Mobilizes Distinct DELLA-Dependent Transcriptomes to Regulate Seed Germination and Floral Development in Arabidopsis. Plant Physiol. **142**: 509–525.

Carretero-Paulet, L., Galstyan, A., Roig-Villanova, I., Martinez-Garcia, J.F., Bilbao-Castro, J.R., and Robertson, D.L. (2010). Genome-Wide Classification and Evolutionary Analysis of the bHLH

Family of Transcription Factors in Arabidopsis, Poplar, Rice, Moss, and Algae. Plant Physiol. **153**: 1398–1412.

Castelain, M., Le Hir, R., and Bellini, C. (2012). The non-DNA-binding bHLH transcription factor PRE3/bHLH135/ATBS1/TMO7 is involved in the regulation of light signaling pathway in Arabidopsis. Physiol. Plant. **145**: 450–460.

Castro, P.H., Couto, D., Freitas, S., Verde, N., Macho, A.P., Huguet, S., Botella, M.A., Ruiz-Albert, J., Tavares, R.M., Bejarano, E.R., and Azevedo, H. (2016). SUMO proteases ULP1c and ULP1d are required for development and osmotic stress responses in Arabidopsis thaliana. Plant Mol. Biol. **92**: 143–159.

Cecchetti, V., Altamura, M.M., Falasca, G., Costantino, P., and Cardarelli, M. (2008). Auxin regulates Arabidopsis anther dehiscence, pollen maturation, and filament elongation. Plant Cell **20**: 1760–1774.

Cecchetti, V., Celebrin, D., Napoli, N., Ghelli, R., Brunetti, P., Costantino, P., and Cardarelli, M. (2017). An auxin maximum in the middle layer controls stamen development and pollen maturation in Arabidopsis. New Phytol. **213**: 1194–1207.

Chandler, P.M., Marion-Poll, A., Ellis, M., and Gubler, F. (2002). Mutants at the Slender1 locus of barley cv himalaya. Molecular and physiological characterization. Plant Physiol. **129**: 181–190.

Chen, L. and Liu, Y.-G. (2014). Male Sterility and Fertility Restoration in Crops. Annu. Rev. Plant Biol. **65**: 579–606.

Chen, M., Chen, J., Fang, J., Guo, Z., and Lu, S. (2014). Down-regulation of S-adenosylmethionine decarboxylase genes results in reduced plant length, pollen viability, and abiotic stress tolerance. Plant Cell. Tissue Organ Cult. **116**: 311–322.

Chen, W., Lv, M., Wang, Y., Wang, P.A., Cui, Y., Li, M., Wang, R., Gou, X., and Li, J. (2019). BES1 is activated by EMS1-TPD1-SERK1/2-mediated signaling to control tapetum development in Arabidopsis thaliana. Nat. Commun. **10**.

Chen, W., Yu, X.-H., Zhang, K., Shi, J., De Oliveira, S., Schreiber, L., Shanklin, J., and Zhang, D. (2011a). Male Sterile2 Encodes a Plastid-Localized Fatty Acyl Carrier Protein Reductase Required for Pollen Exine Development in Arabidopsis. Plant Physiol. **157**: 842–853.

Chen, Y.C.S. and McCormick, S. (1996). sidecar pollen, an Arabidopsis thaliana male gametophytic mutant with aberrant cell divisions during pollen development. Development **122**: 3243–3253.

Chen, Z., Higgins, J.D., Hui, J.T.L., Li, J., Franklin, F.C.H., and Berger, F. (2011b). Retinoblastoma protein is essential for early meiotic events in Arabidopsis. EMBO J. **30**: 744–755.

Cheng, H., Qin, L., Lee, S., Fu, X., Richards, D.E., Cao, D., Luo, D., Harberd, N.P., and Peng, J. (2004). Gibberellin regulates Arabidopsis floral development via suppression of DELLA protein function. Development **131**: 1055–1064.

Cheng, Q., Wang, P., Liu, J., Wu, L., Zhang, Z., Li, T., Gao, W., and Yang, W. (2018). Identification of candidate genes underlying genic male - sterile msc - 1 locus via genome resequencing in Capsicum annuum L . Theor. Appl. Genet. **131**: 1861–1872.

Cheng, Y., Dai, X., and Zhao, Y. (2006). Auxin biosynthesis by the YUCCA flavin monooxygenases controls the formation of floral organs and vascular tissues in Arabidopsis. Genes Dev. **20**: 1790–1799.

Cheng, Y., Zhou, W., El Sheery, N.I., Peters, C., Li, M., Wang, X., and Huang, J. (2011). Characterization of the Arabidopsis glycerophosphodiester phosphodiesterase (GDPD) family

reveals a role of the plastid-localized AtGDPD1 in maintaining cellular phosphate homeostasis under phosphate starvation. Plant J. **66**: 781–795.

Chiba, Y., Shimizu, T., Miyakawa, S., Kanno, Y., Koshiba, T., Kamiya, Y., and Seo, M. (2015). Identification of Arabidopsis thaliana NRT1/PTR FAMILY (NPF) proteins capable of transporting plant hormones. J. Plant Res. **128**: 679–686.

Chico, J.M., Fernández-Barbero, G., Chini, A., Fernández-Calvo, P., Díez-Díaz, M., and Solano, R. (2014). Repression of jasmonate-dependent defenses by shade involves differential regulation of protein stability of MYC transcription factors and their JAZ repressors in Arabidopsis. Plant Cell **26**: 1967–1980.

Choi, H., Ohyama, K., Kim, Y.Y., Jin, J.Y., Lee, S.B., Yamaoka, Y., Muranaka, T., Suh, M.C., Fujioka, S., and Lee, Y. (2014). The role of Arabidopsis ABCG9 and ABCG31 ATP binding cassette transporters in pollen fitness and the deposition of steryl glycosides on the pollen coat. Plant Cell **26**: 310–324.

Clough, S.J. and Bent, A.F. (1998). Floral dip: A simplified method for Agrobacterium-mediated transformation of *Arabidopsis thaliana*. Plant J. **16**: 735–743.

Colcombet, J., Boisson-Dernier, A., Ros-Palau, R., Vera, C.E., and Schroeder, J.I. (2005). Arabidopsis SOMATIC EMBRYOGENESIS RECEPTOR KINASES1 and 2 are essential for tapetum development and microspore maturation. Plant Cell **17**: 3350–3361.

Conti, L., Nelis, S., Zhang, C., Woodcock, A., Swarup, R., Galbiati, M., Tonelli, C., Napier, R., Hedden, P., Bennett, M., and Sadanandom, A. (2014). Small Ubiquitin-like Modifier Protein SUMO Enables Plants to Control Growth Independently of the Phytohormone Gibberellin. Dev. Cell **28**: 102–110.

Conti, L., Price, G., O'Donnell, E., Schwessinger, B., Dominy, P., and Sadanandom, A. (2008). Small ubiquitin-like modifier proteases OVERLY TOLERANT TO SALT1 and -2 regulate salt stress responses in Arabidopsis. Plant Cell **20**: 2894–908.

Cui, J., You, C., Zhu, E., Huang, Q., Ma, H., and Chang, F. (2016). Feedback Regulation of DYT1 by Interactions with Downstream bHLH Factors Promotes DYT1 Nuclear Localization and Anther Development. Plant Cell **28**: 1078–1093.

Davière, J.M. and Achard, P. (2016). A Pivotal Role of DELLAs in Regulating Multiple Hormone Signals. Mol. Plant **9**: 10–20.

Dill, A. and Sun, T.P. (2001). Synergistic derepression of gibberellin signaling by removing RGA and GAI function in Arabidopsis thaliana. Genetics **159**: 777–785.

Dobritsa, A.A., Shrestha, J., Morant, M., Pinot, F., Matsuno, M., Swanson, R., Møller, B.L., and Preuss, D. (2009). CYP704B1 is a long-chain fatty acid ω-Hydroxylase essential for sporopollenin synthesis in pollen of Arabidopsis. Plant Physiol. **151**: 574–589.

Dong, X., Jiang, Y., and Hur, Y. (2019). Genome-wide analysis of glycoside hydrolase family 1 β-glucosidase genes in Brassica rapa and their potential role in Pollen development. Int. J. Mol. Sci. **20**: 1–17.

Dong, X., Yi, H., Han, C.T., Nou, I.S., and Hur, Y. (2016). GDSL esterase/lipase genes in Brassica rapa L.: Genome-wide identification and expression analysis. Mol. Genet. Genomics **291**: 531–542.

Dou, X.Y., Yang, K.Z., Zhang, Y., Wang, W., Liu, X.L., Chen, L.Q., Zhang, X.Q., and Ye, D. (2011). WBC27, an adenosine tri-phosphate-binding cassette protein, controls pollen wall formation and patterning in arabidopsis. J. Integr. Plant Biol. **53**: 74–88.

Edstam, M.M. and Edqvist, J. (2014). Involvement of GPI-anchored lipid transfer proteins in the development of seed coats and pollen in Arabidopsis thaliana. Physiol. Plant. **152**: 32–42.

Eriksson, S., Böhlenius, H., Moritz, T., and Nilsson, O. (2006). GA4 is the active gibberellin in the regulation of LEAFY transcription and Arabidopsis floral initiation. Plant Cell **18**: 2172–2181.

Eudes, A., Mouille, G., Thévenin, J., Goyallon, A., Minic, Z., and Jouanin, L. (2008). Purification, cloning and functional characterization of an endogenous beta-glucuronidase in Arabidopsis thaliana. Plant Cell Physiol. **49**: 1331–1341.

Fellenberg, C., Böttcher, C., and Vogt, T. (2009). Phenylpropanoid polyamine conjugate biosynthesis in Arabidopsis thaliana flower buds. Phytochemistry **70**: 1392–1400.

Fellenberg, C., Milkowski, C., Hause, B., Lange, P.R., Böttcher, C., Schmidt, J., and Vogt, T. (2008). Tapetum-specific location of a cation-dependent O-methyltransferase in Arabidopsis thaliana. Plant J. **56**: 132–145.

Feller, A., Hernandez, J.M., and Grotewold, E. (2006). An ACT-like domain participates in the dimerization of several plant basic-helix-loop-helix transcription factors. J. Biol. Chem. **281**: 28964–28974.

Feng, B., Lu, D., Ma, X., Peng, Y., Sun, Y., Ning, G., and Ma, H. (2012). Regulation of the Arabidopsis anther transcriptome by DYT1 for pollen development. Plant J. **72**: 612–624.

Ferguson, A.C., Pearce, S., Band, L.R., Yang, C., Ferjentsikova, I., King, J., Yuan, Z., Zhang, D., and Wilson, Z.A. (2017). Biphasic regulation of the transcription factor ABORTED MICROSPORES (AMS) is essential for tapetum and pollen development in Arabidopsis. New Phytol. **213**: 778–790.

Ferguson, J.N., Tidy, A.C., Murchie, E.H., and Wilson, Z.A. (2021). The Potential of Resilient Carbon Dynamics for Stabilising Crop Reproductive Development and Productivity During Heat Stress. Plant. Cell Environ.: 1–24.

Ferré-D'Amaré, A.R., Pognonec, P., Roeder, R.G., and Burley, S.K. (1994). Structure and function of the b/HLH/Z domain of USF. EMBO J. **13**: 180–9.

Fleet, C.M. and Sun, T.P. (2005). A DELLAcate balance: The role of gibberellin in plant morphogenesis. Curr. Opin. Plant Biol. **8**: 77–85.

Floris, M., Bassi, R., Robaglia, C., Alboresi, A., and Lanet, E. (2013). Post-transcriptional control of light-harvesting genes expression under light stress. Plant Mol. Biol. **82**: 147–154.

Franklin, K.A. (2008). Shade avoidance. New Phytol. **179**: 930–944.

Fu, Y., Li, M., Zhang, S., Yang, Q., Zhu, E., You, C., Qi, J., Ma, H., and Chang, F. (2020). Analyses of functional conservation and divergence reveal requirement of bHLH010/089/091 for pollen development at elevated temperature in Arabidopsis. J. Genet. Genomics.

Fu, Z., Yu, J., Cheng, X., Zong, X., Xu, J., Chen, M., Li, Z., Zhang, D., and Liang, W. (2014). The Rice Basic Helix-Loop-Helix Transcription Factor TDR INTERACTING PROTEIN2 Is a Central Switch in Early Anther Development. Plant Cell **26**: 1512–1524.

Gawronska, H., Yang, Y.Y., Furukawa, K., Kendrick, R.E., Takahashi, N., and Kamiya, Y. (1995). Effects of low irradiance stress on gibberellin levels in pea seedlings. Plant Cell Physiol. **36**: 1361–1367.

Di Giorgio, J.A.P., Bienert, G.P., Ayub, N.D., Yaneff, A., Barberini, M.L., Mecchia, M.A., Amodeo, G., Soto, G.C., and Muschietti, J.P. (2016). Pollen-specific aquaporins NIP4;1 and NIP4;2 are

required for pollen development and pollination in arabidopsis Thaliana. Plant Cell **28**: 1053–1077.

Gocal, G.F.W., Sheldon, C.C., Gubler, F., Moritz, T., Bagnall, D.J., Macmillan, C.P., Li, S.F., Parish, R.W., Dennis, E.S., Weigel, D., and King, R.W. (2001). GAMYB-like Genes , Flowering , and Gibberellin Signaling in Arabidopsis 1. Plant Physiol. **127**: 1682–1693.

Gómez, M.D., Fuster-Almunia, C., Ocaña-Cuesta, J., Alonso, J.M., and Pérez-Amador, M.A. (2019). RGL2 controls flower development, ovule number and fertility in Arabidopsis. Plant Sci. **281**: 82–92.

Goossens, J., Mertens, J., and Goossens, A. (2017). Role and functioning of bHLH transcription factors in jasmonate signalling. J. Exp. Bot. **68**: 1333–1347.

Gordân, R., Shen, N., Dror, I., Zhou, T., Horton, J., Rohs, R., and Bulyk, M.L. (2013). Genomic Regions Flanking E-Box Binding Sites Influence DNA Binding Specificity of bHLH Transcription Factors through DNA Shape. Cell Rep. **3**: 1093–1104.

Grienenberger, E., Besseau, S., Geoffroy, P., Debayle, D., Heintz, D., Lapierre, C., Pollet, B., Heitz, T., and Legrand, M. (2009). A BAHD acyltransferase is expressed in the tapetum of Arabidopsis anthers and is involved in the synthesis of hydroxycinnamoyl spermidines. Plant J. **58**: 246–259.

Grienenberger, E., Kim, S.S., Lallemand, B., Geoffroy, P., Heintz, D., Souza, C. de A., Heitz, T., Douglas, C.J., and Legrand, M. (2010). Analysis of TETRAKETIDE α-PYRONE REDUCTASE Function in Arabidopsis thaliana Reveals a Previously Unknown, but Conserved, Biochemical Pathway in Sporopollenin Monomer Biosynthesis. Plant Cell **22**: 4067–4083.

Griffiths, J., Murase, K., Rieu, I., Zentella, R., Zhang, Z.L., Powers, S.J., Gong, F., Phillips, A.L., Hedden, P., Sun, T.P., and Thomas, S.G. (2006). Genetic characterization and functional analysis of the GID1 gibberellin receptors in Arabidopsis. Plant Cell **18**: 3399–3414.

Grunewald, S., Marillonnet, S., Hause, G., Haferkamp, I., Neuhaus, H.E., Veß, A., Hollemann, T., and Vogt, T. (2020). The Tapetal Major Facilitator NPF2.8 is Required for Accumulation of Flavonol Glycosides on the Pollen Surface in Arabidopsis thaliana. Plant Cell **32**: tpc.00801.2019.

Gu, J.N., Zhu, J., Yu, Y., Teng, X.D., Lou, Y., Xu, X.F., Liu, J.L., and Yang, Z.N. (2014). DYT1 directly regulates the expression of TDF1 for tapetum development and pollen wall formation in Arabidopsis. Plant J. **80**: 1005–1013.

Gu, Z., Eils, R., and Schlesner, M. (2016). Complex heatmaps reveal patterns and correlations in multidimensional genomic data. Bioinformatics **32**: 2847–2849.

Guan, Y.F., Huang, X.Y., Zhu, J., Gao, J.F., Zhang, H.X., and Yang, Z.N. (2008). Ruptured pollen grain1, a member of the MtN3/ saliva gene family, is crucial for exine pattern formation and cell integrity of microspores in Arabidopsis. Plant Physiol. **147**: 852–863.

Guo, J., Liu, C., Wang, P., Cheng, Q., Sun, L., Yang, W., and Shen, H. (2018). The aborted microspores (AMS)-like gene is required for anther and microspore development in pepper (Capsicum annuum L.). Int. J. Mol. Sci. **19**.

Guo, W., Tzioutziou, N., Stephen, G., Milne, I., Calixto, C., Waugh, R., Brown, J.W., and Zhang, R. (2019). 3D RNA-seq - a powerful and flexible tool for rapid and accurate differential expression and alternative splicing analysis of RNA-seq data for biologists. bioRxiv: 656686.

Haberer, G. (2004). Transcriptional Similarities, Dissimilarities, and Conservation of cis-Elements in Duplicated Genes of Arabidopsis. Plant Physiol. **136**: 3009–3022.

Han, Y., Zhou, S. Da, Fan, J.J., Zhou, L., Shi, Q.S., Zhang, Y.F., Liu, X.L., Chen, X., Zhu, J., and Yang, Z.N. (2021). OsMS188 Is a Key Regulator of Tapetum Development and Sporopollenin Synthesis in Rice. Rice **14**.

Hao, Q., Yin, P., Li, W., Wang, L., Yan, C., Lin, Z., Wu, J.Z., Wang, J., Yan, S.F., and Yan, N. (2011). The Molecular Basis of ABA-Independent Inhibition of PP2Cs by a Subclass of PYL Proteins. Mol. Cell **42**: 662–672.

He, J., Chen, Q., Xin, P., Yuan, J., Ma, Y., Wang, X., Xu, M., Chu, J., Peters, R.J., and Wang, G. (2019). CYP72A enzymes catalyse 13-hydrolyzation of gibberellins. Nat. Plants **5**: 1057–1065.

Heang, D. and Sassa, H. (2012). Antagonistic actions of HLH/bHLH proteins are involved in grain length and weight in rice. PLoS One **7**.

Heim, M.A., Jakoby, M., Werber, M., Martin, C., Weisshaar, B., and Bailey, P.C. (2003). The basic helix-loop-helix transcription factor family in plants: A genome-wide study of protein structure and functional diversity. Mol. Biol. Evol. **20**: 735–747.

Heisler, M.G., Ohno, C., Das, P., Sieber, P., Reddy, G. V., Long, J.A., and Meyerowitz, E.M. (2005). Patterns of auxin transport and gene expression during primordium development revealed by live imaging of the Arabidopsis inflorescence meristem. Curr. Biol. **15**: 1899–1911.

Hellens, R.P., Allan, A.C., Friel, E.N., Bolitho, K., Grafton, K., Templeton, M.D., Karunairetnam, S., Gleave, A.P., and Laing, W.A. (2005). Transient expression vectors for functional genomics, quantification of promoter activity and RNA silencing in plants. Plant Methods **1**: 1–14.

Hermkes, R., Fu, Y.F., Nürrenberg, K., Budhiraja, R., Schmelzer, E., Elrouby, N., Dohmen, R.J., Bachmair, A., and Coupland, G. (2011). Distinct roles for Arabidopsis SUMO protease ESD4 and its closest homolog ELS1. Planta **233**: 63–73.

Higginson, T., Li, S.F., and Parish, R.W. (2003). AtMYB103 regulates tapetum and trichome development in Arabidopsis thaliana. Plant J. **35**: 177–192.

Hisamatsu, T., King, R.W., Helliwell, C.A., and Koshioka, M. (2005). The Involvement of Gibberellin 20-Oxidase Genes in Phytochrome-Regulated Petiole Elongation of Arabidopsis. Plant Physiol. **138**: 1106–1116.

Hong, S.Y., Seo, P.J., Ryu, J.Y., Cho, S.H., Woo, J.C., and Park, C.M. (2013). A competitive peptide inhibitor KIDARI negatively regulates HFR1 by forming nonfunctional heterodimers in Arabidopsis photomorphogenesis. Mol. Cells **35**: 25–31.

Honys, D., Oh, S.A., Reňák, D., Donders, M., Šolcová, B., Johnson, J.A., Boudová, R., and Twell, D. (2006). Identification of microspore-active promoters that allow targeted manipulation of gene expression at early stages of microgametogenesis in Arabidopsis. BMC Plant Biol. **6**: 1–9.

Hord, C.L.H., Chen, C., DeYoung, B.J., Clark, S.E., and Ma, H. (2006). The BAM1/BAM2 receptor-like kinases are important regulators of Arabidopsis early anther development. Plant Cell **18**: 1667–1680.

Hornitschek, P., Kohnen, M. V., Lorrain, S., Rougemont, J., Ljung, K., López-Vidriero, I., Franco-Zorrilla, J.M., Solano, R., Trevisan, M., Pradervand, S., Xenarios, I., and Fankhauser, C. (2012). Phytochrome interacting factors 4 and 5 control seedling growth in changing light conditions by directly controlling auxin signaling. Plant J. **71**: 699–711.

Hou, X., Hu, W.-W., Shen, L., Lee, L.Y.C., Tao, Z., Han, J.-H., and Yu, H. (2008). Global Identification of DELLA Target Genes during Arabidopsis Flower Development. Plant Physiol. **147**: 1126–1142.

Hu, J. et al. (2008). Potential Sites of Bioactive Gibberellin Production during Reproductive Growth in

Arabidopsis. Plant Cell Online **20**: 320–336.

Hu, Y., Zhou, L., Huang, M., He, X., Yang, Y., Liu, X., Li, Y., and Hou, X. (2018). Gibberellins play an essential role in late embryogenesis of Arabidopsis. Nat. Plants **4**: 289–298.

Huang, D.W., Sherman, B.T., and Lempicki, R.A. (2009a). Bioinformatics enrichment tools: Paths toward the comprehensive functional analysis of large gene lists. Nucleic Acids Res. **37**: 1–13.

Huang, D.W., Sherman, B.T., and Lempicki, R.A. (2009b). Systematic and integrative analysis of large gene lists using DAVID bioinformatics resources. Nat. Protoc. **4**: 44–57.

Huang, W.Y., Wu, Y.C., Pu, H.Y., Wang, Y., Jang, G.J., and Wu, S.H. (2017). Plant dual-specificity tyrosine phosphorylation-regulated kinase optimizes light-regulated growth and development in Arabidopsis. Plant Cell Environ. **40**: 1735–1747.

Huq, E., Al-Sady, B., Hudson, M., Kim, C., Apel, K., and Quail, P.H. (2004). Phytochrome-interacting factor 1 is a critical bHLH: Regulator of chlorophyll biosynthesis. Science (80-.). **305**: 1937–1941.

Huq, E. and Quail, P.H. (2002). PIF4, a phytochrome-interacting bHLH factor, functions as a negative regulator of phytochrome B signaling in Arabidopsis. EMBO J. **21**: 2441–2450.

Hwang, J.E., Hong, J.K., Lim, C.J., Chen, H., Je, J., Yang, K.A., Kim, D.Y., Choi, Y.J., Lee, S.Y., and Lim, C.O. (2010). Distinct expression patterns of two Arabidopsis phytocystatin genes, AtCYS1 and AtCYS2, during development and abiotic stresses. Plant Cell Rep. **29**: 905–915.

Ikeda, A., Ueguchi-Tanaka, M., Sonoda, Y., Kitano, H., Koshioka, M., Futsuhara, Y., Matsuoka, M., and Yamaguchi, J. (2001). Slender rice, a constitutive gibberellin response mutant, is caused by a null mutation of the SLR1 gene, an ortholog of the height-regulating gene GAI/RGA/RHT/D8. Plant Cell **13**: 999–1010.

Ito, T.W.F., Yu, H., Das, P., Ito, N., Alves-Ferreira, M., Riechmann, J.L., and Meyerowitz, E.M. (2004). The homeotic protein AGAMOUS controls microsporogenesis by regulation of SPOROCYTELES. Nature **430**: 356–360.

Izhaki, A., Borochov, A., Zamski, E., and Weiss, D. (2002). Gibberellin regulates post-microsporogenesis processes in petunia anthers. Physiol. Plant. **115**: 442–447.

Jeong, H.J., Kang, J.H., Zhao, M., Kwon, J.K., Choi, H.S., Bae, J.H., Lee, H.A., Joung, Y.H., Choi, D., and Kang, B.C. (2014). Tomato Male sterile 1035 is essential for pollen development and meiosis in anthers. J. Exp. Bot. **65**: 6693–6709.

Jia, G., Liu, X., Owen, H.A., and Zhao, D. (2008). Signaling of cell fate determination by the TPD1 small protein and EMS1 receptor kinase. Proc. Natl. Acad. Sci. U. S. A. **105**: 2220–5.

Jiang, Y., Lahlali, R., Karunakaran, C., Kumar, S., Davis, A.R., and Bueckert, R.A. (2015). Seed set, pollen morphology and pollen surface composition response to heat stress in field pea. Plant Cell Environ. **38**: 2387–2397.

Jung, K.-H., Han, M.-J., Lee, Y.-S., Kim, Y.-W., Hwang, I., Kim, M.-J., Kim, Y.-K., Nahm, B.H., and An, G. (2005). Rice Undeveloped Tapetum1 Is a Major Regulator of Early Tapetum Development. Plant Cell **17**: 2705–2722.

Kamiya, Y. and García-Martínez, J.L. (1999). Regulation of gibberellin biosynthesis by light. Curr. Opin. Plant Biol. **2**: 398–403.

Kanno, Y., Jikumaru, Y., Hanada, A., Nambara, E., Abrams, S.R., Kamiya, Y., and Seo, M. (2010). Comprehensive hormone profiling in developing arabidopsis seeds: Examination of the site of

ABA biosynthesis, ABA transport and hormone interactions. Plant Cell Physiol. **51**: 1988–2001.

Kanno, Y., Oikawa, T., Chiba, Y., Ishimaru, Y., Shimizu, T., Sano, N., Koshiba, T., Kamiya, Y., Ueda, M., and Seo, M. (2016). AtSWEET13 and AtSWEET14 regulate gibberellin-mediated physiological processes. Nat. Commun. **7**: 1–11.

Kaul, M.L.. (1988). Male sterility in higher plants. In Monographs on Theoretical and Applied Genetics 10.

Kim, D.H., Yamaguchi, S., Lim, S., Oh, E., Park, J., Hanada, A., Kamiya, Y., and Choi, G. (2008). SOMNUS, a CCCH-type zinc finger protein in Arabidopsis, negatively regulates light-dependent seed germination downstream of PIL5. Plant Cell **20**: 1260–1277.

Kim, M.J., Kim, M., Lee, M.R., Park, S.K., and Kim, J. (2015). LATERAL ORGAN BOUNDARIES DOMAIN (LBD)10 interacts with SIDECAR POLLEN/LBD27 to control pollen development in Arabidopsis. Plant J. **81**: 794–809.

Kim, T.W., Guan, S., Burlingame, A.L., and Wang, Z.Y. (2011). The CDG1 Kinase Mediates Brassinosteroid Signal Transduction from BRI1 Receptor Kinase to BSU1 Phosphatase and GSK3-like Kinase BIN2. Mol. Cell **43**: 561–571.

Kim, Y.J. and Zhang, D. (2018). Molecular Control of Male Fertility for Crop Hybrid Breeding. Trends Plant Sci. **23**: 53–65.

Kinoshita-Tsujimura, K. and Kakimoto, T. (2011). Cytokinin receptors in sporophytes are essential for male and female functions in Arabidopsis thaliana. Plant Signal. Behav. **6**: 66–71.

Klepikova, A. V., Kasianov, A.S., Gerasimov, E.S., Logacheva, M.D., and Penin, A.A. (2016). A high resolution map of the Arabidopsis thaliana developmental transcriptome based on RNA-seq profiling. Plant J. **88**: 1058–1070.

Ko, S.S., Li, M.J., Ku, M.S. Ben, Ho, Y.C., Lin, Y.J., Chuang, M.H., Hsing, H.X., Lien, Y.C., Yang, H.T., Chang, H.C., and Chan, M.T. (2014). The bHLH142 transcription factor coordinates with TDR1 to modulate the expression of EAT1 and regulate pollen development in rice. Plant Cell **26**: 2486–2504.

Kobayashi, K., Awai, K., Takamiya, K.I., and Ohta, H. (2004). Arabidopsis Type B Monogalactosyldiacylglycerol Synthase Genes Are Expressed during Pollen Tube Growth and Induced by Phosphate Starvation. Plant Physiol. **134**: 640–648.

Kohnen, M. V., Schmid-Siegert, E., Trevisan, M., Petrolati, L.A., Sénéchal, F., Müller-Moulé, P., Maloof, J., Xenarios, I., and Fankhauser, C. (2016). Neighbor detection induces organ-specific transcriptomes, revealing patterns underlying hypocotyl-specific growth. Plant Cell **28**: 2889–2904.

Kong, Q., Pattanaik, S., Feller, A., Werkman, J.R., Chai, C., Wang, Y., Grotewold, E., and Yuan, L. (2012). Regulatory switch enforced by basic helix-loop-helix and ACT-domain mediated dimerizations of the maize transcription factor R. Proc. Natl. Acad. Sci. U. S. A. **109**: E2091–E2097.

Kong, X., Luo, X., Qu, G.P., Liu, P., and Jin, J.B. (2017). Arabidopsis SUMO protease ASP1 positively regulates flowering time partially through regulating FLC stability. J. Integr. Plant Biol. **59**: 15–29.

Koornneef, M. and van der Veen, J.H. (1980). Induction and analysis of gibberellin sensitive mutants in Arabidopsis thaliana (L.) heynh. Theor. Appl. Genet. **58**: 257–263.

Korbei, B., Moulinier-Anzola, J., De-Araujo, L., Lucyshyn, D., Retzer, K., Khan, M.A., and Luschnig, C.

(2013). Arabidopsis TOL proteins act as gatekeepers for vacuolar sorting of PIN2 plasma membrane protein. Curr. Biol. **23**: 2500–2505.

Kurepa, J., Walker, J.M., Smalle, J., Gosink, M.M., Davis, S.J., Durham, T.L., Sung, D.Y., and Vierstra, R.D. (2003). The small ubiquitin-like modifier (SUMO) protein modification system in Arabidopsis. Accumulation of sumo1 and -2 conjugates is increased by stress. J. Biol. Chem. **278**: 6862–6872.

Kurepin, L. V., Emery, R.J.N., Pharis, R.P., and Reid, D.M. (2007). Uncoupling light quality from light irradiance effects in Helianthus annuus shoots: Putative roles for plant hormones in leaf and internode growth. J. Exp. Bot. **58**: 2145–2157.

Lahlali, R., Jiang, Y., Kumar, S., Karunakaran, C., Liu, X., Borondics, F., Hallin, E., and Bueckert, R. (2014). ATR-FTIR spectroscopy reveals involvement of lipids and proteins of intact pea pollen grains to heat stress tolerance. Front. Plant Sci. **5**: 1–10.

Lantzouni, O., Alkofer, A., Falter-Braun, P., and Schwechheimer, C. (2020). Growth-regulating factors interact with dellas and regulate growth in cold stress. Plant Cell **32**: 1018–1034.

Lauxmann, M.A. et al. (2016). Reproductive failure in Arabidopsis thaliana under transient carbohydrate limitation: Flowers and very young siliques are jettisoned and the meristem is maintained to allow successful resumption of reproductive growth. Plant Cell Environ. **39**: 745–767.

Law, C.W., Chen, Y., Shi, W., and Smyth, G.K. (2014). voom: precision weights unlock linear model analysis tools for RNA-seq read counts. Genome Biol. **15**.

LeClere, S., Tellez, R., Rampey, R.A., Matsuda, S.P.T., and Bartel, B. (2002). Characterization of a family of IAA-amino acid conjugate hydrolases from Arabidopsis. J. Biol. Chem. **277**: 20446–20452.

Lee, S., Cheng, H., King, K.E., Wang, W., He, Y., Hussain, A., Lo, J., Harberd, N.P., and Peng, J. (2002). Gibberellin regulates Arabidopsis seed germination via RGL2,a GAI/RGA-like gene whose expression is up-regulated following imbibition. Genes Dev. **16**: 646–658.

Lee, Y.H. and Tegeder, M. (2004). Selective expression of a novel high-affinity transport system for acidic and neutral amino acids in the tapetum cells of Arabidopsis flowers. Plant J. **40**: 60–74.

Leivar, P. and Quail, P.H. (2011). PIFs: pivotal components in a cellular signaling hub Phytochrome signal perception and transduction. Trends Plant **16**: 19–28.

Leivar, P., Tepperman, J.M., Cohn, M.M., Monte, E., Al-Sady, B., Erickson, E., and Quail, P.H. (2012). Dynamic Antagonism between Phytochromes and PIF Family Basic Helix-Loop-Helix Factors Induces Selective Reciprocal Responses to Light and Shade in a Rapidly Responsive Transcriptional Network in Arabidopsis. Plant Cell **24**: 1398–1419.

Leydon, A.R., Beale, K.M., Woroniecka, K., Castner, E., Chen, J., Horgan, C., Palanivelu, R., and Johnson, M.A. (2013). Three MYB transcription factors control pollen tube differentiation required for sperm release. Curr. Biol. **23**: 1209–1214.

Li, H., Yuan, Z., Vizcay-Barrena, G., Yang, C., Liang, W., Zong, J., Wilson, Z.A., and Zhang, D. (2011). PERSISTENT TAPETAL CELL1 encodes a PHD-finger protein that is required for tapetal cell death and pollen development in rice. Plant Physiol. **156**: 615–630.

Li, L. et al. (2012). Linking photoreceptor excitation to changes in plant architecture. Genes Dev. **26**: 785–790.

Li, S.F., Iacuone, S., and Parish, R.W. (2007). Suppression and restoration of male fertility using a

transcription factor. Plant Biotechnol. J. **5**: 297–312.

Li, Y., Wang, H., Li, X., Liang, G., and Yu, D. (2017a). Two DELLA-interacting proteins bHLH48 and bHLH60 regulate flowering under long-day conditions in Arabidopsis thaliana. J. Exp. Bot. **68**: 2757–2767.

Li, Z., Wang, Y., Huang, J., Ahsan, N., Biener, G., Paprocki, J., Thelen, J.J., Raicu, V., and Zhao, D. (2017b). Two SERK receptor-like kinases interact with EMS1 to control anther cell fate determination. Plant Physiol. **173**: 326–337.

Liang, Y., Tan, Z.M., Zhu, L., Niu, Q.K., Zhou, J.J., Li, M., Chen, L.Q., Zhang, X.Q., and Ye, D. (2013). MYB97, MYB101 and MYB120 Function as Male Factors That Control Pollen Tube-Synergid Interaction in Arabidopsis thaliana Fertilization. PLoS Genet. **9**.

Lippman, Z.B. and Zamir, D. (2007). Heterosis: revisiting the magic. Trends Genet. **23**: 60–66.

Liu, B., De Storme, N., and Geelen, D.N.V. (2017a). Gibberellin induces diploid pollen formation by interfering with meiotic cytokinesis. Plant Physiol. **173**: 338–353.

Liu, J.X., Srivastava, R., and Howell, S. (2009). Overexpression of an arabidopsis gene encoding a subtilase (AtSBT5.4) produces a clavata-like phenotype. Planta **230**: 687–697.

Liu, L., Jiang, Y., Zhang, X., Wang, X., Wang, Y., Han, Y., Coupland, G., Jin, J.B., Searle, I., Fu, Y.F., and Chen, F. (2017b). Two SUMO proteases SUMO PROTEASE RELATED TO FERTILITY1 and 2 are required for fertility in arabidopsis. Plant Physiol. **175**: 1703–1719.

Liu, L., Li, C., Liang, Z., and Yu, H. (2018). Characterization of multiple C2 domain and transmembrane region proteins in arabidopsis. Plant Physiol. **176**: 2119–2132.

Liu, M.-J., Wu, S.-H., Chen, H.-M., and Wu, S.-H. (2012). Widespread translational control contributes to the regulation of Arabidopsis photomorphogenesis. Mol. Syst. Biol. **8**: 1–14.

Liu, X. et al. (2019). A putative bHLH transcription factor is a candidate gene for male sterile 32, a locus affecting pollen and tapetum development in tomato. Hortic. Res. **6**.

Liu, Y., Li, X., Li, K., Liu, H., and Lin, C. (2013). Multiple bHLH Proteins form Heterodimers to Mediate CRY2-Dependent Regulation of Flowering-Time in Arabidopsis. PLoS Genet. **9**.

Lou, Y., Xu, X., Zhu, J., Gu, J., Blackmore, S., and Yang, Z. (2014). The tapetal AHL family protein TEK determines nexine formation in the pollen wall. Nat. Commun. **5**: 3855.

Lou, Y., Zhou, H., Han, Y., Zeng, Q., Zhu, J., and Yang, Z. (2017). Positive regulation of AMS by TDF1 and the formation of a TDF1 – AMS complex are required for anther development in Arabidopsis thaliana. New Phytol.

Lu, J.Y., Xiong, S.X., Yin, W., Teng, X.D., Lou, Y., Zhu, J., Zhang, C., Gu, J.N., Wilson, Z.A., and Yang, Z.N. (2020). MS1, a direct target of MS188, regulates the expression of key sporophytic pollen coat protein genes in Arabidopsis. J. Exp. Bot. **71**: 4877–4889.

De Lucas, M., Davière, J.M., Rodríguez-Falcón, M., Pontin, M., Iglesias-Pedraz, J.M., Lorrain, S., Fankhauser, C., Blázquez, M.A., Titarenko, E., and Prat, S. (2008). A molecular framework for light and gibberellin control of cell elongation. Nature **451**: 480–484.

Ludwig, S.R., Habera, L.F., Dellaporta, S.L., and Wessler, S.R. (1989). Lc, a member of the maize R gene family responsible for tissue-specific anthocyanin production, encodes a protein similar to transcriptional activators and contains the myc-homology region. Proc. Natl. Acad. Sci. U. S. A. **86**: 7092–7096.

Luo, W. and Brouwer, C. (2013). Pathview: An R/Bioconductor package for pathway-based data integration and visualization. Bioinformatics **29**: 1830–1831.

Ma, L., Li, J., Qu, L., Hager, J., Chen, Z., and Zhao, H. (2001). Light Control of Arabidopsis Development Entails Coordinated Regulation of Genome Expression and Cellular Pathways. Plant Cell **13**: 2589–2607.

Ma, X., Feng, B., and Ma, H. (2012). AMS-dependent and independent regulation of anther transcriptome and comparison with those affected by other Arabidopsis anther genes.

Marín-de la Rosa, N. et al. (2015). Genome Wide Binding Site Analysis Reveals Transcriptional Coactivation of Cytokinin-Responsive Genes by DELLA Proteins. PLoS Genet. **11**: 1–20.

Marín-de la Rosa, N. et al. (2014). Large-Scale Identification of Gibberellin-Related Transcription Factors Defines Group VII ETHYLENE RESPONSE FACTORS as Functional DELLA Partners. Plant Physiol. **166**: 1022–1032.

Mashiguchi, K., Asami, T., and Suzuki, Y. (2009). Genome-wide identification, structure and expression studies, and mutant collection of 22 early nodulin-like protein genes in arabidopsis. Biosci. Biotechnol. Biochem. **73**: 2452–2459.

Matsuno, M. et al. (2009). Evolution of a novel phenolic pathway for pollen development. Science (80-.). **325**: 1688–1692.

Maxwell, B.B. and Keiber, J.J. (2010). Cytokinin Signal Transduction. In Plant Hormones: Biosynthesis, Signal Transduction, Action!, P.J. Davies, ed (Springer Netherlands), pp. 329–357.

Mayfield, J.A., Fiebig, A., Johnstone, S.E., and Preuss, D. (2001). Gene families from the Arabidopsis thaliana pollen coat proteome. Science (80-.). **292**: 2482–2485.

Mayfield, J.A. and Preuss, D. (2000). Rapid initiation of Arabidopsis pollination requires the oleosin-domain protein GRP17. Nat. Cell Biol. **2**: 128–130.

Mi, H., Huang, X., Muruganujan, A., Tang, H., Mills, C., Kang, D., and Thomas, P.D. (2017). PANTHER version 11: Expanded annotation data from Gene Ontology and Reactome pathways, and data analysis tool enhancements. Nucleic Acids Res. **45**: D183–D189.

Millar, A.A. and Gubler, F. (2005). The Arabidopsis GAMYB-Like Genes, MYB33 and MYB65, Are MicroRNA-Regulated Genes That Redundantly Facilitate Anther Development. Plant Cell **17**: 705–721.

Morrell, R. and Sadanandom, A. (2019). Dealing With Stress: A Review of Plant SUMO Proteases. Front. Plant Sci. **10**: 1–19.

Murre, C., McCaw, P.S., and Baltimore, D. (1989). A new DNA binding and dimerization motif in immunoglubin enhancer binding, dauhterless, MyoD, and myc proteins. Cell **56**: 777–783.

Nakazawa, M., Yabe, N., Ichikawa, T., Yamamoto, Y.Y., Yoshizumi, T., Hasunuma, K., and Matsui, M. (2001). DFL1, an auxin-responsive GH3 gene homologue, negatively regulates shoot cell elongation and lateral root formation, and positively regulates the light response of hypocotyl length. Plant J. **25**: 213–221.

Nan, G.L., Zhai, J., Arikit, S., Morrow, D., Fernandes, J., Mai, L., Nguyen, N., Meyers, B.C., and Walbot, V. (2017). MS23, a master basic helix-loop-helix factor, regulates the specification and development of the tapetum in maize. Dev. **144**: 163–172.

Nguyen, T.D., Jang, S., Soh, M.S., Lee, J., Yun, S.D., Oh, S.A., and Park, S.K. (2019). High daytime temperature induces male sterility with developmental defects in male reproductive organs of

Arabidopsis. Plant Biotechnol. Rep. **13**: 635–643.

Oh, E., Kang, H., Yamaguchi, S., Park, J., Lee, D., Kamiya, Y., and Choi, G. (2009). Genome-wide analysis of genes targeted by PHYTOCHROME INTERACTING FACTOR 3-LIKE5 during seed germination in arabidopsis. Plant Cell **21**: 403–419.

Oh, E., Zhu, J.Y., Bai, M.Y., Arenhart, R.A. ugusto, Sun, Y., and Wang, Z.Y. (2014). Cell elongation is regulated through a central circuit of interacting transcription factors in the Arabidopsis hypocotyl. Elife **3**: 1–19.

Oh, S.A., Park, K.S., Twell, D., and Park, S.K. (2010). The SIDECAR POLLEN gene encodes a microspore-specific LOB/AS2 domain protein required for the correct timing and orientation of asymmetric cell division. Plant J. **64**: 839–850.

Oliveros, J.C. (2007). VENNY. An interactive tool for comparing lists with Venn Diagrams.: http://bioinfogp.cnnb.csic.es/tools/venny/index.ht.

Orosa-Puente, B. et al. (2018). Root branching toward water involves posttranslational modification of transcription factor ARF7. Science (80-.). **362**: 1407–1410.

Ortega-Amaro, M.A., Rodriguez-Hernandez, A.A., Rodriguez-Kessler, M., Hernandez-Lucero, E., Rosales-Mendoza, S., Ibanez-Salazar, A., Delgado-Sanchez, P., and Jimenez-Bremont, J.F. (2015). Overexpression of AtGRDP2, a novel glycine-rich domain protein, accelerates plant growth and improves stress tolerance. Front. Plant Sci. **5**: 1–16.

Pan, X., Yan, W., Chang, Z., Xu, Y., Luo, M., Xu, C., Chen, Z., Wu, J., and Tang, X. (2020). OsMYB80 Regulates Anther Development and Pollen Fertility by Targeting Multiple Biological Pathways. Plant Cell Physiol. **61**: 988–1004.

Parish, R.W., Phan, H.A., Iacuone, S., and Li, S.F. (2012). Tapetal development and abiotic stress: A centre of vulnerability. Funct. Plant Biol. **39**: 553–559.

Patro, R., Duggal, G., Love, M.I., Irizarry, R.A., Kingsford, C., and Biology, C. (2017). Salmon: fast and bias-aware quantification of transcript expression using dual-phase inference. Nat. Methods **14**: 417–419.

Peng, C., P., R., D. E., K., and K. E., C. (1997). The Arabidopsis GAI gene defines a signalling pathway that negatively regulates gibberellin responses. Genes Dev **11**: 3194–3205.

Peng, J. et al. (1999). “Green revolution” genes encode mutant gibberellin response modulators. Nature **400**: 256–261.

Pereira, A.M., Masiero, S., Nobre, M.S., Costa, M.L., Solís, M.T., Testillano, P.S., Sprunck, S., and Coimbra, S. (2014). Differential expression patterns of arabinogalactan proteins in Arabidopsis thaliana reproductive tissues. J. Exp. Bot. **65**: 5459–5471.

Pham, V.N., Kathare, P.K., and Huq, E. (2018). Phytochromes and Phytochrome Interacting Factors 1 [OPEN]. **176**: 1025–1038.

Phan, H.A., Iacuone, S., Li, S.F., and Parish, R.W. (2011). The MYB80 Transcription Factor Is Required for Pollen Development and the Regulation of Tapetal Programmed Cell Death in *Arabidopsis thaliana*. Plant Cell **23**: 2209–2224.

Piffanelli, P., Ross, J.H.E., and Murphy, D.J. (1998). Biogenesis and function of the lipidic structures of pollen grains. Sex. Plant Reprod. **11**: 65–80.

Pireyre, M. and Burow, M. (2015). Regulation of MYB and bHLH transcription factors: A glance at the protein level. Mol. Plant **8**: 378–388.

Plackett, A.R.G. et al. (2012). Analysis of the developmental roles of the arabidopsis gibberellin 20-oxidases demonstrates that GA20ox1, -2, and -3 are the dominant paralogs. Plant Cell **24**: 941–960.

Plackett, A.R.G., Ferguson, A.C., Powers, S.J., Wanchoo-Kohli, A., Phillips, A.L., Wilson, Z.A., Hedden, P., and Thomas, S.G. (2014). DELLA activity is required for successful pollen development in the Columbia ecotype of Arabidopsis. New Phytol. **201**: 825–836.

Plackett, A.R.G., Powers, S.J., Phillips, A.L., Wilson, Z.A., Hedden, P., and Thomas, S.G. (2017). The early inflorescence of Arabidopsis thaliana demonstrates positional effects in floral organ growth and meristem patterning. Plant Reprod. **31**: 171–191.

Plegt, L. and Bino, R.J. (1989). β-Glucuronidase activity during development of the male gametophyte from transgenic and non-transgenic plants. MGG Mol. Gen. Genet. **216**: 321–327.

Prasad, P.V.V. and Djanaguiraman, M. (2011). High night temperature decreases leaf photosynthesis and pollen function in grain sorghum. Funct. Plant Biol. **38**: 993–1003.

Qi, T., Huang, H., Song, S., and Xie, D. (2015). Regulation of jasmonate-mediated stamen development and seed production by a bHLH-MYB complex in arabidopsis. Plant Cell **27**: 1620–1633.

Qi, T., Huang, H., Wu, D., Yan, J., Qi, Y., Song, S., and Xie, D. (2014). Arabidopsis DELLA and JAZ proteins bind the WD-Repeat/ bHLH/MYB complex to modulate gibberellin and jasmonate signaling synergy. Plant Cell **26**: 1118–1133.

Ramsay, N.A. and Glover, B.J. (2005). MYB-bHLH-WD40 protein complex and the evolution of cellular diversity. Trends Plant Sci. **10**: 63–70.

Reeves, P.H., Murtas, G., Dash, S., and Coupland, G. (2002). early in short days 4, a mutation in Arabidopsis that causes early flowering and reduces the mRNA abundance of the floral repressor FLC. Development **129**: 5349–5361.

Riechmann, J.L. et al. (2000). Arabidopsis transcription factors: genome-wide comparative analysis among eukaryotes. Science **290**: 2105–2110.

Rieu, I., Eriksson, S., Powers, S.J., Gong, F., Griffiths, J., Woolley, L., Benlloch, R., Nilsson, O., Thomas, S.G., Hedden, P., and Phillips, A.L. (2008a). Genetic analysis reveals that C19-GA 2-oxidation is a major gibberellin inactivation pathway in Arabidopsis. Plant Cell **20**: 2420–2436.

Rieu, I., Ruiz-Rivero, O., Fernandez-Garcia, N., Griffiths, J., Powers, S.J., Gong, F., Linhartova, T., Eriksson, S., Nilsson, O., Thomas, S.G., Phillips, A.L., and Hedden, P. (2008b). The gibberellin biosynthetic genes AtGA20ox1 and AtGA20ox2 act, partially redundantly, to promote growth and development throughout the Arabidopsis life cycle. Plant J. **53**: 488–504.

Rieu, I., Twell, D., and Firon, N. (2017). Pollen development at high temperature: From acclimation to collapse. Plant Physiol. **173**: 1967–1976.

Rijpkema, A.S., Vandenbussche, M., Koes, R., Heijmans, K., and Gerats, T. (2010). Variations on a theme: Changes in the floral ABCs in angiosperms. Semin. Cell Dev. Biol. **21**: 100–107.

Ritchie, M.E., Phipson, B., Wu, D., Hu, Y., Law, C.W., Shi, W., and Smyth, G.K. (2015). Limma powers differential expression analyses for RNA-sequencing and microarray studies. Nucleic Acids Res. **43**: e47.

Rizza, A., Walia, A., Lanquar, V., Frommer, W.B., and Jones, A.M. (2017). In vivo gibberellin gradients visualized in rapidly elongating tissues. Nat. Plants.

Roshchina, V. V. (2003). Autofluorescence of Plant Secreting Cells as a Biosensor and Bioindicator Reaction. J. Fluoresc. **13**: 403–418.

Rubinelli, P., Hu, Y., and Ma, H. (1998). Identification, sequence analysis and expression studies of novel anther-specific genes of Arabidopsis thaliana. Plant Mol. Biol. **37**: 607–619.

Sadanandom, A., Ádám, É., Orosa, B., Viczián, A., Klose, C., Zhang, C., Josse, E.M., Kozma-Bognár, L., and Nagy, F. (2015). SUMOylation of phytochrome-B negatively regulates light-induced signaling in Arabidopsis thaliana. Proc. Natl. Acad. Sci. U. S. A. **112**: 11108–11113.

Sanders, P.M., Bui, A.Q., Weterings, K., McIntire, K.N., Hsu, Y.C., Lee, P.Y., Truong, M.T., Beals, T.P., and Goldberg, R.B. (1999). Anther developmental defects in *Arabidopsis thaliana* male-sterile mutants. Sex. Plant Reprod. **11**: 297–322.

Schiefthaler, U., Balasubramanian, S., Sieber, P., Chevalier, D., Wisman, E., and Schneitz, K. (1999). Molecular analysis of NOZZLE , a gene involved in pattern formation and early sporogenesis during sex organ development in Arabidopsis thaliana. Proc. Natl. Acad. Sci. U. S. A. **96**: 11664–11669.

Schmid, M., Davison, T.S., Henz, S.R., Pape, U.J., Demar, M., Vingron, M., Schölkopf, B., Weigel, D., and Lohmann, J.U. (2005). A gene expression map of Arabidopsis thaliana development. Nat. Genet. **37**: 501–506.

Scott, R.J. (2004). Stamen Structure and Function. Plant Cell Online **16**: S46–S60.

Sellaro, R., Pac, M., and Casal, J.J. (2017). Meta-Analysis of the Transcriptome Reveals a Core Set of Shade-Avoidance Genes in Arabidopsis. Photochem. Photobiol. **93**: 692–702.

Shang, Y. et al. (2010). The Mg-Chelatase H Subunit of *Arabidopsis* Antagonizes a Group of WRKY Transcription Repressors to Relieve ABA-Responsive Genes of Inhibition. Plant Cell **22**: 1909–1935.

Shen, H., Zhu, L., Castillon, A., Majee, M., Downie, B., and Huq, E. (2008). Light-induced phosphorylation and degradation of the negative regulator phytochrome-interacting factor1 from Arabidopsis depend upon its direct physical interactions with photoactivated phytochromes. Plant Cell **20**: 1586–1602.

Shi, J., Cui, M., Yang, L., Kim, Y.J., and Zhang, D. (2015). Genetic and Biochemical Mechanisms of Pollen Wall Development. Trends Plant Sci. **20**: 741–753.

Shinozaki, K. and Yamaguchi-Shinozaki, K. (2007). Gene networks involved in drought stress response and tolerance. J. Exp. Bot. **58**: 221–227.

Silverstone, A.L., Chang, C.W., Krol, E., and Sun, T.P. (1997). Developmental regulation of the gibberellin biosynthetic gene GA 1 in Arabidopsis thaliana. Plant J. **12**: 9–19.

Silverstone, A.L., Jung, H.S., Dill, A., Kawaide, H., Kamiya, Y., and Sun, T.P. (2001). Repressing a repressor: Gibberellin-induced rapid reduction of the RGA protein in Arabidopsis. Plant Cell **13**: 1555–66.

Smyth, D.R., Bowman, J.L., and Meyerowitz, E.M. (1990). Early Flower Development in Arabidopsis. Plant Cell **2**: 755–767.

Soneson, C., Love, M.I., and Robinson, M.D. (2016). Differential analyses for RNA-seq: Transcript-level estimates improve gene-level inferences [version 2; referees: 2 approved]. F1000Research **4**: 1–22.

Sorensen, A.M., Kröber, S., Unte, U.S., Huijser, P., Dekker, K., and Saedler, H. (2003). The

Arabidopsis aborted microspores (ams) gene encodes a MYC class transcription factor. Plant J. **33**: 413–423.

Staswick, P.E., Serban, B., Rowe, M., Tiryaki, I., Maldonado, M.T., Maldonado, M.C., and Suza, W. (2005). Characterization of an Arabidopsis Enzyme Family That Conjugates Amino Acids to Indole-3-Acetic Acid. Plant Cell **17**: 616–627.

De Storme, N. and Geelen, D. (2020). High temperatures alter cross-over distribution and induce male meiotic restitution in Arabidopsis thaliana. Commun. Biol. **3**: 1–15.

Takase, T., Nakazawa, M., Ishikawa, A., Kawashima, M., Ichikawa, T., Takahashi, N., Shimada, H., Manabe, K., and Matsui, M. (2004). ydk1-D, an auxin-responsive GH3 mutant that is involved in hypocotyl and root elongation. Plant J. **37**: 471–483.

Takei, K., Yamaya, T., and Sakakibara, H. (2004). Arabidopsis CYP735A1 and CYP735A2 encode cytokinin hydroxylases that catalyse the biosynthesis of trans-Zeatin. J. Biol. Chem. **279**: 41866–41872.

Tanaka, S.I., Mochizuki, N., and Nagatani, A. (2002). Expression of the AtGH3a gene, an Arabidopsis homologue of the soybean GH3 gene, is regulated by phytochrome B. Plant Cell Physiol. **43**: 281–289.

Tiwari, S.B., Wang, X., and Guilfoyle, T.J. (2001). AUX / IAA Proteins Are Active Repressors , and Their Stability and Activity Are Modulated by Auxin Author (s): Shiv B . Tiwari , Xiao-Jun Wang , Gretchen Hagen and Tom J . Guilfoyle Published by : American Society of Plant Biologists (ASPB) Stable URL. Plant Cell **13**: 2809–2822.

Toledo-Ortiz, G., Huq, E., and Quail, P.H. (2003). The Arabidopsis Basic / Helix-Loop-Helix Transcription Factor Family. Plant Cell **15**: 1749–1770.

Trapalis, M., Li, S.F., and Parish, R.W. (2017). The Arabidopsis GASA10 gene encodes a cell wall protein strongly expressed in developing anthers and seeds. Plant Sci. **260**: 71–79.

Truernit, E., Stadler, R., Baier, K., and Sauer, N. (1999). A male gametophyte-specific monosaccharide transporter in Arabidopsis. Plant J. **17**: 191–201.

Tyler, L., Thomas, S.G., Hu, J., Dill, A., Alonso, J.M., Ecker, J.R., and Sun, T.-P. (2004). Della proteins and gibberellin-regulated seed germination and floral development in Arabidopsis. Plant Physiol. **135**: 1008–19.

Ueguchi-Tanaka, M., Ashikari, M., Nakajima, M., Itoh, H., Katoh, E., Kobayashi, M., Chow, T.Y., Hsing, Y.I.C., Kitano, H., Yamaguchi, I., and Matsuoka, M. (2005). GIBBERELLIN INSENSITIVE DWARF1 encodes a soluble receptor for gibberellin. Nature **437**: 693–698.

Updegraff, E.P., Zhao, F., and Preuss, D. (2009). The extracellular lipase EXL4 is required for efficient hydration of Arabidopsis pollen. Sex. Plant Reprod. **22**: 197–204.

Urbanová, T., Tarkowská, D., Novák, O., Hedden, P., and Strnad, M. (2013). Analysis of gibberellins as free acids by ultra performance liquid chromatography-tandem mass spectrometry. Talanta **112**: 85–94.

Varbanova, M. et al. (2007). Methylation of gibberellins by Arabidopsis GAMT1 and GAMT2. Plant Cell **19**: 32–45.

Vizcay-Barrena, G. and Wilson, Z.A. (2006). Altered tapetal PCD and pollen wall development in the Arabidopsis ms1 mutant. J. Exp. Bot. **57**: 2709–2717.

Wang, F., Muto, A., van de Velde, J., Neyt, P., Himanen, K., Vandepoele, K., and Van Lijsebettens,

M. (2015). Functional analysis of the Arabidopsis tetraspanin gene family in plant growth and development. Plant Physiol. **169**: 2200–2214.

Wang, H., Lu, Y., Jiang, T., Berg, H., Li, C., and Xia, Y. (2013). The Arabidopsis U-box/ARM repeat E3 ligase AtPUB4 influences growth and degeneration of tapetal cells, and its mutation leads to conditional male sterility. Plant J. **74**: 511–523.

Wang, K., Guo, Z.-L., Zhou, W.-T., Zhang, C., Zhang, Z.-Y., Lou, Y., Xiong, S.-X., Yao, X., Fan, J.-J., Zhu, J., and Yang, Z.-N. (2018). The regulation of sporopollenin biosynthesis genes for rapid pollen wall formation. Plant Physiol. **178**: 283–294.

Wang, X. et al. (2019). ABRE-BINDING FACTORS play a role in the feedback regulation of ABA signaling by mediating rapid ABA induction of ABA co-receptor genes. New Phytol. **221**: 341–355.

Waters, B.M., Chu, H.H., DiDonato, R.J., Roberts, L.A., Eisley, R.B., Lahner, B., Salt, D.E., and Walker, E.L. (2006). Mutations in Arabidopsis Yellow Stripe-Like1 and Yellow Stripe-Like3 reveal their roles in metal ion homeostasis and loading of metal ions in seeds. Plant Physiol. **141**: 1446–1458.

Wen, C.K. and Chang, C. (2002). Arabidopsis RGL1 encodes a negative regulator of gibberellin responses. Plant Cell **14**: 87–100.

Wilson, Z.A., Morroll, S.M., Dawson, J., Swarup, R., and Tighe, P.J. (2001). The Arabidopsis MALE STERILITY1 (MS1) gene is a transcriptional regulator of male gametogenesis, with homology to the PHD-finger family of transcription factors. Plant J. **28**: 27–39.

Wit, M. De, Galv, V.C., and Fankhauser, C. (2016). Light-Mediated Hormonal Regulation of Plant Growth and Development. Annu. Rev. Plant Biol. **67**: 513–537.

Wuest, S.E., O'Maoileidigh, D.S., Rae, L., Kwasniewska, K., Raganelli, A., Hanczaryk, K., Lohan, A.J., Loftus, B., Graciet, E., and Wellmer, F. (2012). Molecular basis for the specification of floral organs by APETALA3 and PISTILLATA. Proc. Natl. Acad. Sci. U. S. A. **109**: 13452–13457.

Xie, Y., Tan, H., Ma, Z., and Huang, J. (2016). DELLA Proteins Promote Anthocyanin Biosynthesis via Sequestering MYBL2 and JAZ Suppressors of the MYB/bHLH/WD40 Complex in Arabidopsis thaliana. Mol. Plant **9**: 711–721.

Xiong, S.X., Lu, J.Y., Lou, Y., Teng, X.D., Gu, J.N., Zhang, C., Shi, Q.S., Yang, Z.N., and Zhu, J. (2016). The transcription factors MS188 and AMS form a complex to activate the expression of CYP703A2 for sporopollenin biosynthesis in Arabidopsis thaliana. Plant J. **88**: 936–946.

Xiong, S.X., Zeng, Q.Y., Hou, J.Q., Hou, L.L., Zhu, J., Yang, M., Yang, Z.N., and Lou, Y. (2020). The temporal regulation of TEK contributes to pollen wall exine patterning. PLoS Genet. **16**: e1008807.

Xu, J., Ding, Z., Vizcay-Barrena, G., Shi, J., Liang, W., Yuan, Z., Werck-Reichhart, D., Schreiber, L., Wilson, Z. a, and Zhang, D. (2014). ABORTED MICROSPORES Acts as a Master Regulator of Pollen Wall Formation in Arabidopsis. Plant Cell **26**: 1544–1556.

Xu, J., Yang, C., Yuan, Z., Zhang, D., Gondwe, M.Y., Ding, Z., Liang, W., Zhang, D., and Wilson, Z.A. (2010). The ABORTED MICROSPORES regulatory network is required for postmeiotic male reproductive development in Arabidopsis thaliana. Plant Cell **22**: 91–107.

Xue, Z., Xu, X., Zhou, Y., Wang, X., Zhang, Y., Liu, D., Zhao, B., Duan, L., and Qi, X. (2018). Deficiency of a triterpene pathway results in humidity-sensitive genic male sterility in rice. Nat. Commun. **9**.

Yang, C. and Li, L. (2017). Hormonal regulation in shade avoidance. Front. Plant Sci. **8**: 1–8.

Yang, C., Vizcay-Barrena, G., Conner, K., and Wilson, Z. a (2007). MALE STERILITY1 is required for tapetal development and pollen wall biosynthesis. Plant Cell **19**: 3530–3548.

Yang, S., Xie, L., Mao, H., Puah, C.S., Yang, W., Jiang, L., Sundaresan, V., and Ye, D. (2003). TAPETUM DETERMINANT1 Is Required for Cell Specialization in the Arabidopsis Anther. Plant Cell **15**: 2792–2804.

Yang, T., Sun, Y., Wang, Y., Zhou, L., Chen, M., Bian, Z., Lian, Y., Xuan, L., Yuan, G., Wang, X., and Wang, C. (2020). AtHSPR is involved in GA- and light intensity-mediated control of flowering time and seed set in Arabidopsis. J. Exp. Bot. **2**: 1–17.

Yang, W.C., Ye, D., Xu, J., and Sundaresan, V. (1999). The SPOROCYTELESS gene of Arabidopsis is required for initiation of sporogenesis and encodes a novel nuclear protein. Genes Dev **13**: 2108–17.

Yang, X., Wu, D., Shi, J., He, Y., Pinot, F., Grausem, B., Yin, C., Zhu, L., Chen, M., Luo, Z., Liang, W., and Zhang, D. (2014). Rice CYP703A3, a cytochrome P450 hydroxylase, is essential for development of anther cuticle and pollen exine. J. Integr. Plant Biol. **56**: 979–994.

Yoshida, H. et al. (2014). DELLA protein functions as a transcriptional activator through the DNA binding of the INDETERMINATE DOMAIN family proteins. Proc. Natl. Acad. Sci. U. S. A. **111**: 7861–7866.

Yuan, L., Graff, L., Loqué, D., Kojima, S., Tsuchiya, Y.N., Takahashi, H., and Von Wirén, N. (2009). AtAMT1;4, a pollen-specific high-affinity ammonium transporter of the plasma membrane in arabidopsis. Plant Cell Physiol. **50**: 13–25.

Zentella, R., Zhang, Z.-L., Park, M., Thomas, S.G., Endo, A., Murase, K., Fleet, C.M., Jikumaru, Y., Nambara, E., Kamiya, Y., and Sun, T. (2007). Global Analysis of DELLA Direct Targets in Early Gibberellin Signaling in *Arabidopsis*. Plant Cell **19**: 3037–3057.

Zhang, B., Chopra, D., Schrader, A., and Hülskamp, M. (2019). Evolutionary comparison of competitive protein-complex formation of MYB, bHLH, and WDR proteins in plants. J. Exp. Bot. **70**: 3197–3209.

Zhang, C., Xu, T., Ren, M.Y., Zhu, J., Shi, Q.S., Zhang, Y.F., Qi, Y.W., Huang, M.J., Song, L., Xu, P., and Yang, Z.N. (2020). Slow development restores the fertility of photoperiod-sensitive male-sterile plant lines. Plant Physiol. **184**: 923–932.

Zhang, R. et al. (2017). A high quality Arabidopsis transcriptome for accurate transcript-level analysis of alternative splicing. Nucleic Acids Res. **45**: 5061–5073.

Zhang, W., Sun, Y., Timofejeva, L., Chen, C., Grossniklaus, U., and Ma, H. (2006). Regulation of Arabidopsis tapetum development and function by DYSFUNCTIONAL TAPETUM1 (DYT1) encoding a putative bHLH transcription factor. Development **133**: 3085–3095.

Zhang, Z.B. et al. (2007). Transcription factor AtMYB103 is required for anther development by regulating tapetum development, callose dissolution and exine formation in Arabidopsis. Plant J. **52**: 528–538.

Zhao, D.-Z., Wang, G., and Speal, B. (2002). The EXCESS MICROSPOROCYTES1 gene encodes a putative leucine-rich repeat receptor protein kinase that controls somatic and reproductive cell fates in the Arabidopsis anther. Genes Dev.: 2021–2031.

Zhu, E., You, C., Wang, S., Cui, J., Niu, B., Wang, Y., Qi, J., Ma, H., and Chang, F. (2015). The DYT1-interacting proteins bHLH010, bHLH089 and bHLH091 are redundantly required for Arabidopsis

anther development and transcriptome. Plant J. **83**: 976–990.

Zhu, J. et al. (2020). Slowing development restores the fertility of thermo-sensitive male-sterile plant lines. Nat. Plants **6**.

Zhu, J., Chen, H., Li, H., Gao, J.F., Jiang, H., Wang, C., Guan, Y.F., and Yang, Z.N. (2008). Defective in Tapetal Development and Function 1 is essential for anther development and tapetal function for microspore maturation in Arabidopsis. Plant J. **55**: 266–277.

Zhu, J., Lou, Y., Xu, X., and Yang, Z.N. (2011). A genetic pathway for tapetum development and function in Arabidopsis. J. Integr. Plant Biol. **53**: 892–900.

APPENDIX I: CONSTRUCT MAPS

pGBGWY-bHLH91

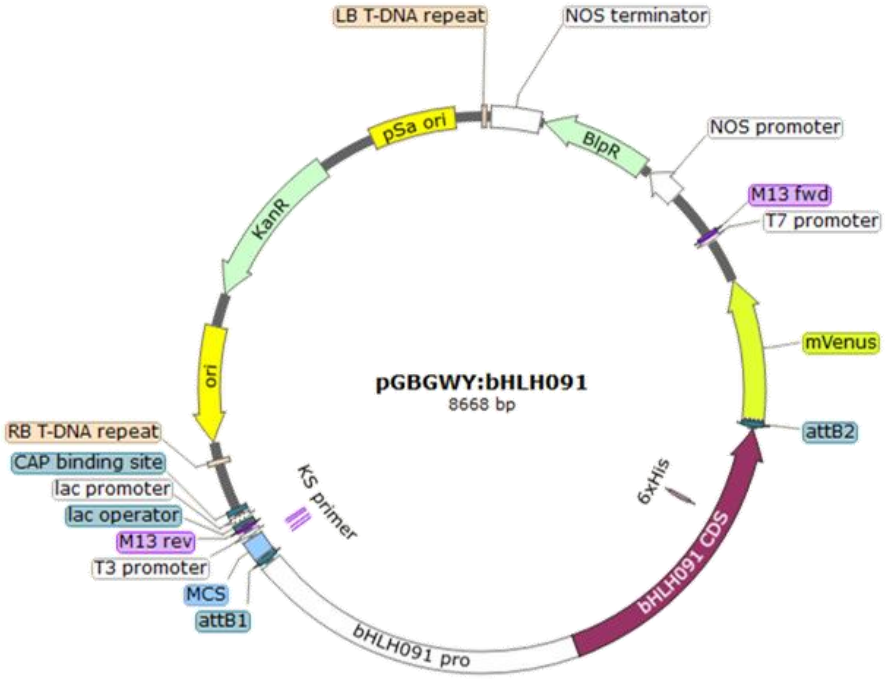

pGHGWC-bHLH091

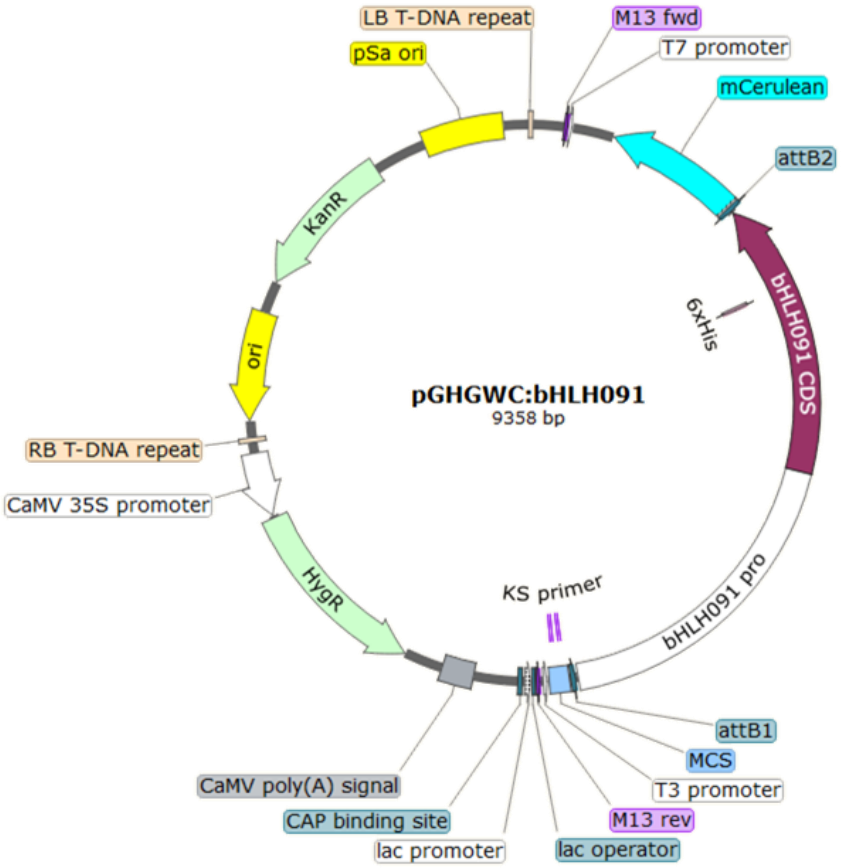

pGHGWG-bHLH089-1

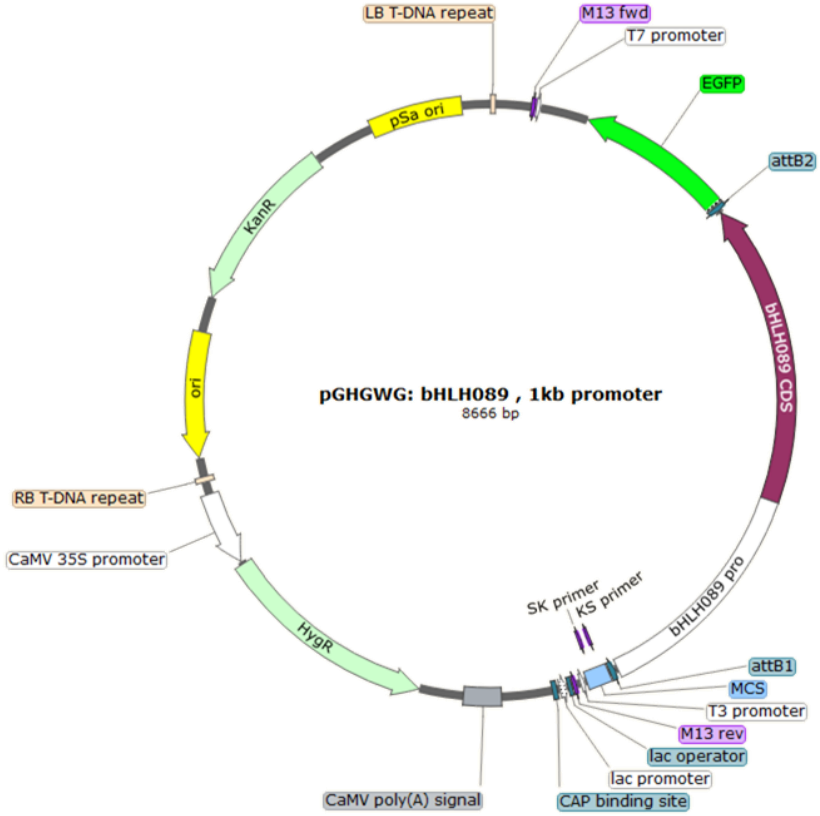

pGHGWG-bHLH089-2

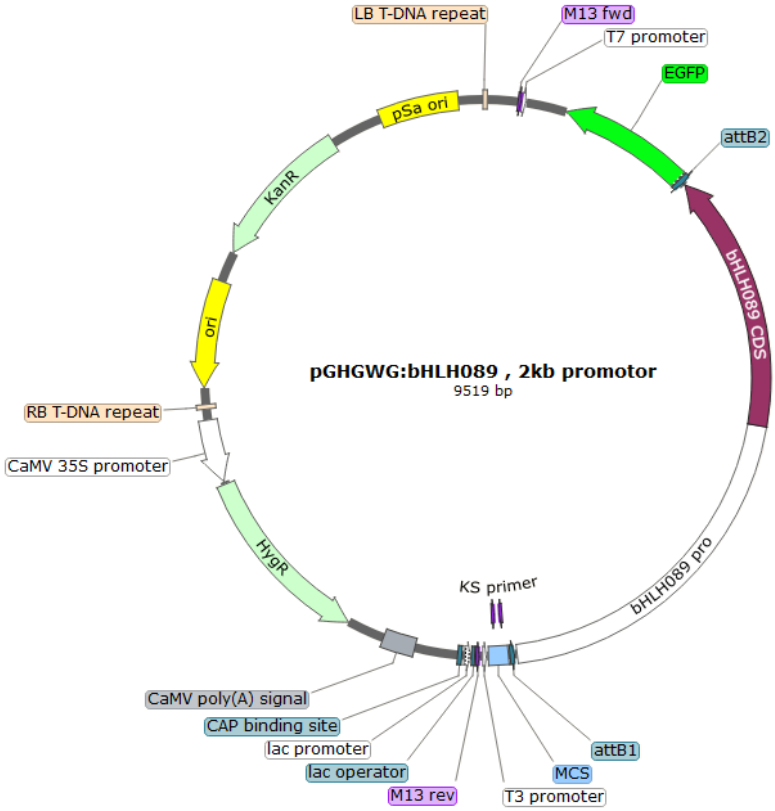

pGREEN-MS2-LUC

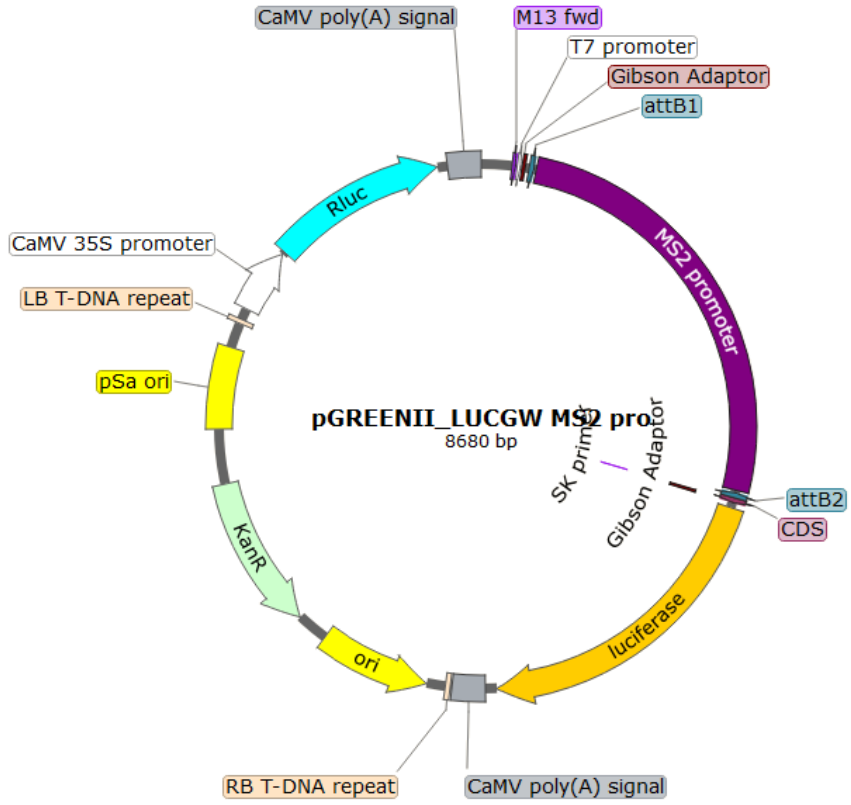

pGWB3-bHLH010

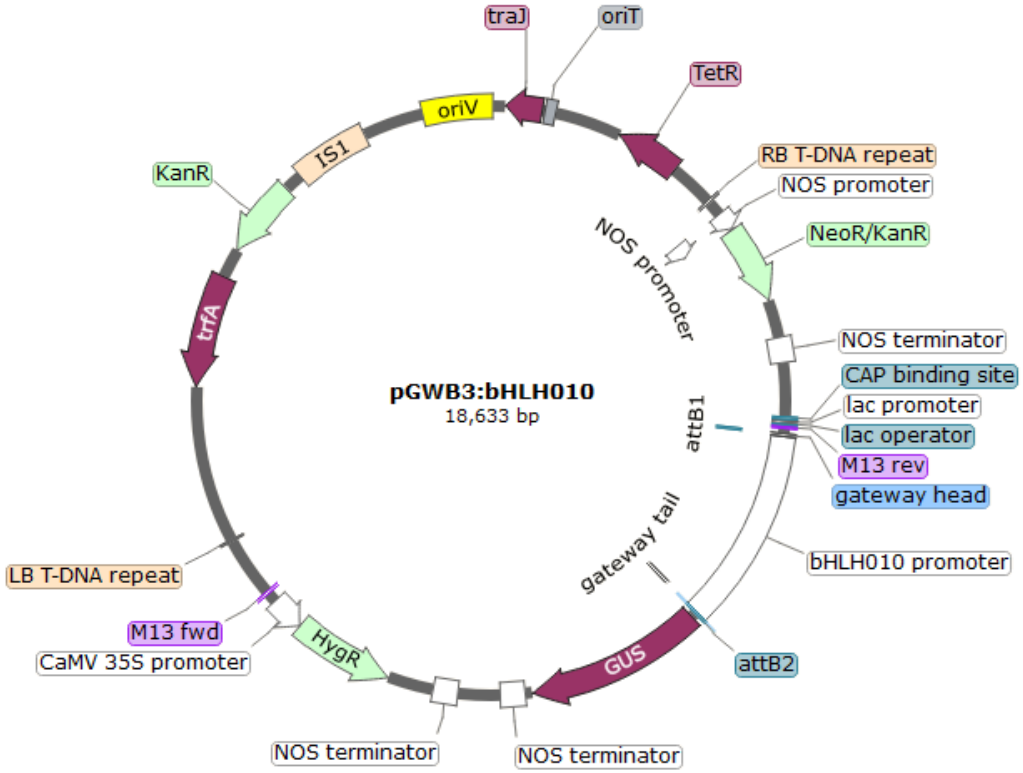

pGWB3-bHLH091

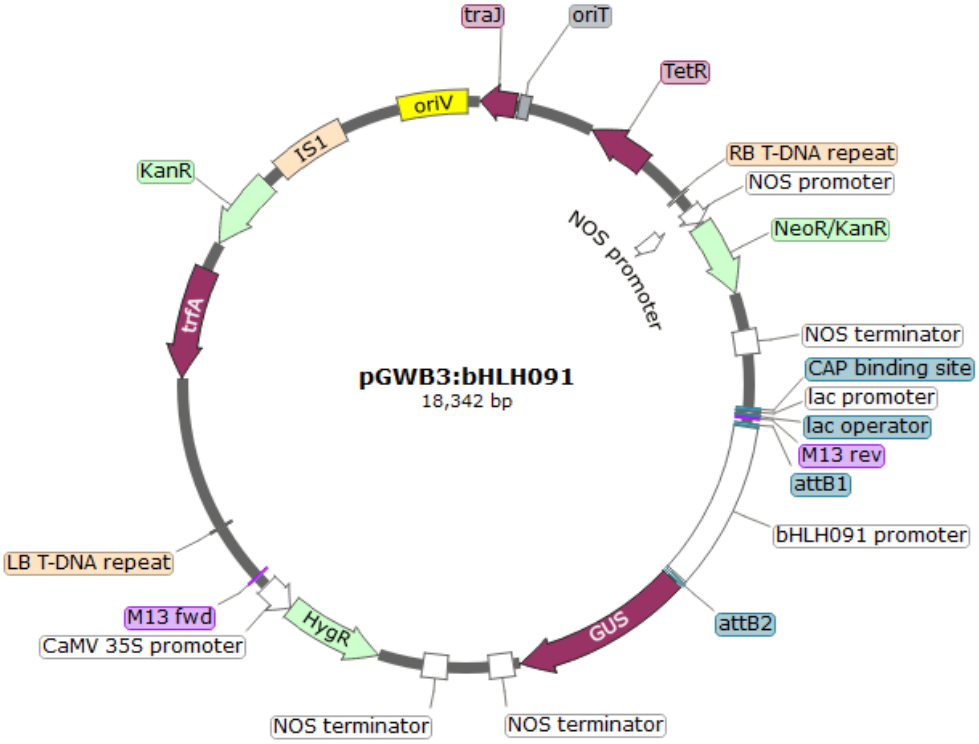

pGWB453-bHLH089-1

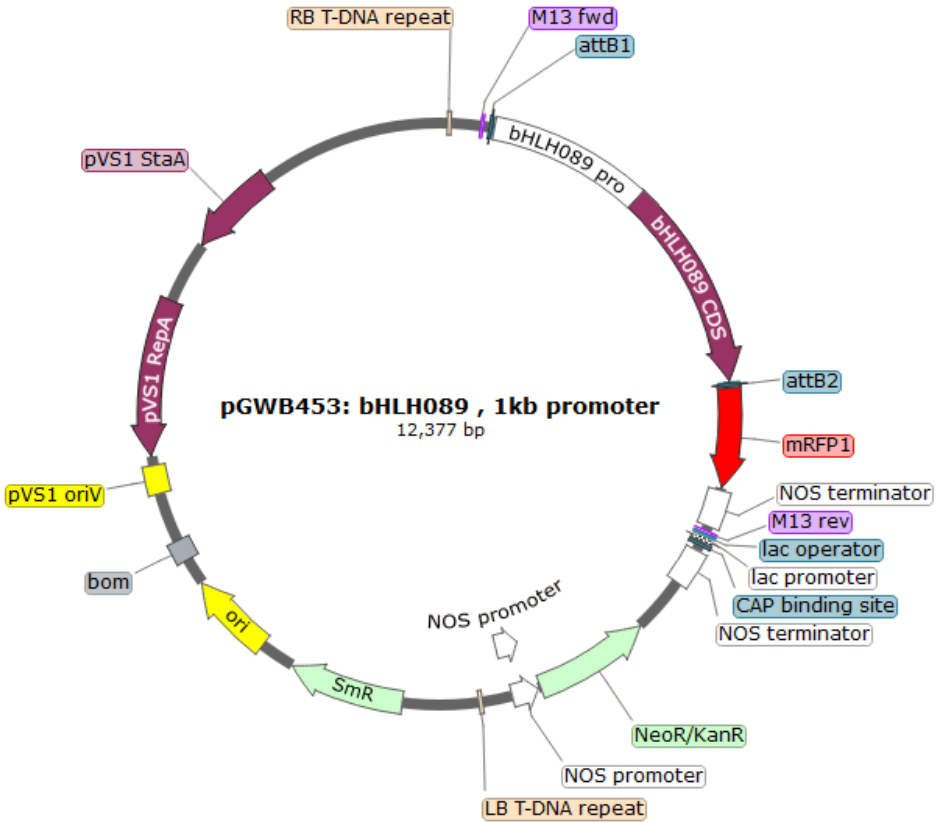

pGWB453-bHLH089-2

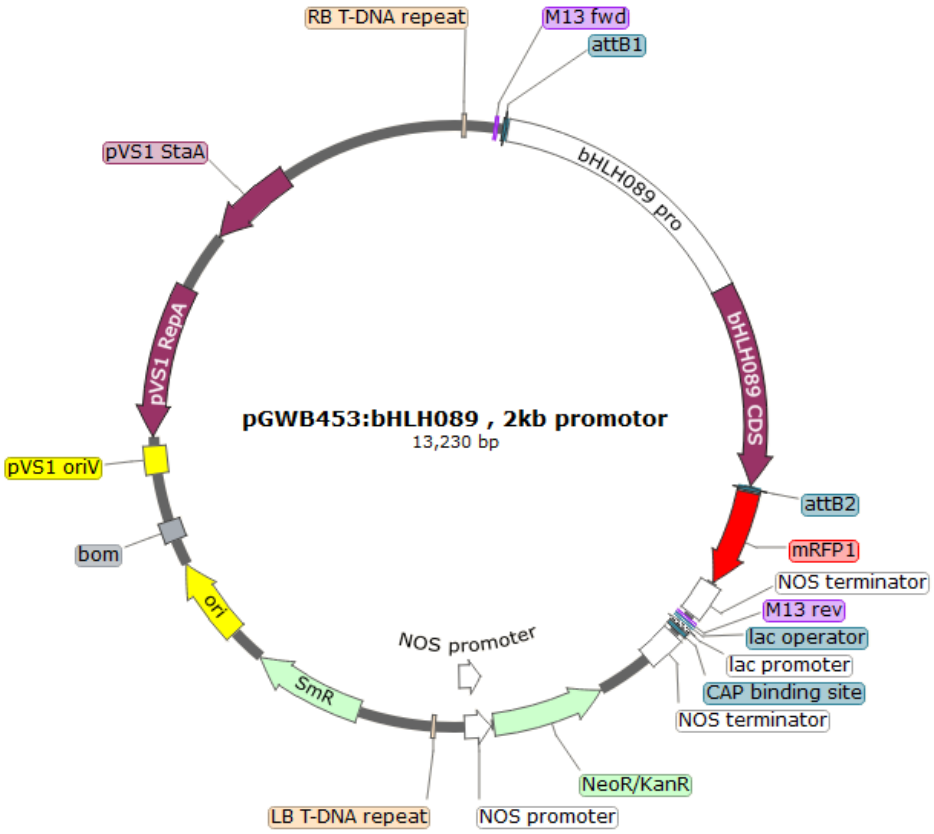

pUBC-AMS-YFP

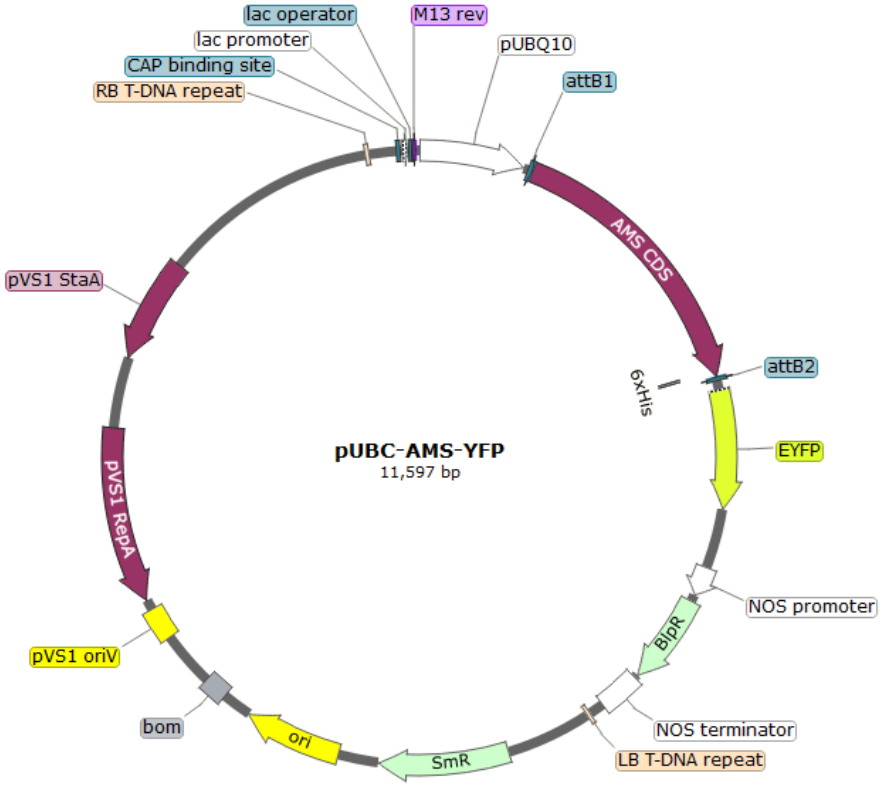

pUBC-bHLH010-cYFP

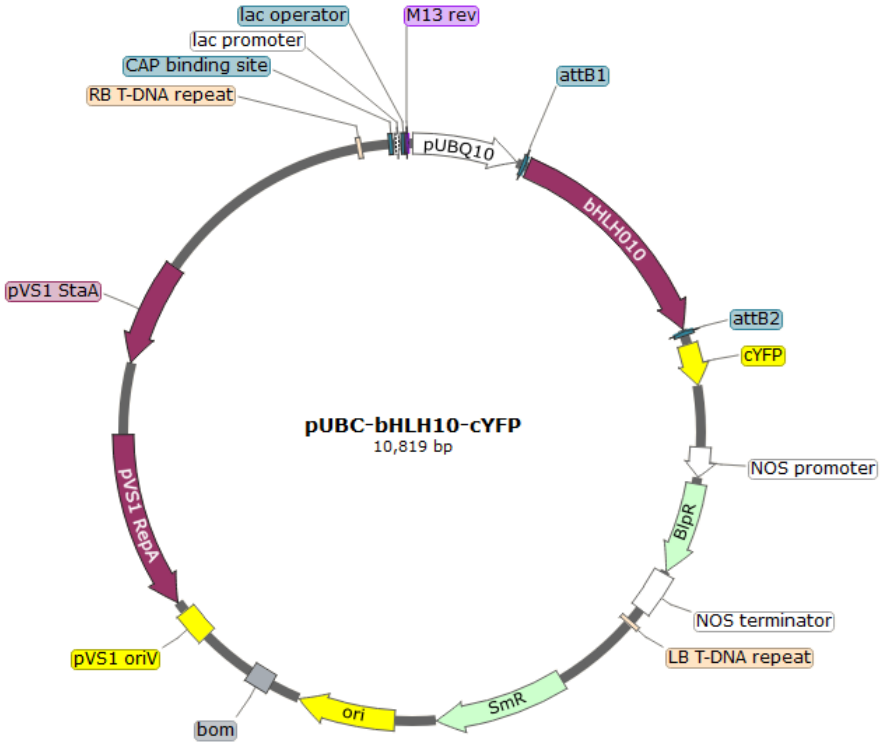

pUBC-bHLH010-nYFP

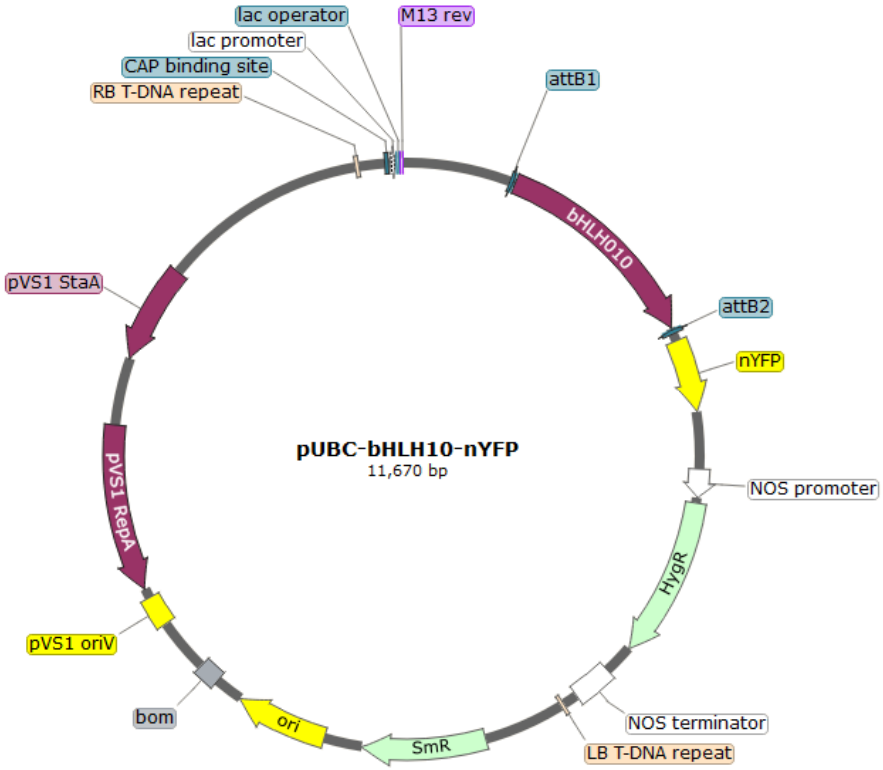

pUBC-bHLH010-YFP

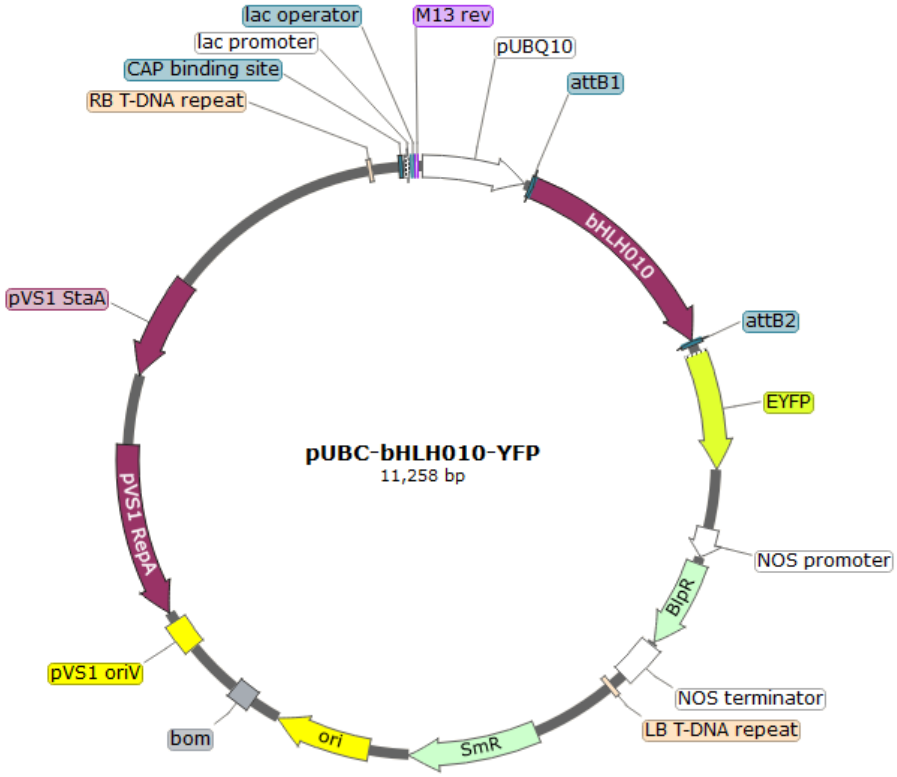

pUBC-bHLH089-cYFP

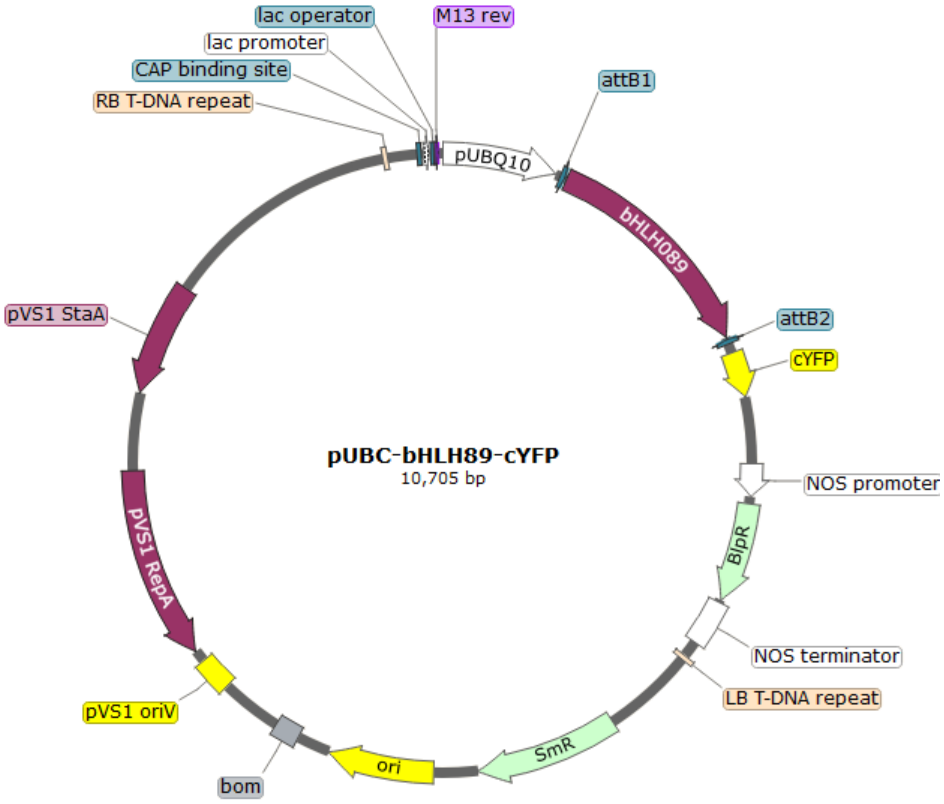

pUBC-bHLH089-nYFP

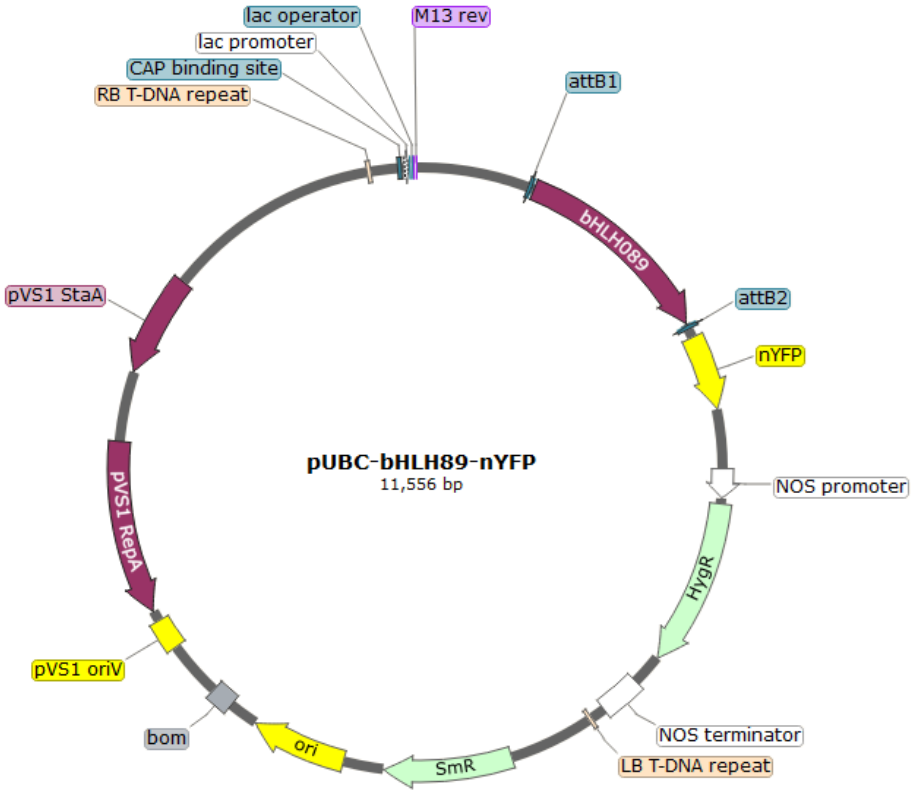

pUBC-bHLH089-YFP

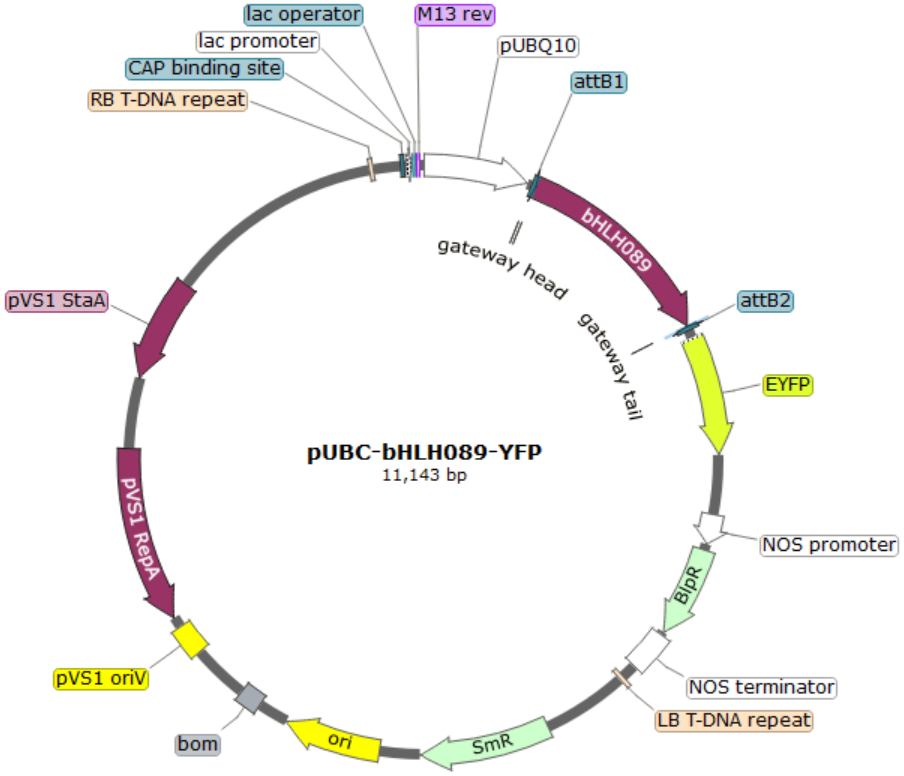

pUBC-bHLH091-cYFP

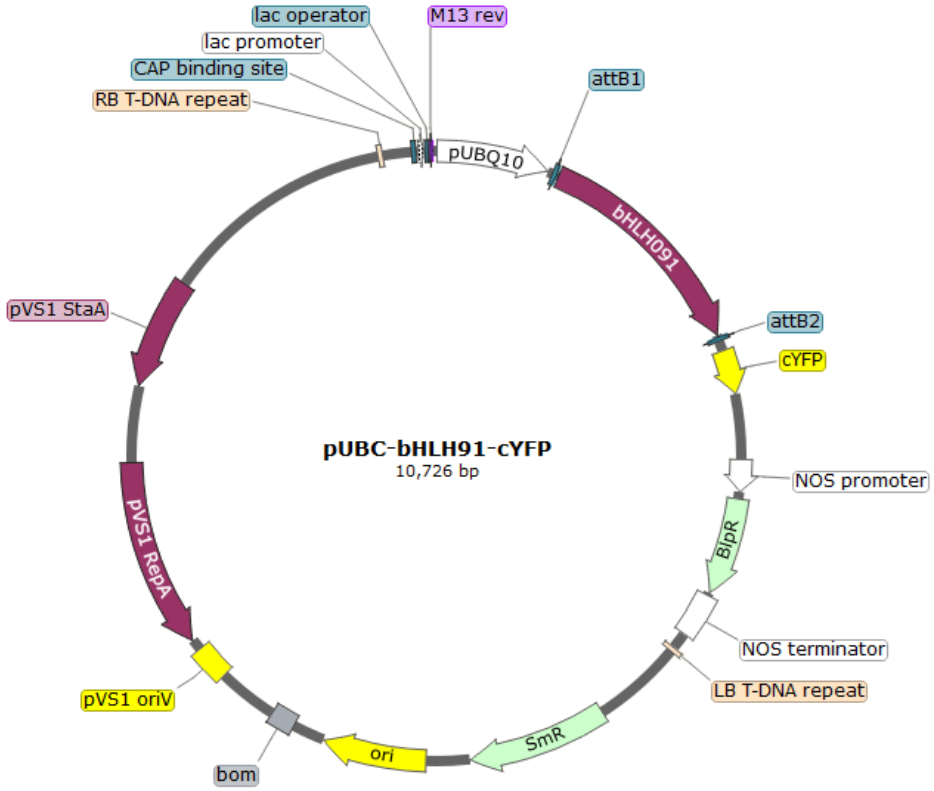

pUBC-bHLH091-nYFP

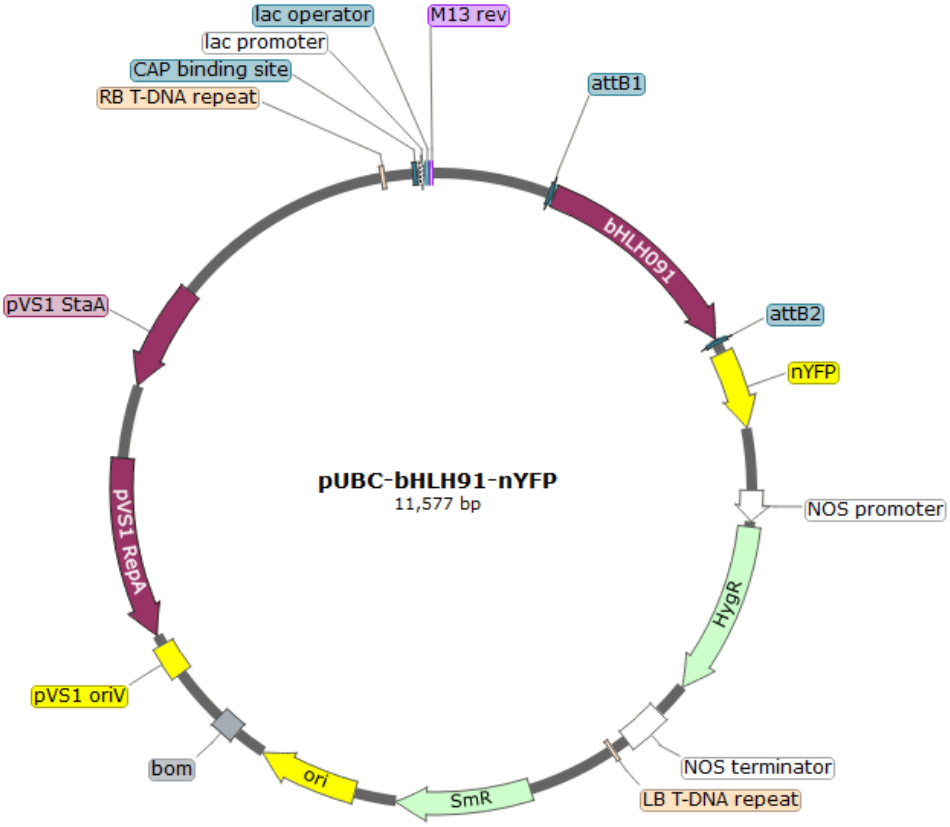

pUBC-bHLH091-YF

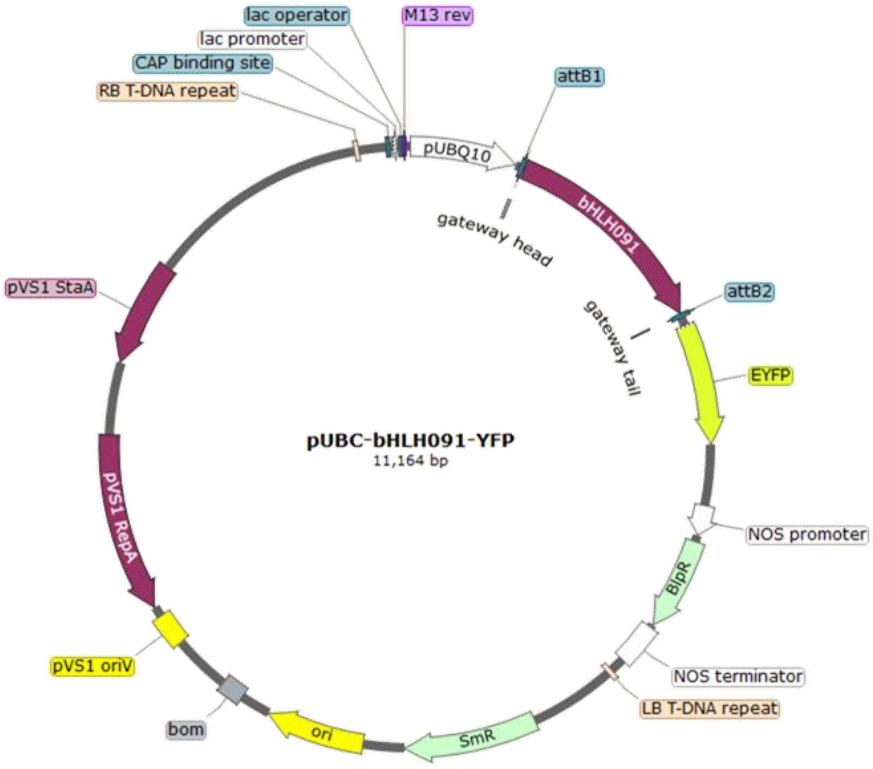

pUBC-DYT1-YFP

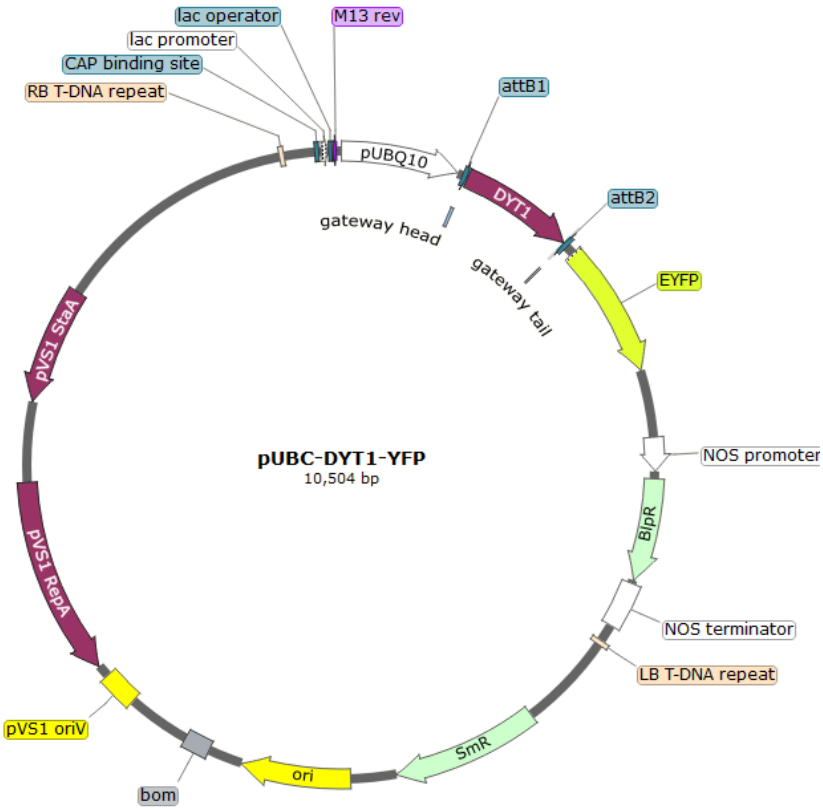

pUBC-GAI-cYFP

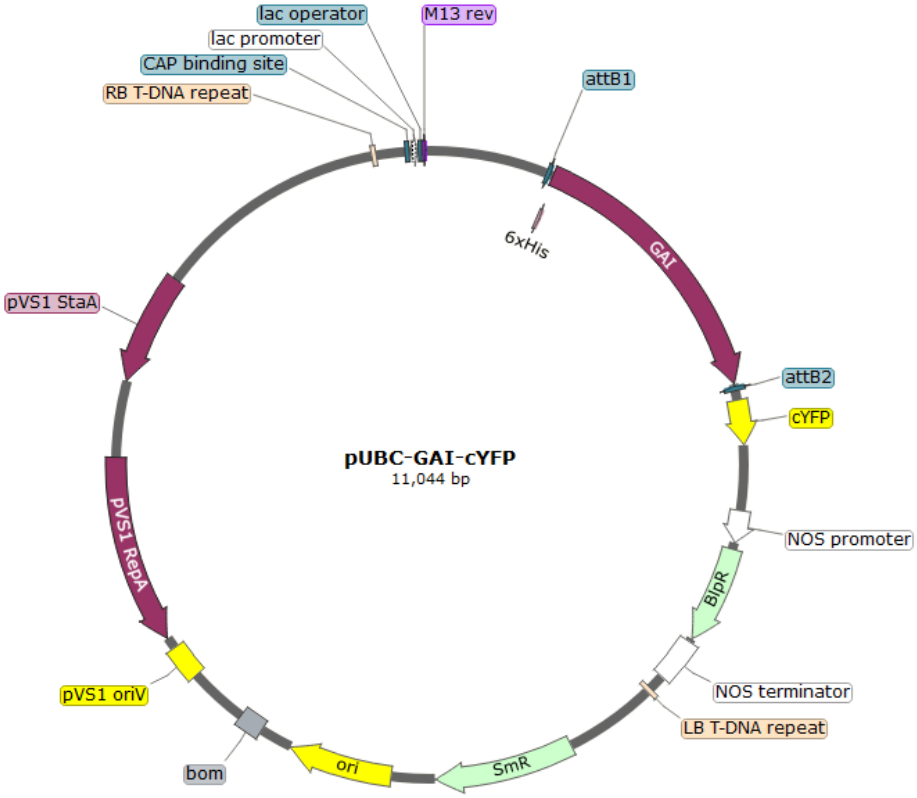

pUBC-MYB33-cYFP

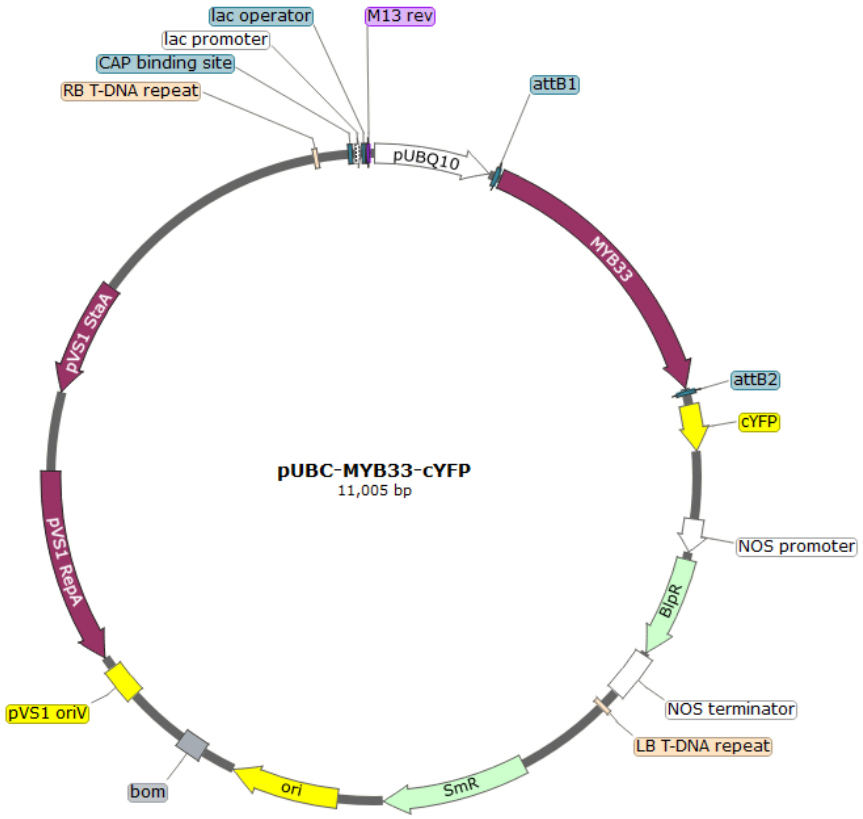

pUBC-MYB65-cYFP

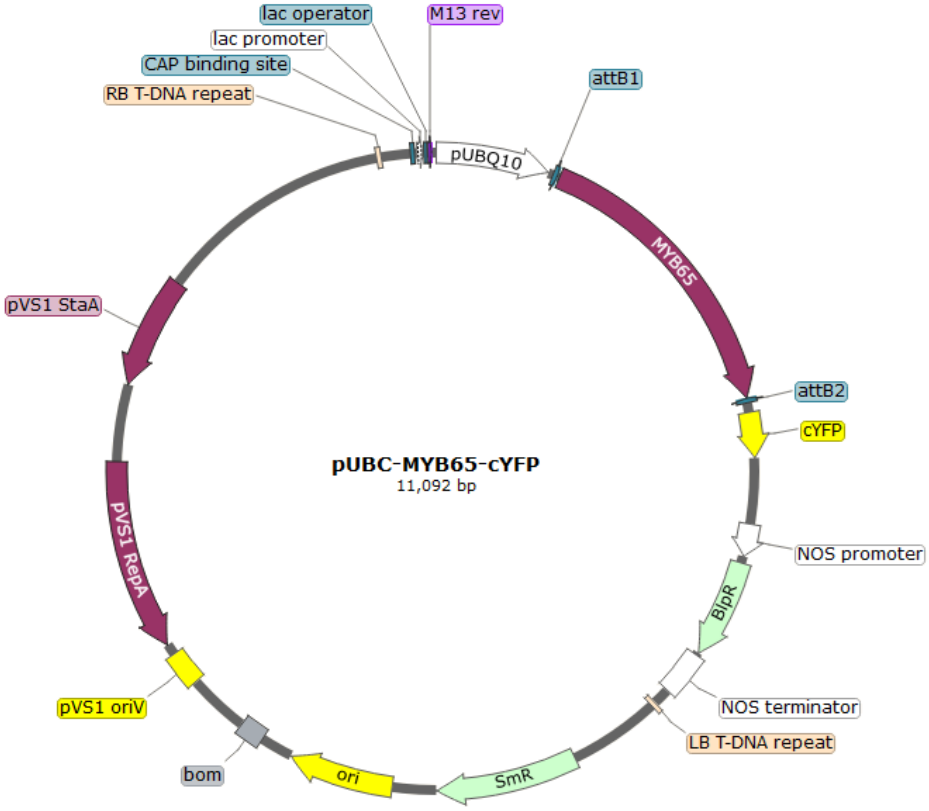

pUBC-RGL2-cYFP

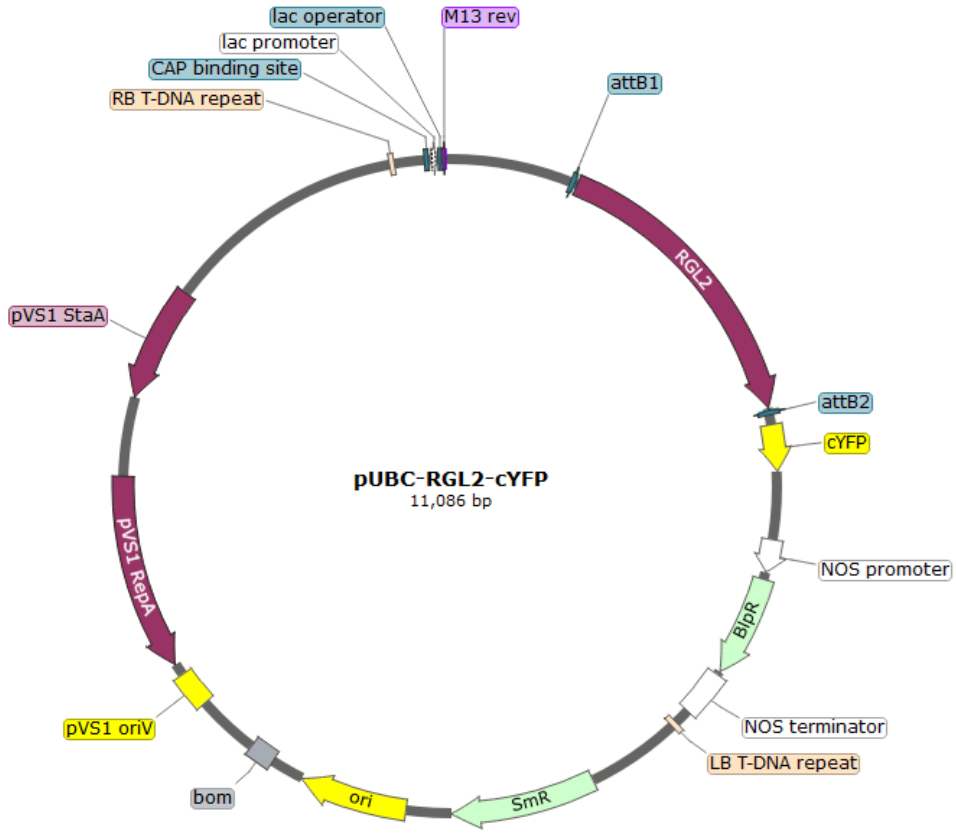

pUBC-RGL3-cYFP

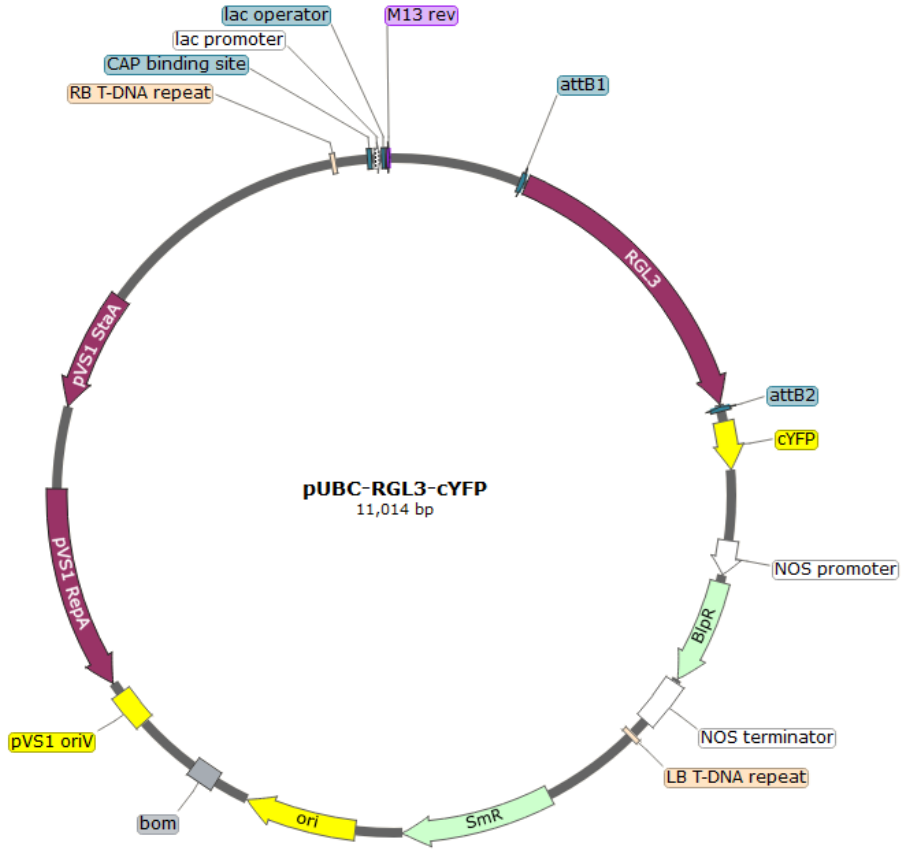

APPENDIX II: BHLH89, 91 & 10 PROTEIN HOMOLOGY

Protein alignments of bHLH89, -91 and -10 with bHLH domain highlighted in blue, BIF domain in grey and SUMO/SIM sites highlighted in green.

bHLH089 x bHLH010; 59.25% identity

Score	Expect	Method	Identities	Positives	Gaps
459 bits(1182)	4e-165	Compositional matrix adjust.	269/454(59%)	318/454(70%)	56/454(12%)

```
Query  10   IGCFDPNAPAEMTAESSFSPSEPPPT---ITVIGSNSNSNCSLE--DLSAFHLSPQDSSL  64
            +GCFDPN PAE+T ESSFS +EPPP    + V GS SNSNCS+E  +LS FHLSPQD
Sbjct  1    MGCFDPNTPAEVTVESSFSQAEPPPPPPQVLVAGSTSNSNCSVEVEELSEFHLSPQDC--  58

Query  65   PASASAYAHQLHINATPN----CDHQFQSSMHQTLQDPSYAQQSNHWDNGYQDFVNLGPN  120
               AS+   Q HIN  P     CD    + +HQ     S+ QQ ++WDNGYQDFVNLGPN
Sbjct  59   -PQASSTPLQFHINPPPPPPPPCDQLHNNLIHQM---ASHQQQHSNWDNGYQDFVNLGPN  114

Query  121  H-TTPDLLSLLQLPRSSLPPFANPS------IQDIIMTTSSSVAAYDPLFHLNFPLQPP-  172
             TTPDLLSLL LPR SLPP  +PS        DI+ ++S++   YDPLFHLNFP+QP
Sbjct  115  SATTPDLLSLLHLPRCSLPPNHHPSSMLPTSFSDIMSSSSAAAVMYDPLFHLNFPMQPRD  174

Query  173  -----NGS-FMGV-DQDQTETNQGVNLMYDEENN-----------NLDDGLNRKGRGSKK  214
                 NGS  +GV DQ Q + N G+N++Y E  N              ++G+ RKGRGS+K
Sbjct  175  QNQLRNGSCLLGVEDQIQMDANGGMNVLYFEGANNNNGGFENEILEFNNGVTRKGRGSRK  234

Query  215  RKIFPTERERRVHFKDRFGDLKNLIPNPTKNDRASIVGEAIDYIKELLRTIDEFKLLVEK  274
             +  PTERERRVHF DRF DLKNLIPNPTK DRASIVGEAIDYIKELLRTI+EFK+LVEK
Sbjct  235  SRTSPTERERRVHFNDRFFDLKNLIPNPTKIDRASIVGEAIDYIKELLRTIEEFKMLVEK  294

Query  275  KRV-----KQRNR---------EGDDVVDENFKAQSEVVEQCLINKKNNALRCSWLKRKS  320
            KR      K+R R         + ++    N+K QSEV + C     NN+LRCSWLKRKS
Sbjct  295  KRCGRFRSKKRARVGEGGGGEDQEEEEDTVNYKPQSEVDQSCFNKNNNNSLRCSWLKRKS  354

Query  321  KFTDVDVRIIDDEVTIKIVQKKKINCLLFVSKVVDQLELDLHHVAGAQIGEHHSFLFNAK  380
            K T+VDVRIIDDEVTIK+VQKKKINCLLF +KV+DQL+LDLHHVAG QIGEH+SFLFN K
Sbjct  355  KVTEVDVRIIDDEVTIKLVQKKKINCLLFTTKVLDQLQLDLHHVAGGQIGEHYSFLFNTK  414

Query  381  ISEGSSVYASAIADRVMEVLKKQYMEALSANNGY  414
            I EGS VYAS IAD +MEV++KQYMEA+ + NGY
Sbjct  415  ICEGSCVYASGIADTLMEVVEKQYMEAVPS-NGY  447
```

bHLH091 x bHLH010; 45.14% identity

Score	Expect	Method	Identities	Positives	Gaps
312 bits(799)	4e-107	Compositional matrix adjust.	209/463(45%)	275/463(59%)	59/463(12%)

```
Query  7    CFDPN--SMVDNNGGFCAAETTFTVSHQFQPPLGSTTNSFDDDLKLPTMDEFSVFPSVIS  64
            CFDPN  + V     F  AE              GST+NS +  +++  + EF + P
Sbjct  3    CFDPNTPAEVTVESSFSQAEPPPPPPQVLVA--GSTSNS-NCSVEVEELSEFHLSPQDCP  59

Query  65   LPNSETQNQNISN-----------NNHLINQMI----QESNWGVSEDNSNFFMNTSHPNT  109
              +S     +I+            +N+LI+QM     Q SNW   ++    F+N   PN+
Sbjct  60   QASSTPLQFHINPPPPPPPPCDQLHNNLIHQMASHQQQHSNW---DNGYQDFVNLG-PNS  115

Query  110  TTTPIPDLLSLLHLPRCSM---SLPSSDI----------MAGSCFTYDPLFHLNLPPQPP  156
              TTP  DLLSLLHLPRCS+     PSS +           + +   YDPLFHLN P QP
Sbjct  116  ATTP--DLLSLLHLPRCSLPPNHHPSSMLPTSFSDIMSSSSAAAVMYDPLFHLNFPMQPR  173
```

```
Query  157  LIPSNDYSGYLLGIDTNTTTQRDESNVG--------DENNNAQFDSGIIEFSKEIRRKGR  208
                    LLG++         ++N G           NNN   F++ I+EF+   + RKGR
Sbjct  174  DQNQLRNGSCLLGVEDQIQM---DANGGMNVLYFEGANNNNGGFENEILEFNNGVTRKGR  230

Query  209  GKRKNKPFTTERERRCHLNERYEALKLLIPSPSKGDRASILQDGIDYINELRRRVSELKY  268
            G RK++   TERERR H N+R+  LK LIP+P+K DRASI+ + IDYI EL R + E K
Sbjct  231  GSRKSRTSPTERERRVHFNDRFFDLKNLIPNPTKIDRASIVGEAIDYIKELLRTIEEFKM  290

Query  269  LVERKRCGGRHKNNEVDDNNNNKNLDDHGNEDDDDDDENMEKKPESDVIDQC---SSNNS  325
            LVE+KRCG              +  +  G ED +++++ +  KP+S+V   C    ++NNS
Sbjct  291  LVEKKRCG------RFRSKKRARVGEGGGGEDQEEEEDTVNYKPQSEVDQSCFNKNNNNS  344

Query  326  LRCSWLQRKSKVTEVDVRIVDDEVTIKVVQKKKINCLLLVSKVLDQLQLDLHHVAGGQIG  385
            LRCSWL+RKSKVTEVDVRI+DDEVTIK+VQKKKINCLL  +KVLDQLQLDLHHVAGGQIG
Sbjct  345  LRCSWLKRKSKVTEVDVRIIDDEVTIKLVQKKKINCLLFTTKVLDQLQLDLHHVAGGQIG  404

Query  386  EHYSFLFNTKIYEGSTIYASAIANRVIEVVDKHYMASLPNSNY  428
            EHYSFLFNTKI EGS +YAS IA+ ++EVV+K YM ++P++ Y
Sbjct  405  EHYSFLFNTKICEGSCVYASGIADTLMEVVEKQYMEAVPSNGY  447
```

bHLH089 x bHLH091; 43.86% identity

Score	Expect	Method	Identities	Positives	Gaps
314 bits(805)	2e-108	Compositional matrix adjust.	200/456(44%)	267/456(58%)	78/456(17%)

```
Query  6    MFEEIGCFDPNAPAE-----MTAESSFSPS---EPPPTITVIGSNSNS---NCSLEDLSA  54
            M+EE  CFDPN+  +       AE++F+ S   +PP     +GS +NS   +  L  +
Sbjct  1    MYEESSCFDPNSMVDNNGGFCAAETTFTVSHQFQPP-----LGSTTNSFDDDLKLPTMDE  55

Query  55   FHLSPQDSSLPASASAYAHQLHINATPNCDHQFQSSMHQTLQDPSYAQQSNHWDNGYQDF  114
            F + P   SLP S +   +        N +H     ++Q +Q+ ++       ++    F
Sbjct  56   FSVFPSVISLPNSETQNQN------ISNNNHL----INQMIQESNWGVS----EDNSNFF  101

Query  115  VNLG-PNHTT---PDLLSLLQLPRSSLPPFANPSIQDIIMTTSSSVAAYDPLFHLNFPLQ  170
            +N   PN TT   PDLLSLL LPR S+   + PS  DI+   + S   YDPLFHLN P Q
Sbjct  102  MNTSHPNTTTTPIPDLLSLLHLPRCSM---SLPS-SDIM---AGSCFTYDPLFHLNLPPQ  154

Query  171  PP-------NGSFMGVDQDQTETNQGVNLMYDEENNNLDDGL-------NRKGRGSKKRK  216
            PP        +G  +G+D + T      N+  +  N   D G+         RKGRG +K K
Sbjct  155  PPLIPSNDYSGYLLGIDTNTTTQRDESNVGDENNNAQFDSGIIEFSKEIRRKGRGKRKNK  214

Query  217  IFPTERERRVHFKDRFGDLKNLIPNPTKNDRASIVGEAIDYIKELLRTIDEFKLLVEKKR  276
             F TERERR H   +R+  LK LIP+P+K DRASI+ + IDYI EL R + E K LVE+KR
Sbjct  215  PFTTERERRCHLNERYEALKLLIPSPSKGDRASILQDGIDYINELRRRVSELKYLVERKR  274

Query  277  VKQRNREGDDVVDENF--------------------KAQSEVVEQCLINKKNNALRCSWL  316
               R++  +   + N                     K +S+V++QC     NN+LRCSWL
Sbjct  275  CGGRHKNNEVDDNNNNKNLDDHGNEDDDDDDENMEKKPESDVIDQC---SSNNSLRCSWL  331

Query  317  KRKSKFTDVDVRIIDDEVTIKIVQKKKINCLLFVSKVVDQLELDLHHVAGAQIGEHHSFL  376
            +RKSK T+VDVRI+DDEVTIK+VQKKKINCLL VSKV+DQL+LDLHHVAG QIGEH+SFL
Sbjct  332  QRKSKVTEVDVRIVDDEVTIKVVQKKKINCLLLVSKVLDQLQLDLHHVAGGQIGEHYSFL  391

Query  377  FNAKISEGSSVYASAIADRVMEVLKKQYMEALSANN  412
            FN KI EGS++YASAIA+RV+EV+ K YM +L  +N
Sbjct  392  FNTKIYEGSTIYASAIANRVIEVVDKHYMASLPNSN  427
```